STUDIES OF THE MOLECULAR MECHANISM AND SIGNALING REGULATION OF AUTOPHAGY IN *SACCHAROMYCES CEREVISIAE*

by

Zhifen Yang

A dissertation submitted in partial fulfillment
of the requirements for the degree of
Doctor of Philosophy
(Molecular, Cellular and Developmental Biology)
in The University of Michigan
2010

Doctoral Committee:

Professor Daniel J. Klionsky, Chair
Professor Lois Weisman
Associate Professor Anuj Kumar
Associate Professor Ken Cadigan

DEDICATION

This thesis is dedicated to all the people who have encouraged and supported me during the years of my PhD study: to my parents, for their eternal love, endless care and always giving me strength and courage; to my brother, for bringing me all the joy in my childhood, guiding me forward, supporting me whatever the way I have chosen and keeping me confident and strong; to all my teachers and mentors, for giving me knowledge, teaching me the meaning of life; to my friends, for bringing me fun and joy; to Wei, for his unquestioned love, encouragement and support; finally, to the luck that brings me all these people in my life.

ACKNOWLEDGEMENTS

I would like to give my special thanks to my graduate mentor, Dr. Daniel J. Klionsky for his invaluable assistance in providing me precious training and supervision. I feel very fortunate and honored to work in his laboratory. I have learned a lot from his scientific expertise, logical thinking and passion towards scientific research and education, and these invaluable lessons will guide and encourage me forward in my future research career.

I would like to thank my thesis committee members, Dr. Lois Weisman, Dr. Anuj Kumar and Dr. Ken Cadigan, for giving me insightful suggestions and criticisms for my projects. I would like to also thank Dr. Jesse C. Hay and Dr. Anuj Kumar for giving me opportunities to do rotations in their laboratories. Additionally, I am also grateful to Dr. Ken Inoki and Dr. Sungki Hong in the Inoki laboratory for helping me in my kinase experiments.

I am grateful to all the former and current members of the Klionsky lab that I have worked with in the past six years. I feel appreciation for their kind assistance, good suggestions and ideas. I would like to especially thank Dr. Ju Huang and Dr. Usha Nair for helping me on the Atg22 project, Dr. Wei-Lien Yen and Mr. Ke Wang for helping me on the Pho85 project, and also Mr. Jiefei Geng with whom I had a pleasant collaboration on both the Atg22 and Pho85 projects. I also want to thank Dr. Tomohiro Yorimitsu, Dr. Tomotake Kanki and Dr. Usha Nair for helpful advice in my research. Additionally, I am also grateful to have Dr. Wei-Lien Yen, Dr. Ju Huang, Dr. Congcong He and Dr. Usha Nair as my colleagues and good friends.

Finally, I am thankful to Huazhong Agricultural University where I got my undergraduate and master, and the National Key Laboratory of Crop Genetic Improvement where I started my biological research; and to the MCDB Department and Rackham Graduate School of the University of Michigan for providing me funding and the opportunity to complete my Ph.D. study.

I am thankful to the journals Current Topics in Microbiology and Immunology, Current Opinion in Cell Biology, Molecular Biology of the Cell, and Autophagy, for their permission to reproduce my publications.

Chapter 1 is reprinted from Current Topics in Microbiology and Immunology, Vol.335, Autophagy in Infection and Immunity, Zhifen Yang and Daniel J. Klionsky, An Overview of the Molecular Mechanism of Autophagy, pg. 1-35, Copyright 2009, with permission.

Chapter 2 is reprinted from Current Opinion in Cell Biology, Zhifen Yang and Daniel J. Klionsky, Mammalian Autophagy: Core Molecular Machinery and Signaling Regulation, in press, with minor modifications.

Chapter 3 is reprinted from Molecular Biology of the Cell, Vol.17, Zhifen Yang, Ju Huang, Jiefei Geng, Usha Nair and Daniel J. Klionsky, Atg22 Recycles Amino Acids to Link the Degradative and Recycling Functions of Autophagy, pg. 5094-5104, Copyright 2006, with the permission of MBC, Online:**http://www.molbiolcell.org**, by The American Society for Cell Biology.

Chapter 5 is reprinted from Autophagy, Volume 3, Issue 2, Zhifen Yang and Daniel J. Klionsky, Permeases Recycle Amino Acids Resulting from Autophagy, pg. 149-150 Copyright 2007, with permission from Landes Bioscience.

TABLE OF CONTENTS

LIST OF TABLES

LIST OF FIGURES

CHAPTER 1

An overview of the molecular mechanism of autophagy

ABSTRACT

Autophagy is a highly conserved cellular degradation process in which portions of cytosol and organelles are sequestered into a double-membrane vesicle, an autophagosome, and delivered into a degradative organelle, the vacuole/lysosome, for breakdown and eventual recycling of the resulting macromolecules. This process relieves the cell from various stress conditions. Autophagy plays a critical role during cellular development and differentiation, functions in tumor suppression, and may be linked to lifespan extension. Autophagy also has diverse roles in innate and adaptive immunity, such as resistance to pathogen invasion. Substantial progress has been made in the identification of many autophagy-related, *ATG*, genes that are essential to drive this cellular process, including both selective and non-selective types of autophagy. Identification of the *ATG* genes in yeast, and the finding of orthologs in other organisms, reveals the conservation of the autophagic machinery in all eukaryotes. Here, we summarize our current knowledge about the machinery and molecular mechanism of autophagy.

Introduction

Autophagy, "self-eating" at the subcellular level, has gained tremendous attention in the past few years, and our knowledge concerning the mechanism of autophagy has expanded dramatically (Yorimitsu and Klionsky, 2005b). There are three major types of autophagy in eukaryotic cells, macroautophagy, microautophagy and chaperone-mediated autophagy (CMA), and they are mechanistically different from each other (Klionsky, 2005; Massey et al., 2004). Both macro- and microautophagy involve dynamic membrane rearrangement to engulf portions of the cytoplasm, and they have the capacity for sequestration of large structures, such as entire organelles. Microautophagy involves the direct engulfment of cytoplasm at the lysosome surface by invagination, protrusion, and septation of the lysosome membrane. In contrast, during macroautophagy, portions of cytoplasm are sequestered into a *de novo* formed double-membrane vesicle, termed an autophagosome. Subsequently, the completed autophagosome fuses with the lysosome/vacuole and the inner single-membrane vesicle is released into the lumen. In either case, the membrane of the resulting autophagic body is lysed to allow breakdown of the contents, and the resulting macromolecules are transported back into the cytosol through membrane permeases for reuse. In contrast, CMA does not involve a similar type of membrane rearrangement; instead, it translocates unfolded, soluble proteins directly across the limiting membrane of the lysosome.

In this chapter, we will focus on macroautophagy, hereafter referred to as autophagy. Autophagy is an evolutionarily conserved process that occurs ubiquitously in all eukaryotic cells (Reggiori and Klionsky, 2002) and has many physiological roles. Autophagy is active at a basal level for the turnover of long-lived proteins and also for the

removal of superfluous or damaged organelles. This latter function might provide a connection to autophagy's proposed role in lifespan extension (Levine and Klionsky, 2004). On the other hand, autophagy is induced as a cellular response to various stress conditions, such as nutrient limitation, heat and oxidative stress. Autophagy also plays a role in cellular development and differentiation (Levine and Klionsky, 2004). Moreover, autophagy is implicated in a wide range of diseases (Huang and Klionsky, 2007; Mizushima et al., 2008; Shintani and Klionsky, 2004a), including cancer and neurodegenerative disorders such as Alzheimer's, Parkinson's and Huntington's diseases. In addition, autophagy has diverse roles in innate and adaptive immunity (Levine and Deretic, 2007). For example, autophagy can eliminate invasive pathogens, including viruses, parasites and bacteria; autophagy also promotes MHC class II presentation of microbial (and self) antigens. Finally, in the absence of apoptosis, autophagy may participate in a type of programmed cell death, termed type II programmed cell death, that is distinct from apoptosis, although the physiological relevance of the former is not clear (Levine and Yuan, 2005).

The morphology of autophagy was first identified in mammalian cells in the 1950s, and extensive morphological and pharmacological studies defined the basic steps of this process. Subsequent work in various fungi starting in the 1990s allowed the identification of individual molecular components that participate in autophagy. To date, there are 31 AuTophaGy-related (*ATG*) genes (Huang and Klionsky, 2007; Klionsky et al., 2003). The *ATG* genes were discovered from genetic screens for mutants that affected protein turnover (non-specific autophagy), peroxisome degradation (pexophagy) and delivery of a resident vacuolar hydrolase (the cytoplasm to vacuole targeting (Cvt) pathway). Although the Cvt, pexophagy and autophagy pathway are morphologically and mechanistically similar and

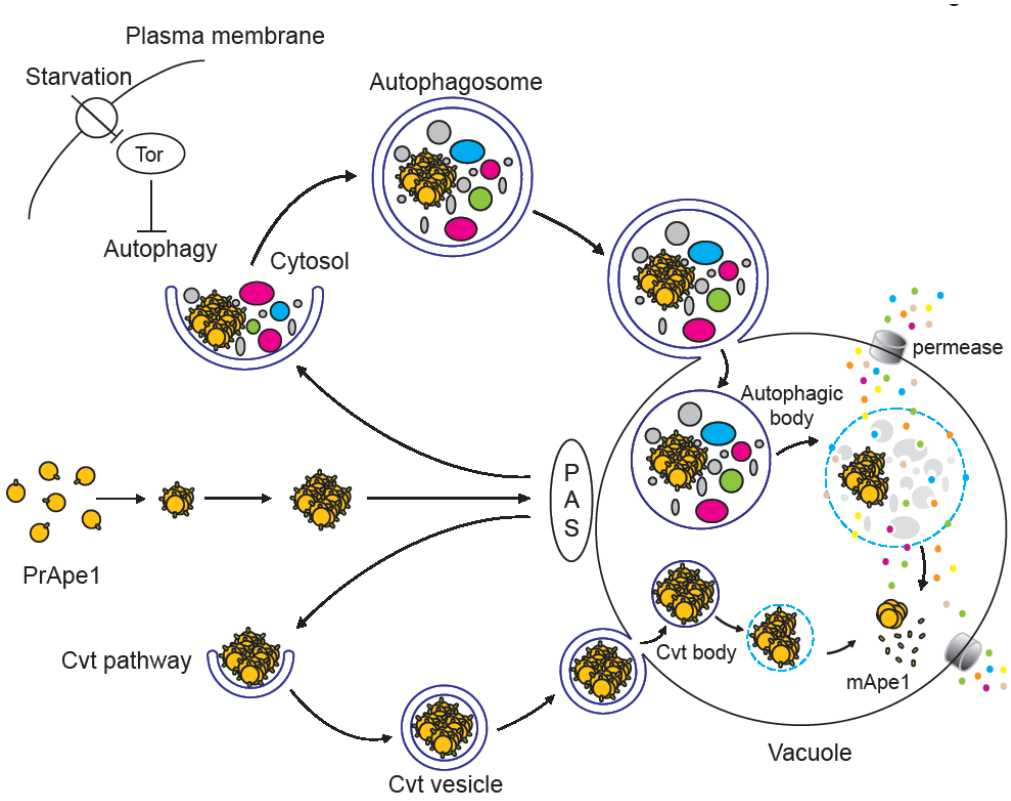

Figure 1.1. Schematic overview of autophagy and the Cvt pathway in yeast. Both pathways involve the engulfment of cargos within distinct double-membrane vesicles, which are thought to originate from the phagophore assembly site (PAS). The Cvt pathway is biosynthetic and is used for the delivery of two resident vacuolar hydrolases, aminopeptidase I (Ape1) and α-mannosidase (Ams1), and it occurs under vegetative conditions. The Cvt vesicle is approximately 140-160 nm in diameter and appears to closely enwrap the specific cargo, the Cvt complex (consisting of prApe1 and the Atg19 receptor), and exclude bulk cytoplasm. In contrast, autophagy is degradative and is induced by inactivation of Tor kinase upon nutrient starvation. The autophagosome, which is 300-900 nm in diameter, sequesters cytoplasm, including organelles, and can also specifically sequester the Cvt complex. Once completed, the double-membrane vesicles dock and fuse with the vacuole, and release the inner single-membrane vesicles (autophagic or Cvt body) into the lumen. Subsequently, these vesicles are broken down, allowing the maturation of prApe1 and the degradation of cytoplasm, with recycling of the resulting macromolecules through vacuolar permeases. This figure is modified from Figure 1 of Yorimitsu and Klionsky (2005b).

share most of the Atg components, they differ in several aspects (Figure 1.1). Autophagy and pexophagy are degradative, whereas the Cvt pathway is biosynthetic. Autophagy is generally considered non-selective, whereas pexophagy and the Cvt pathway are highly selective. The Cvt pathway is used for delivery of two resident vacuolar hydrolases, aminopeptidase I (Ape1) and α-mannosidase (Ams1) (Hutchins and Klionsky, 2001; Scott et al., 1997). A double-membrane vesicle that sequesters these two proteins is termed a Cvt vesicle, which is relatively consistent in size, but significantly smaller than the autophagosome; being 140-160 nm in diameter compared to the 300-900 nm autophagosome (Baba et al., 1997). Similarly, the vesicle formed during pexophagy, the pexophagosome, is also larger than the Cvt vesicle in order to accommodate its specific cargos, peroxisomes (Hutchins et al., 1999). In contrast to the autophagosome, both the Cvt vesicle and pexophagosome appear to closely enwrap the cargo and exclude bulk cytoplasm.

These dynamic pathways can be broken down into a series of steps (Figure 1.2), including induction, cargo recognition and packaging, vesicle nucleation, vesicle expansion and completion, Atg protein cycling, vesicle fusion with the vacuole/lysosome, vesicle breakdown and recycling of the resulting macromolecules (Huang and Klionsky, 2007). Thus, the Atg proteins can be classified into several different groups according to their functions at the different steps of the pathway. Many orthologs of the *ATG* gene products have also been identified and studied in higher eukaryotes, such as worms, insects, plants and mammals, and they have essentially similar roles as those in yeast (Xie and Klionsky, 2007; Yorimitsu and Klionsky, 2005b). Continued investigation of functions of the *ATG* gene products in yeast will largely expand our understanding of autophagy. In this

chapter, we will mainly discuss the molecular machinery of autophagy, with an emphasis on yeast.

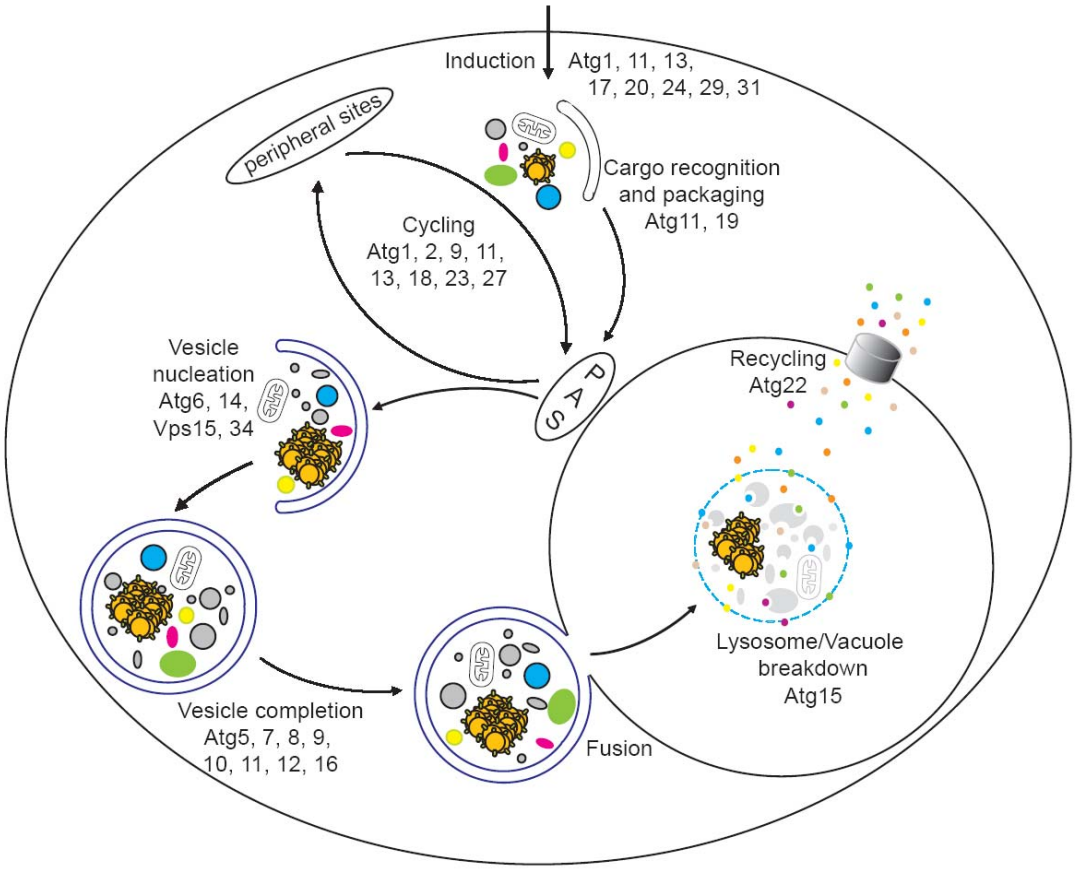

Figure 1.2. Schematic representation of autophagy and autophagy-related pathways. These dynamic pathways can be broken down into a series of steps including induction, cargo recognition and packaging, vesicle nucleation, vesicle expansion and completion, Atg protein cycling, vesicle fusion with the vacuole/lysosome, vesicle breakdown and recycling of the resulting macromolecules. The Atg proteins can be classified into several different groups according to their functions at the different steps of the pathway. The Atg1 complex may act at multiple steps of the pathway including induction and Atg protein cycling. During the vesicle formation process, several Atg proteins are involved in cycling between the peripheral sites and the PAS. *PAS*, phagophore assembly site; thought to be the organizing site for phagophore formation. This figure is modified from Figure 2 of Huang and Klionsky (2007).

Induction and Regulation of Autophagy

Insufficient autophagy can be deleterious (Komatsu et al., 2007a; Kuma et al., 2004), but excessive levels may also be harmful. Accordingly, autophagy is a tightly regulated process in all eukaryotes. The induction and regulation of autophagy have been studied extensively in yeast, mammalian cells and *Drosophila*. Several signaling pathways, as summarized in the following, are involved in the control of autophagy.

TORC1. The protein target of rapamycin, Tor, plays a major regulatory role in autophagy induction (Carrera, 2004). Tor forms two functionally distinct protein complexes, Tor complex 1 and 2 (TORC1 and TORC2) (Loewith et al., 2002), and TORC1 has the primary role in regulating autophagy. Under nutrient rich conditions, TORC1 is active, and inhibits autophagy, whereas upon nutrient deprivation, TORC1 is inhibited, which allows an increase of autophagic activity (Noda and Ohsumi, 1998).

In yeast, TORC1 acts on autophagy in two ways (Klionsky, 2005). First, TORC1 regulates the Atg1-Atg13-Atg17 kinase complex (Figure 1.3A). The formation of this ternary complex correlates with an increase in autophagic activity. Atg1, a serine/threonine kinase, is one of the key Atg proteins required for both autophagy and the Cvt pathway (Matsuura et al., 1997). Based on yeast two-hybid data and affinity isolation, Atg1 is found to be in a complex with Atg13 and Atg17 (Kabeya et al., 2005; Kamada et al., 2000). The observation that Atg17 interacts with Atg13 in the absence of Atg1, but not vice versa, suggests that Atg13 mediates the interaction between Atg1 and Atg17. TORC1 regulates directly or indirectly the Atg13 phosphorylation state. Under nutrient-rich conditions, Atg13 is highly phosphorylated, and has a lower affinity for Atg1 and Atg17. Upon inactivation of TORC1 by rapamycin or nutrient deprivation, Atg13 is rapidly and partially

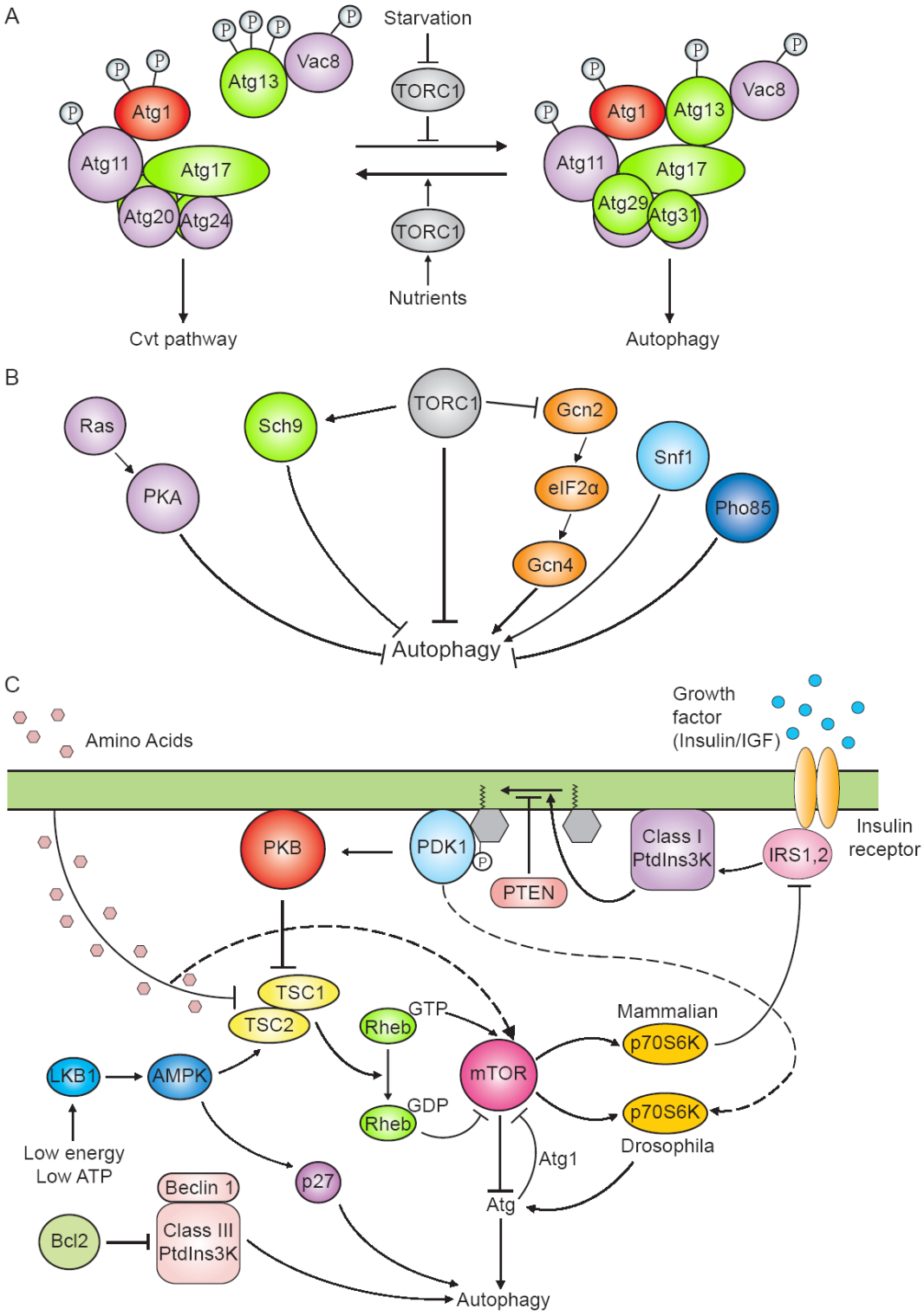
A
Starvation
TORC1
TORC1
Nutrients
Atg1
Atg13
Vac8
Atg11
Atg17
Atg20
Atg24
Atg29
Atg31
Cvt pathway
Autophagy
B
TORC1
Ras
Sch9
Gcn2
PKA
eIF2α
Snf1
Pho85
Gcn4
Autophagy
C
Amino Acids
Growth factor (Insulin/IGF)
PKB
PDK1
PTEN
Class I PtdIns3K
IRS1,2
Insulin receptor
TSC1
TSC2
Rheb
GTP
GDP
Mammalian
p70S6K
mTOR
LKB1
AMPK
Low energy
Low ATP
p27
Atg1
Atg
Beclin 1
Bcl2
Class III PtdIns3K
Autophagy

Figure 1.3. Regulation of autophagy induction in yeast and mammalian cells. (A) Regulatory complex for autophagy induction in yeast. In yeast, autophagy is mainly a starvation response, and Tor kinase complex 1 (TORC1) regulates the induction of autophagy upon sensing the nutrient conditions. Atg1 kinase, which is essential for both autophagy and the Cvt pathway, forms a putative complex with several Atg proteins that are primarily required for autophagy (*in green*) or the Cvt pathway (*in purple*). Under nutrient-rich conditions, TORC1 is active and Atg13 is highly phosphorylated, and this hyperphosphorylated Atg13 has a lower affinity for Atg1 and Atg17. Upon inactivation of TORC1 by nutrient starvation, Atg13 is rapidly and partially dephosphorylated, leading to a higher affinity for Atg1 and Atg17. The formation of Atg1—Atg13—Atg17 ternary complex allows the activation of Atg1 kinase activity, which may regulate the switch between autophagy and the Cvt pathway in response to environmental changes. The function of additional components of the putative complex depicted here, including Atg20, Atg24, Atg29, Atg31 and Vac8, are not known. Atg11 may function in part as a scaffold protein. This figure is modified from Figure 2 of Yorimitsu and Klionsky (2005b). **(B) Multiple nutrient-sensing kinase signaling pathways converge on autophagy in yeast.** TORC1 plays a major role in the regulation of autophagy. Ras is active under nutrient-rich conditions, and allows the activation of PKA, which inhibits autophagy. The PKA and Sch9 signaling pathways cooperatively regulate the induction of autophagy in parallel with Tor, although Sch9 is also a direct substrate of TORC1. The eIF2α kinase signaling pathway positively regulates autophagy, and Gcn2 might be another target of TORC1. Snf1 and Pho85 are additional positive and negative regulatory components, respectively, of autophagy in yeast. **(C) Regulation of autophagy in mammalian cells.** mTor activation depends on several inputs, including nutrients (amino acids), energy (ATP) and growth factor (insulin/IGF). In response to insulin receptor stimulation, a class I phosphoinositide 3-kinase (PtdIns3K) is activated and generates PtdIns(3,4)P_2 and PtdIns(3,4,5)P_3 at the plasma membrane, and the latter two activate 3-phosphoinositide-dependent protein kinase 1 (PDK1) and protein kinase B (PKB)/Akt. PKB phosphorylates and inhibits the GTPase-activating protein complex TSC1—TSC2, leading to the stabilization of Rheb-GTP, which stimulates mTor, causing inhibition of autophagy. PTEN, a 3' phosphoinositide phosphatase, antagonizes PKB, and has a stimulatory effect on autophagy. Both mTor and PDK1 stimulate p70S6 kinase (p70S6K). In one model, under nutrient-rich conditions, activation of S6K directly stimulates autophagy, or it is stimulated indirectly through inhibition of PtdIns3K, allowing a basal level of autophagy for homeostatic purposes. Under starvation conditions, inhibition of mTor prevents further activation of S6K, which limits and prevents excessive autophagy. Both ATP and amino acids deprivation result in mTor inactivation independent of the insulin signaling pathway. Amino acids activate mTor via inhibition of the TSC1—TSC2 complex or are sensed by mTor directly. Energy stress

causes activation of the LKB1—AMPK pathway, which inhibits mTor by activating TSC1—TSC2. AMPK phosphorylates and stabilizes p27, a cylin-kinase inhibitor, leading to activation of autophagy. An anti-apoptotic protein, Bcl-2, associates with Beclin 1, the mammalian homolog of Atg6, and inhibits a class III PtdIns3K complex, whereas the latter serves a stimulatory role in autophagy. Also shown is the notion that Atg1 overexpression negatively feeds back on Tor activity in *Drosophila*.

dephosphorylated, leading to a higher affinity for Atg1 and Atg17. The identities of the phosphatase(s) that control Atg13 phosphorylation are currently unknown. The interaction of Atg1 with hypophosphorylated Atg13 and Atg17 allows the activation of Atg1 kinase activity. Loss of interaction between Atg1 and Atg13, or between Atg13 and Atg17, leads to a decrease in Atg1 kinase activity and decreased autophagy. The kinase activity of Atg1 is essential for both autophagy and the Cvt pathway, although a higher level of kinase activity appears to be needed for the Cvt pathway (Abeliovich et al., 2003; Cheong et al., 2008; Kabeya et al., 2005; Kamada et al., 2000). It is possible that the kinase activity of Atg1 is critical for the magnitude of autophagy, but not its initiation (Nair and Klionsky, 2005). The downstream substrate of Atg1 kinase is unclear, and it is still a matter of debate whether Atg1 primarily acts on autophagy through its kinase activity or through a structural role during autophagic complex formation. However, one role of the Atg1-Atg13-Atg17 ternary complex is thought to be that of regulating the switch between autophagy and the Cvt pathway in response to environmental changes.

Homologs of Atg1 are involved in autophagy in various multicellular organisms such as *Dictyostelium discoideum* (Otto et al., 2004), *Drosophila melanogaster* (Scott et al., 2004), *C.elegans* (Melendez et al., 2003), *Arabidopsis thaliana* (Hanaoka et al., 2002), and mammals (Yan et al., 1998; Yan et al., 1999). In *Drosophila*, Atg1 activity is modulated by

TORC1 as in yeast, because the induction of autophagy that results from the overexpression of Atg1 is suppressed when the TORC1 signaling pathway is impaired (Scott et al., 2007). Normally, a feedback mechanism may occur in which Atg1 downregulates Tor activity, resulting in a further activation of Atg1 and a further increase in autophagy (Figure 1.3C). Because these studies are based on overexpressed Atg1, however, the physiological significance is not clear at present. In mammals, the uncoordinated 51-like kinases 1 and 2 (Ulk1 and Ulk2) appear to be the functionally equivalent mammalian homologs of yeast Atg1. Knockdown of *ULK1* inhibits the induction of autophagy by rapamycin treatment, indicating that Ulk1 functions downstream of mTOR in autophagy regulation (Chan et al., 2007). In contrast to the result in *Drosophila*, overexpression of *ULK1* or *ULK2* suppresses autophagy. Furthermore, moderate expression of kinase-dead *ULK* mutants also efficiently suppresses autophagy, indicating that kinase activity of the Ulk proteins is critical during this process (Hara et al., 2008). FIP200 is a recently identified Ulk-interacting protein that is required for autophagy (Hara et al., 2008). Ulk and FIP200 function together and form a complex that is essential during an early step in autophagosome formation; FIP200 is thus thought to be a counterpart of yeast Atg17. Further identification and analysis of a functional homolog of mammalian Atg13 might help clarify the functional relationship between yeast and mammalian Atg1 complex.

Second, TORC1 acts through its downstream effectors to control autophagy. Several, but not all, TORC1 readouts, including autophagy, are regulated through protein phosphatase type 2A (PP2A) and/or 2A-related protein phosphatase (Sit4) (De Virgilio and Loewith, 2006). PP2A and Sit4 are in distinct complexes containing Tap42. Under nutrient

rich conditions, Tap42 is phosphorylated and tightly associates with PP2A and Sit4. Starvation or rapamycin treatment causes dephosphorylation and dissociation of Tap42 or a change in conformation, resulting in activation of Sit4. TORC1 may directly phosphorylate Tap42, or may indirectly regulate Tap42 via Tip41. Upon inactivation of TORC1, Tip41 is dephosphorylated and has a high affinity for Tap42 resulting in the inhibition of the latter. One report suggests that Tap42 does not transmit the signal from TORC1 to regulate autophagy (Kamada et al., 2000). However, more recent data indicate a role for Tap42 in the negative regulation of this process (Yorimitsu et al., 2009).

The conserved Tor protein in mammalian cells (mTor) also senses nutrient status and modulates autophagy, but the mechanism of regulation is more complex than in fungi, which are not responsive to hormones. As shown in Figure 1.3C, the regulatory cascade upstream of mTor includes an insulin receptor, insulin-receptor substrates 1 and 2, class I phosphoinositide 3-kinase (PtdIns3K), 3-phosphoinositide-dependent protein kinase 1 (PDK1) and protein kinase B (PKB)/Akt (Meijer and Codogno, 2006). mTor activity is controlled by the heterodimer TSC1-TSC2 which acts as a GTPase-activating protein (GAP) for the GTPase Rheb. The GDP-bound form of Rheb inhibits mTor, whereas the GTP-bound form stimulates the enzyme. PKB phosphorylates and inhibits the TSC1-TSC2 complex, leading to activation of mTor signaling. PTEN, a 3' phosphoinositide phosphatase, antagonizes PKB, and has a stimulatory effect on autophagy (Arico et al., 2001). The best characterized signaling pathway, located downstream of mTor, includes components such as ribosomal subunit S6 kinase (p70S6K). In one model, S6K exerts a negative feedback on mTor signaling by phosphorylating IRS1 to downregulate insulin signaling, leading to a decline in PI(3,4,5)P3, an inhibitor of autophagy; this feedback

regulation may ensure a basal level of autophagy even under nutrient-rich conditions (Klionsky, 2005).

Ras/cAMP-dependent protein kinase A (PKA). In addition to TORC1, the Ras/PKA signaling pathway also regulates autophagy from yeast to mammals (Budovskaya et al., 2004; Furuta et al., 2004; Mavrakis et al., 2006; Schmelzle et al., 2004; Yorimitsu et al., 2007). Under nutrient-rich conditions in yeast, two redundant small GTPases, Ras1 and Ras2, are activated, and stimulate adenylyl cyclase to produce cAMP. cAMP binds to the PKA regulatory subunit (Bcy1) and allows its dissociation from the three PKA catalytic subunits (Tpk1, Tpk2 and Tpk3), resulting in the activation of PKA (Thevelein and de Winde, 1999). Constitutive activation of PKA through a dominant hyperactive allele of *RAS2*, $RAS2^{G19V}$, or deletion of *BCY1*, prevents the induction of autophagy by nutrient starvation or rapamycin, whereas inactivation of PKA by a dominant negative allele of *RAS2*, $RAS2^{G22A}$, induces autophagy in rich condition without rapamycin (Budovskaya et al., 2004; Schmelzle et al., 2004). Thus, in addition to TORC1, Ras/PKA is another negative regulator of autophagy (Figure 1.3B). Among the Atg proteins, Atg1, Atg13, Atg18 and Atg21 contain PKA phosphorylation sites. However, it is still unclear whether the phosphorylation of these Atg proteins by PKA has any functional link to autophagy (Budovskaya et al., 2005).

Sch9 is a homologue of mammalian PKB or p70S6 kinase (Urban et al., 2007). A recent report shows that PKA and Sch9 signaling pathways cooperatively regulate the induction of autophagy (Yorimitsu et al., 2007). Simultaneous inactivation of PKA and Sch9 triggers induction of autophagy in rich conditions independent of effects on TORC1, whereas further inactivation of TORC1 causes an additive effect. These observations

suggest a model wherein PKA, Sch9 and TORC1, at least in part, regulate autophagy in parallel (Figure 1.3B). This model is supported by the finding that TORC1 and Ras/PKA function as two parallel pathways that independently act in regulating cell growth (Zurita-Martinez and Cardenas, 2005). However, Sch9 is a direct substrate of TORC1 (Urban et al., 2007); furthermore, it is also suggested that TORC1 transmits signals through the Ras/PKA pathway to its downstream targets (Schmelzle et al., 2004). Therefore, the connection among PKA, Sch9 and TORC1 with regard to their effects in autophagy regulation is still not clear.

eIF2α kinase signaling and GCN4 general control. In response to amino acid starvation, budding yeast initiate a general amino acid control to induce the transcription of numerous genes. Central to this response is Gcn4, a master transcriptional activator of gene expression (Hinnebusch, 2005). Gcn4 synthesis is mainly regulated at the translational level. Derepression of *GCN4* mRNA translation requires a protein kinase, Gcn2, whose only known substrate is the α subunit of translation initiation factor 2 (eIF2). The eIF2α kinase signaling pathway is also involved in the regulation of autophagy from yeast to mammals (Figure 1.3B) (Talloczy et al., 2002). Upon loss of Gcn2 or Gcn4, or in the presence of the eIF2α nonphosphorylatable mutant *SUI2-S51A*, autophagic activity is impaired. Intriguingly, TORC1 is implicated in the eIF2α kinase signaling pathway because rapamycin activates Gcn2, at least in part, through de-phosphorylation of Ser577 (Kubota et al., 2003). Thus, Gcn2 might be another target of TORC1.

Other signaling pathways controlling autophagy. Snf1, the closest yeast homologue of the mammalian AMP-activated protein kinase, and Pho85, a cyclin-dependent kinase (CDK), antagonistically control autophagy in yeast (Figure 1.3B) (Wang et al., 2001b).

Snf1, which is activated upon glucose depletion to allow transcription of glucose-repressed genes, is required for starvation-induced autophagy. Pho85, which has multiple functions through association with its ten different cyclins (Pcls), is a negative regulator of autophagy, although the functions of the various Pcl proteins and the pathways that they regulate are currently unknown (Carroll and O'Shea, 2002).

In mammalian cells, AMPK is also required for autophagy (Meley et al., 2006). During energy stress, AMP accumulation causes activation of the LKB1-AMPK pathway, which inhibits mTor by activating TSC1/TSC2 (Hoyer-Hansen and Jaattela, 2007). Furthermore, AMPK phosphorylates p27, a cylin-kinase inhibitor, thereby stabilizing p27, whereas ectopic expression of wild-type or a stabilized p27 mutant induces autophagy (Liang et al., 2007).

The Cvt Pathway and Other Selective Types of Autophagy

Although autophagy is generally considered as a nonselective pathway for the degradation of bulk cytoplasmic components, recent findings indicate that there exist many types of selective autophagy in both yeast and higher eukaryotes. In yeast, even bulk autophagy can be selective; cytosolic acetaldehyde dehydrogenase, Ald6, is preferentially sequestered into autophagosomes relative to other cytosolic proteins (Onodera and Ohsumi, 2004). Several organelles are selectively degraded through autophagy. For example, the selective degradation of mitochondria is termed mitophagy (Kim et al., 2007). This type of selective process is thought to play a crucial role in mitochondrial homeostasis, however, the mechanism underlying mitophagy remains unclear. The use of electron microscopy to observe mitochondrial degradation indicates that mitophagy occurs both selectively and nonselectively. A recent report demonstrates that mature ribosomes are rapidly degraded by autophagy in yeast, through a process termed ribophagy. This degradation involves a type of selective autophagy in that it specifically requires catalytic activity of the Ubp3/Bre5 ubiquitin protease (Kraft et al., 2008).

In fungi such as *Saccharomyces cerevisiae*, *Pichia pastoris*, *Hansenula polymorpha*, and *Yarrowia lipolytica*, peroxisomes are selectively engulfed and degraded through two morphologically distinct autophagic degradation processes, micro- and macropexophagy (Gunkel et al., 1999; Hutchins and Klionsky, 2001; Sakai et al., 2006; Tuttle et al., 1993; Veenhuis et al., 1983). When fungi grow on specific carbon sources, such as oleic acid or methanol, peroxisome proliferation is induced to adapt to the new physiological conditions that require peroxisome metabolism. When peroxisomes proliferation becomes unnecessary and peroxisomes become superfluous, as occurs after shifting to a preferred

carbon source such as glucose, peroxisomes are rapidly and specifically degraded. The two main modes of pexophagy, micro- and macropexophagy share most of the molecular components with non-specific autophagy. However, the presence of Pex14 at the peroxisomal membrane is necessary for the specific recognition of the organelle by the macropexophagy machinery (Bellu et al., 2001). A specificity factor, Atg11, which is required for the Cvt pathway, is also essential for the selective transport of peroxisomes to the vacuole (Kim et al., 2001). A recently identified pexophagy-specific protein, PpAtg30, functions as a peroxisome receptor through interactions with PpPex3, PpPex14, PpAtg11 and PpAtg17, to delivers peroxisomes to the site for pexophagosome formation (Farre et al., 2008). Furthermore, a fully functional actin cytoskeleton is required for selective autophagy, including the Cvt pathway and pexophagy, but not for nonselective autophagy (Reggiori et al., 2005a).

The Cvt pathway is a unique type of specific autophagy. The mechanism of the selective recognition and packaging of prApe1 has been relatively well clarified (Figure 1.4). The Ape1 protein is synthesized in the cytoplasm as a precursor form (prApe1) (Klionsky et al., 1992). After synthesis, prApe1 assembles into a dodecamer (Kim et al., 1997), which is further packaged into a larger oligomeric structure, called the Ape1 complex (Shintani et al., 2002). The prApe1 propeptide contains vacuolar targeting information (Martinez et al., 1997; Oda et al., 1996). In addition, the propeptide also mediates the interaction between prApe1 and its receptor protein, Atg19, to form the Cvt complex in the cytosol (Scott et al., 2001). Another Cvt cargo, Ams1, also binds Atg19 via a site that is distinct from the prApe1 binding site, and is concentrated at the Cvt complex (Shintani et al., 2002). The Cvt complex is subsequently enwrapped by a double membrane

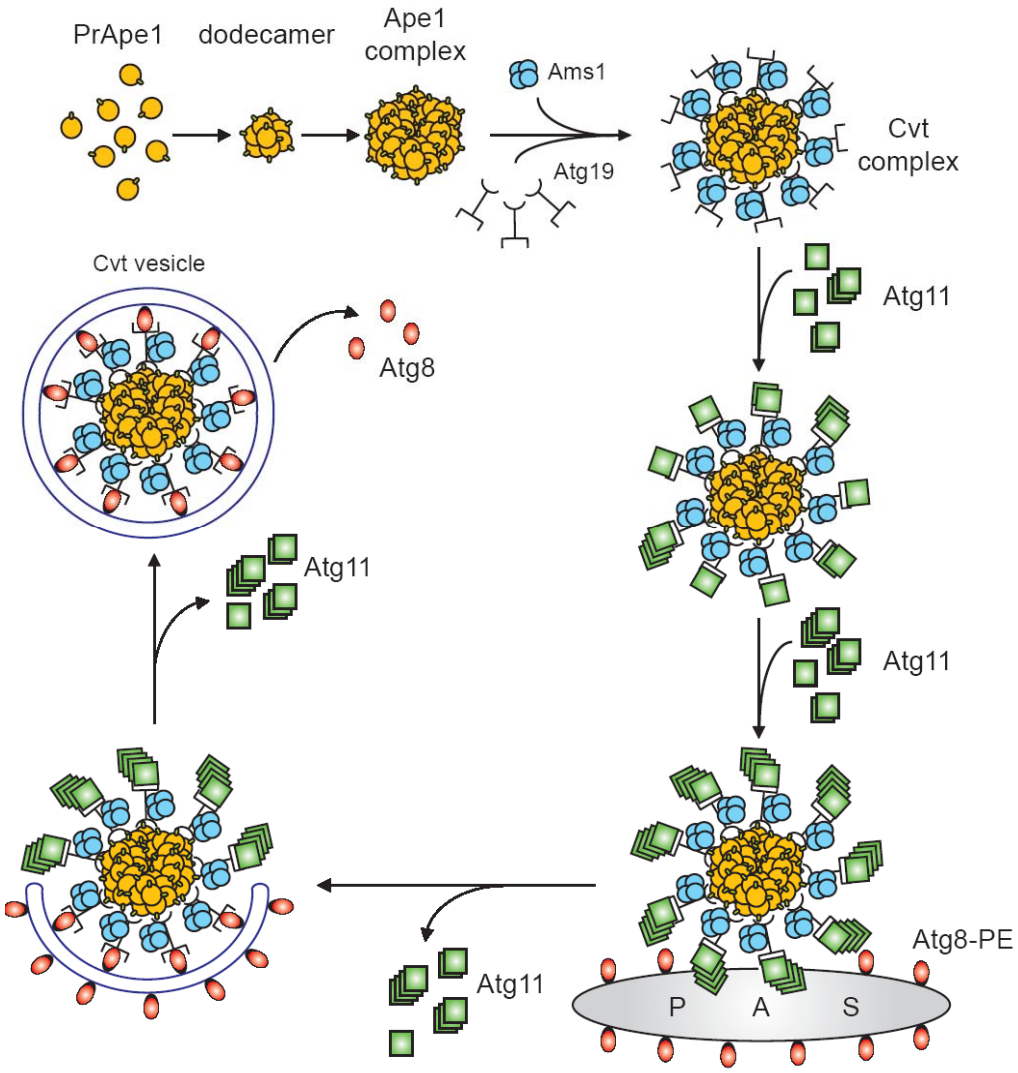

Figure 1.4. Temporal order of action of cargo recognition, packaging and sequestration in the Cvt pathway. A selective type of autophagy, the Cvt pathway, specifically transports the vacuolar hydrolases precursor Ape1 and Ams1 into the vacuole. Precursor Ape1 is synthesized in the cytosol, assembled into a dodecamer, and then further packaged into a larger oligomeric structure, called the Ape1 complex. Atg19 binds to the propeptide of prApe1 to form the Cvt complex in the cytosol; Ams1 is also incorporated into this complex via binding to Atg19. Atg11 subsequently associates with Atg19, acting as an adapter to bring the Cvt complex to the phagophore assembly site or PAS, a potential site for Cvt vesicle formation. The PAS may organize the formation of the sequestering vesicle, or it may literally become the sequestering vesicle as shown. Atg11 assembles with the Cvt

complex before targeting to the PAS, and it forms a homodimer or homo-oligomer at the PAS, although it is not clear whether this self-interaction occurs before or after the arrival at this site. Several Atg components, including Atg8, are recruited to the PAS independent of Atg11. Atg8 is conjugated into Atg8—PE for subsequent vesicle formation. Atg8—PE interacts with Atg19, and allows the correct incorporation of the Cvt complex into the forming vesicle. Atg19 is delivered into the vacuole together with the cargo proteins and degraded there. The scaffold protein Atg11, however, dissociates from the Cvt complex before vesicle completion, although the exact timing and mechanism of its release remain to be resolved. This figure is modified from Figure 3 of Yorimitsu and Klionsky (2005b).

that forms a Cvt vesicle. The Cvt complex can be also sequestered within autophagsomes, depending on the nutrient conditions (Baba et al., 1997), but this still occurs through a selective process that involves Atg19.

Atg11 subsequently associates with Atg19, acting like an adapter or tethering protein to bring the Cvt complex to the phagophore assembly site (PAS), a potential site for the formation of the Cvt vesicle and autophagosome. Several lines of evidence support the idea that Atg11 assembles with the Cvt complex before targeting to the PAS (Yorimitsu and Klionsky, 2005a). However, how Atg11 guides the Cvt complex to the PAS is still unclear. A C-terminal coiled-coil domain of Atg11 is critical for interaction with the C terminus of Atg19, whereas the N-terminal and/or central coiled-coil domains contain information necessary for the Cvt complex to be targeted to the PAS (Yorimitsu and Klionsky, 2005a). Besides Atg19, Atg11 has several other interacting partners, including Atg1, Atg9, Atg17, Atg20 and itself (Chang and Huang, 2007; He et al., 2006; Yorimitsu and Klionsky, 2005a). Atg9, the only characterized transmembrane protein that is required for sequestering vesicle formation, interacts with Atg11 independent of Atg1 or Atg19, suggesting that there are distinct and multiple populations of Atg11 within the cell. Atg11

homo-oligomerization may allow various Atg11 populations, along with its various interacting partners, to be delivered to the PAS (Yorimitsu and Klionsky, 2005a). A point mutation (H192L) in Atg9 disrupts the interaction with Atg11, preventing movement of Atg9 to the PAS and blocking the Cvt pathway, but not bulk autophagy (He et al., 2006), in agreement with the finding that Atg11 is not required for non-specific autophagy (Kim et al., 2001).

After the arrival of the Atg11-Atg19-cargo complex at the PAS, Atg19 interacts with Atg8—PE to allow the transfer of the Atg19-cargo complex to the forming Cvt vesicle (or autophagosome); interaction between these two proteins may ensure the incorporation of the Cvt complex into the Cvt vesicle (Shintani et al., 2002). Unlike most receptors that recycle between donor and acceptor membranes, Atg19 is delivered into the vacuole together with the cargo proteins and degraded there. The scaffold protein Atg11, however, does not appear to remain associated with the Cvt complex; rather it is thought to be released from Atg19 after delivery to the PAS and dissociate from the complex before vesicle formation (Kim et al., 2001). It remains unknown whether there is a role for Atg11 during the process of Cvt vesicle completion, and the exact timing and mechanism of its release remains to be resolved. However, disassembly of the homo-oligomerized Atg11 requires the Atg1-Atg13-Atg17 kinase complex (Yorimitsu and Klionsky, 2005a).

Increasing evidence indicates that selective autophagy also occurs in mammals. For example, the p62/SQSTM1/sequestosome protein preferentially recognizes polyubiquitinated protein aggregates and connects these with the autophagic machinery through interaction with the Atg8 mammalian homolog, LC3 (Bjorkoy et al., 2005; Komatsu et al., 2007b). Thus, p62 could function as a receptor protein similar to Atg19 to

link polyubiquitinated proteins to autophagosomes. Another recent example of selective autophagy is seen with the clearance of mitochondria and ribosomes during reticulocyte maturation (Kundu et al., 2008). In this case, Ulk1 plays a critical role in selective autophagy, but is not essential for the induction of starvation-induced bulk autophagy. Selectivity is also seen with the degradation of peroxisomes in mammalian cells (Iwata et al., 2006). Finally, some pathogens are selectively targeted by autophagy, such as *Mycobacterium tuberculosis* and *Streptococcus pyogenes* (Gutierrez et al., 2004; Nakagawa et al., 2004). It is important to note, however, that other microbes including bacteria and viruses regulate autophagy for their own survival (Nakagawa et al., 2004; Ogawa et al., 2005; Orvedahl and Levine, 2008). *Shigella*, an invasive bacteria, is able to escape autophagy by secreting IcsB on the bacterial surface. The IcsB protein interacts with VirG, which prevents the latter from binding Atg5 and triggering specific autophagic sequestration (Ogawa et al., 2005).

Phosphatidylinositol 3-kinase Complex

The class III phosphatidylinositol 3-kinase (PtdIns3K) is known to participate in various membrane trafficking events. Vps34 is the only PtdIns3K in yeast, and it forms at least two distinct complexes, complex I and II (Figure 1.5). Each complex contains three common components, Vps34, Vps15 and Vps30/Atg6 (Kihara et al., 2001). The function of Vps34 is dependent on a serine/threonine kinase, Vps15, which is required for Vps34 membrane association and activity (Stack et al., 1995). The role of Vps30/Atg6 within these PtdIns3K complexes is not well understood. These three common proteins are involved in both autophagy, the Cvt pathway and the sorting of carboxypeptidase Y (CPY), which is normally transported from the late Golgi to the vacuole through the CPY pathway. In addition, each complex contains another specific component, Atg14 (complex I) or Vps38 (complex II), which is thought to act as a connector between Vps30 and Vps15-Vps34. The region containing the coiled-coil domain I and II within N terminal half of Atg14 is responsible for the interaction between Vps34 and Vps30/Atg6. Loss of Atg14 disrupts complex I and causes a defect only in autophagy and the Cvt pathway, whereas Vps38 deletion disrupts complex II and blocks only the CPY pathway. The association of Atg14 or Vps38 confers functional specificity on the two PtdIns3K complexes by targeting Vps34 to distinct compartments, thus regulating different protein trafficking events. Vps15-Vps34 complexed with Vps30 and Atg14 localizes to the PAS, functioning in autophagy and the Cvt pathway; Vps15-Vps34 complexed with Vps30 and Vps38 localizes to endosomes, and functions in the CPY pathway (Obara et al., 2006).

PtdIns3K is a lipid kinase and the kinase activity of Vps34 is essential for autophagy and the Cvt pathway. One possible role of PtdIns3K is to produce PtdIns(3)P at the PAS to

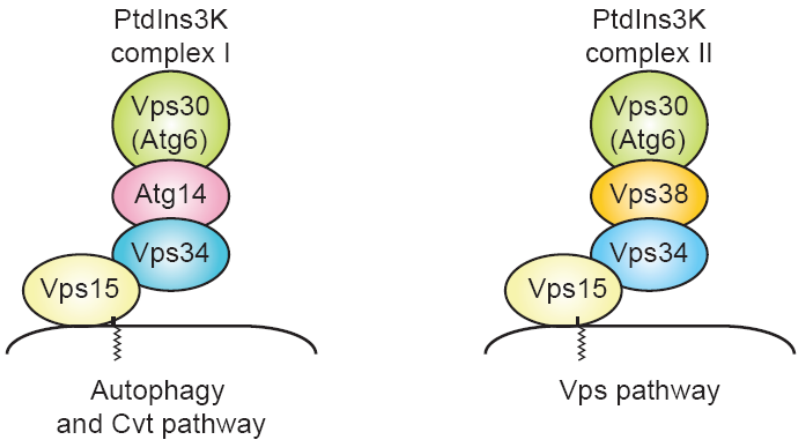

Figure 1.5. Two phosphatidylinositol 3-kinase (PtdIns3K) complexes in yeast. Each complex contains three common components, Vps15, Vps34 and Vps30/Atg6. Vps34 is the PtdIns3K enzyme, and Vps15 is thought to be a regulatory component; the function of Vps30/Atg6 is not known. In addition, each complex contains another specific component, Atg14 (complex I) or Vps38 (complex II), which is thought to act as a connector between Vps30 and Vps15-Vps34. Complex I functions in autophagy and the Cvt pathway, whereas complex II acts in the Vps pathway, including the CPY and MVB pathways. This figure is modified from Figure 5a of Yorimitsu and Klionsky (2005b).

recruit PtdIns(3)P-binding proteins, which in turn recruit additional downstream effectors to the PAS. PtdIns(3)P is bound by proteins that have specific binding sites, such as the PX (phox-homology) domain and the FYVE (for conserved in Fab1, YOTB, Vac1 and EEA1) zinc finger domain (Ellson et al., 2002; Stenmark et al., 2002). Two PX domain-containing proteins, Atg20 and Atg24, bind to PtdIns(3)P (Nice et al., 2002). These proteins are essential only for the Cvt pathway, not bulk autophagy. Their functional PX domains are necessary for membrane localization to the PAS and the endosome, which in turn depend on PtdIns3K complex I and complex II, respectively. The role of endosomal localization is unknown since the CPY pathway is normal in the absence of Atg20 or Atg24; however, the endosomal localization is not necessary for Cvt transport. Atg20 and Atg24 interact with

each other, and Atg24 and possibly Atg20 interact with Atg17 (Nice et al., 2002). In addition, Atg20 interacts with Atg11 (Yorimitsu and Klionsky, 2005a). Thus, the Atg20-Atg24 complex might be part of the Atg1 kinase complex. Atg18 and Atg21 are also PtdIns(3)P-binding proteins, although neither of them contain known phosphoinositide-binding domains. Both proteins are recruited to the PAS in a manner dependent on PtdIns3K complex I (Guan et al., 2001; Stromhaug et al., 2004). Atg18 is needed for the correct movement of Atg9, but the function of Atg21 is not known.

In contrast to yeast, there are two types of PtdIns3K in mammalian cells: class I and class III PtdIns3K. Mammalian class III PtdIns3K, hVps34—similar to yeast Vps34—generates PtdIns(3)P, and plays a stimulatory role in autophagy (Figure 3C). It forms a complex with its regulator, p150, the homologue of Vps15, and its accessory protein Beclin 1, the homolog of Vps30/Atg6 (Liang et al., 1999; Panaretou et al., 1997). Class I PtdIns3K uses PtdIns(4,5)P_2 as substrate to yield PtdIns(3,4,5)P_3. It functions at the plasma membrane, and acts through an insulin signaling cascade to activate mTOR and PKB, hence it has an inhibitory role on autophagy (Jacinto and Hall, 2003). A major pathway by which amino acids control mTor is not mediated through class I PtdIns3K, but instead through activation of the class III PtdIns3K, hVps34 (Nobukuni et al., 2005). Thus, hVps34 might also have an inhibitory effect on autophagy in mammalian cells. The specific function of PtdIns(3)P in mammalian cells has not yet been clarified, but it could function similar to that in yeast. Moreover, the effectors of PtdIns(3)P are also not clear. Atg20 and Atg24 do not have mammalian homologs. Atg18 has a human homolog and binds to PtdIns(3)P, but its role in autophagy has not yet been elucidated (Jeffries et al., 2004).

Two Ubiquitin-like Protein Conjugation Systems

There are two protein conjugation systems that function in selective and non-selective autophagy, and they include the ubiquitin-like proteins Atg12 and Atg8 (Figure 1.6) (Ohsumi, 2001). Both conjugation systems are evolutionarily conserved from yeast to humans. Although Atg12 and Atg8 do not have apparent sequence homology with ubiquitin, each of them contains a ubiquitin-fold at the C terminus, based on the crystal structures of Atg12 and Atg8 homologs from plants and mammals, respectively (Paz et al., 2000; Suzuki et al., 2005).

Atg12 is covalently attached to Atg5 through an isopeptide bond between a C-terminal glycine of Atg12 and an internal lysine residue of Atg5. The conjugation reaction is catalyzed by two additional proteins, Atg7 and Atg10 (Mizushima et al., 1998a). Atg7 is homologous to the E1 ubiquitin-activating enzyme, Uba1, in the ATP-binding region and the active cysteine residue, but not in terms of its overall structure (Tanida et al., 1999). Atg10 functions as an E2 ubiquitin-conjugating enzyme although Atg10 shows no homology to the E2 enzymes that participate in the ubiquitin system (Shintani et al., 1999). As occurs during ubiquitination, Atg7 hydrolyzes ATP resulting in the activation of Atg12 via the formation of a high-energy thioester bond between the C-terminal glycine of Atg12 and the active cysteine 507 of Atg7; subsequently, the activated Atg12 is directly transferred to the active cysteine 133 of Atg10 to form an Atg12-Atg10 thioester; finally, Atg12 is transferred to the target protein Atg5 to form the final conjugate. Atg5 is further bound noncovalently to another coiled-coil protein, Atg16, to form an Atg12—Atg5-Atg16 multimeric structure through homo-oligomerization of Atg16. This multimer has a molecular mass of approximately 350 kDa in yeast, which is predicted to

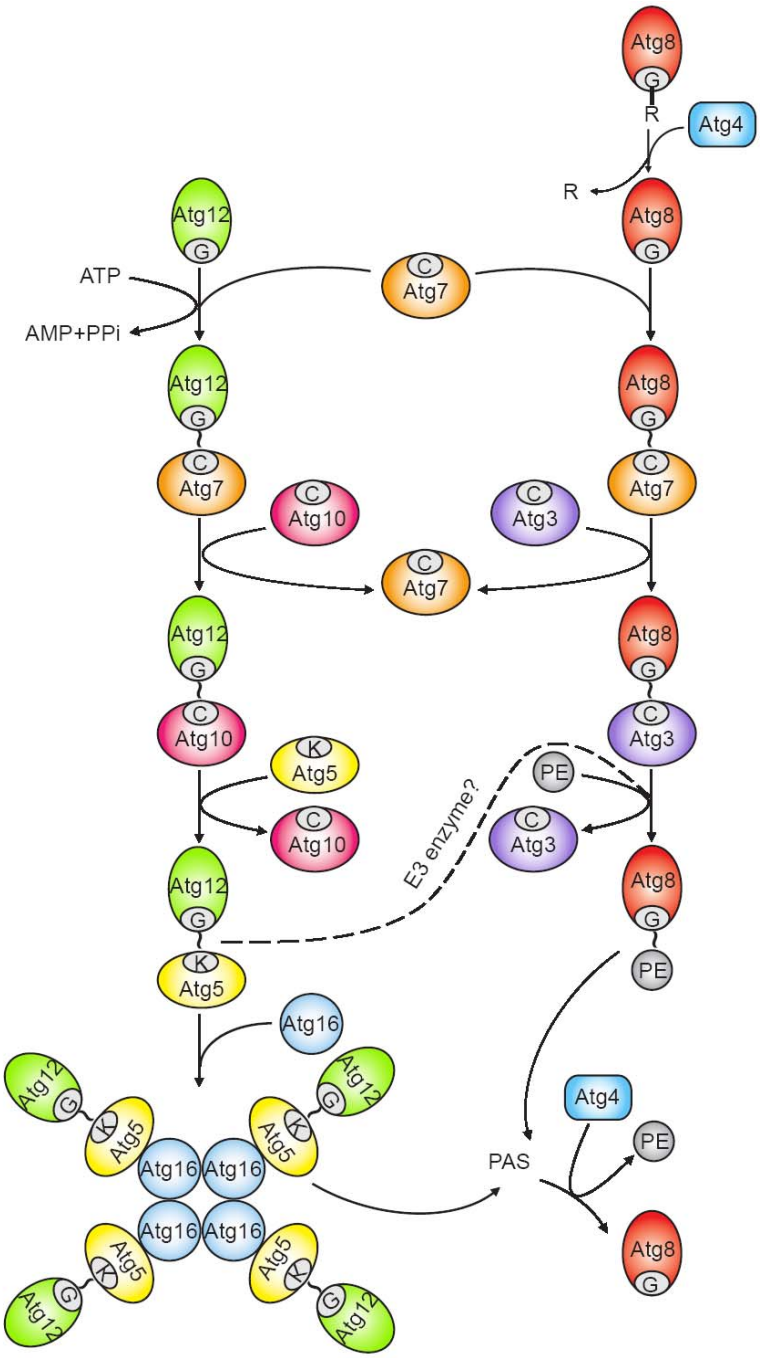

Figure 1.6. Two ubiquitin-like protein conjugation systems. The conjugation of Atg12 to Atg5 starts with activation by Atg7, which is homologous to the E1 ubiquitin-activating enzyme. Atg7 hydrolyzes ATP, resulting in the activation of Atg12 via the formation of a thioester bond between

the C-terminal glycine of Atg12 and the active site cysteine of Atg7; subsequently, the activated Atg12 is transferred to the active site cysteine of Atg10, an E2-like enzyme, which catalyzes the conjugation of Atg12 to Atg5 through the formation of an isopeptide bond between the activated glycine of Atg12 and an internal lysine residue of Atg5. Atg12—Atg5 is finally assembled with Atg16. Atg16 forms a tetramer to allow the formation of an Atg12—Atg5-Atg16 multimeric structure. The conjugation of Atg8—PE starts with the cleavage of the C-terminal arginine of Atg8 by the protease Atg4. The exposed glycine of Atg8 is then bound to the active site cysteine of the same E1-like enzyme, Atg7. The activated Atg8 is then transferred to another E2-like enzyme, Atg3. Eventually, Atg3 catalyzes the conjugation of Atg8 to form Atg8—PE. The Atg12—Atg5 conjugate might function as an E3, ubiquitin ligase-like enzyme, to promote Atg8—PE conjugation. Both the Atg12—Atg5-Atg16 complex and Atg8—PE localize to the PAS to facilitate vesicle formation. The Atg8—PE that resides on the outer face of the sequestering vesicle is released from the membrane by a second Atg4-dependent cleavage. This figure is modified from Figure 4 of Yorimitsu and Klionsky (2005b).

represent a tetramer of the Atg12—Atg5-Atg16 complex, which it is functionally essential for autophagy (Kuma et al., 2002). The Atg16 complex has recently been shown to specify the site of LC3 lipidation for membrane biogenesis in mammalian autophagy (Fujita et al., 2008).

A second ubiquitin-like protein, Atg8, is conjugated to a membrane lipid, phosphatidylethanolamine (PE) (Ichimura et al., 2000). The C-terminal arginine 117 residue of newly synthesized Atg8 is initially proteolytically cleaved by a cysteine protease, Atg4, exposing a glycine (Kirisako et al., 2000). The glycine is then bound to the active cysteine 507 of Atg7, the same E1-like enzyme used in the Atg12—Atg5 conjugation system. The activated Atg8 is then transferred to another E2-like enzyme, Atg3, at the active cysteine 234 residue via a thioester bond. The region around cysteine 234 of Atg3 shows partial homology to the corresponding region surrounding cysteine 133 of Atg10. Eventually, Atg8 is conjugated to PE through an amide bond between the C-terminal

glycine and the amino group of PE. Atg8—PE is tightly associated with membranes as an integral membrane protein. An *in vitro* reconstitution of the Atg8—PE conjugation process, using purified Atg7, Atg3 and Atg8ΔR (Atg8 lacking the last arginine residue), demonstrates that Atg7 and Atg3 are minimal catalysts (Ichimura et al., 2004). Unlike the Atg12—Atg5 conjugate, Atg8—PE conjugation is a reversible process in which Atg4 liberates Atg8 from its target lipid. The liberated Atg8 is recycled and used in another conjugation reaction to allow efficient progression of autophagy and the Cvt pathway (Kirisako et al., 2000).

Both the Atg12 and Atg8 conjugation systems are evolutionarily conserved. The mammalian homologs for each component of the yeast Atg12—Atg5 conjugation systems (Atg5, Atg7, Atg10 and Atg12) have been characterized, and they function in a similar manner as their counterparts in yeast (Mizushima et al., 1998b; Mizushima et al., 2002; Tanida et al., 1999). There is also a mammalian Atg16-like protein, Atg16L, which forms an approximately 800 kDa protein complex with the Atg12—Atg5 conjugate, again mediated by the homo-oligomerization of Atg16L (Mizushima et al., 2003). There are at least four mammalian Atg8 homologs, MAP1LC3, GATE16, GABARAP and Atg8L. All proteins possess a conserved glycine residue near their C terminus, and are conjugated to PE in the same manner as occurs in yeast via the catalysts Atg4, Atg7 and Atg3 (Hemelaar et al., 2003; Kabeya et al., 2000; Kabeya et al., 2004; Tanida et al., 2003; Tanida et al., 2006; Tanida et al., 2002). Among them, LC3 is most abundant in autophagosomal membranes and is well established as a marker to monitor the autophagosome and autophagic activity.

During autophagosome formation, both the Atg12—Atg5-Atg16 complex and the Atg8—PE conjugate localize at the PAS (Kim et al., 2002; Suzuki et al., 2001). Electron

microscopy analysis clearly shows that these two conjugates decorate the expanding phagophore (Kabeya et al., 2000; Kirisako et al., 1999; Mizushima et al., 2003; Mizushima et al., 2001). The Atg12—Atg5-Atg16 complex is mainly localized on the outer side of the phagophore and released into the cytosol before or after autophagosome completion. These observations suggest that the Atg12—Atg5-Atg16 complex might serve as a coat component to drive the expansion and/or curvature of the membrane leaflet during autophagosome formation. Recent data, however, indicate that the Atg12—Atg5 conjugate might function as an E3, ubiquitin ligase, for Atg8—PE conjugation (Figure 1.6), although it is not essential for the latter process to occur (Hanada et al., 2007). In contrast, Atg8—PE displays an apparently symmetrical distribution on both sides of the phagophore. The Atg8—PE that resides on the surface that becomes the outer face of the sequestering vesicle is released from the membrane by a second Atg4-dependent cleavage, whereas the inner population remains inside the vesicle and is delivered into the vacuole/lysosome where it is degraded (Huang et al., 2000; Kabeya et al., 2000; Kirisako et al., 1999). Accordingly, Atg8—PE is another scaffold candidate to drive membrane expansion and vesicle completion. Upon autophagy induction, Atg8 protein levels increase and this is needed to accommodate the larger-sized autophagosome relative to the Cvt vesicle. A quantitative correlation between the amount of Atg8 and the size of the sequestering vesicle has recently been determined (Xie et al., 2008). Atg8 is also suggested to act during the expansion of the autophagosomal membrane by mediating membrane tethering and hemifusion (Nakatogawa et al., 2007), although the physiological significance of this activity is not yet known.

Atg9 and Its Cycling Systems

One of the intriguing questions concerning autophagy is the source of the lipid that is used for autophagosome formation and the mechanism used for lipid movement to the site of autophagosome assembly. Atg9 is an integral membrane protein and is thought to be a "membrane carrier" during the assembly process (He et al., 2006; Noda et al., 2000). Unlike most other Atg proteins, which display primarily a single punctate localization at the PAS, Atg9 localizes to multiple punctate structures, including the PAS (Reggiori et al., 2005b; Reggiori et al., 2004a). The cycling of Atg9 between the PAS and the non-PAS punctate structures is essential for autophagosome formation. Potentially, membrane could be delivered to the PAS through this shuttling process. In yeast, several Atg9 non-PAS puncta are found to localize adjacent to or at the surface of mitochondria (Reggiori et al., 2005b). It is still unclear, however, whether Atg9 is an integral component of the mitochondrial outer membrane or the membrane component of an organelle or other structure associated with mitochondria. Moreover, a population of the Atg9 peripheral pool does not co-localize with either the PAS or mitochondria, but rather is dispersed throughout the cytosol. This portion of Atg9 is thought to be associated with membranes in the process of trafficking between the PAS and the membrane donor sites.

The anterograde movement of Atg9 to the PAS involves several Atg proteins (Figure 1.7). In the absence of Atg11, the transport of Atg9 to the PAS is blocked (He et al., 2006; Shintani and Klionsky, 2004b). The efficient anterograde movement of Atg9 to the PAS also involves Atg23 and Atg27, which form a cycling unit with Atg9 (Legakis et al., 2007; Yen et al., 2007). Atg23 is a peripheral membrane protein, whereas Atg27 is a type I transmembrane protein. Both of these proteins are required for the Cvt pathway and

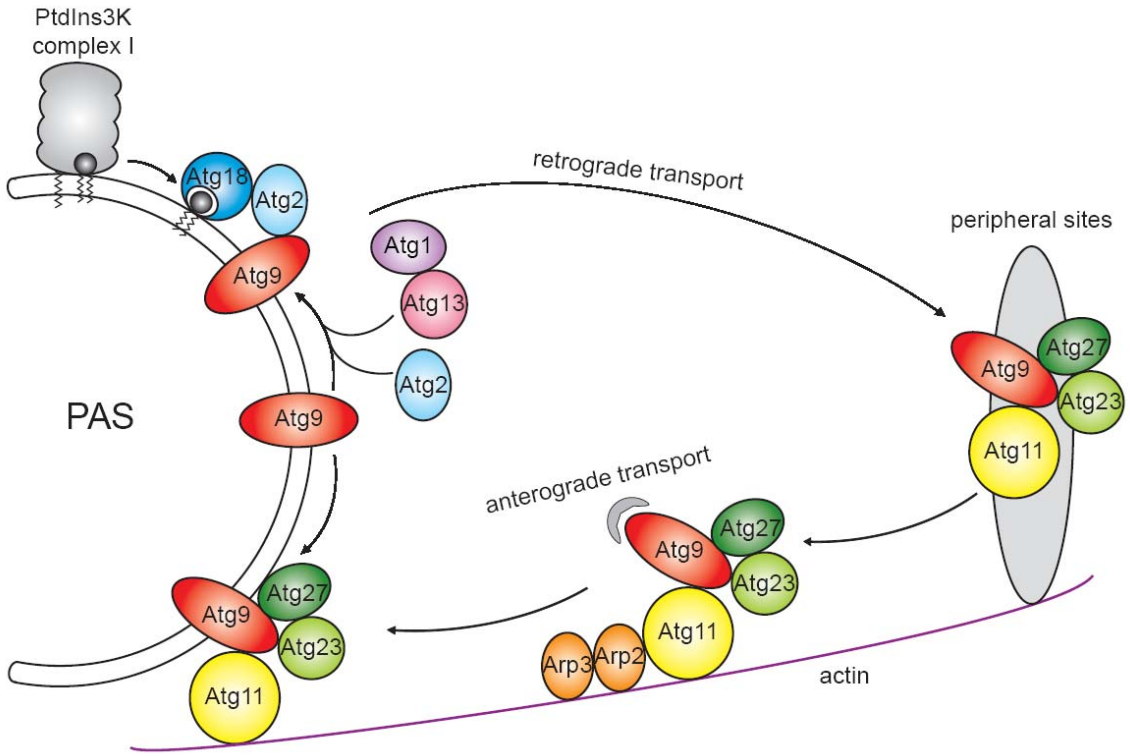

Figure 1.7. Cycling of Atg9. In yeast, Atg9 cycles between the PAS and non-PAS punctate structures (peripheral sites), some of which are found to localize adjacent to or at the surface of mitochondria. The efficient anterograde movement of Atg9 to the PAS requires Atg11, Atg23, Atg27, and the actin cytoskeletion. Atg9, Atg23 and Atg27 are in a heterotrimeric complex, and their movement to the PAS is interdependent. Atg11 acts as a potential adaptor between Atg9 and actin, and between Atg9 and the Arp2/3 complex, while the latter may provide the force to push the cargo (Atg9 and its associated membrane) away from the peripheral sites and toward the PAS. The retrograde transport of Atg9 from the PAS back to the peripheral sites depends on the Atg1—Atg13 kinase complex, Atg2, Atg18 and the PtdIns3K complex I. The Atg1—Atg13 complex promotes the association of Atg2 and the PtdIns(3)P binding protein Atg18 with Atg9, and the formation of this ternary complex initiates Atg9 retrieval for another round of membrane delivery.

efficient autophagy. Similar to Atg9, they localize to the PAS and several other punctate structures. Current evidence suggests that Atg9, Atg23 and Atg27 are in a heterotrimeric complex, and travel together to the PAS. Based on fluorescence microscopy, the antergrade transport of these three proteins is found to be largely interdependent. In the absence of Atg23 or Atg27, Atg9 is at multiple punctate sites other than the PAS, whereas Atg23 is dispersed throughout the cytosol without either Atg9 or Atg27.

The actin cytoskeleton also participates in Atg9 anterograde movement (He et al., 2006). Disruption of the actin cytoskeleton prevents correct targeting of Atg9 to the PAS. Moreover, an actin-related protein, Arp2, interacts with Atg9 and directly regulates the dynamics of Atg9 PAS targeting (Monastyrska et al., 2008). Arp2 is one subunit of the Arp2/3 complex, the nucleation factor of branched actin filaments. Thus, one model is that Atg11 acts as an adaptor between the cargo (Atg9 and actin), while the Arp2/3 complex provides the force to push the cargo (Atg9 and its associated membrane) away from the membrane donor and toward the forming autophagosome (He et al., 2006; Monastyrska et al., 2008; Monastyrska et al., 2006).

The retrieval of Atg9 from the PAS back to the peripheral, non-PAS sites depends on the Atg1-Atg13 kinase complex, Atg2, Atg18 and the PtdIns3K complex I (Figure 1.7); the absence of any of these proteins results in the accumulation of Atg9 at the PAS (Reggiori et al., 2004a). Similarly, the retrieval of Atg23 and Atg27 requires the Atg1-Atg13 complex; however, only Atg23 retrieval needs a high level of Atg1 kinase activity (Legakis et al., 2007; Yen et al., 2007). Atg2 and Atg18 are two interacting peripheral membrane proteins (Suzuki et al., 2007). They can both interact with Atg9, and the interaction of Atg18 with Atg9 requires Atg2 and Atg1 (Reggiori et al., 2004a; Wang et al., 2001a). The PAS

localization of Atg2 and Atg18 depends on each other, Atg1, Atg13, Atg9 and the PtdIns3K complex I. Atg18 can bind two phosphoinositides, PtdIns(3)P and PtdIns(3,5)P_2, but only the former is essential for autophagy (Stromhaug et al., 2004). One model is that once the Atg1-Atg13 complex and Atg9 are recruited to the PAS separately, Atg1-Atg13 promotes Atg9 interaction with Atg2 and Atg18, and the formation of this ternary complex allows Atg9 to be released for another round of membrane delivery (Reggiori et al., 2004a).

Recent studies on mammalian Atg9 (mAtg9) have revealed that mAtg9 resides in a juxtanuclear region corresponding to the *trans*-Golgi network (TGN) and late endosomes (Young et al., 2006). Starvation triggers the distribution of mAtg9 from the TGN to a dispersed peripheral endosomal pool, and knockdown of Ulk1, the mammalian ortholog of Atg1, restricts mAtg9 to the TGN. These observations lead to the idea that mAtg9 traffics between the TGN and late endosomes, and that, potentially, membranes are delivered from the TGN to the forming autophagosomes.

de novo Vesicle Formation

Unlike most other intracellular trafficking processes, autophagy undergoes *de novo* formation of double-membrane vesicles. This is a *de novo* process in that the sequestering vesicles do not bud from a pre-existing organelle. Instead, these vesicles are thought to form by expansion of a membrane core of unknown origin, termed the phagophore (Mizushima et al., 2001; Noda et al., 2002; Seglen et al., 1990). Figure 1.8 shows a hypothetical model for *de novo* vesicle formation. The proposed site for vesicle formation is the phagophore assembly site (Kim et al., 2002; Suzuki et al., 2001). In yeast, the PAS is a perivacuolar site and is defined in part as the site where almost all of the Atg proteins reside, at least transiently (Suzuki et al., 2001). The PAS can be also defined as a hybrid of the phagophore and its associated Atg proteins (Xie and Klionsky, 2007). In mammalian cells, colocalization of the Atg proteins has also been observed, although a comprehensive study has been lacking (Yamada et al., 2005; Young et al., 2006). In these observations, cells lack a single specialized site for autophagosome formation that is similar to the yeast PAS, and instead display multiple sites of Atg protein colocalization, possibly corresponding to multiple PAS.

Understanding the nature of the PAS is a key to studying this novel type of membrane-forming process. However, the PAS is poorly characterized. Although the role of the PAS is not fully understood, one model suggests that the PAS serves to facilitate the nucleation and/or expansion of the phagophore, the precursor of the autophagosome, through recruitment of Atg proteins (Mizushima et al., 2001; Suzuki et al., 2007). In addition, membrane has to be delivered to the phagophore; although the origin of this membrane is also not clear, it appears to include the early secretory pathway and, in yeast,

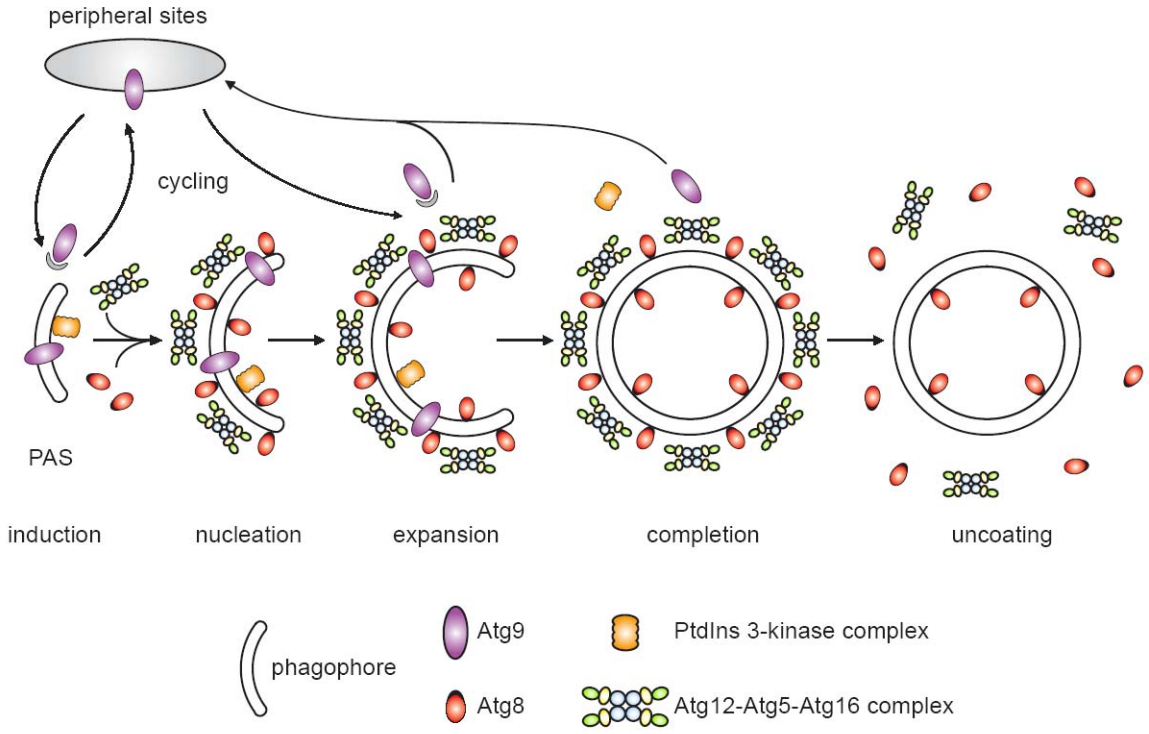

Figure 1.8. Schematic depiction of double-membrane vesicle formation. The PAS serves to facilitate the nucleation and/or expansion of the phagophore, the precursor of the autophagosome, through recruitment of Atg proteins. Atg9 and the PtdIns3K complex I are recruited relatively early to the PAS, and act in membrane nucleation. Atg9 cycles between peripheral sites and the PAS; potentially, Atg9 cycling delivers lipids to the expanding membrane. The Atg12—Atg5-Atg16 complex and the Atg8—PE conjugate, components of the vesicle-forming machinery, are subsequently recruited to the PAS, and mediate the expansion of the sequestering vesicle. The Atg12—Atg5-Atg16 complex may in part behave like a coat or may function as an E3 ubiquitin ligase-like enzyme, whereas Atg8—PE acts in the elongation of the vesicle as a structural component. Before or immediately after the autophagosome is completed, most of the Atg components, including the putative coat proteins, dissociate from the vesicle; the portion of Atg8—PE on the outer surface of the vesicle is normally cleaved off by the Atg4 protease. Finally, the sequestering vesicle can fuse with the vacuole.

the mitochondria (Reggiori et al., 2005b; Reggiori et al., 2004b).

A recent systematic analysis demonstrated that the Atg proteins depend on each other for PAS recruitment (Cheong et al., 2008; Kawamata et al., 2008; Suzuki et al., 2007). In particular, Atg11 and Atg17 act as scaffold proteins for PAS assembly, meaning they may be the initial factors responsible for subsequent recruitment of the remaining Atg proteins. Atg11 is essential for PAS organization under vegetative conditions, whereas Atg17 (and associated proteins) plays a critical role during starvation. In cells lacking both Atg11 and Atg17, there is a complete absence of PAS localization of other Atg proteins. Starvation-induced PAS assembly, however, requires more than Atg17. In addition to the Atg1—Atg13—Atg17 ternary complex, Atg17 also interacts with two autophagy-specific proteins, Atg29 and Atg31 (Kawamata et al., 2008). Cells lacking Atg11 and any of the components in the Atg17 complex display essentially the same phenotype as the *atg11*Δ *atg17*Δ double mutant, suggesting these two complexes function as a PAS-organization center to induce the ordered recruitment of Atg proteins (Cheong et al., 2008; Kawamata et al., 2008). Although Atg1 kinase activity is not essential for PAS recruitment of other Atg proteins, it might play a role in disassembly of the PAS or the dissociation of Atg proteins from the PAS. A dynamic process of Atg protein cycling is thought to be critical for proper autophagosome expansion (Cheong et al., 2008). This concept fits with the idea that Atg1 kinase activity is related to the size of the sequestering vesicle (Noda et al., 2002).

Among the remaining Atg proteins, Atg9 is recruited relatively early to the PAS, and this also requires the function of the PtdIns3K complex I. Atg9 and the PtdIns3K complex I may play some role in membrane nucleation and facilitating the subsequent recruitment

of certain Atg components, including the Atg12—Atg5-Atg16 complex and the Atg8—PE conjugate. In their absence, these two conjugates can be formed, but they become completely diffuse in the cytosol without any punctate localization. The PAS localization of Atg8—PE depends on the Atg12—Atg5-Atg16 complex (Suzuki et al., 2001).

As mentioned above, before or immediately after the autophagosome is completed, most of the Atg components dissociate from the vesicle. The sequestering vesicle must be completed before fusion with the vacuole. The Atg12—Atg5-Atg16 complex may in part behave like a coat to prevent premature fusion; the portion of Atg8—PE on the outer surface of the vesicle might also play such a role. Atg8—PE is normally cleaved off by the Atg4 protease prior to vesicle fusion. Furthermore, there may be certain unknown factors that can sense the completion of the double-membrane vesicle and trigger the disassembly of the vesicle-forming machinery. Atg1 is one possible candidate, because it functions at later stages in the vesicle-forming process, such as Atg9 retrieval and Atg11 release from the PAS, and its kinase activity has been also suggested to play a role in the disassembly of the PAS or the dissociation of Atg proteins from the PAS (Cheong et al., 2008; Reggiori et al., 2004a; Yorimitsu and Klionsky, 2005a).

Vesicle Docking and Fusion with the Vacuole

Once the double-membrane vesicle is formed, it is targeted to the vacuole for the fusion process. Molecular genetic studies have indicated that the machinery involved in homotypic vacuole fusion is also essential for the fusion of autophagosomes and Cvt vesicles with the vacuole (Figure 1.9). This machinery includes the SNARE proteins Vam3, Vam7, Vti1 and Ykt6, the NSF Sec18, the α-SNAP Sec17, the Rab GTPase Ypt7 and the class C Vps/HOPS complex; the two recently characterized proteins, Mon1 and Ccz1, are also part of the fusion machinery (Klionsky, 2005; Wang and Klionsky, 2003). Mon1 and Ccz1 form a complex, and are critical for the Ypt7-dependent tethering/docking stage leading to the subsequent formation of the SNARE complex (Wang et al., 2003). The class C Vps/HOPS complex functions in concert with Ypt7 during the tethering/docking stage (Wang and Klionsky, 2003). After fusion, the autophagosome inner single-membrane vesicle is released inside the vacuole lumen, which is termed the autophagic body.

In mammalian cells, maturation of autophagosomes includes several fusion events with vesicles originating from early and late endosomes, as well as lysosomes. Fusion with endosomes to become amphisomes allows convergence of the endocytic and autophagic pathways; subsequent fusion of autophagosomes or amphisomes with lysosomes generates autolysosomes (Berg et al., 1998; Tooze et al., 1990). In some cases where it is not possible to distinguish the precise nature of the compartment, the term “autophagic vacuoles” is used to cover all three autophagic structures: autophagosomes, amphisomes and autolysosomes. Mammalian Vtilb is involved in the fusion of autophagsomes with multivesicular endosomes (Atlashkin et al., 2003), and the Rab GTPase Rab7 plays a role in the fusion with lysosomes (Jager et al., 2004).

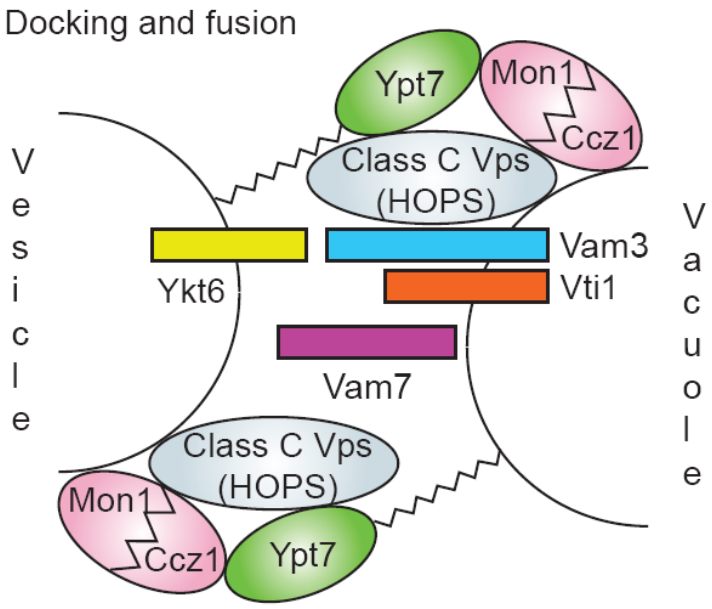

Figure 1.9. Vesicle docking and fusion with the vacuole. The SNARE proteins Vam3, Vam7, Vti1 and Ykt6, function in various membrane fusion events, including the process of autophagosome fusion with the vacuole. Also shown is the Mon1—Ccz1 complex and the class C Vps/HPOS complex, which function in concert at the Ypt7-dependent tethering/docking stage. This figure is modified from Figure 7 of Klionsky (2005).

Vesicle Breakdown and Recycling of the Resulting Macromolecules

Upon release into the vacuole, the single-membrane subvacuolar vesicle, the autophagic or Cvt body, is broken down inside the vacuolar lumen. This process depends on proper vacuole function (including vacuolar acidification) and the activity of vacuolar resident hydrolases (including Pep4 and Prb1). In addition to these factors, Atg15, a putative lipase, is also implicated at this step and seems likely to function directly in the intravacuolar lysis of the autophagic/Cvt body (Epple et al., 2001; Teter et al., 2001). Atg15 contains a lipase active-site motif, and mutations in the corresponding active site eliminate its function. Atg15 is targeted to the vacuolar lumen via the multivesicular body (MVB) pathway (Epple et al., 2003). Atg15 seems to function as a general lipase because it is also involved in the disintegration of intravacuolar MVB vesicles.

The main purpose of autophagy is to degrade cytoplasm and recycle the resulting macromolecules for the synthesis of essential components to overcome various stress conditions. Accordingly, the resulting macromolecules must be released back to the cytosol for reuse; however, little is known about this process. Atg22, a putative amino acid effluxer on the vacuolar membrane, has been found to play such role in mediating the efflux of leucine, and other amino acids resulting from autophagic degradation (Yang et al., 2006). In addition, Avt3 and Avt4 seem to be part of the same family of permeases (Russnak et al., 2001). Upon elimination of all three partially redundant vacuolar effluxers, cells rapidly lose viability under starvation conditions, whereas supplementation with leucine partially restores viability. Although a mammalian homolog of Atg22 has not been identified, homologs of Avt3 and Avt4 have been characterized as SLC36A1/LYAAT-1 (lysosomal amino acid transporter 1) (Sagne et al., 2001), and SLC36A4/LYAAT-2,

respectively. How autophagy contributes to the recycling of other macromolecules, such as carbonhydrate or lipids, remains unknown.

Conclusion

As a conserved cellular degradative pathway in eukaryotes, autophagy protects cells during various types of stress. Defects in autophagy have been linked to human diseases, indicating its crucial physiological significance. Autophagy involves dynamic membrane rearrangement for sequestration of cytoplasm and its delivery into the vacuole/lysosome. Significant breakthroughs in understanding the molecular mechanism of autophagy have been achieved from studies in yeast and other model systems. Currently, analyses of autophagy, pexophagy and the Cvt pathway in fungi have identified 31 *ATG* genes, corresponding to the unique molecular machinery that drives these pathways. However, the fundamental biochemical questions that concern the functions of Atg proteins still need to be resolved, especially those related to sequestering vesicle formation, such as the ordered vesicle assembly process and the origin of the lipid membrane. In addition, as more examples of selective types of autophagy emerge, continued studies on the specific nature of autophagy are becoming increasingly important. Yeast remains a powerful system to address these questions. Further studies of autophagy-related pathways will facilitate our understanding of the molecular mechanism and regulation of these pathways, and may allow the practical use of autophagy for therapeutic purposes.

References

Abeliovich, H., Zhang, C., Dunn, W.A., Jr., Shokat, K.M., and Klionsky, D.J. (2003). Chemical genetic analysis of Apg1 reveals a non-kinase role in the induction of autophagy. Mol Biol Cell *14*, 477-490.

Arico, S., Petiot, A., Bauvy, C., Dubbelhuis, P.F., Meijer, A.J., Codogno, P., and Ogier-Denis, E. (2001). The tumor suppressor PTEN positively regulates macroautophagy by inhibiting the phosphatidylinositol 3-kinase/protein kinase B pathway. J Biol Chem *276*, 35243-35246.

Atlashkin, V., Kreykenbohm, V., Eskelinen, E.L., Wenzel, D., Fayyazi, A., and Fischer von Mollard, G. (2003). Deletion of the SNARE vti1b in mice results in the loss of a single SNARE partner, syntaxin 8. Mol Cell Biol *23*, 5198-5207.

Baba, M., Osumi, M., Scott, S.V., Klionsky, D.J., and Ohsumi, Y. (1997). Two distinct pathways for targeting proteins from the cytoplasm to the vacuole/lysosome. J Cell Biol *139*, 1687-1695.

Bellu, A.R., Komori, M., van der Klei, I.J., Kiel, J.A., and Veenhuis, M. (2001). Peroxisome biogenesis and selective degradation converge at Pex14p. J Biol Chem *276*, 44570-44574.

Berg, T.O., Fengsrud, M., Stromhaug, P.E., Berg, T., and Seglen, P.O. (1998). Isolation and characterization of rat liver amphisomes. Evidence for fusion of autophagosomes with both early and late endosomes. J Biol Chem *273*, 21883-21892.

Bjørkøy, G., Lamark, T., Brech, A., Outzen, H., Perander, M., Overvatn, A., Stenmark, H., and Johansen, T. (2005). p62/SQSTM1 forms protein aggregates degraded by autophagy and has a protective effect on huntingtin-induced cell death. J Cell Biol *171*, 603-614.

Budovskaya, Y.V., Stephan, J.S., Deminoff, S.J., and Herman, P.K. (2005). An evolutionary proteomics approach identifies substrates of the cAMP-dependent protein kinase. Proc Natl Acad Sci U S A *102*, 13933-13938.

Budovskaya, Y.V., Stephan, J.S., Reggiori, F., Klionsky, D.J., and Herman, P.K. (2004). The Ras/cAMP-dependent protein kinase signaling pathway regulates an early step of the autophagy process in *Saccharomyces cerevisiae*. J Biol Chem *279*, 20663-20671.

Carrera, A.C. (2004). TOR signaling in mammals. J Cell Sci *117*, 4615-4616.

Carroll, A.S., and O'Shea, E.K. (2002). Pho85 and signaling environmental conditions. Trends Biochem Sci *27*, 87-93.

Chan, E.Y.W., Kir, S., and Tooze, S.A. (2007). siRNA screening of the kinome identifies ULK1 as a multidomain modulator of autophagy. J Biol Chem *282*, 25464-25474.

Chang, C.Y., and Huang, W.-P. (2007). Atg19 mediates a dual interaction cargo sorting mechanism in selective autophagy. Mol Biol Cell *18*, 919-929.

Cheong, H., Nair, U., Geng, J., and Klionsky, D.J. (2008). The Atg1 Kinase Complex Is Involved in the Regulation of Protein Recruitment to Initiate Sequestering Vesicle Formation for Nonspecific Autophagy in *Saccharomyces cerevisiae*. Mol Biol Cell *19*, 668-681.

De Virgilio, C., and Loewith, R. (2006). Cell growth control: little eukaryotes make big contributions. Oncogene *25*, 6392-6415.

Ellson, C.D., Andrews, S., Stephens, L.R., and Hawkins, P.T. (2002). The PX domain: a new phosphoinositide-binding module. J Cell Sci *115*, 1099-1105.

Epple, U.D., Eskelinen, E.L., and Thumm, M. (2003). Intravacuolar membrane lysis in *Saccharomyces cerevisiae*. Does vacuolar targeting of Cvt17/Aut5p affect its function? J Biol Chem *278*, 7810-7821.

Epple, U.D., Suriapranata, I., Eskelinen, E.L., and Thumm, M. (2001). Aut5/Cvt17p, a putative lipase essential for disintegration of autophagic bodies inside the vacuole. J Bacteriol *183*, 5942-5955.

Farre, J.C., Manjithaya, R., Mathewson, R.D., and Subramani, S. (2008). PpAtg30 tags peroxisomes for turnover by selective autophagy. Dev Cell *14*, 365-376.

Fujita, N., Itoh, T., Omori, H., Fukuda, M., Noda, T., and Yoshimori, T. (2008). The Atg16L complex specifies the site of LC3 lipidation for membrane biogenesis in autophagy. Mol Biol Cell *19*, 2092-2100.

Furuta, S., Hidaka, E., Ogata, A., Yokota, S., and Kamata, T. (2004). Ras is involved in the negative control of autophagy through the class I PI3-kinase. Oncogene *23*, 3898-3904.

Guan, J., Stromhaug, P.E., George, M.D., Habibzadegah-Tari, P., Bevan, A., Dunn, W.A., Jr., and Klionsky, D.J. (2001). Cvt18/Gsa12 is required for cytoplasm-to-vacuole transport, pexophagy, and autophagy in *Saccharomyces cerevisiae* and *Pichia pastoris*. Mol Biol Cell *12*, 3821-3838.

Gunkel, K., van der Klei, I.J., Barth, G., and Veenhuis, M. (1999). Selective peroxisome degradation in *Yarrowia lipolytica* after a shift of cells from acetate/oleate/ethylamine into glucose/ammonium sulfate-containing media. FEBS Lett *451*, 1-4.

Gutierrez, M.G., Master, S.S., Singh, S.B., Taylor, G.A., Colombo, M.I., and Deretic, V. (2004). Autophagy is a defense mechanism inhibiting BCG and *Mycobacterium tuberculosis* survival in infected macrophages. Cell *119*, 753-766.

Hanada, T., Noda, N.N., Satomi, Y., Ichimura, Y., Fujioka, Y., Takao, T., Inagaki, F., and Ohsumi, Y. (2007). The Atg12−Atg5 conjugate has a novel E3-like activity for protein lipidation in autophagy. J Biol Chem *282*, 37298-37302.

Hanaoka, H., Noda, T., Shirano, Y., Kato, T., Hayashi, H., Shibata, D., Tabata, S., and Ohsumi, Y. (2002). Leaf senescence and starvation-induced chlorosis are accelerated by the disruption of an Arabidopsis autophagy gene. Plant Physiol *129*, 1181-1193.

Hara, T., Takamura, A., Kishi, C., Iemura, S., Natsume, T., Guan, J.L., and Mizushima, N. (2008). FIP200, a ULK-interacting protein, is required for autophagosome formation in mammalian cells. J Cell Biol *181*, 497-510.

He, C., Song, H., Yorimitsu, T., Monastyrska, I., Yen, W.-L., Legakis, J.E., and Klionsky, D.J. (2006). Recruitment of Atg9 to the preautophagosomal structure by Atg11 is essential for selective autophagy in budding yeast. J Cell Biol *175*, 925-935.

Hemelaar, J., Lelyveld, V.S., Kessler, B.M., and Ploegh, H.L. (2003). A single protease, Apg4B, is specific for the autophagy-related ubiquitin-like proteins GATE-16, MAP1-LC3, GABARAP, and Apg8L. J Biol Chem *278*, 51841-51850.

Hinnebusch, A.G. (2005). Translational regulation of *GCN4* and the general amino acid control of yeast. Annu Rev Microbiol *59*, 407-450.

Høyer-Hansen, M., and Jaattela, M. (2007). AMP-activated protein kinase: a universal regulator of autophagy? Autophagy *3*, 381-383.

Huang, J., and Klionsky, D.J. (2007). Autophagy and human disease. Cell Cycle *6*, 1837-1849.

Huang, W.-P., Scott, S.V., Kim, J., and Klionsky, D.J. (2000). The itinerary of a vesicle component, Aut7p/Cvt5p, terminates in the yeast vacuole via the autophagy/Cvt pathways. J Biol Chem *275*, 5845-5851.

Hutchins, M.U., and Klionsky, D.J. (2001). Vacuolar localization of oligomeric alpha-mannosidase requires the cytoplasm to vacuole targeting and autophagy pathway components in *Saccharomyces cerevisiae*. J Biol Chem *276*, 20491-20498.

Hutchins, M.U., Veenhuis, M., and Klionsky, D.J. (1999). Peroxisome degradation in *Saccharomyces cerevisiae* is dependent on machinery of macroautophagy and the Cvt pathway. J Cell Sci *112 (Pt 22)*, 4079-4087.

Ichimura, Y., Imamura, Y., Emoto, K., Umeda, M., Noda, T., and Ohsumi, Y. (2004). In vivo and in vitro reconstitution of Atg8 conjugation essential for autophagy. J Biol

Chem *279*, 40584-40592.

Ichimura, Y., Kirisako, T., Takao, T., Satomi, Y., Shimonishi, Y., Ishihara, N., Mizushima, N., Tanida, I., Kominami, E., Ohsumi, M., Noda, T., Ohsumi, Y. (2000). A ubiquitin-like system mediates protein lipidation. Nature *408*, 488-492.

Iwata, J., Ezaki, J., Komatsu, M., Yokota, S., Ueno, T., Tanida, I., Chiba, T., Tanaka, K., and Kominami, E. (2006). Excess peroxisomes are degraded by autophagic machinery in mammals. J Biol Chem *281*, 4035-4041.

Jacinto, E., and Hall, M.N. (2003). Tor signalling in bugs, brain and brawn. Nat Rev Mol Cell Biol *4*, 117-126.

Jager, S., Bucci, C., Tanida, I., Ueno, T., Kominami, E., Saftig, P., and Eskelinen, E.L. (2004). Role for Rab7 in maturation of late autophagic vacuoles. J Cell Sci *117*, 4837-4848.

Jeffries, T.R., Dove, S.K., Michell, R.H., and Parker, P.J. (2004). PtdIns-specific MPR pathway association of a novel WD40 repeat protein, WIPI49. Mol Biol Cell *15*, 2652-2663.

Kabeya, Y., Kamada, Y., Baba, M., Takikawa, H., Sasaki, M., and Ohsumi, Y. (2005). Atg17 functions in cooperation with Atg1 and Atg13 in yeast autophagy. Mol Biol Cell *16*, 2544-2553.

Kabeya, Y., Mizushima, N., Ueno, T., Yamamoto, A., Kirisako, T., Noda, T., Kominami, E., Ohsumi, Y., and Yoshimori, T. (2000). LC3, a mammalian homologue of yeast Apg8p, is localized in autophagosome membranes after processing. EMBO J *19*, 5720-5728.

Kabeya, Y., Mizushima, N., Yamamoto, A., Oshitani-Okamoto, S., Ohsumi, Y., and Yoshimori, T. (2004). LC3, GABARAP and GATE16 localize to autophagosomal membrane depending on form-II formation. J Cell Sci *117*, 2805-2812.

Kamada, Y., Funakoshi, T., Shintani, T., Nagano, K., Ohsumi, M., and Ohsumi, Y. (2000). Tor-mediated induction of autophagy via an Apg1 protein kinase complex. J Cell Biol *150*, 1507-1513.

Kawamata, T., Kamada, Y., Kabeya, Y., Sekito, T., and Ohsumi, Y. (2008). Organization of the Pre-Autophagosomal Structure Responsible for Autophagosome Formation. Mol Biol Cell.

Kihara, A., Noda, T., Ishihara, N., and Ohsumi, Y. (2001). Two distinct Vps34 phosphatidylinositol 3-kinase complexes function in autophagy and carboxypeptidase Y sorting in *Saccharomyces cerevisiae*. J Cell Biol *152*, 519-530.

Kim, I., Rodriguez-Enriquez, S., and Lemasters, J.J. (2007). Selective degradation of mitochondria by mitophagy. Arch Biochem Biophys *462*, 245-253.

Kim, J., Huang, W.-P., Stromhaug, P.E., and Klionsky, D.J. (2002). Convergence of multiple autophagy and cytoplasm to vacuole targeting components to a perivacuolar membrane compartment prior to *de novo* vesicle formation. J Biol Chem *277*, 763-773.

Kim, J., Kamada, Y., Stromhaug, P.E., Guan, J., Hefner-Gravink, A., Baba, M., Scott, S.V., Ohsumi, Y., Dunn, W.A., Jr., and Klionsky, D.J. (2001). Cvt9/Gsa9 functions in sequestering selective cytosolic cargo destined for the vacuole. J Cell Biol *153*, 381-396.

Kim, J., Scott, S.V., Oda, M.N., and Klionsky, D.J. (1997). Transport of a large oligomeric protein by the cytoplasm to vacuole protein targeting pathway. J Cell Biol *137*, 609-618.

Kirisako, T., Baba, M., Ishihara, N., Miyazawa, K., Ohsumi, M., Yoshimori, T., Noda, T., and Ohsumi, Y. (1999). Formation process of autophagosome is traced with Apg8/Aut7p in yeast. J Cell Biol *147*, 435-446.

Kirisako, T., Ichimura, Y., Okada, H., Kabeya, Y., Mizushima, N., Yoshimori, T., Ohsumi, M., Takao, T., Noda, T., and Ohsumi, Y. (2000). The reversible modification regulates the membrane-binding state of Apg8/Aut7 essential for autophagy and the cytoplasm to vacuole targeting pathway. J Cell Biol *151*, 263-276.

Klionsky, D.J. (2005). The molecular machinery of autophagy: unanswered questions. J Cell Sci *118*, 7-18.

Klionsky, D.J., Cregg, J.M., Dunn, W.A., Jr., Emr, S.D., Sakai, Y., Sandoval, I.V., Sibirny, A., Subramani, S., Thumm, M., Veenhuis, M., and Ohsumi, Y. (2003). A unified nomenclature for yeast autophagy-related genes. Dev Cell *5*, 539-545.

Klionsky, D.J., Cueva, R., and Yaver, D.S. (1992). Aminopeptidase I of *Saccharomyces cerevisiae* is localized to the vacuole independent of the secretory pathway. J Cell Biol *119*, 287-299.

Komatsu, M., Ueno, T., Waguri, S., Uchiyama, Y., Kominami, E., and Tanaka, K. (2007a). Constitutive autophagy: vital role in clearance of unfavorable proteins in neurons. Cell Death Differ *14*, 887-894.

Komatsu, M., Waguri, S., Koike, M., Sou, Y.S., Ueno, T., Hara, T., Mizushima, N., Iwata, J., Ezaki, J., Murata, S., Hamazaki, J., Nishito, Y., Iemura, S., Natsume, T., Yanagawa, T., Uwayama, J., Warabi, E., Yoshida, H., Ishii, T., Kobayashi, A., Yamamoto, M., Yue, Z., Uchiyama, Y., Kominami, E., Tanaka, K. (2007b). Homeostatic levels of p62 control cytoplasmic inclusion body formation in autophagy-deficient mice. Cell *131*, 1149-1163.

Kraft, C., Deplazes, A., Sohrmann, M., and Peter, M. (2008). Mature ribosomes are selectively degraded upon starvation by an autophagy pathway requiring the Ubp3p/Bre5p

ubiquitin protease. Nat Cell Biol *10*, 602-610.

Kubota, H., Obata, T., Ota, K., Sasaki, T., and Ito, T. (2003). Rapamycin-induced translational derepression of GCN4 mRNA involves a novel mechanism for activation of the eIF2α kinase GCN2. J Biol Chem *278*, 20457-20460.

Kuma, A., Hatano, M., Matsui, M., Yamamoto, A., Nakaya, H., Yoshimori, T., Ohsumi, Y., Tokuhisa, T., and Mizushima, N. (2004). The role of autophagy during the early neonatal starvation period. Nature *432*, 1032-1036.

Kuma, A., Mizushima, N., Ishihara, N., and Ohsumi, Y. (2002). Formation of the approximately 350-kDa Apg12−Apg5·Apg16 multimeric complex, mediated by Apg16 oligomerization, is essential for autophagy in yeast. J Biol Chem *277*, 18619-18625.

Kundu, M., Lindsten, T., Yang, C.Y., Wu, J., Zhao, F., Zhang, J., Selak, M.A., Ney, P.A., and Thompson, C.B. (2008). Ulk1 plays a critical role in the autophagic clearance of mitochondria and ribosomes during reticulocyte maturation. Blood *112*, 1493-1502.

Legakis, J.E., Yen, W.-L., and Klionsky, D.J. (2007). A cycling protein complex required for selective autophagy. Autophagy *3*, 422-432.

Levine, B., and Deretic, V. (2007). Unveiling the roles of autophagy in innate and adaptive immunity. Nat Rev Immunol *7*, 767-777.

Levine, B., and Klionsky, D.J. (2004). Development by self-digestion: molecular mechanisms and biological functions of autophagy. Dev Cell *6*, 463-477.

Levine, B., and Yuan, J. (2005). Autophagy in cell death: an innocent convict? J Clin Invest *115*, 2679-2688.

Liang, J., Shao, S.H., Xu, Z.X., Hennessy, B., Ding, Z., Larrea, M., Kondo, S., Dumont, D.J., Gutterman, J.U., Walker, C.L.*, et al.* (2007). The energy sensing LKB1-AMPK pathway regulates p27(kip1) phosphorylation mediating the decision to enter autophagy or apoptosis. Nat Cell Biol *9*, 218-224.

Liang, X.H., Jackson, S., Seaman, M., Brown, K., Kempkes, B., Hibshoosh, H., and Levine, B. (1999). Induction of autophagy and inhibition of tumorigenesis by *beclin 1*. Nature *402*, 672-676.

Loewith, R., Jacinto, E., Wullschleger, S., Lorberg, A., Crespo, J.L., Bonenfant, D., Oppliger, W., Jenoe, P., and Hall, M.N. (2002). Two TOR complexes, only one of which is rapamycin sensitive, have distinct roles in cell growth control. Mol Cell *10*, 457-468.

Martinez, E., Jimenez, M.A., Segui-Real, B., Vandekerckhove, J., and Sandoval, I.V. (1997). Folding of the presequence of yeast pAPI into an amphipathic helix determines transport of the protein from the cytosol to the vacuole. J Mol Biol *267*, 1124-1138.

Massey, A., Kiffin, R., and Cuervo, A.M. (2004). Pathophysiology of

chaperone-mediated autophagy. Int J Biochem Cell Biol *36*, 2420-2434.

Matsuura, A., Tsukada, M., Wada, Y., and Ohsumi, Y. (1997). Apg1p, a novel protein kinase required for the autophagic process in *Saccharomyces cerevisiae*. Gene *192*, 245-250.

Mavrakis, M., Lippincott-Schwartz, J., Stratakis, C.A., and Bossis, I. (2006). Depletion of type IA regulatory subunit (RIα) of protein kinase A (PKA) in mammalian cells and tissues activates mTOR and causes autophagic deficiency. Hum Mol Genet *15*, 2962-2971.

Meijer, A.J., and Codogno, P. (2006). Signalling and autophagy regulation in health, aging and disease. Mol Aspects Med *27*, 411-425.

Meléndez, A., Talloczy, Z., Seaman, M., Eskelinen, E.L., Hall, D.H., and Levine, B. (2003). Autophagy genes are essential for dauer development and life-span extension in C. elegans. Science *301*, 1387-1391.

Meley, D., Bauvy, C., Houben-Weerts, J.H., Dubbelhuis, P.F., Helmond, M.T., Codogno, P., and Meijer, A.J. (2006). AMP-activated protein kinase and the regulation of autophagic proteolysis. J Biol Chem *281*, 34870-34879.

Mizushima, N., Kuma, A., Kobayashi, Y., Yamamoto, A., Matsubae, M., Takao, T., Natsume, T., Ohsumi, Y., and Yoshimori, T. (2003). Mouse Apg16L, a novel WD-repeat protein, targets to the autophagic isolation membrane with the Apg12-Apg5 conjugate. J Cell Sci *116*, 1679-1688.

Mizushima, N., Levine, B., Cuervo, A.M., and Klionsky, D.J. (2008). Autophagy fights disease through cellular self-digestion. Nature *451*, 1069-1075.

Mizushima, N., Noda, T., Yoshimori, T., Tanaka, Y., Ishii, T., George, M.D., Klionsky, D.J., Ohsumi, M., and Ohsumi, Y. (1998a). A protein conjugation system essential for autophagy. Nature *395*, 395-398.

Mizushima, N., Sugita, H., Yoshimori, T., and Ohsumi, Y. (1998b). A new protein conjugation system in human. The counterpart of the yeast Apg12p conjugation system essential for autophagy. J Biol Chem *273*, 33889-33892.

Mizushima, N., Yamamoto, A., Hatano, M., Kobayashi, Y., Kabeya, Y., Suzuki, K., Tokuhisa, T., Ohsumi, Y., and Yoshimori, T. (2001). Dissection of autophagosome formation using Apg5-deficient mouse embryonic stem cells. J Cell Biol *152*, 657-668.

Mizushima, N., Yoshimori, T., and Ohsumi, Y. (2002). Mouse Apg10 as an Apg12-conjugating enzyme: analysis by the conjugation-mediated yeast two-hybrid method. FEBS Lett *532*, 450-454.

Monastyrska, I., He, C., Geng, J., Hoppe, A.D., Li, Z., and Klionsky, D.J. (2008).

Arp2 links Autophagic Machinery with the Actin Cytoskeleton. Mol Biol Cell.

Monastyrska, I., Shintani, T., Klionsky, D.J., and Reggiori, F. (2006). Atg11 directs autophagosome cargoes to the PAS along actin cables. Autophagy *2*, 119-121.

Nair, U., and Klionsky, D.J. (2005). Molecular mechanisms and regulation of specific and nonspecific autophagy pathways in yeast. J Biol Chem *280*, 41785-41788.

Nakagawa, I., Amano, A., Mizushima, N., Yamamoto, A., Yamaguchi, H., Kamimoto, T., Nara, A., Funao, J., Nakata, M., Tsuda, K.*, et al.* (2004). Autophagy defends cells against invading group A *Streptococcus*. Science *306*, 1037-1040.

Nakatogawa, H., Ichimura, Y., and Ohsumi, Y. (2007). Atg8, a ubiquitin-like protein required for autophagosome formation, mediates membrane tethering and hemifusion. Cell *130*, 165-178.

Nice, D.C., Sato, T.K., Stromhaug, P.E., Emr, S.D., and Klionsky, D.J. (2002). Cooperative binding of the cytoplasm to vacuole targeting pathway proteins, Cvt13 and Cvt20, to phosphatidylinositol 3-phosphate at the pre-autophagosomal structure is required for selective autophagy. J Biol Chem *277*, 30198-30207.

Nobukuni, T., Joaquin, M., Roccio, M., Dann, S.G., Kim, S.Y., Gulati, P., Byfield, M.P., Backer, J.M., Natt, F., Bos, J.L.*, et al.* (2005). Amino acids mediate mTOR/raptor signaling through activation of class 3 phosphatidylinositol 3OH-kinase. Proc Natl Acad Sci U S A *102*, 14238-14243.

Noda, T., Kim, J., Huang, W.P., Baba, M., Tokunaga, C., Ohsumi, Y., and Klionsky, D.J. (2000). Apg9p/Cvt7p is an integral membrane protein required for transport vesicle formation in the Cvt and autophagy pathways. J Cell Biol *148*, 465-480.

Noda, T., and Ohsumi, Y. (1998). Tor, a phosphatidylinositol kinase homologue, controls autophagy in yeast. J Biol Chem *273*, 3963-3966.

Noda, T., Suzuki, K., and Ohsumi, Y. (2002). Yeast autophagosomes: de novo formation of a membrane structure. Trends Cell Biol *12*, 231-235.

Obara, K., Sekito, T., and Ohsumi, Y. (2006). Assortment of phosphatidylinositol 3-kinase complexes--Atg14p directs association of complex I to the pre-autophagosomal structure in *Saccharomyces cerevisiae*. Mol Biol Cell *17*, 1527-1539.

Oda, M.N., Scott, S.V., Hefner-Gravink, A., Caffarelli, A.D., and Klionsky, D.J. (1996). Identification of a cytoplasm to vacuole targeting determinant in aminopeptidase I. J Cell Biol *132*, 999-1010.

Ogawa, M., Yoshimori, T., Suzuki, T., Sagara, H., Mizushima, N., and Sasakawa, C. (2005). Escape of intracellular Shigella from autophagy. Science *307*, 727-731.

Ohsumi, Y. (2001). Molecular dissection of autophagy: two ubiquitin-like systems.

Nat Rev Mol Cell Biol *2*, 211-216.

Onodera, J., and Ohsumi, Y. (2004). Ald6p is a preferred target for autophagy in yeast, *Saccharomyces cerevisiae*. J Biol Chem *279*, 16071-16076.

Orvedahl, A., and Levine, B. (2008). Viral evasion of autophagy. Autophagy *4*, 280-285.

Otto, G.P., Wu, M.Y., Kazgan, N., Anderson, O.R., and Kessin, R.H. (2004). Dictyostelium macroautophagy mutants vary in the severity of their developmental defects. J Biol Chem *279*, 15621-15629.

Panaretou, C., Domin, J., Cockcroft, S., and Waterfield, M.D. (1997). Characterization of p150, an adaptor protein for the human phosphatidylinositol (PtdIns) 3-kinase. Substrate presentation by phosphatidylinositol transfer protein to the p150·Ptdins 3-kinase complex. J Biol Chem *272*, 2477-2485.

Paz, Y., Elazar, Z., and Fass, D. (2000). Structure of GATE-16, membrane transport modulator and mammalian ortholog of autophagocytosis factor Aut7p. J Biol Chem *275*, 25445-25450.

Reggiori, F., and Klionsky, D.J. (2002). Autophagy in the eukaryotic cell. Eukaryot Cell *1*, 11-21.

Reggiori, F., Monastyrska, I., Shintani, T., and Klionsky, D.J. (2005a). The actin cytoskeleton is required for selective types of autophagy, but not nonspecific autophagy, in the yeast *Saccharomyces cerevisiae*. Mol Biol Cell *16*, 5843-5856.

Reggiori, F., Shintani, T., Nair, U., and Klionsky, D.J. (2005b). Atg9 cycles between mitochondria and the pre-autophagosomal structure in yeasts. Autophagy *1*, 101-109.

Reggiori, F., Tucker, K.A., Stromhaug, P.E., and Klionsky, D.J. (2004a). The Atg1-Atg13 complex regulates Atg9 and Atg23 retrieval transport from the pre-autophagosomal structure. Dev Cell *6*, 79-90.

Reggiori, F., Wang, C.-W., Nair, U., Shintani, T., Abeliovich, H., and Klionsky, D.J. (2004b). Early stages of the secretory pathway, but not endosomes, are required for Cvt vesicle and autophagosome assembly in *Saccharomyces cerevisiae*. Mol Biol Cell *15*, 2189-2204.

Russnak, R., Konczal, D., and McIntire, S.L. (2001). A family of yeast proteins mediating bidirectional vacuolar amino acid transport. J Biol Chem *276*, 23849-23857.

Sagne, C., Agulhon, C., Ravassard, P., Darmon, M., Hamon, M., El Mestikawy, S., Gasnier, B., and Giros, B. (2001). Identification and characterization of a lysosomal transporter for small neutral amino acids. Proc Natl Acad Sci U S A *98*, 7206-7211.

Sakai, Y., Oku, M., van der Klei, I.J., and Kiel, J.A. (2006). Pexophagy: autophagic

degradation of peroxisomes. Biochim Biophys Acta *1763*, 1767-1775.

Schmelzle, T., Beck, T., Martin, D.E., and Hall, M.N. (2004). Activation of the RAS/cyclic AMP pathway suppresses a TOR deficiency in yeast. Mol Cell Biol *24*, 338-351.

Scott, R.C., Juhasz, G., and Neufeld, T.P. (2007). Direct induction of autophagy by Atg1 inhibits cell growth and induces apoptotic cell death. Curr Biol *17*, 1-11.

Scott, R.C., Schuldiner, O., and Neufeld, T.P. (2004). Role and regulation of starvation-induced autophagy in the Drosophila fat body. Dev Cell *7*, 167-178.

Scott, S.V., Baba, M., Ohsumi, Y., and Klionsky, D.J. (1997). Aminopeptidase I is targeted to the vacuole by a nonclassical vesicular mechanism. J Cell Biol *138*, 37-44.

Scott, S.V., Guan, J., Hutchins, M.U., Kim, J., and Klionsky, D.J. (2001). Cvt19 is a receptor for the cytoplasm-to-vacuole targeting pathway. Mol Cell *7*, 1131-1141.

Seglen, P.O., Gordon, P.B., and Holen, I. (1990). Non-selective autophagy. Semin Cell Biol *1*, 441-448.

Shintani, T., Huang, W.-P., Stromhaug, P.E., and Klionsky, D.J. (2002). Mechanism of cargo selection in the cytoplasm to vacuole targeting pathway. Dev Cell *3*, 825-837.

Shintani, T., and Klionsky, D.J. (2004a). Autophagy in health and disease: a double-edged sword. Science *306*, 990-995.

Shintani, T., and Klionsky, D.J. (2004b). Cargo proteins facilitate the formation of transport vesicles in the cytoplasm to vacuole targeting pathway. J Biol Chem *279*, 29889-29894.

Shintani, T., Mizushima, N., Ogawa, Y., Matsuura, A., Noda, T., and Ohsumi, Y. (1999). Apg10p, a novel protein-conjugating enzyme essential for autophagy in yeast. EMBO J *18*, 5234-5241.

Stack, J.H., DeWald, D.B., Takegawa, K., and Emr, S.D. (1995). Vesicle-mediated protein transport: regulatory interactions between the Vps15 protein kinase and the Vps34 PtdIns 3-kinase essential for protein sorting to the vacuole in yeast. J Cell Biol *129*, 321-334.

Stenmark, H., Aasland, R., and Driscoll, P.C. (2002). The phosphatidylinositol 3-phosphate-binding FYVE finger. FEBS Lett *513*, 77-84.

Stromhaug, P.E., Reggiori, F., Guan, J., Wang, C.-W., and Klionsky, D.J. (2004). Atg21 is a phosphoinositide binding protein required for efficient lipidation and localization of Atg8 during uptake of aminopeptidase I by selective autophagy. Mol Biol Cell *15*, 3553-3566.

Suzuki, K., Kirisako, T., Kamada, Y., Mizushima, N., Noda, T., and Ohsumi, Y.

(2001). The pre-autophagosomal structure organized by concerted functions of APG genes is essential for autophagosome formation. EMBO J *20*, 5971-5981.

Suzuki, K., Kubota, Y., Sekito, T., and Ohsumi, Y. (2007). Hierarchy of Atg proteins in pre-autophagosomal structure organization. Genes Cells *12*, 209-218.

Suzuki, N.N., Yoshimoto, K., Fujioka, Y., Ohsumi, Y., and Inagaki, F. (2005). The crystal structure of plant ATG12 and its biological implication in autophagy. Autophagy *1*, 119-126.

Tallóczy, Z., Jiang, W., Virgin, H.W.t., Leib, D.A., Scheuner, D., Kaufman, R.J., Eskelinen, E.L., and Levine, B. (2002). Regulation of starvation- and virus-induced autophagy by the eIF2alpha kinase signaling pathway. Proc Natl Acad Sci U S A *99*, 190-195.

Tanida, I., Komatsu, M., Ueno, T., and Kominami, E. (2003). GATE-16 and GABARAP are authentic modifiers mediated by Apg7 and Apg3. Biochem Biophys Res Commun *300*, 637-644.

Tanida, I., Mizushima, N., Kiyooka, M., Ohsumi, M., Ueno, T., Ohsumi, Y., and Kominami, E. (1999). Apg7p/Cvt2p: A novel protein-activating enzyme essential for autophagy. Mol Biol Cell *10*, 1367-1379.

Tanida, I., Sou, Y.S., Minematsu-Ikeguchi, N., Ueno, T., and Kominami, E. (2006). Atg8L/Apg8L is the fourth mammalian modifier of mammalian Atg8 conjugation mediated by human Atg4B, Atg7 and Atg3. FEBS J *273*, 2553-2562.

Tanida, I., Tanida-Miyake, E., Komatsu, M., Ueno, T., and Kominami, E. (2002). Human Apg3p/Aut1p homologue is an authentic E2 enzyme for multiple substrates, GATE-16, GABARAP, and MAP-LC3, and facilitates the conjugation of hApg12p to hApg5p. J Biol Chem *277*, 13739-13744.

Teter, S.A., Eggerton, K.P., Scott, S.V., Kim, J., Fischer, A.M., and Klionsky, D.J. (2001). Degradation of lipid vesicles in the yeast vacuole requires function of Cvt17, a putative lipase. J Biol Chem *276*, 2083-2087.

Thevelein, J.M., and de Winde, J.H. (1999). Novel sensing mechanisms and targets for the cAMP-protein kinase A pathway in the yeast *Saccharomyces cerevisiae*. Mol Microbiol *33*, 904-918.

Tooze, J., Hollinshead, M., Ludwig, T., Howell, K., Hoflack, B., and Kern, H. (1990). In exocrine pancreas, the basolateral endocytic pathway converges with the autophagic pathway immediately after the early endosome. J Cell Biol *111*, 329-345.

Tuttle, D.L., Lewin, A.S., and Dunn, W.A., Jr. (1993). Selective autophagy of peroxisomes in methylotrophic yeasts. Eur J Cell Biol *60*, 283-290.

Urban, J., Soulard, A., Huber, A., Lippman, S., Mukhopadhyay, D., Deloche, O., Wanke, V., Anrather, D., Ammerer, G., Riezman, H*., et al.* (2007). Sch9 is a major target of TORC1 in *Saccharomyces cerevisiae*. Mol Cell *26*, 663-674.

Veenhuis, M., Douma, A., Harder, W., and Osumi, M. (1983). Degradation and turnover of peroxisomes in the yeast Hansenula polymorpha induced by selective inactivation of peroxisomal enzymes. Arch Microbiol *134*, 193-203.

Wang, C.-W., Kim, J., Huang, W.P., Abeliovich, H., Stromhaug, P.E., Dunn, W.A., Jr., and Klionsky, D.J. (2001a). Apg2 is a novel protein required for the cytoplasm to vacuole targeting, autophagy, and pexophagy pathways. J Biol Chem *276*, 30442-30451.

Wang, C.-W., and Klionsky, D.J. (2003). The molecular mechanism of autophagy. Mol Med *9*, 65-76.

Wang, C.-W., Stromhaug, P.E., Kauffman, E.J., Weisman, L.S., and Klionsky, D.J. (2003). Yeast homotypic vacuole fusion requires the Ccz1-Mon1 complex during the tethering/docking stage. J Cell Biol *163*, 973-985.

Wang, Z., Wilson, W.A., Fujino, M.A., and Roach, P.J. (2001b). Antagonistic controls of autophagy and glycogen accumulation by Snf1p, the yeast homolog of AMP-activated protein kinase, and the cyclin-dependent kinase Pho85p. Mol Cell Biol *21*, 5742-5752.

Xie, Z., and Klionsky, D.J. (2007). Autophagosome formation: core machinery and adaptations. Nat Cell Biol *9*, 1102-1109.

Xie, Z., Nair, U., and Klionsky, D.J. (2008). Atg8 controls phagophore expansion during autophagosome formation. Mol Biol Cell *19*, 3290-3298.

Yamada, T., Carson, A.R., Caniggia, I., Umebayashi, K., Yoshimori, T., Nakabayashi, K., and Scherer, S.W. (2005). Endothelial nitric-oxide synthase antisense (NOS3AS) gene encodes an autophagy-related protein (APG9-like2) highly expressed in trophoblast. J Biol Chem *280*, 18283-18290.

Yan, J., Kuroyanagi, H., Kuroiwa, A., Matsuda, Y., Tokumitsu, H., Tomoda, T., Shirasawa, T., and Muramatsu, M. (1998). Identification of mouse ULK1, a novel protein kinase structurally related to *C. elegans* UNC-51. Biochem Biophys Res Commun *246*, 222-227.

Yan, J., Kuroyanagi, H., Tomemori, T., Okazaki, N., Asato, K., Matsuda, Y., Suzuki, Y., Ohshima, Y., Mitani, S., Masuho, Y*., et al.* (1999). Mouse ULK2, a novel member of the UNC-51-like protein kinases: unique features of functional domains. Oncogene *18*, 5850-5859.

Yang, Z., Huang, J., Geng, J., Nair, U., and Klionsky, D.J. (2006). Atg22 recycles amino acids to link the degradative and recycling functions of autophagy. Mol Biol Cell *17*,

5094-5104.

Yen, W.-L., Legakis, J.E., Nair, U., and Klionsky, D.J. (2007). Atg27 is required for autophagy-dependent cycling of Atg9. Mol Biol Cell *18*, 581-593.

Yorimitsu, T., He, C., Wang, K., and Klionsky, D.J. (2009). Tap42-associated protein phosphatase type 2A negatively regulates induction of autophagy. Autophagy *5*.

Yorimitsu, T., and Klionsky, D.J. (2005a). Atg11 links cargo to the vesicle-forming machinery in the cytoplasm to vacuole targeting pathway. Mol Biol Cell *16*, 1593-1605.

Yorimitsu, T., and Klionsky, D.J. (2005b). Autophagy: molecular machinery for self-eating. Cell Death Differ *12 Suppl 2*, 1542-1552.

Yorimitsu, T., Zaman, S., Broach, J.R., and Klionsky, D.J. (2007). Protein kinase A and Sch9 cooperatively regulate induction of autophagy in *Saccharomyces cerevisiae*. Mol Biol Cell *18*, 4180-4189.

Young, A.R.J., Chan, E.Y.W., Hu, X.W., Köchl, R., Crawshaw, S.G., High, S., Hailey, D.W., Lippincott-Schwartz, J., and Tooze, S.A. (2006). Starvation and ULK1-dependent cycling of mammalian Atg9 between the TGN and endosomes. J Cell Sci *119*, 3888-3900.

Zurita-Martinez, S.A., and Cardenas, M.E. (2005). Tor and cyclic AMP-protein kinase A: two parallel pathways regulating expression of genes required for cell growth. Eukaryot Cell *4*, 63-71.

CHAPTER 2

Mammalian autophagy: core molecular machinery and signaling regulation

ABSTRACT

Autophagy, or self-eating, is a cellular catabolic pathway that is evolutionarily conserved from yeast to mammals. Central to this process is the formation of the autophagosome, a double-membrane vesicle responsible for the delivery of long-lived proteins and excess or damaged organelle into the lysosome for degradation and reuse of the resulting macromolecules. In addition to the hallmark discovery of core molecular machinery components involved in autophagosome formation, complex signaling cascades controlling autophagy have also begun to emerge, with mTOR as a central but far from exclusive player. Malfunction of autophagy has been linked to a wide range of human pathologies, including cancer, neurodegeneration and pathogen infection. Here we highlight the recent advances in identifying and understanding the core molecular machinery and signaling pathways that are involved in mammalian autophagy.

INTRODUCTION

Autophagy, literally meaning "self-eating", embraces three major intracellular pathways in eukaryotic cells, macroautophagy, microautophagy and chaperone-mediated autophagy (CMA), which share a common destiny of lysosomal degradation, but are mechanistically different from one another (Klionsky, 2005; Massey et al., 2006). During macroautophagy, intact organelles (such as mitochondria) and portions of the cytosol are sequestered into a double-membrane vesicle, termed an autophagosome. Subsequently, the completed autophagosome matures by fusing with an endosome and/or lysosome, thereby forming an autolysosome. This latter step exposes the cargo to lysosomal hydrolases to allow its breakdown, and the resulting macromolecules are transported back into the cytosol through membrane permeases for reuse (Figure 2.1). By contrast, microautophagy involves the direct engulfment of cytoplasm at the lysosome surface, whereas CMA translocates unfolded, soluble proteins directly across the limiting membrane of the lysosome.

In this review, we will focus on mammalian macroautophagy (hereafter referred to as autophagy), which plays important physiological roles in human health and disease. The basal, constitutive level of autophagy plays an important role in cellular homeostasis through the elimination of damaged/old organelles as well as the turnover of long-lived proteins and protein aggregates, and thus maintains quality control of essential cellular components. On the other hand, when cells encounter environmental stresses, such as nutrient starvation, hypoxia, oxidative stress, pathogen infection, radiation, or anticancer drug treatment, the level of autophagy can be dramatically augmented as a cytoprotective response, resulting in adaptation and survival; however, dysregulated or excessive

autophagy may lead to cell death. Thus, defective autophagy has been implicated in the pathogenesis of diverse diseases, such as certain types of neuronal degeneration and cancer, and also in aging (Mizushima et al., 2008).

Although autophagy was first identified in mammalian cells approximately 50 years ago, our molecular understanding of it only started in the past decade, largely based on the discovery of autophagy-related (*ATG*) genes initially in yeast followed by the identification of homologs in higher eukaryotes (Yang and Klionsky, 2009). Among these Atg proteins, one subset is essential for autophagosome formation, and is referred to as the "core" molecular machinery (Xie and Klionsky, 2007). These core Atg proteins are composed of four subgroups: (1) The Atg1/unc-51-like kinase (ULK) complex; (2) two ubiquitn-like protein (Atg12 and Atg8/LC3) conjugation systems; (3) the class III phosphatidylinositol 3-kinase (PtdIns3K)/Vps34 complex I; and (4) two transmembrane proteins, Atg9/mAtg9 (and associated proteins involved in its movement such as Atg18/WIPI-1) and VMP1. The proposed site for autophagosome formation, to which most of the core Atg proteins are recruited, is termed the phagophore assembly site (PAS).

In this review, we mainly highlight the recent advances in mammalian autophagy in terms of the molecular machinery involved in the formation and maturation of autophagosomes and the signaling cascades needed for the regulation of autophagy. The clarification of how autophagy is modulated in response to intracellular and extracellular stresses relies largely on the elucidation of the signaling network upstream of the Atg machinery.

Core molecular machinery

ULK complexes

The yeast serine/threonine kinase Atg1 plays a key role in the induction of autophagy, acting downstream of the target of rapamycin (TOR) complex 1 (TORC1). A family of mammalian Atg1 proteins has been identified; among these, unc-51-like kinase 1 (ULK1) and 2 have the highest similarity with yeast Atg1 and appear to be closely related. siRNA knockdown of ULK1 or ULK2 blocks autophagy in HEK293 cells (Jung et al., 2009). However, *ULK1*$^{-/-}$ mice display normal autophagy in response to nutrient deprivation, but delay mitochondrial clearance during reticulocyte maturation (Kundu et al., 2008). The basis for these differences is not known. It is possible that in some tissues, ULK2 can compensate for the deficiency of ULK1. Furthermore, a role of ULK3 in autophagy induction in oncogene-induced cell senescence has been described recently (Young et al., 2009). Thus, at least three ULKs are involved in mammalian autophagy regulation and they have mechanistically different roles *in vivo*.

Yeast Atg1 exists in a complex with Atg13 and Atg17. Atg13 is phosphorylated in a TORC1-dependent manner and the phosphorylation state of Atg13 modulates its binding to Atg1 and Atg17; inactivation of TORC1 leads to dephosphorylation of Atg13, increasing Atg1−Atg13−Atg17 complex formation and activating autophagy (Kamada et al., 2000; Yang and Klionsky, 2009). ULK1 and ULK2 are also in a large complex that includes the mammalian homolog of Atg13 (mAtg13) and the scaffold protein FIP200 (an ortholog of yeast Atg17) (Ganley et al., 2009; Hosokawa et al., 2009; Jung et al., 2009). mAtg13 is essential for autophagy, and it directly interacts with ULK1, ULK2 and FIP200 independent of its phosphorylation state (Hosokawa et al., 2009; Jung et al., 2009). FIP200

is also required for autophagy and binds to ULK1 and ULK2 independent of nutrient status (Hara et al., 2008), in contrast to the yeast Atg1−Atg17 interaction. In addition, under nutrient-rich conditions, the large ULK1−Atg13−FIP200 complex contains mammalian TORC1 (mTORC1); conversely, following nutrient deprivation, mTORC1 is quickly dissociated from the ULK1 complex (Hosokawa et al., 2009). There are several phosphorylation events within this complex, including phosphorylation of mAtg13 by ULK1, ULK2, and mTORC1, phosphorylation of FIP200 by ULK1 and ULK2, and phosphorylation of ULK1 and ULK2 by mTORC1 (Figure 2.1) (Hosokawa et al., 2009; Jung et al., 2009). Under conditions that induce autophagy, a decrease in mTORC1 activity leads to dephosphorylation of ULK1, ULK2, and mAtg13, activation of ULK1 and ULK2, and phosphorylation of mAtg13 and FIP200 by ULK1 and ULK2 (Hosokawa et al., 2009; Jung et al., 2009). Further studies are required to characterize the functional significance of these phosphorylation events. Recently, a new, mAtg13-interacting protein, Atg101, was found to interact with ULK1 in a mAtg13-dependent manner, and is essential for autophagy (Mercer et al., 2009). However, the role of the ULK1−Atg13−Atg101 complex in autophagy regulation remains unclear.

Two ubiquitin-like proteins, Atg12 and Atg8/LC3, and their conjugation systems

Studies in yeast and mammals have identified two ubiquitin-like proteins, Atg12 and Atg8/LC3, and their respective, partially overlapping, conjugation systems, which are proposed to act during elongation and expansion of the phagophore membrane. Atg12 is conjugated to Atg5 in a reaction that requires Atg7 and Atg10 (E1 and E2-like enzymes, respectively). The Atg12–Atg5 conjugate then interacts non-covalently with Atg16L, which oligomerizes to form a large multimeric complex called the Atg16L complex.

Atg8/LC3 is cleaved at its C terminus by Atg4 to generate the cytosolic LC3-I with a C-terminal glycine residue, which is conjugated to phosphatidylethanolamine (PE) in a reaction that requires Atg7 and the E2-like enzyme Atg3. The lipidated form of LC3 (LC3-II) is attached to both faces of the phagophore membrane, but is ultimately removed from the autophagosome outer membrane, which is followed by fusion of the autophagosome with a late endosome/lysosome (Yang and Klionsky, 2009).

Recent work suggests that these two ubiquitination-like systems are closely connected. On the one hand, the Atg16L complex is localized to the phagophore and it can act as a novel E3-like enzyme, determining the sites of Atg8/LC3 lipidation (Fujita et al., 2008b; Hanada et al., 2007). On the other hand, the Atg8/LC3 conjugation machinery seems to be essential for the formation of the Atg16L complex. In Atg3-deficient mice, where no LC3-II can be detected, Atg12–Atg5 conjugation is markedly reduced, and dissociation of the Atg16L complex from the phagophore is delayed; autophagosomes are smaller than in the wild type and appear either open-ended or multi-lamellar (Sou et al., 2008), indicating a role for the Atg16L complex and LC3 lipidation for the elongation and closure of the phagophore. This hypothesis is futher supported by the observation that overexpression of an inactive mutant of Atg4 inhibits the lipidation of LC3, and in these cells a significant number of nearly complete autophagosomes are not closed (Fujita et al., 2008a).

Class III phosphatidylinositol 3-kinase complex

In yeast, the only phosphatidylinositol 3-kinase (PtdIns3K) is Vps34, and it exists in two different complexes, complex I and II. Complex I, consisting of Vps34, Vps15, Atg6, and Atg14, is required for the induction of autophagy, and the lipid kinase activity of Vps34 is essential for generating phosphatidylinositol (3)-phosphate (PtdIns(3)P) at the

PAS to allow the recruitment of other Atg proteins. Complex II, consisting of Vps34, Vps15, Atg6, and Vps38, is required for the vacuolar sorting of carboxypeptidase Y. In mammals, there are two types of PtdIns3K: class I and III. Formation of the mammalian class III PtdIns3K complex, including hVps34, Beclin 1 (a homolog of Atg6), and p150 (a homolog of Vps15), is conserved. The orthologs of Atg14 and Vps38 have recently been identified and are called Atg14-like protein (Atg14L, or Barkor) and ultraviolet irradiation resistant-associated gene (UVRAG), respectively (Itakura et al., 2008; Liang et al., 2006; Sun et al., 2008).

Atg14L plays an important role in mammalian autophagy. Under nutrient-rich conditions, a subpopulation of Atg14L localizes to the ER; upon starvation, Atg14L localizes to Atg16L-positive and LC3-positive structures, indicating the phagophore and autophagosome, respectively, independently of the interaction of Atg14L with hVps34 and Beclin 1 (Itakura et al., 2008; Matsunaga et al., 2009). Importantly, depletion of Atg14L reduces Atg16L and LC3 puncta formation (Matsunaga et al., 2009). Overexpression of Atg14L stimulates the kinase activity of hVps34, and induces autophagy, whereas *Atg14L* knockdown reduces PtdIns(3)P production, and inhibits autophagy (Sun et al., 2008; Zhong et al., 2009). Thus, a possible role of Atg14L is to direct the class III PtdIns3K complex to the phagophore to initiate the recruitment of Atg machinery.

Recent studies suggest that UVRAG participates in at least four different mechanisms to regulate autophagy. First, UVRAG competes with Atg14L for binding to Beclin 1; the interactions of Atg14L and UVRAG with the Beclin 1−hVps34−p150 complex are mutually exclusive (Itakura et al., 2008; Sun et al., 2008). Second, UVRAG interacts with Bif-1 (Bax-interacting factor 1); Bif-1 is required for autophagy and colocalizes with Atg5,

LC3, and mAtg9 during starvation (Takahashi et al., 2007). It is proposed that the recruitment of Bif-1 via UVRAG may provide the machinery to deform membranes, as Bif-1 has an N-BAR domain and shows membrane binding and bending activities (Takahashi et al., 2009). Third, UVRAG interacts with the class C Vps/HOPS proteins, promoting autophagosome fusion with the late endosome/lysosome, thereby accelerating delivery and degradation of autophagic cargo (Liang et al., 2008). Fourth, the recently identified Rubicon (RUN domain and cysteine-rich domain containing, Beclin 1-interacting) protein forms a complex with UVRAG−Beclin 1−hVps34−p150; this complex localizes to the late endosome/lysosome and negatively regulates autophagosome maturation (Matsunaga et al., 2009; Zhong et al., 2009). Rubicon reduces hVps34 activity and inhibits autophagy.

In addition to hVps34, Atg14L, and UVRAG, Beclin 1 also interacts with Ambra 1 (activating molecule in Beclin 1-regulated autophagy). Ambra 1 functions as a positive regulator of autophagy and the mechanism remains unclear (Fimia et al., 2007). Collectively, there exist multiple mammalian hVps34−Beclin 1 complexes that may participate in distinct steps of autophagy regulation (Figure 2.1), either at the early stage to promote autophagosome formation or at the later stage to promote autophagosome maturation.

Transmembrane proteins in mammalian autophagy

Mammalian Atg9 (mAtg9) and vacuole membrane protein 1 (VMP1) are the two transmembrane proteins so far identified that are required for mammalian autophagy. mAtg9, with both the N and C termini in the cytosol, spans the membrane six times. It is located in the *trans*-Golgi network and late endosomes, and upon starvation or rapamycin

treatment, redistributes to peripheral sites, overlapping with GFP-LC3-positive autophagosomes. The cycling of mAtg9 after starvation is ULK1-dependent, and also requires the kinase activity of hVps34 (Young et al., 2006), which is similar to the yeast protein (Reggiori et al., 2004). Although its functions remain unclear, based on the existing data from yeast Atg9, mAtg9 potentially contributes to the delivery of membrane to the forming autophagosome, an attrative model that needs to be experimentally tested in mammalian cells.

In contrast to mAtg9, VMP1 has no known homologs in yeast. The localization of VMP1 is controversial: in mammalian cells it is localized to the plasma membrane and also colocalizes with LC3 and Beclin 1 upon autophagy induction (Ropolo et al., 2007), whereas the VMP1 homolog in *Dictyostelium discoideum* localizes to the ER (Calvo-Garrido et al., 2008). In mammalian cells, ectopical overexpression of VMP1 triggers autophagy even under nutrient-rich conditions, whereas depletion of VMP1 blocks starvation-induced and rapamycin-induced autophagy (Ropolo et al., 2007). Importantly, VMP1 interacts with Beclin 1, and this interaction is essential for autophagy induced by VMP1 overexpression (Ropolo et al., 2007). VMP1 might function as a transmembrane protein that recruits Beclin 1 and other components in the class III PtdIns3K complex to the phagophore. This is supported by a recent finding that a novel VMP1-interacting protein, TP53INP2 (tumor protein 53-induced nuclear protein 2), is essential for the translocation of Beclin 1 and LC3 to autophagosomes upon autophagy stimulation, potentially through its interaction with VMP1 (Nowak et al., 2009). TP53INP2 is essential for autophagy. It translocates from the nucleus to autophagosomes upon autophagy induction, where it interacts with LC3 as well as VMP1, but not Beclin 1.

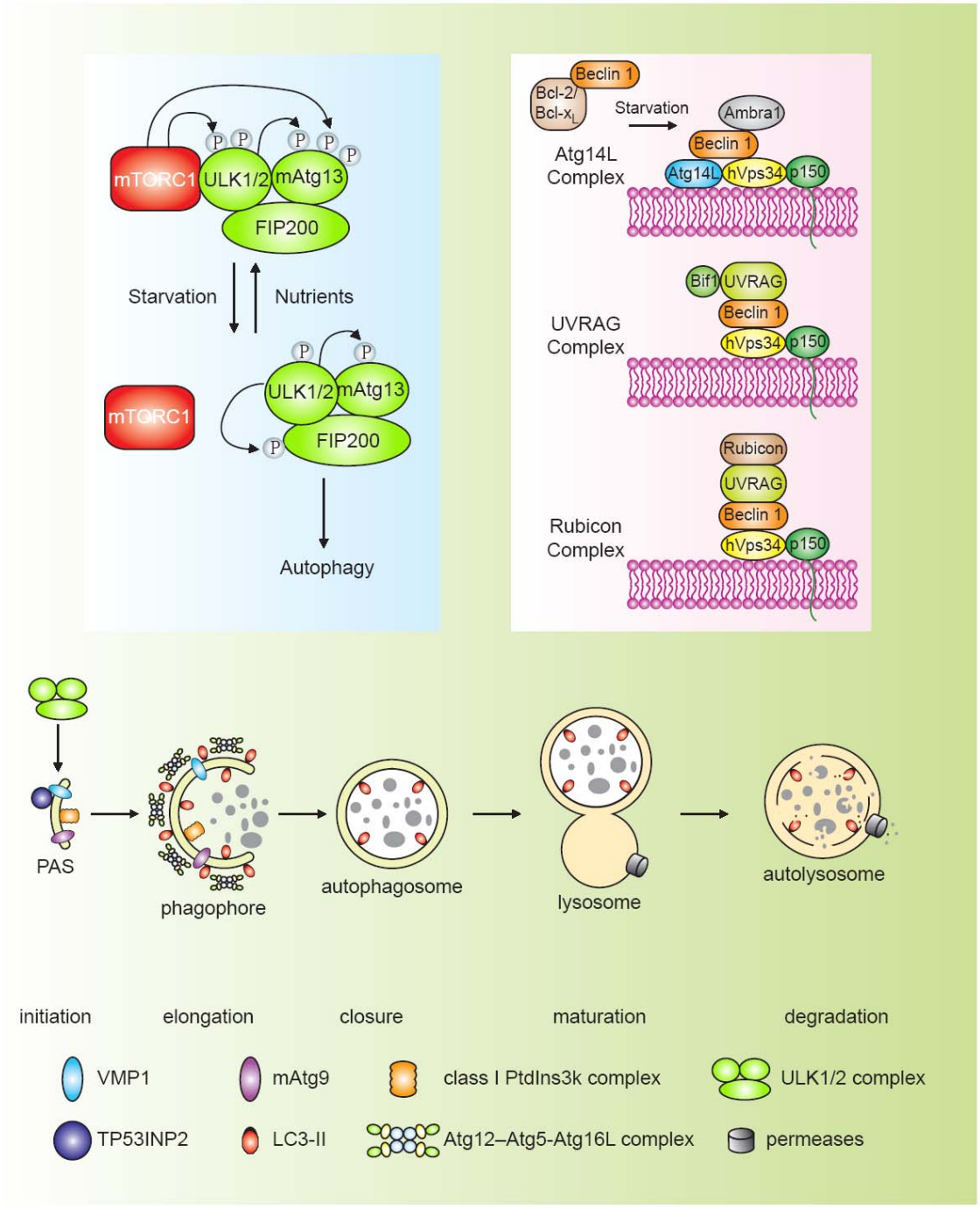
mTORC1
ULK1/2
mAtg13
FIP200
Starvation
Nutrients
Autophagy
Beclin 1
Bcl-2/
Bcl-x$_L$
Starvation
Ambra1
Atg14L
Complex
Atg14L
hVps34
p150
Bif1
UVRAG
UVRAG
Complex
Rubicon
Rubicon
Complex
PAS
phagophore
autophagosome
lysosome
autolysosome
initiation
elongation
closure
maturation
degradation
VMP1
mAtg9
class I PtdIns3k complex
ULK1/2 complex
TP53INP2
LC3-II
Atg12–Atg5-Atg16L complex
permeases

Figure 2.1. **Schematic depiction of the autophagy pathway and its core molecular machinery in mammalian cells.** Mammalian autophagy proceeds through a series of steps, including initiation at the PAS (phagophore assembly site), elongation and expansion of the phagophore, closure and completion of the autophagosome, autophagosome maturation via docking and fusion with an endosome and/or lysosome, breakdown and degradation of the autophagosome inner membrane and cargo, and recycling of the resulting macromolecules. Regulatory components for autophagy induction include the ULK1 and ULK2 complexes that contain various Atg proteins (light blue box at left) that are required for autophagy. The association of mTORC1 with this complex and the activity of mTORC1 depend on the nutrient status. Under nutrient-rich conditions, mTORC1 is associated with the ULK1 and ULK2 complexes, and phosphorylates ULK1, ULK2, and mAtg13; upon inactivation of mTORC1 by nutrient starvation, mTORC1 disassociates, mAtg13, ULK1 and ULK2 are partially dephosphorylated, and activation of ULK1 and ULK2 promotes phosphosphorylation of FIP200. There are at least three class III PtdIns3K complexes (light red box at right), that are involved in autophagosome formation or clearance. The Atg14L (Atg14L−Beclin 1−hVps34−p150) and UVRAG (UVRAG−Beclin 1−hVps34−p150) complexes are required for autophagy, whereas Rubicon complex (Rubicon−UVRAG−Beclin 1−hVps34−p150) negatively regulates autophagy. Ambra1 and Bif-1 are essential for the induction of autophagy, through direct interaction with Beclin 1 and UVRAG, respectively; whereas Bcl-2 binds to Beclin 1 and disrupts the Beclin 1-associated hVps34 complex, thereby inhibiting autophagy.

Signaling pathways regulating autophagy

PtdIns3K-Akt-mTORC1

The target of rapamycin (TOR) is a highly conserved serine/threonine protein kinase that acts as a central sensor of growth factors, nutrient signals, and engery status. TOR serves as a master regulator of autophagy (Codogno and Meijer, 2005). TOR exists in two distinct complexes, TORC1 and TORC2 that are conserved from yeast to mammals, and TORC1 has a primary function in regulating autophagy. In yeast, inhibiting the TORC1 complex during nitrogen starvation or by rapamycin stimulates autophagy (Yang and Klionsky, 2009). The mammalian TORC1 (mTORC1) is also sensitive to rapamycin, which in many settings stimulates autophagy. However, a recent report challenged this view by showing that rapamycin and siRNA knockdown of one of the key downstream effectors of mTORC1, S6 kinase 1 (S6K1), inhibit autophagy in cancer cells (Zeng and Kinsella, 2008), and a more recent finding shows that mTORC1 regulates autophagy through an unknown mechanism that is essentially insensitive to rapamycin (Thoreen et al., 2009).

mTORC1 integrates upstream activating signals that inhibit autophagy through the class I PtdIns3K-protein kinase B (PKB, also known as Akt) pathway (Figure 2.2). Upon association with growth factor, receptor tyrosine kinases undergo autophosphorylation and become activated, leading to the stimulation of two key signal transducing components: the small GTPase Ras and class I PtdIns3K. Class I PtdIns3K catalyzes the production of PtdIns(3)P at the plasma membrane, which increases membrane recruitment of both PKB and its activator PDK1 (phosphoinositide-dependent protein kinase 1), leading to the activation of PKB. PtdIns3K kinase activity can be opposed by PTEN, a

3'-phosphoinositide phosphatase, subsequently decreasing PKB activity, and inhibiting mTOR. PtdIns3K-PKB activation suppresses autophagy in mammalian cells. PKB further activates mTORC1 through inhibiting a downstream protein complex, the tuberous sclerosis complex 1/2 (TSC1/TSC2). The TSC1/TSC2 heterodimer, which is a stable complex, senses the upstream inputs from various kinases, including PKB and ERK1/2 (Inoki et al., 2002; Ma et al., 2005). Phosphorylation of TSC2 by PKB or ERK1/2 leads to the disruption of its complex with TSC1, and results in mTOR activation. TSC1/TSC2 acts as the GTPase-activating protein for Rheb, a small GTP-binding protein that binds to and activates mTOR in its GTP-bound form. Ras has opposing roles in autophagy regulation: it inhibits autophagy by activating the PtdIns3K-PKB-mTORC1 pathway, and at the same time, it may induce autophagy via the Raf-1-MEK1/2-ERK1/2 pathway (Furuta et al., 2004; Pattingre et al., 2003). Finally, the mTORC2 complex is also involved in autophagy regulation. Full activation of PKB requires mTORC2 (Sarbassov et al., 2005), and inhibition of PKB, caused by mTORC2 depletion, reduces the phosphorylation of, and therefore activates, the forkhead box O (FoxO3) transcription factor, which stimulates autophagy in muscle cells independent of the activity of mTORC1 (Mammucari et al., 2007).

AMPK

The AMP-activated protein kinase (AMPK) is another sensor of cellular bioenergetics, specifically in response to energy stress. During nutrient and energy depletion, AMPK is activated by a decreased ATP/AMP ratio through the upstream LKB1 kinase (encoded by the Peutz-Jeghers syndrome gene). Active AMPK leads to phosphorylation and activation of TSC1/TSC2 and inhibition of mTORC1 activity. Thus, the phosphorylation of

TSC1/TSC2 by AMPK and PKB has opposite effects on mTORC1 and connects mTORC1 with energy and growth factor signaling, respectively (Figure 2.2). Recently, it is reported that AMPK regulates mTORC1 signaling through an alternative mechanism, whereby AMPK directly phosphorylates Raptor, a subunit of mTORC1, and this Raptor phosphorylation is important for the inhibition of mTORC1 signaling by AMPK (Gwinn et al., 2008). Thus, AMPK serves as a positive regulator of autophagy. Under stress conditions, the LKB1-AMPK pathway phosphorylates and stabilizes $p27^{kip1}$, a cell cycle inhibitor, and stabilized $p27^{kip1}$ induces autophagy (Liang et al., 2007). An increase in the cytosolic free Ca^{2+} concentration and cytokines (such as TRAIL) activates AMPK via activation of the Ca^{2+}/calmodulin-dependent kinase kinase-β (CaMKKβ) and transforming growth factor-β-activating kinase 1 (TAK1), respectively, and these pathways are required for Ca^{2+}-induced or TRAIL-induced autophagy (Herrero-Martin et al., 2009; Hoyer-Hansen et al., 2007). Moreover, AMPK activity contributes to the induction of autophagy during hypoxia (Papandreou et al., 2008).

p53

The p53 tumor suppressor, the "guardian of the cellular genome", has dual positive and negative regulatory roles in autophagy induction (Figure 2.2) (Levine and Abrams, 2008). Upon genotoxic stress or oncogenic activation, the activation of p53 induces autophagy; p53 activates AMPK, which in turn, activates the TSC1/TSC2 complex, leading to the inhibition of the mTORC1 pathway (Feng et al., 2005). p53 can also induce autophagy through upregulation of the damage-regulated modulator of autophagy (DRAM) (Crighton et al., 2006).

Remarkably, chemical inhibition of p53, knockdown of *p53* with siRNA, or deletion

of the *p53* gene can trigger the onset of autophagy (Tasdemir et al., 2008). Several stimuli, including starvation or ER stress, can induce HDM2-dependent proteasomal degradation of p53 to favor autophagy induction, positioning p53 as a negative regulator of autophagy. HDM2, the p53-specific E3 ubiquitin ligase, targets p53 to proteasome-mediated destruction. The inhibition of HDM2 blocks the depletion of p53 and also prevents the activation of autophagy (Tasdemir et al., 2008). More importantly, it is the cytoplasmic p53 that exerts its inhibitory function towards autophagy, in contrast to the transcriptionally active nuclear p53 that promotes autophagy. Upon reintroduction into $p53^{-/-}$ cancer cells, mutants of p53 that are restricted to the cytosol effectively inhibit autophagy, whereas mutants of p53 that accumulate within the nucleus fail to block autophagy (Tasdemir et al., 2008). The inhibitory role of cytoplasmic p53 in autophagy may contribute to the strong oncogenic action of certain p53 mutants that are preferentially localized to the cytosol (Morselli et al., 2008).

Bcl-2 protein family

In mammals, the Bcl-2 protein family plays a dual role in autophagy regulation. Anti-apoptotic proteins, such as Bcl-2, Bcl-X_L, Bcl-w, and Mcl-1, can inhibit autophagy, whereas pro-apoptotic BH3-only proteins, such as BNIP3, Bad, Bik, Noxa, Puma, and BimEL, can induce autophagy (Levine et al., 2008). The binding of Bcl-2 to Beclin 1 disrupts the association of Beclin 1 with hVps34, decreases Beclin 1-associated hVps34 PtdIns3K activity and thereby inhibits autophagy. There are at least three distinct mechanisms that may account for the release of Beclin 1 from its inhibitory interaction with Bcl-2/Bcl-X_L (Figure 2.2). One model depicts that the BH3 domain of BH3-only proteins such as Bad, may competitively disrupt the inhibitory interaction of Beclin 1 and

Bcl-2/Bcl-X_L (Maiuri et al., 2007). A second mechanism for the dissociation of Beclin 1 from its inhibitory interaction with Bcl-2 involves the phosphorylation of Bcl-2 by the stress-activated c-Jun N-terminal Kinase 1 (JNK1). Starvation induces the phosphorylation of Bcl-2 at residues T69, S70, and S87 of the non-structured loop; expression of a non-phosphorylatable Bcl-2 mutant (T69A, S70A, and S87A) or inhibition of JNK1 abolishes the starvation-triggered dissociation of Bcl-2 from Beclin 1, and inhibits autophagy; expression of a constitutively active JNK1 results in constitutive Bcl-2 multisite phosphorylation, dissociation of Bcl-2 from Beclin 1 and stimulation of autophagy (Wei et al., 2008). Third, a recent finding shows that the activation of Beclin 1 to induce autophagy involves the phosphorylation of Beclin 1 by the death-associated protein kinase (DAPK). DAPK physically interacts with Beclin 1, and phosphorylates Beclin 1 on Thr119 located at a crucial position within the BH3 domain of Beclin 1, and thus promotes the dissociation of Beclin 1 from its inhibitor, Bcl-X_L, and autophagy induction (Zalckvar et al., 2009).

Figure 2.2. **Signaling cascades involved in the regulation of mammalian autophagy.** Autophagy is regulated by a complex signaling network of various stimulatory (arrowheads) and inhibitory (bars) inputs. Activation of growth factor receptors stimulates the class I PtdIns3K complex and small GTPase Ras, which leads to activation of the PtdIns3K-PKB-mTORC1 pathway and the Raf-1-MEK1/2-ERK1/2 pathway, respectively. PKB and ERK1/2 phosphorylates and inhibits the GTPase-activating protein complex TSC1/TSC2, leading to the stabilization of Rheb-GTPase, which, in turn, activates mTORC1, causing inhibition of autophagy. Activated ERK1/2 also stimulates autophagy. mTORC2 inhibits autophagy through the phosphorylation and activation of PKB. Metabolic stress, such as high AMP/ATP ratios resulting from energy depletion, or an increase in the cytosolic free Ca^{2+} concentration or cytokines, cause the AMP-activated protein kinase (AMPK) to be phosphorylated and activated by LKB1, CaMKKβ and TAK1, respectively. AMPK phosphorylates and activates TSC1/TSC2, leading to inactivation of

mTORC1 and autophagy induction. Genotoxic and oncogenic stresses result in nuclear p53 stabilization and activation, which stimulates autophagy through activation of AMPK or upregulation of DRAM. In contrast, cytoplasmic p53 has an inhibitory effect on autophagy. Anti-apoptotic proteins, Bcl-2 or Bcl-X_L, associate with Beclin 1 and inhibit the Beclin 1-associated class III PtdIns3K complex, causing inhibition of autophagy. For additional details, see the main text.

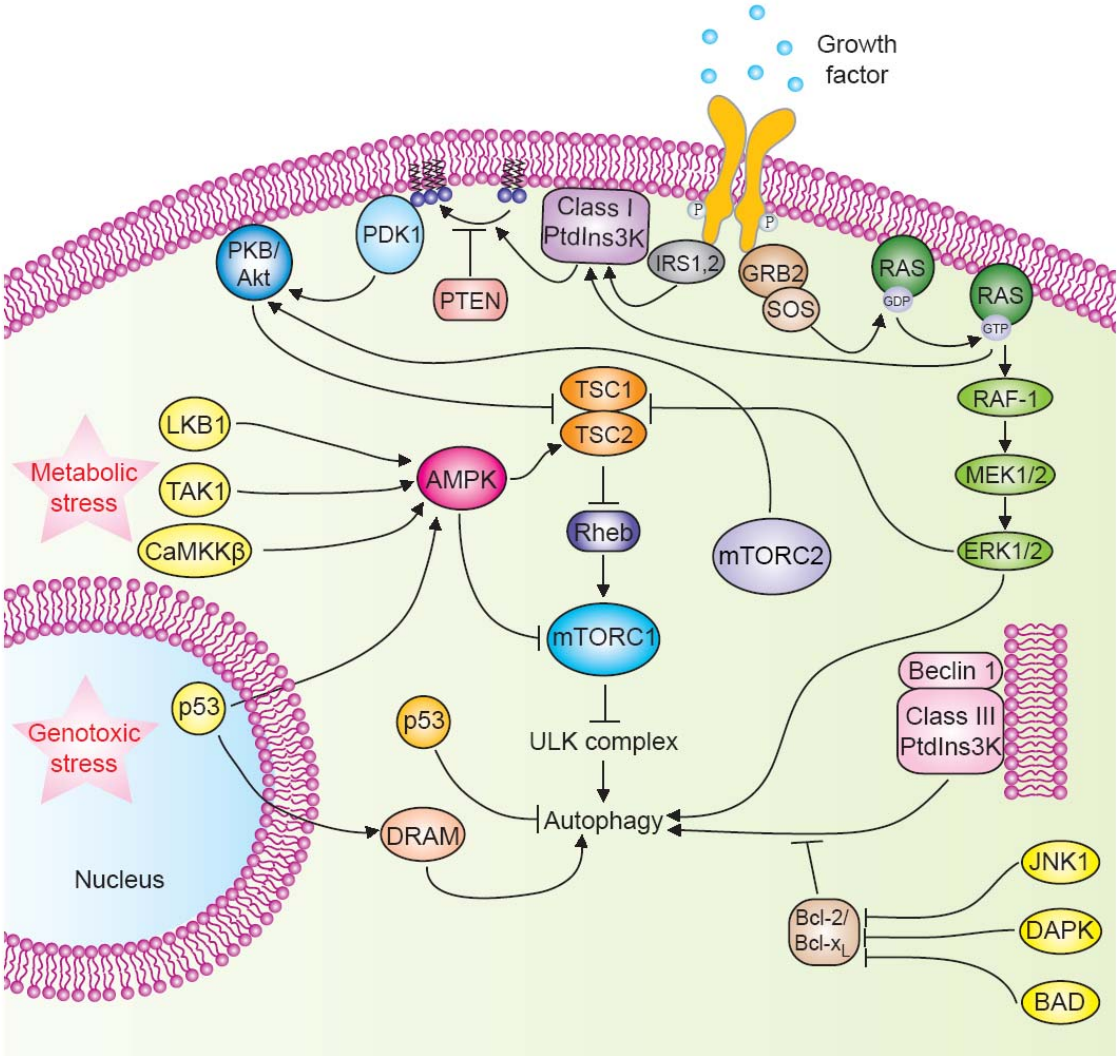

Concluding remarks

In the past decade there has been a tremendous advance in our understanding of the molecular machinery involved in mammalian autophagy. Nonetheless, many outstanding questions remain to be answered, including the mystery of the membrane source for autophagosome formation. By comparison, our knowledge about the signaling regulation of autophagy is relatively limited, in particular, with regard to the complex coordination between autophagy machinery and signaling inputs. As an intracellular self-destructive system, autophagy must be tightly regulated in order to adapt to different intracellular and extracellular stresses. This raises a fundamental question: How does the cell determine the specificity and magnitude of autophagy based on the inputs from a variety of signaling mechanisms? Mammalian autophagy has gained tremendous attention because of its implications in a wide range of physiological processes and diseases in humans. Our current understanding of this process and continued examination of its mechanism and regulation hold the potential for practical modulation of autophagy and its use as a therapeutic intervention.

REFERENCES

Calvo-Garrido, J., Carilla-Latorre, S., Lazaro-Dieguez, F., Egea, G., and Escalante, R. (2008). Vacuole membrane protein 1 is an endoplasmic reticulum protein required for organelle biogenesis, protein secretion, and development. Mol Biol Cell *19*, 3442-3453.

Codogno, P., and Meijer, A.J. (2005). Autophagy and signaling: their role in cell survival and cell death. Cell Death Differ *12 Suppl 2*, 1509-1518.

Crighton, D., Wilkinson, S., O'Prey, J., Syed, N., Smith, P., Harrison, P.R., Gasco, M., Garrone, O., Crook, T., and Ryan, K.M. (2006). DRAM, a p53-induced modulator of autophagy, is critical for apoptosis. Cell *126*, 121-134.

Feng, Z., Zhang, H., Levine, A.J., and Jin, S. (2005). The coordinate regulation of the p53 and mTOR pathways in cells. Proc Natl Acad Sci U S A *102*, 8204-8209.

Fimia, G.M., Stoykova, A., Romagnoli, A., Giunta, L., Di Bartolomeo, S., Nardacci, R., Corazzari, M., Fuoco, C., Ucar, A., Schwartz, P*., et al.* (2007). Ambra1 regulates autophagy and development of the nervous system. Nature *447*, 1121-1125.

Fujita, N., Hayashi-Nishino, M., Fukumoto, H., Omori, H., Yamamoto, A., Noda, T., and Yoshimori, T. (2008a). An Atg4B mutant hampers the lipidation of LC3 paralogues and causes defects in autophagosome closure. Mol Biol Cell *19*, 4651-4659.

Fujita, N., Itoh, T., Omori, H., Fukuda, M., Noda, T., and Yoshimori, T. (2008b). The Atg16L complex specifies the site of LC3 lipidation for membrane biogenesis in autophagy. Mol Biol Cell *19*, 2092-2100.

Furuta, S., Hidaka, E., Ogata, A., Yokota, S., and Kamata, T. (2004). Ras is involved in the negative control of autophagy through the class I PI3-kinase. Oncogene *23*, 3898-3904.

Ganley, I.G., Lam du, H., Wang, J., Ding, X., Chen, S., and Jiang, X. (2009). ULK1.ATG13.FIP200 complex mediates mTOR signaling and is essential for autophagy. J Biol Chem *284*, 12297-12305.

Gwinn, D.M., Shackelford, D.B., Egan, D.F., Mihaylova, M.M., Mery, A., Vasquez, D.S., Turk, B.E., and Shaw, R.J. (2008). AMPK phosphorylation of raptor mediates a metabolic checkpoint. Mol Cell *30*, 214-226.

Hanada, T., Noda, N.N., Satomi, Y., Ichimura, Y., Fujioka, Y., Takao, T., Inagaki, F., and Ohsumi, Y. (2007). The Atg12-Atg5 conjugate has a novel E3-like activity for protein lipidation in autophagy. J Biol Chem *282*, 37298-37302.

Hara, T., Takamura, A., Kishi, C., Iemura, S., Natsume, T., Guan, J.L., and Mizushima, N. (2008). FIP200, a ULK-interacting protein, is required for autophagosome formation in

mammalian cells. J Cell Biol *181*, 497-510.

Herrero-Martin, G., Høyer-Hansen, M., Garcia-Garcia, C., Fumarola, C., Farkas, T., Lopez-Rivas, A., and Jaattela, M. (2009). TAK1 activates AMPK-dependent cytoprotective autophagy in TRAIL-treated epithelial cells. EMBO J *28*, 677-685.

Hosokawa, N., Hara, T., Kaizuka, T., Kishi, C., Takamura, A., Miura, Y., Iemura, S., Natsume, T., Takehana, K., Yamada, N.*, et al.* (2009). Nutrient-dependent mTORC1 association with the ULK1-Atg13-FIP200 complex required for autophagy. Mol Biol Cell *20*, 1981-1991.

Høyer-Hansen, M., Bastholm, L., Szyniarowski, P., Campanella, M., Szabadkai, G., Farkas, T., Bianchi, K., Fehrenbacher, N., Elling, F., Rizzuto, R.*, et al.* (2007). Control of macroautophagy by calcium, calmodulin-dependent kinase kinase-β, and Bcl-2. Mol Cell *25*, 193-205.

Inoki, K., Li, Y., Zhu, T., Wu, J., and Guan, K.-L. (2002). TSC2 is phosphorylated and inhibited by Akt and suppresses mTOR signalling. Nat Cell Biol *4*, 648-657.

Itakura, E., Kishi, C., Inoue, K., and Mizushima, N. (2008). Beclin 1 forms two distinct phosphatidylinositol 3-kinase complexes with mammalian Atg14 and UVRAG. Mol Biol Cell *19*, 5360-5372.

Jung, C.H., Jun, C.B., Ro, S.H., Kim, Y.M., Otto, N.M., Cao, J., Kundu, M., and Kim, D.H. (2009). ULK-Atg13-FIP200 complexes mediate mTOR signaling to the autophagy machinery. Mol Biol Cell *20*, 1992-2003.

Kamada, Y., Funakoshi, T., Shintani, T., Nagano, K., Ohsumi, M., and Ohsumi, Y. (2000). Tor-mediated induction of autophagy via an Apg1 protein kinase complex. J Cell Biol *150*, 1507-1513.

Klionsky, D.J. (2005). The molecular machinery of autophagy: unanswered questions. J Cell Sci *118*, 7-18.

Kundu, M., Lindsten, T., Yang, C.Y., Wu, J., Zhao, F., Zhang, J., Selak, M.A., Ney, P.A., and Thompson, C.B. (2008). Ulk1 plays a critical role in the autophagic clearance of mitochondria and ribosomes during reticulocyte maturation. Blood *112*, 1493-1502.

Levine, B., and Abrams, J. (2008). p53: The Janus of autophagy? Nat Cell Biol *10*, 637-639.

Levine, B., Sinha, S., and Kroemer, G. (2008). Bcl-2 family members: dual regulators of apoptosis and autophagy. Autophagy *4*, 600-606.

Liang, C., Feng, P., Ku, B., Dotan, I., Canaani, D., Oh, B.H., and Jung, J.U. (2006). Autophagic and tumour suppressor activity of a novel Beclin1-binding protein UVRAG. Nat Cell Biol *8*, 688-699.

Liang, C., Lee, J.S., Inn, K.S., Gack, M.U., Li, Q., Roberts, E.A., Vergne, I., Deretic, V., Feng, P., Akazawa, C., and Jung, J.U. (2008). Beclin1-binding UVRAG targets the class C Vps complex to coordinate autophagosome maturation and endocytic trafficking. Nat Cell Biol *10*, 776-787.

Liang, J., Shao, S.H., Xu, Z.X., Hennessy, B., Ding, Z., Larrea, M., Kondo, S., Dumont, D.J., Gutterman, J.U., Walker, C.L.*, et al.* (2007). The energy sensing LKB1-AMPK pathway regulates p27(kip1) phosphorylation mediating the decision to enter autophagy or apoptosis. Nat Cell Biol *9*, 218-224.

Ma, L., Chen, Z., Erdjument-Bromage, H., Tempst, P., and Pandolfi, P.P. (2005). Phosphorylation and functional inactivation of TSC2 by Erk implications for tuberous sclerosis and cancer pathogenesis. Cell *121*, 179-193.

Maiuri, M.C., Le Toumelin, G., Criollo, A., Rain, J.C., Gautier, F., Juin, P., Tasdemir, E., Pierron, G., Troulinaki, K., Tavernarakis, N.*, et al.* (2007). Functional and physical interaction between Bcl-X(L) and a BH3-like domain in Beclin-1. EMBO J *26*, 2527-2539.

Mammucari, C., Milan, G., Romanello, V., Masiero, E., Rudolf, R., Del Piccolo, P., Burden, S.J., Di Lisi, R., Sandri, C., Zhao, J.*, et al.* (2007). FoxO3 controls autophagy in skeletal muscle in vivo. Cell Metab *6*, 458-471.

Massey, A.C., Zhang, C., and Cuervo, A.M. (2006). Chaperone-mediated autophagy in aging and disease. Curr Top Dev Biol *73*, 205-235.

Matsunaga, K., Saitoh, T., Tabata, K., Omori, H., Satoh, T., Kurotori, N., Maejima, I., Shirahama-Noda, K., Ichimura, T., Isobe, T.*, et al.* (2009). Two Beclin 1-binding proteins, Atg14L and Rubicon, reciprocally regulate autophagy at different stages. Nat Cell Biol *11*, 385-396.

Mercer, C.A., Kaliappan, A., and Dennis, P.B. (2009). A novel, human Atg13 binding protein, Atg101, interacts with ULK1 and is essential for macroautophagy. Autophagy *5*, 649-662.

Mizushima, N., Levine, B., Cuervo, A.M., and Klionsky, D.J. (2008). Autophagy fights disease through cellular self-digestion. Nature *451*, 1069-1075.

Morselli, E., Tasdemir, E., Maiuri, M.C., Galluzzi, L., Kepp, O., Criollo, A., Vicencio, J.M., Soussi, T., and Kroemer, G. (2008). Mutant p53 protein localized in the cytoplasm inhibits autophagy. Cell Cycle *7*, 3056-3061.

Nowak, J., Archange, C., Tardivel-Lacombe, J., Pontarotti, P., Pebusque, M.J., Vaccaro, M.I., Velasco, G., Dagorn, J.C., and Iovanna, J.L. (2009). The TP53INP2 protein is required for autophagy in mammalian cells. Mol Biol Cell *20*, 870-881.

Papandreou, I., Lim, A.L., Laderoute, K., and Denko, N.C. (2008). Hypoxia signals

autophagy in tumor cells via AMPK activity, independent of HIF-1, BNIP3, and BNIP3L. Cell Death Differ *15*, 1572-1581.

Pattingre, S., Bauvy, C., and Codogno, P. (2003). Amino acids interfere with the ERK1/2-dependent control of macroautophagy by controlling the activation of Raf-1 in human colon cancer HT-29 cells. J Biol Chem *278*, 16667-16674.

Reggiori, F., Tucker, K.A., Stromhaug, P.E., and Klionsky, D.J. (2004). The Atg1-Atg13 complex regulates Atg9 and Atg23 retrieval transport from the pre-autophagosomal structure. Dev Cell *6*, 79-90.

Ropolo, A., Grasso, D., Pardo, R., Sacchetti, M.L., Archange, C., Lo Re, A., Seux, M., Nowak, J., Gonzalez, C.D., Iovanna, J.L., and Vaccaro, M.I. (2007). The pancreatitis-induced vacuole membrane protein 1 triggers autophagy in mammalian cells. J Biol Chem *282*, 37124-37133.

Sarbassov, D.D., Guertin, D.A., Ali, S.M., and Sabatini, D.M. (2005). Phosphorylation and regulation of Akt/PKB by the rictor-mTOR complex. Science *307*, 1098-1101.

Sou, Y.S., Waguri, S., Iwata, J., Ueno, T., Fujimura, T., Hara, T., Sawada, N., Yamada, A., Mizushima, N., Uchiyama, Y*., et al.* (2008). The Atg8 conjugation system is indispensable for proper development of autophagic isolation membranes in mice. Mol Biol Cell *19*, 4762-4775.

Sun, Q., Fan, W., Chen, K., Ding, X., Chen, S., and Zhong, Q. (2008). Identification of Barkor as a mammalian autophagy-specific factor for Beclin 1 and class III phosphatidylinositol 3-kinase. Proc Natl Acad Sci U S A *105*, 19211-19216.

Takahashi, Y., Coppola, D., Matsushita, N., Cualing, H.D., Sun, M., Sato, Y., Liang, C., Jung, J.U., Cheng, J.Q., Mule, J.J*., et al.* (2007). Bif-1 interacts with Beclin 1 through UVRAG and regulates autophagy and tumorigenesis. Nat Cell Biol *9*, 1142-1151.

Takahashi, Y., Meyerkord, C.L., and Wang, H.G. (2009). Bif-1/endophilin B1: a candidate for crescent driving force in autophagy. Cell Death Differ *16*, 947-955.

Tasdemir, E., Maiuri, M.C., Galluzzi, L., Vitale, I., Djavaheri-Mergny, M., D'Amelio, M., Criollo, A., Morselli, E., Zhu, C., Harper, F*., et al.* (2008). Regulation of autophagy by cytoplasmic p53. Nat Cell Biol *10*, 676-687.

Thoreen, C.C., Kang, S.A., Chang, J.W., Liu, Q., Zhang, J., Gao, Y., Reichling, L.J., Sim, T., Sabatini, D.M., and Gray, N.S. (2009). An ATP-competitive mammalian target of rapamycin inhibitor reveals rapamycin-resistant functions of mTORC1. J Biol Chem *284*, 8023-8032.

Wei, Y., Pattingre, S., Sinha, S., Bassik, M., and Levine, B. (2008). JNK1-mediated

phosphorylation of Bcl-2 regulates starvation-induced autophagy. Mol Cell *30*, 678-688.

Xie, Z., and Klionsky, D.J. (2007). Autophagosome formation: core machinery and adaptations. Nat Cell Biol *9*, 1102-1109.

Yang, Z., and Klionsky, D.J. (2009). An overview of the molecular mechanism of autophagy. Curr Top Microbiol Immunol *335*, 1-32.

Young, A.R.J., Chan, E.Y.W., Hu, X.W., Köchl, R., Crawshaw, S.G., High, S., Hailey, D.W., Lippincott-Schwartz, J., and Tooze, S.A. (2006). Starvation and ULK1-dependent cycling of mammalian Atg9 between the TGN and endosomes. J Cell Sci *119*, 3888-3900.

Young, A.R.J., Narita, M., Ferreira, M., Kirschner, K., Sadaie, M., Darot, J.F., Tavare, S., Arakawa, S., Shimizu, S., and Watt, F.M. (2009). Autophagy mediates the mitotic senescence transition. Genes Dev *23*, 798-803.

Zalckvar, E., Berissi, H., Mizrachy, L., Idelchuk, Y., Koren, I., Eisenstein, M., Sabanay, H., Pinkas-Kramarski, R., and Kimchi, A. (2009). DAP-kinase-mediated phosphorylation on the BH3 domain of beclin 1 promotes dissociation of beclin 1 from Bcl-X_L and induction of autophagy. EMBO Rep *10*, 285-292.

Zeng, X., and Kinsella, T.J. (2008). Mammalian target of rapamycin and S6 kinase 1 positively regulate 6-thioguanine-induced autophagy. Cancer Res *68*, 2384-2390.

Zhong, Y., Wang, Q.J., Li, X., Yan, Y., Backer, J.M., Chait, B.T., Heintz, N., and Yue, Z. (2009). Distinct regulation of autophagic activity by Atg14L and Rubicon associated with Beclin 1-phosphatidylinositol-3-kinase complex. Nat Cell Biol *11*, 468-476.

CHAPTER 3

Atg22 recycles amino acids to link the degradative and recycling functions of autophagy

ABSTRACT

In response to stress conditions (such as nutrient limitation, or accumulation of damaged organelles) and certain pathological situations, eukaryotic cells use autophagy as a survival mechanism. During nutrient stress the main purpose of autophagy is to degrade cytoplasmic materials within the lysosome/vacuole lumen and generate an internal nutrient pool that is recycled back to the cytosol. This study elucidates a molecular mechanism for linking the degradative and recycling roles of autophagy. We show that in contrast to published studies Atg22 is not directly required for the breakdown of autophagic bodies within the lysosome/vacuole. Instead, we demonstrate that Atg22, Avt3 and Avt4 are redundant vacuolar effluxers, which mediate the efflux of leucine and other amino acids resulting from autophagic degradation. The release of autophagic amino acids allows the maintenance of protein synthesis and viability during nitrogen starvation. We propose a "recycling" model that includes the efflux of macromolecules from the lysosome/vacuole as the final step of autophagy.

INTRODUCTION

Autophagy is a carefully orchestrated process responsible for the rapid degradation of large portions of cytoplasm in the lysosome/vacuole lumen (Kim and Klionsky, 2000). The identification of over 20 conserved autophagy-related (*ATG*) genes in the yeast *S. cerevisiae* (Klionsky et al., 2003) has provided some insight into the molecular basis behind autophagy. In this process, cytoplasm is nonselectively sequestered by a double-membrane vesicle, an autophagosome, which fuses with the lysosome/vacuole. The resulting single-membrane intravacuolar autophagic body is subsequently lysed, the cargos are typically degraded, and the resulting macromolecules reused to synthesize essential cellular components. For ease of description, autophagy can be separated into several steps including induction, vesicle formation, retrieval of Atg proteins, fusion with the lysosome/vacuole and processing of the cargo (Klionsky, 2005).

It has long been assumed that during extreme conditions, such as nutrient shortage, autophagy provides an internal nutrient pool to maintain the metabolism essential for survival. One example of this function is illustrated by the observation that the survival of neonatal mice is dependent upon the amino acids produced by autophagy for the maintenance of energy homeostasis and viability (Kuma et al., 2004). Another example of the survival-promoting role of autophagy in mammalian cells is the recent evidence showing that in the absence of apoptosis, Bax- and Bak-deficient mice activate autophagy, maintain ATP production, and ultimately sustain viability for several weeks following growth factor withdrawal (Lum et al., 2005).

Although the accumulated evidence suggests that the recycling of degradation products generated by autophagy is a critical part of its function, no experimental data have

ever demonstrated the existence of such a process. In fact, while virtually all reviews that discuss autophagy refer to breakdown in the lysosome/vacuolar lumen followed by recycling of the resulting macromolecules, none of the accompanying models include the recycling step as part of the autophagic process, and no mechanistic information has been published that directly connect autophagy with cytosolic amino acid levels. However, autophagy would be largely pointless, at least as a starvation response, without this final step.

One purpose of autophagy is to degrade cytoplasmic components and recycle the resulting macromolecules that are essential for cell survival when nutrients are scarce. Accordingly, it must break down the single-membrane autophagic body that results from fusion of the autophagosome with the vacuole. This breakdown event depends on the acidic pH of the vacuole lumen and Prb1. Two other proteins have also been reported to be involved in this step, Atg15/Cvt17 (Epple et al., 2001; Teter et al., 2001) and Atg22/Aut4 (Suriapranata et al., 2000). Atg15 is a putative lipase and seems likely to function directly in the intravacuolar lysis of autophagic bodies. In contrast, Atg22 is a putative integral membrane protein located in the limiting membrane of the vacuole, with limited homologies to permeases. It was suggested that the breakdown of autophagic bodies depends on Atg22, because starving *atg22Δ*/*aut4Δ* mutant cells exhibit a slight accumulation of autophagic bodies inside the vacuole, and are partially defective in total protein turnover (Suriapranata et al., 2000). In contrast, the cytoplasm to vacuole targeting (Cvt) pathway, a type of specific autophagy involved in biosynthetic delivery to the vacuole (Kim and Klionsky, 2000) is normal in the *atg22Δ* mutant cells. In particular, the breakdown of the single-membrane intravacuolar Cvt bodies was unaffected by the

absence of Atg22 (Suriapranata et al., 2000). These data imply a fundamental difference in the composition of the membranes that form the Cvt/autophagic bodies and/or the breakdown process used in the Cvt and autophagy pathways.

In this paper, we carefully examined the role of Atg22 in autophagy and the breakdown of autophagic bodies. In contrast to previously published data, we find that Atg22 is not directly required for the steps of autophagy up to and including vesicle breakdown. Instead, our results suggest that Atg22 functions as an amino acid effluxer on the vacuolar membrane. In addition, two other vacuolar amino acid effluxers, Avt3 and Avt4, which seem to be part of the same family as Atg22, were discovered to be also required for maintenance of viability under nitrogen starvation conditions in the absence of leucine in a leucine auxotrophic strain. Finally, these results support a model wherein the efflux of amino acids resulting from the breakdown of autophagic bodies within the vacuole lumen constitutes the final step of autophagy.

MATERIALS AND METHODS

Strains, Plasmids and Media

The yeast *S. cerevisiae* strains used in this study are listed in Table 2.1. For gene disruptions, the entire coding region was replaced with either the *Kluveromyces lactis URA3*, or the *S. cerevisiae TRP1*, *LEU2*, or *URA3* genes using PCR primers containing ~60 bases of identity to the regions flanking the open reading frame.

Cells were grown in rich (YPD; 1% yeast extract, 2% peptone, 2% glucose) or synthetic minimal media (SMD; 0.67% yeast nitrogen base, 2% glucose, amino acids and vitamins as needed). Starvation experiments were conducted in synthetic medium lacking nitrogen (SD-N; 0.17% yeast nitrogen base without amino acids, 2% glucose).

Table 2.1. Yeast strains used in this study.

Strain	Genotype	Reference
BY4742	MATα, *leu2- 0*, *his3- 1*, *lys2- 0*, *ura3- 0*	ResGen/Invitrogen
SEY6210	*MATα ura3-52 leu2-3,112 his3-Δ200 trp1-Δ901 lys2-801 suc2-Δ9 mel GAL*	(Robinson et al., 1988)
TN124	*MATα leu2–3,112 ura3–52 trp1 pho8Δ::PHO8Δ60 pho13Δ::LEU2*	
WCG4a	*MATα his3-11,15 leu2-3,112 ura3*	(Thumm et al., 1994)
WHY1	SEY6210 *atg1Δ::HIS5 S.p.*	(Shintani et al., 2002)
YTS178	SEY6210 *vac8Δ::HIS5 S.p.*	(Cheong et al., 2005)
ZFY1	WCG4a *atg22Δ::HIS3*	This study
ZFY2	WCG4a *pep4Δ::LEU2*	This study

ZFY4	WCG4a *atg1Δ::URA3*	This study
ZFY6	SEY6210 *atg22Δ::TRP1*	This study
ZFY8	SEY6210 *atg22Δ::TRP1 vac8Δ::URA3*	This study
ZFY14	TN124 *atg22Δ::TRP1*	This study
ZFY15	SEY6210 *ATG22-GFP::HIS3*	This study
ZFY16	BY4742 *ATG22-GFP::HIS3*	This study
ZFY19	SEY6210 *avt3Δ::HIS3*	This study
ZFY20	SEY6210 *avt3Δ::HIS3 avt4Δ::URA3*	This study
ZFY22	SEY6210 *avt3Δ::HIS3 avt4Δ::URA3 atg22Δ::TRP1*	This study
ZFY32	SEY6210 *avt4Δ::HIS3*	This study
ZFY36	SEY6210 *ATG22-HA::TRP1*	This study
ZFY38	SEY6210 *ATG22-protein A::TRP1 pep4Δ::LEU2*	This study

Microscopy

For fluorescent microscopy, cultures were grown in SMD until early log phase. To label the vacuolar membrane, the cells were pelleted and resuspended in fresh SMD at OD_{600} = 1.0. FM 4-64 was added to a final concentration of 8 μM, and the culture was incubated at 30°C for 30 min. The cells were washed and resuspended in either SMD or SD-N at OD_{600} = 1.0. After a 2 h incubation, the samples were examined using a DeltaVision Spectris microscope (Applied Precision, Issaquah, WA) fitted with differential interference contrast optics and Olympus camera IX-HLSH100 with softWoRx software

(Applied Precision). Electron microscopy was performed essentially as described previously (Kaiser and Schekman, 1990). Briefly, cells were fixed in potassium permanganate and embedded in Spurr's resin. After resin polymerization, 65-75 nm sections were mounted on nickel grids. The grids were stained with 1% uranyl acetate followed by lead citrate, and then they were imaged using a Philips CM-100 transmission electron microscope.

Yeast Vacuolar Amino Acid Analysis

The Cu^{2+} method (Ohsumi et al., 1988) was used for extraction of vacuolar amino acid pools from yeast cells. In summary, cells at OD_{600} = 1.6 were harvested, washed twice with distilled water, resuspended in AA buffer (2.5 mM potassium phosphate buffer, pH 6.0, 0.6 M sorbitol, 10 mM Glucose, 0.2 mM $CuCl_2$), and incubated at 30°C for 10 min. Cell suspensions was collected by filtration on membrane filters (0.45 μm, Millipore, Bedford, MA) and washed five times with the AA buffer lacking 0.2 mM $CuCl_2$. The cells retained on the filter were resuspended in distilled water and boiled for 15 min, then subjected to ultracentrifugation at 100,000 *g* for 1 h. The supernatant was collected as the vacuolar fraction. The amino acid analysis was performed at the Protein Chemistry Laboratory (Texas A&M University, College Station, TX) using a Hewlett Packard AminoQuant II system, and the data were analyzed and reviewed by Dr. Henriette A. Remmer (Protein Structure Facility, University of Michigan, Ann Arbor, MI).

Subcellular Fractionation

Cells were grown to mid-log phase in SMD medium and converted to spheroplasts as described previously (Kim et al., 1999). Supernatant and pellet fractions were generated by

centrifugation at 13, 000 × *g* for 5 min. All samples were collected by trichloroacetic acid (TCA) precipitation and subjected to immunoblotting as described previously (Kim et al., 1999).

Autophagy Assays

The alkaline phosphate assay to measure activity from Pho8Δ60 has been described previously (Abeliovich et al., 2003; Noda et al., 1995). The green fluorescent protein (GFP)-Atg8 processing assay was carried out as described previously (Cheong et al., 2005).

RESULTS

atg22Δ Cells Display Normal Autophagy

The Cvt pathway shares most of the components needed for autophagy. In both pathways, the basic mechanism of cytoplasm-to-vacuole transport involves the formation of a double-membrane vesicle that enwraps cytoplasmic components, and delivers them into the vacuole for subsequent degradation. We began our analysis with an interest in what is typically viewed as the last step of autophagy, intravacuolar vesicle breakdown. The putative lipase Atg15 is needed for the disintegration of both Cvt and autophagic bodies (Teter et al., 2001). In contrast, it was reported that another protein, Atg22, is only needed for breakdown of autophagic bodies (Suriapranata et al., 2000). This finding was intriguing because it implied a difference between the membrane composition of Cvt vesicles and autophagosomes. The conclusion about the pathway specificity of Atg22 is based on the following observations: 1) Electron microscopy revealed that Atg22-deleted cells accumulate a low level of autophagic bodies within the vacuole lumen, 2) the *atg22Δ* mutant displayed a partial reduction in total protein turnover under starvation conditions, and 3) processing of prApe1 seemed normal in this mutant (Suriapranata et al., 2000). However, other assays including the analysis of Pho8Δ60 (Noda et al., 1995), the most commonly used procedure for monitoring autophagy, were not used to examine the *atg22Δ* mutant. If the breakdown of autophagic vesicles really depends on Atg22, we should observe a general autophagy-defective phenotype in *atg22Δ* mutant cells.

To make a quantitative measurement of autophagy in the *atg22Δ* mutant, we analyzed the truncated version of Pho8, Pho8Δ60, which resides in the cytosol and can be only delivered into the vacuolar lumen by autophagy. Once it enters into the vacuole, it is

processed by removal of a C-terminal propeptide to generate the active form. As a nonspecific cargo, Pho8Δ60 serves as a protein marker for bulk autophagy. The Pho8Δ60 activity was measured in wild-type, *atg22Δ* and *atg8Δ* cells under vegetative and starvation conditions (Figure 2.1A). As expected, wild-type cells showed Pho8Δ60-dependent alkaline phosphatase activity that increased between 2 and 4 h of starvation, whereas the *atg8Δ* autophagy-defective strain retained a background level of activity. The *atg22Δ* mutant demonstrated an increase of Pho8Δ60 activity similar to that observed in the wild-type strain indicating normal breakdown of autophagic bodies.

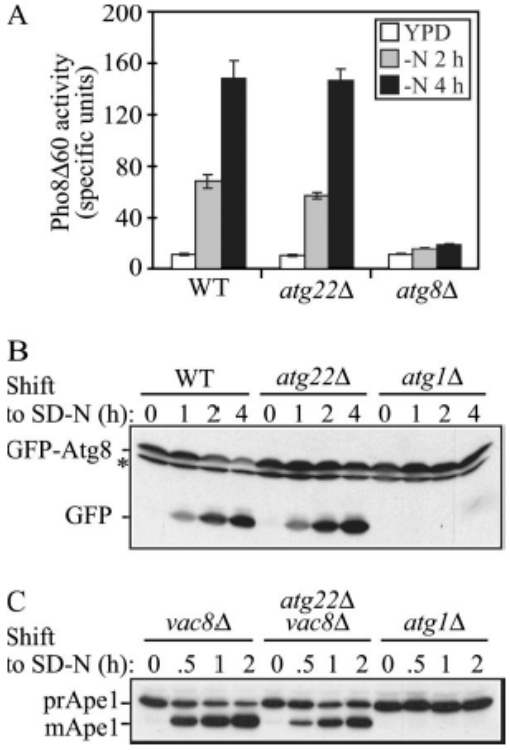

Figure 2.1. **The *atg22Δ* mutant displays normal autophagy**. (A) Pho8Δ60 activity, a marker for nonspecific autophagy, indicates this process is normal in *atg22Δ* cells. The Pho8Δ60-dependent alkaline phosphatase activity was measured before and 2 or 4 h after shifting from YPD to SD-N medium. The error bars indicate the SD of two independent experiments. (B) GFP-Atg8p processing is normal in the *atg22Δ* mutant. The wild-type (WT, SEY6210), *atg1Δ* (WHY1), and

atg22Δ (ZFY6) strains expressing GFP-Atg8 were grown in SMD to mid log phase and shifted to SD-N to induce autophagy. At the indicated times, aliquots were removed and examined by immunoblot using anti-GFP antibody. The position of free GFP, indicating autophagy-dependent processing of GFP-Atg8, is indicated. The asterisk indicates a non-specific band. (C) In the *atg22Δ* mutant autophagic delivery of prApe1 is normal in the Cvt pathway-defective *vac8Δ* background. The *vac8Δ* (YTS178), *atg22Δ vac8Δ* (ZFY8), and *atg1Δ* (WHY1) strains were cultured as described above. At the indicated times, aliquots were taken and checked by immunoblot using anti-Ape1 antiserum. The positions of precursor and mature Ape1 are indicated.

In addition to Pho8Δ60, there are several other assays available to monitor autophagy, each one reflecting a different parameter of the process. For example, Atg8 is an ubiquitin-like protein that is conjugated to phosphatidylethanolamine and seems to be the only Atg protein, aside from the cargo receptor Atg19, which remains associated with the completed autophagosome and autophagic body. The population of GFP-tagged Atg8 that is within the lumen of these vesicles becomes trapped. When the autophagic bodies are broken down, Atg8 is degraded, whereas the GFP moiety remains relatively stable. Thus, the generation of free GFP reflects the delivery of autophagosomes, and in particular the vesicle inner membrane, to the vacuole, and it can also be used to monitor the efficiency of lysis of the autophagic bodies (Cheong et al., 2005). Wild-type, *atg22Δ* and *atg1Δ* strains were transformed with a plasmid encoding GFP-Atg8, grown in synthetic complete medium (SMD) with auxotrophic amino acids and shifted to SD-N to induce autophagy. At the indicated time, aliquots were removed and analyzed by western blot using antiserum against GFP. As shown in Figure 2.1B, wild-type cells displayed an increase in the level of free GFP over time in starvation conditions. In contrast, the *atg1Δ* mutant that is defective in autophagy accumulated only full-length GFP-Atg8. In the *atg22Δ* cells, free GFP was detected in increasing amounts as starvation proceeded, similar to the result seen with the

wild-type strain. Thus, by this assay as well, autophagic bodies were broken down in the *atg22Δ* mutant.

To extend our analysis, we chose to examine the autophagy pathway by monitoring the maturation of prApe1, a marker for specific autophagy, in the Cvt pathway-defective *vac8Δ* background (Cheong et al., 2005). In this background, the maturation of prApe1 under starvation conditions is due to autophagy, allowing us to use a western blot-based "pulse/chase" analysis. Cells were grown to early log phase in SMD medium, shifted to SD-N and protein extracts examined by western blot. The *vac8Δ* strain accumulated only prApe1 during vegetative growth, but it was able to efficiently deliver the precursor to the vacuole by autophagy, where it was processed to the mature form (Figure 2.1C). The *atg1Δ* mutant again served as a negative control and accumulated only the precursor form, prApe1, under both conditions. As with *vac8Δ* cells, we observed the mature aminopeptidase I (Ape1) band by immunoblot in the *vac8Δ atg22Δ* double deletion mutant after shifting to starvation conditions, supporting our conclusion of a normal autophagy pathway in the absence of Atg22. We also examined the kinetics of prApe1 maturation through the Cvt pathway in the *atg22Δ* mutant using a radioactive pulse-chase analysis and found essentially normal processing (our unpublished data) in agreement with the previously published results (Suriapranata et al., 2000). Taken together, these data suggested that Atg22 is not defective in either autophagy or the Cvt pathway.

Breakdown of Autophagic Bodies is Kinetically Delayed in the atg22Δ Mutant.

Suriapranata et al., (2000) observed the accumulation of autophagic bodies with 350 nm diameter inside the vacuole by electron microscopy in the *atg22Δ* mutant, which suggests a defective autophagy phenotype. However, based on our data, the *atg22Δ* mutant

displayed normal autophagy, at levels similar to the wild-type strain. This finding suggested that the vacuolar lysis of autophagic bodies should be also normal. To address this apparent discrepancy, we examined the vacuolar accumulation of autophagic bodies using electron microscopy. To minimize potential differences, we chose the same strain background, WCG4a, as used in the previous study. Autophagic bodies are single-membrane vesicles that result from the fusion of autophagosomes with the vacuole; once delivered into the vacuolar lumen, they are broken down in a Pep4-dependent manner. Therefore, we chose the wild-type and *pep4Δ* mutant strain as negative and positive controls, respectively.

We first examined the cells after shifting to SD-N for 4 h. As shown in Figure 2.2A, the *pep4Δ* mutant accumulated autophagic bodies within the vacuole lumen as expected. In contrast, the wild-type strain did not accumulate autophagic bodies at all (our unpublished data), because they were rapidly broken down. As with the *pep4Δ* strain, we also observed the accumulation of some autophagic bodies inside the vacuole in the *atg22Δ* mutant. To compare the accumulation phenotype between the *atg22Δ* and *pep4Δ* mutants, we quantified the data (Figure 2.2B). We determined the number of autophagic bodies per vacuole, only counting those cells containing similar sized vacuoles. In the *atg22Δ* mutant, the highest proportion of the vacuoles at the 4-h time point contained zero autophagic bodies, and the average number was 3.74 ± 3.87 (Figure 2.2C). However, in the *pep4Δ* mutant, the average number of accumulated autophagic bodies per vacuole was 10.14 ± 4.03, with seven to nine autphagic bodies in 32% of the vacuoles. Thus, the *atg22Δ* mutant accumulated far fewer autophagic bodies than the *pep4Δ* mutant. This result suggested two possibilities: either fewer autophagosomes were produced in the *atg22Δ*

mutant, or the breakdown of the autophagic bodies was partially defective and/or kinetically delayed.

The normal autophagy phenotype observed in the *atg22Δ* mutant excluded the first possibility. To test the second possibility, we extended our electron microscopy analysis by observing the accumulation of autophagic bodies in cells starved for 6 h. As shown in Figures 2.2, A and B, *atg22Δ* mutant cells accumulated fewer autophagic bodies at 6 h compared to cells that had been starved for 4 h. The percentage of vacuoles containing zero autophagic bodies increased from 31.5% at 4 h to 38.9% at 6 h. Similarly, the vacuoles containing one to three autophagic bodies increased from 22% to 29.6%. The average number of autophagic bodies per vacuole decreased to 2.24 ± 2.31 (Figure 2.2C). In contrast, in the *pep4Δ* mutant, it was difficult to discern the vacuole boundary because the organelles were essentially filled with autophagic bodies at this time point. The average number of autophagic bodies increased to 15.01 ± 2.86, and >75% of the cells contained 13 to 18 autophagic bodies. Taken together, this result strongly supported our hypothesis that autophagic bodies in the *atg22Δ* mutant were indeed gradually broken down, with the rate of degradation much slower than in the wild-type strain. Thus, partially accumulated autophagic bodies seen in this mutant might be due to a kinetic delay in the breakdown process.

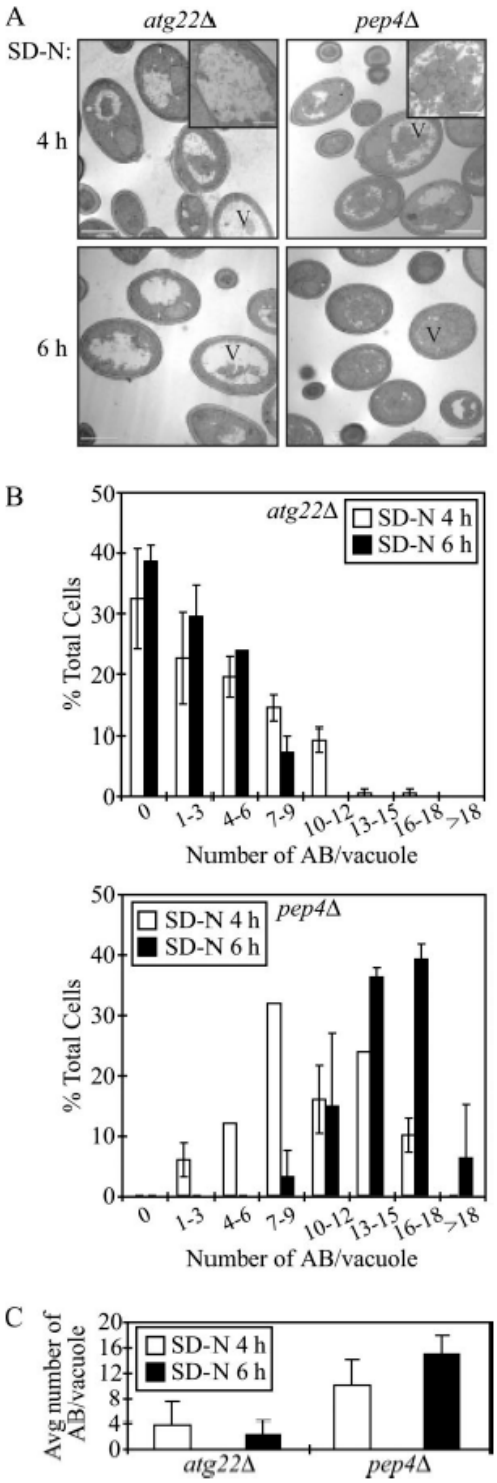
A
atg22Δ
pep4Δ
SD-N:
4 h
6 h
V
B
atg22Δ
SD-N 4 h
SD-N 6 h
% Total Cells
0
10
20
30
40
50
0
1-3
4-6
7-9
10-12
13-15
16-18
>18
Number of AB/vacuole
pep4Δ
SD-N 4 h
SD-N 6 h
% Total Cells
Number of AB/vacuole
C
Avg number of AB/vacuole
SD-N 4 h
SD-N 6 h
0
4
8
12
16
20
atg22Δ
pep4Δ

Figure 2.2. **The *atg22Δ* mutant cells display a kinetic delay in the breakdown of autophagic bodies**. (A) The *atg22Δ* (ZFY1), and *pep4Δ* (ZFY2) strains were grown to mid-log phase in YPD, and shifted to SD-N medium for 4 and 6 h. Cells were fixed and then examined by electron microscopy as described in MATERIALS AND METHODS. The bars in the main images (X7,900) and insets (X19,000) represent 2 and 0.5 μm, respectively. (B) Quantification of autophagic body (AB) accumulation. The number of autophagic bodies in ~100 or 50 cells containing vacuoles of similar size in *atg22Δ* and *pep4Δ* cells, respectively, were quantified. The error bars represent the SD. (C) The average number of vacuoles from the quantification in (B) is depicted.

Atg22 is a Vacuolar Integral Membrane Protein.

To identify the molecular function of Atg22, we searched databases, but we found that Atg22 does not show significant similarity with characterized proteins in other organisms. *ATG22* encodes a protein of 528 amino acids with a predicted molecular mass of 58 kDa. Based on TMpred hydrophobicity analysis (http://www.ch.embnet.org/software/ TMPRED_form.html), Atg22 is predicted to contain 11 to 12 transmembrane helices (Figure 2.3A). A computer-based analysis was carried out to identify all members of the major facilitator superfamily (permeases) in *S. cerevisiae* that are characterized by two structural units of six transmembrane-spanning α-helical segments connected by a cytoplasmic loop (Nelissen et al., 1997). These parameters allowed the consideration of proteins with a length of 500-600 amino acids, making up a total of 12 transmembrane-spanning segments. Within this study, Atg22 is characterized as a predicted permease with unknown function. Additionally, Atg22 shows limited similarity with some putative transporters, such as the multidrug-efflux transporter Bmr3 from *B. subtilis* (Ohki and Murata, 1997; Suriapranata et al., 2000). To gain more insight about Atg22, we performed several experiments to examine the biosynthesis of the protein.

First, to assess whether Atg22 is an integral membrane protein, we carried out subcellular fractionation. We generated a functional C-terminal 3xHA fusion at the chromosomal *ATG22* locus. Lysed spheroplasts of the strain expressing Atg22-3xHA (ZFY36) were separated into soluble and pelletable fractions. As shown in Figure 2.3B, Atg22 was found predominantly in the pellet fraction when spheroplasts were lysed in the presence of buffer alone. Similarly, 1.0 M KCl did not extract Atg22 into the supernatant fraction (our unpublished data), and Na_2CO_3 at pH 10.5 solubilized only a small amount of the protein, indicating that Atg22 is not a peripheral membrane protein. In contrast, extraction with Triton X-100 completely solubilized Atg22 into the supernatant fraction. Cytosolic Pgk1 was almost completely absent from the pellet fraction, indicating the successful lysis of spheroplasts and separation of soluble and pelletable fractions. Vma4, a peripheral vacuole membrane protein, was extracted into the supernatant fraction in the presence of KCl (our unpublished data) and Na_2CO_3. Pho8, an integral membrane protein, served as a positive control, and displayed a similar fractionation pattern as seen with Atg22. Thus, combined with the hydrophobicity analysis, this result strongly indicated that Atg22 is an integral membrane protein.

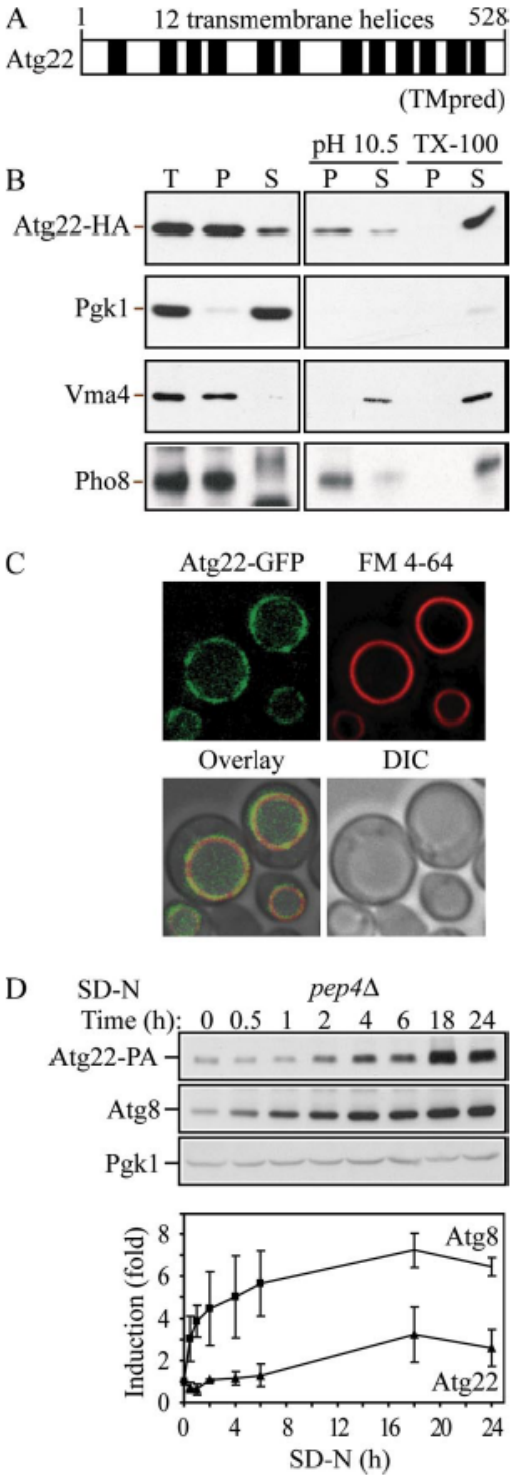
A
1
12 transmembrane helices
528
Atg22
(TMpred)
B
pH 10.5
TX-100
T P S P S P S
Atg22-HA
Pgk1
Vma4
Pho8
C
Atg22-GFP
FM 4-64
Overlay
DIC
D
SD-N
pep4Δ
Time (h): 0 0.5 1 2 4 6 18 24
Atg22-PA
Atg8
Pgk1
Induction (fold)
Atg8
Atg22
SD-N (h)

Figure 2.3. **Atg22 is an integral vacuolar membrane protein**. (A) Hydrophobicity analysis based on TMpred (Hofmann and Stoffel, 1993) predicts 12 transmembrane helices, which are indicated schematically. (B) Atg22 is an integral membrane protein. Cells expressing Atg22-3xHA (ZFY36) were grown in YPD, converted to spheroplasts, and osmotically lysed and fractionated into total (T), supernatant (S), and pellet (P) fractions, as described in MATERIALS AND METHODS. The resulting pellet was subjected to the indicated treatment: 0.5 mM Na_2CO_3, pH 10.5, or 1% Triton X-100. After centrifugation, S and P fractions were collected and analyzed by immunoblots with anti-hemagglutinin (HA) antibody or the indicated antisera. The positions of Atg22-HA, and the markers Pgk1 (cytosolic), Vma4 (peripheral membrane) and Pho8 (integral membrane) are indicated. (C) Atg22 is localized on the vacuolar membrane. Cells expressing Atg22-GFP (ZFY16) were grown in YPD, treated with FM 4-64 to label vacuoles and analyzed by fluorescence microscopy as described in MATERIALS AND METHODS. DIC, differential interference contrast. (D) The expression level of Atg22 seemed constant under vegetative growth and was induced under nitrogen starvation conditions. Cells expressing Atg22-Protein A (ZFY38) in the background of *pep4Δ* were grown in YPD and shifted to SD-N. At the indicated times, aliquots were removed and analyzed by immunoblot using anti-protein A (PA) antidody and antisera to Atg8 and Pgk1; Pgk1 was used as a loading control. The blot is shown for a representative experiment and the graph plots the data for the three independent experiments. The error bars represent the SD.

Suriapranata et al., (2000) visualized the intracellular localization of Atg22 at the vacuolar membrane, using a plasmid-based fusion protein consisting of GFP fused at the N terminus of Atg22, under the control of the *MET25* promoter. Because of the differences in the phenotype of the *atg22Δ* mutant in our current studies compared to the previously published data, we also examined the subcellular localization of Atg22. The gene encoding GFP was integrated in-frame at the 3' end of *ATG22* at the chromosomal locus, under the control of its native promoter. Cells expressing Atg22-GFP were grown to mid-log phase, treated with FM 4-64, and imaged with a fluorescence microscope. As shown in Figure 2.3C, Atg22 localized primarily to the vacuolar membrane, and it overlapped with the FM 4-64-labeled vacuole. Thus, our result was consistent with that in

the previous study. Taken together, Atg22 is a vacuolar integral membrane protein.

In addition, we also examined the expression level of Atg22 under both vegetative growth and nitrogen starvation conditions. We generated a functional C-terminal 3xProtein A fusion at the chromosomal *ATG22* locus. To eliminate the cleavage of protein A by vacuolar hydrolases, we knocked out the gene encoding vacuolar proteinase A, *PEP4*. The *pep4*Δ cells expressing Atg22-3xProtein A were grown to mid-log phase and then incubated in nitrogen starvation medium. At the indicated time, aliquots were removed and analyzed by western blot using antiserum against protein A. As shown in Figure 2.3D, Atg22 displayed an approximately threefold increase after 18-h starvation, relative to the loading control Pgk1, which displayed a constant level over time. This finding is in agreement with published data indicating a 2.7-fold increase in expression of Atg22 after 1 d of nitrogen depletion (Gasch et al., 2000). As a comparison, we examined Atg8, which is induced by nitrogen starvation (Huang et al., 2000). This protein increased its accumulation in the *pep4Δ* strain immediately when cells were shifted to SD-N, whereas the increase in Atg22 was apparent only after starvation for 2 h. Atg8 also showed a substantially higher level of induction, but both proteins seemed to reach a maximum after 18 h.

Atg22 is a Leucine Effluxer on the Vacuolar Membrane.

Autophagy genes are dispensable for vegetative growth, but they are required for survival during nutrient starvation conditions (Levine and Klionsky, 2004). It has been assumed that an internal nutrient pool provided by autophagy, helps yeast cells sustain viability to survive nutrient deprivation. Accordingly, testing for viability during nitrogen starvation has been used as an assay to assess autophagic capacity. Although *atg22Δ* cells

were not autophagy-defective by most assays, electron microscopy revealed that deletion of Atg22 caused the partial-accumulation of autophagic bodies. Because breakdown of autophagic bodies is required for recycling the cargo contained within, deletion of Atg22 might also cause a loss of viability during nitrogen starvation. To test this possibility, we examined the viability of *atg22Δ* cells incubated in SD-N, by using wild-type and *atg1Δ* cells as positive and negative controls, respectively. As expected, *atg1Δ* cells exhibited a dramatic decrease in cell viability after 4-d starvation, whereas wild-type cells maintained robust viability even under prolonged nitrogen starvation (Figure 2.4A). The *atg22Δ* cells gradually lost viability through 12 d of starvation. The *ATG22* gene expressed on a plasmid restored the viability of the *atg22Δ* cells to the wild-type level (Figure 2.4B), indicating that the loss of viability was due to the absence of Atg22. Thus, there was a certain discrepancy in the data: *atg22Δ* cells displayed normal autophagy by most criteria, but they were starvation sensitive, a characteristic of *atg* mutants.

To resolve this discrepancy, we examined the reason for the starvation sensitivity of the *atg22Δ* strain. Atg22 is an integral vacuolar membrane protein, and its protein sequence places it in a family of permeases. Accordingly, we decided to test whether it was a vacuolar permease. We hypothesized that the absence of a permease would cause a loss of viability in strains that lack the biosynthetic capacity for the substrate of the permease under starvation conditions. To test our hypothesis, we decided to identify the substrate for the putative permease Atg22. The *atg22Δ* strain was auxotrophic for histidine, leucine, lysine and uracil. Thus, we decided to test whether one of these four components could rescue the starvation sensitive phenotype seen in *atg22Δ* cells. Wild-type, *atg1Δ*, and *atg22Δ* cells were starved in SD-N containing each of these components separately

(Figures 2.4, C and D, our unpublished data). The addition of histidine, lysine or uracil was not able to restore viability to the *atg22Δ* strain in SD-N. Similarly, the addition of other amino acids such as isoleucine that could be synthesized by the cell did not affect viability. In contrast, the addition of leucine, or complementation of the *leu2* defect by transformation with a plasmid carrying the *LEU2* gene, restored viability to the wild-type level (Figures 2.4, E and F). These results led us to conclude that Atg22 was a leucine effluxer on the vacuolar membrane.

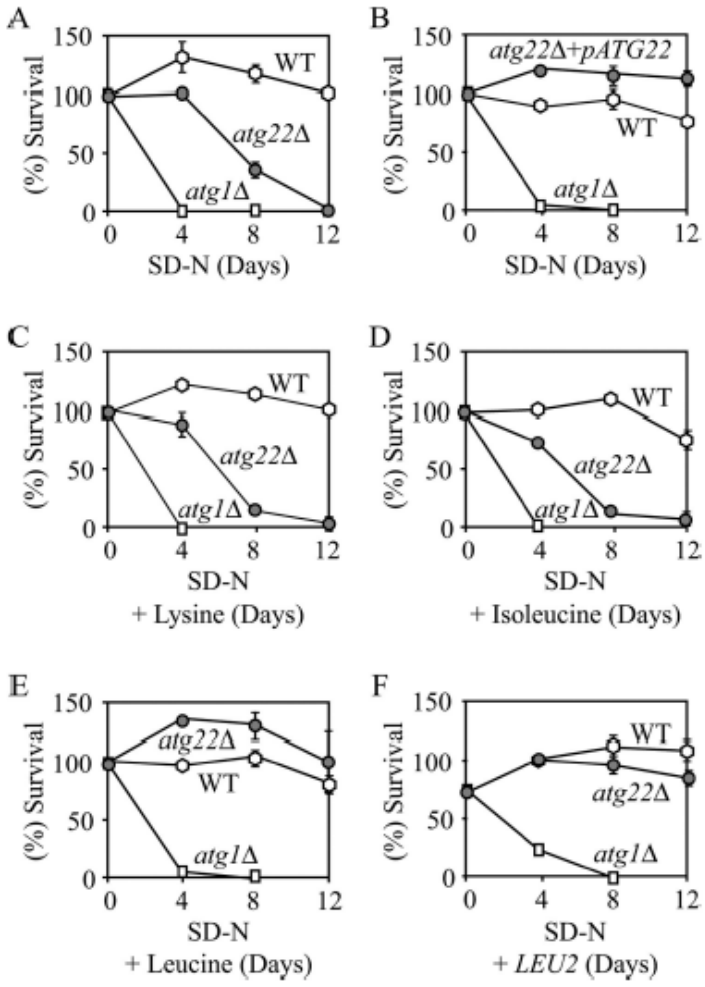

Figure 2.4. ***atg22Δ* mutant cells displayed a loss of viability in starvation conditions**. The wild-type (SEY6210), *atg22Δ* (ZFY6), and *atg1Δ* (WHY1) cells were grown in SMD containing auxotrophic amino acids and nucleosides to OD_{600} = 1.0, and then they were shifted to SD-N. The SD-N included no addition (A), 30 µg/ml lysine (C), 30 µg/ml isoleucine (D), 50 µg/ml leucine (E). Cells harbored the plasmid pCu-ATG22, expressing Atg22 from the *CUP1* promoter (B), or the pRS425 (*LEU2*) plasmid (F). At the indicated day, viability was determined by removing aliquots, plating on YPD in triplicate, and counting the number of colonies per plate after 2-3 d growth. The addition of leucine, or the *LEU2* or *ATG22* genes restored viability of *atg22Δ* cells to wild-type levels. The addition of histidine or uracil resulted in essentially the same loss of viability as seen with lysine. The error bars indicate the SD of two independent experiments.

To obtain direct evidence for the role of Atg22 as a vacuolar leucine effluxer, we decided to examine vacuolar levels of leucine. In addition, we considered the possibility that Atg22 might share substrates with two other vacuolar amino acid effluxers, Avt3 and Avt4, which belong to a family of yeast vacuolar amino acid transporters, designated as Avt1-7, in the yeast *S. cerevisiae* (Russnak et al., 2001). Among this family, Avt1 is required for uptake of neutral amino acids including tyrosine, isoleucine and glutamine; leucine and asparagine might also be substrates because competitive inhibition studies by Sato et al., (1984) have shown that leucine/isoleucine and asparagine/glutamine use the same vacuolar uptake system. Avt3 and Avt4, two closely related proteins, display the same specificity as Avt1, but are synergistically involved in the efflux of amino acids from the vacuole into the cytosol, whereas Avt6 is responsible for the efflux of aspartate and glutamate. Thus, we decided to extend our analysis to Avt3/Avt4. Accordingly, we generated *avt3Δ avt4Δ* double mutant and *atg22Δ avt3Δ avt4Δ* triple mutant strains, and then we carried out amino acid analysis to examine vacuolar levels of various amino acids. The vacuolar amino acid fraction was extracted from log phase-grown cells, as described in

MATERIALS AND METHODS. We normalized the concentrations of the analyzed amino acids to that for arginine, which is stored in the vacuole, but is not a substrate for the Avt3/Avt4 permeases.

As shown in Figure 2.5, the most striking accumulation in all three mutant strains was seen with tyrosine, which showed a sixfold accumulation in the *atg22Δ* cells relative to the wild-type strain. A similar result was seen with the *avt3Δ avt4Δ* double mutant, whereas the triple mutant displayed an even higher level of accumulation, ~8.5-fold higher than wild type. This result confirmed the validity of the analysis because tyrosine is a known substrate of the Avt3/Avt4 effluxers and should accumulate within the vacuole in the corresponding mutant strain. This finding also implicated Atg22 as a vacuolar effluxer for tyrosine.

We were not able to examine levels of glutamine or asparagine, two other substrates of the Avt3/Avt4 effluxers because the concentrations of these amino acids could not be determined separately from glutamate and aspartate, respectively, by the methodology used; however, we continued the analysis by monitoring the levels of leucine and isoleucine, two putative substrates, as well as three control hydrophobic amino acids: valine, methionine and phenylalanine. None of these amino acids displayed as great a-fold increase in accumulation in the mutant strains as seen with tyrosine (Figure 2.5A); however, we also examined the absolute values and the change in concentration in each amino acid (Figure 2.5, B and C). For example, the level of leucine in the *atg22Δ avt3Δ avt4Δ* triple mutant increased to 20.07 nmol/10^8 cells, compared with 15.58 nmol for the wild-type strain, representing a difference of 4.49 nmol, or a 1.3-fold increase. A similar change was seen in the isoleucine levels. In constrast, the control amino acids showed either a minimal

increase or a decrease in concentration (Figure 2.5, B and C). The values for leucine and isoleucine showed a much lower-fold increase than tyrosine; however, this is partly due to the relatively low level of tyrosine accumulation in the vacuoles of wild-type cells. For tyrosine and leucine, the triple mutant demonstrated a greater accumulation of predicted substrate amino acids than seen with either the *atg22Δ* single mutant, or the *avt3Δ avt4Δ* double mutant. Taken together, these results suggested that Atg22 is a vacuolar effluxer for leucine, isoleucine and tyrosine, sharing the same substrates with Avt3 and Avt4.

Figure 2.5. **Yeast vacuoles accumulated a high level of tyrosine, isoleucine and leucine in the absence of Atg22 and/or Avt3/Avt4**. The wild-type (SEY6210), *atg22Δ* (ZFY6), *avt3Δ avt4Δ* (ZFY20), and *avt3Δ avt4Δ atg22Δ* (ZFY22) cells were grown in YPD medium and harvested at log phase. The preparation of vacuolar amino acid pools and analysis of amino acid composition are described in MATERIALS AND METHODS. The results represent the mean and SD of three experiments. The amino acid concentration was normalized to the highest concentration of arginine among three experiments. The results are displayed as the ratio to wild type (A), the absolute values expressed as nanomoles/10^8 cells (B), and the difference from wild type for tyrosine, isoleucine, leucine, valine, methionine and phenylalanine for the wild-type, *atg22Δ* (I), *avt3Δ avt4Δ* (II), *avt3Δ avt4Δ atg22Δ* (III) strains (C). Tyrosine, isoleucine, and leucine accumulated in the mutants, compared to the controls valine, methionine, and phenylalanine. The table lists the vacuolar amino acid level shown in the graph in (B).

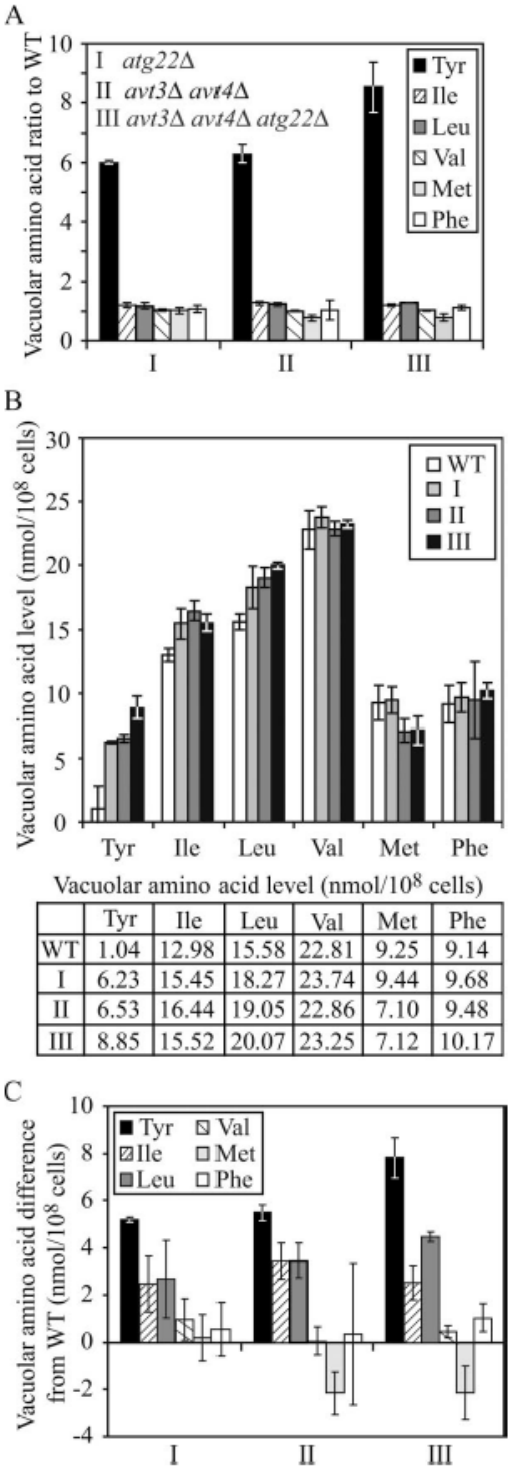

Vacuolar amino acid level (nmol/10^8 cells)

	Tyr	Ile	Leu	Val	Met	Phe
WT	1.04	12.98	15.58	22.81	9.25	9.14
I	6.23	15.45	18.27	23.74	9.44	9.68
II	6.53	16.44	19.05	22.86	7.10	9.48
III	8.85	15.52	20.07	23.25	7.12	10.17

Putative Amino Acid Permeases Mediate the Connection Between Autophagy and Maintenance of Protein Synthesis under Amino Acid Starvation Conditions.

Recently, Onodera and Ohsumi (2005) reported an interesting new phenotype for autophagy-defective mutants (Onodera and Ohsumi, 2005). They found that bulk protein synthesis was substantially reduced under nitrogen starvation conditions in mutants, such as *atg7Δ*, *atg1Δ* and *pep4Δ* cells, compared to the wild-type. They also demonstrated that the synthesis of certain proteins, such as the vacuolar proteinases Ape1 and Prc1 (carboxypeptidase Y), which are up-regulated at the protein expression level upon nitrogen starvation, was dramatically abrogated in the *atg7Δ* strain. Additionally, the total intracellular amino acid pool was reduced in *atg7Δ* cells. They interpreted these results to indicate that free amino acids pools generated during autophagy were a limiting factor for protein synthesis under starvation conditions. Here, we were interested in identifying the mechanistic connection between autophagy and maintenance of amino acid levels and hence protein sysnthesis. Based on the data we have already shown, we hypothesized that in a strain auxotrophic for a particular amino acid, a defect in efflux from the vacuole lumen for this amino acid would cause an intracellular shortage, which would result in a decline in the ability of the cell to maintain general protein synthesis. Because Atg22 may function in part as a leucine effluxer on the vacuolar membrane and our strain is auxotrophic for leucine, we decided to test the protein synthesis capacity in the *atg22Δ* mutant in the presence and absence of leucine.

We first verified that the absence of a single amino acid would induce autophagy by using the GFP-Atg8 processing assay. The *atg22Δ* strain (*his3 leu2 lys2 ura3*) was grown in synthetic complete medium (SMD) lacking either leucine or lysine. Either condition induced autophagy at levels similar to those seen with nitrogen starvation based on

processing of GFP-Atg8 (our unpublished data). Next, we carried out a protein synthesis assay. Cells were grown in SMD and then shifted to SMD-leucine or SMD-lysine, conditions that we had demonstrated would induce autophagy. To examine the effect on protein synthesis, we took advantage of the starvation-induced increase in Ape1 and Prc1 synthesis. Pgk1 did not show a substantial change in protein levels under these conditions and served as a loading control. Using immunoblot analysis, we quantified the protein levels of Ape1 and Prc1 in wild-type, *atg1Δ*, and *atg22Δ* cells. Under both SMD-leucine and SMD-lysine conditions, there was clear protein synthesis in wild-type cells, with up to a 19-fold increase in the Ape1 level and up to a 4.5-fold increase in the level of Prc1 (Figure 2.6, A, B, and D). In contrast, synthesis of Ape1 and Prc1 was essentially blocked in the *atg1Δ* cells under both SMD-leucine and SMD-lysine conditions, in agreement with the previous study by Onodera and Ohsumi (Onodera and Ohsumi, 2005). In *atg22Δ* cells, in SMD-leucine both Ape1 and Prc1 synthesis were minimally elevated even after 12-h starvation, and gradually increased by 14- and 3.4-fold , respectively, only after prolonged (24-h) starvation (Figure 2.6, A, C, and E). In contrast, in SMD-lysine Ape1 and Prc1 synthesis seemed similar to wild type and increased by 17- and 4.2-fold, respectively, with a substantial increase as early as 2 h. Thus, in the *atg22Δ* cells, a reduced level of Ape1 and Prc1 synthesis was only observed under SMD-leucine conditions, supporting our conclusion that Atg22 functions in part as a vacuolar leucine effluxer. Furthermore, this result supported our hypothesis that under amino acid deprivation conditions, permeases mediate the connection between autophagy and the maintenance of amino acid levels in the cytosol, and hence protein synthesis levels, through the efflux of amino acids resulting from autophagy.

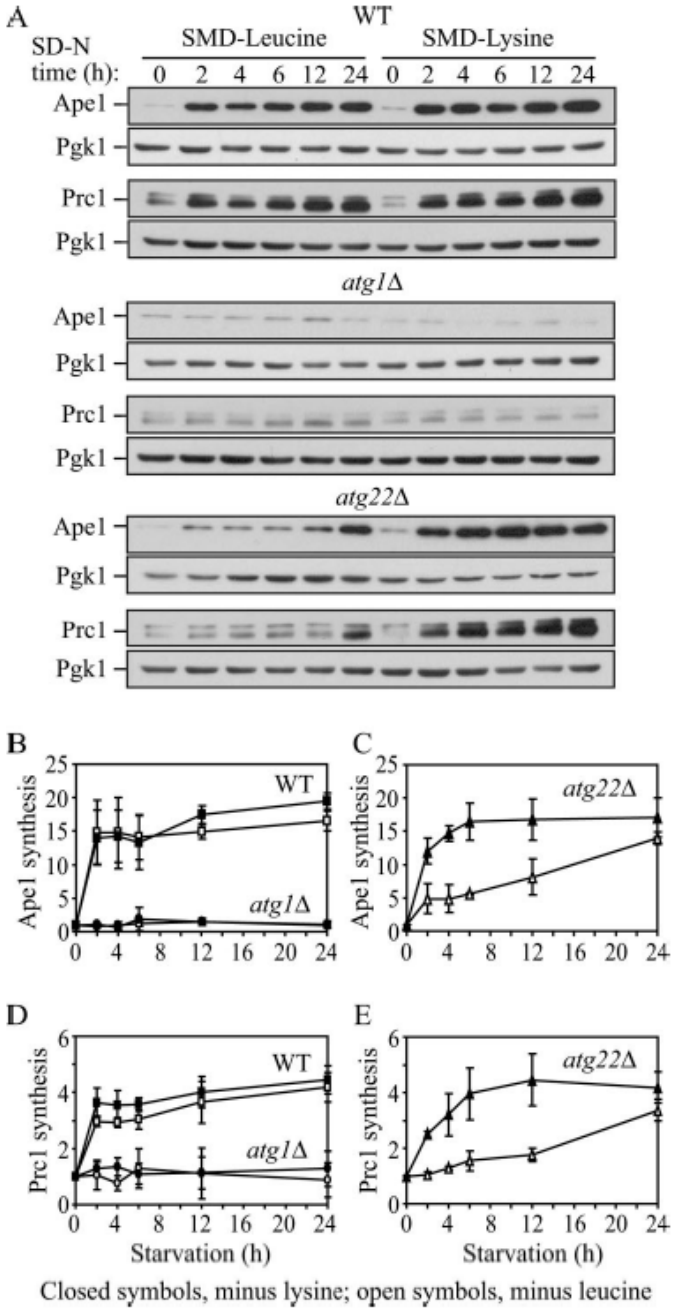

Figure 2.6. **Protein synthesis dependent upon autophagic amino acids was partially defective in *atg22Δ* mutant cells**. (A) The wild-type (SEY6210), *atg1Δ* (WHY1), and *atg22Δ* (ZFY6) cells were grown in SMD and then shifted to SMD-leucine or SMD-lysine to induce autophagy. At the indicated incubation time, aliquots were removed and cell lysates (1.0 OD_{600} unit of cells) were

analyzed by immunoblot with antiserum against Ape1, Prc1, and Pgk1. Pgk1 was used as a loading control. (B-E) Quantification of immunoblots from SMD-leucine (open symbols) or SMD-lysine (closed symbols) in the wild-type (square), *atg1Δ* (circle), and *atg22Δ* (triangle) cells. Band intensities were quantified using NIH Image 1.62 (by Wayne Rasband, National Institutes of Health, Bethesda. MD). The data are the average of three independent experiments and the error bars indicate the SD.

Vacuolar Release of Amino Acids during Starvation Is Essential for Survival.

Having established that permeases mediate autophagy and its physiological role in terms of maintenance of protein synthesis under conditions of amino acid starvation, we decided to investigate whether they are also needed for cell viability, examining the Atg22 and Avt3/Avt4 proteins. Based on our data, the *atg22Δ* cells gradually lost viability through 12 d of starvation (Figure 2.4A), and Ape1 and Prc1 protein synthesis in the *atg22Δ* cells was severely but not completely blocked in SMD-leucine (Figure 2.6). Thus, we hypothesized that Avt3/Avt4 could partially compensate for the defect seen in the absence of Atg22. To address this possibility, we examined an *avt3Δ avt4Δ* strain auxotrophic for both leucine and lysine. Ape1 and Prc1 synthesis were compared under either SMD-leucine or SMD-lysine conditions (Figure 2.7, A, B, and D). Pgk1 again served as a loading control. In the *avt3Δ avt4Δ* cells, Ape1 and Prc1 synthesis was delayed and showed a clear increase only after 12-h starvation in SMD-leucine, whereas there was normal synthesis in SMD-lysine, in support of a role for Avt3/Avt4 as leucine permeases. Accordingly, we hypothesized that the absence of Atg22 along with Avt3/Avt4 might completely block Ape1 and Prc1 synthesis. Thus, we further tested protein synthesis in the *atg22Δ avt3Δ avt4Δ* strain. Ape1 and Prc1 synthesis was hardly detected even after 24-h

starvation in SMD-leucine in the triple deletion strain, but it was relatively unaffected in SMD-lysine conditions (Figure 2.7, A, C, and E). Taken together, these results supported the premise that Atg22, Avt3 and Avt4 are redundant with regard to their function as leucine effluxers on the vacuolar membrane.

To bring our analysis full circle, we decided to examine viability in *avt3Δ avt4Δ* and *atg22Δ avt3Δ avt4Δ* cells. The *avt3Δ avt4Δ* strain was transformed with a plasmid carrying the *TRP1* gene to balance the prototrophy of the *atg22Δ*::*TRP1* deletion, leaving both strains auxotrophic for leucine and lysine. The two strains were then grown in SMD to mid-log phase and incubated in SD-N, or SD-N containing leucine, and viability was measured as described previously. The *avt3Δ avt4Δ* culture lost viability between 5 and 6 d in SD-N (Figure 2.7F), whereas the *atg22Δ avt3Δ avt4Δ* cells displayed a slightly more severe phenotype, completely losing viability by day 4 (Figure 2.7G). Addition of leucine rescued the loss of viability for both mutants for several days, probably until these nutrients became limiting. These results combined with the result seen with *atg22Δ* cells shown in Figure 2.4, suggested that if the efflux of amino acids resulting from autophagy was blocked, the cytosolic shortage of these amino acids would cause a decreased level of general protein synthesis, and, ultimately, cells would lose the ability to survive starvation of the corresponding amino acids.

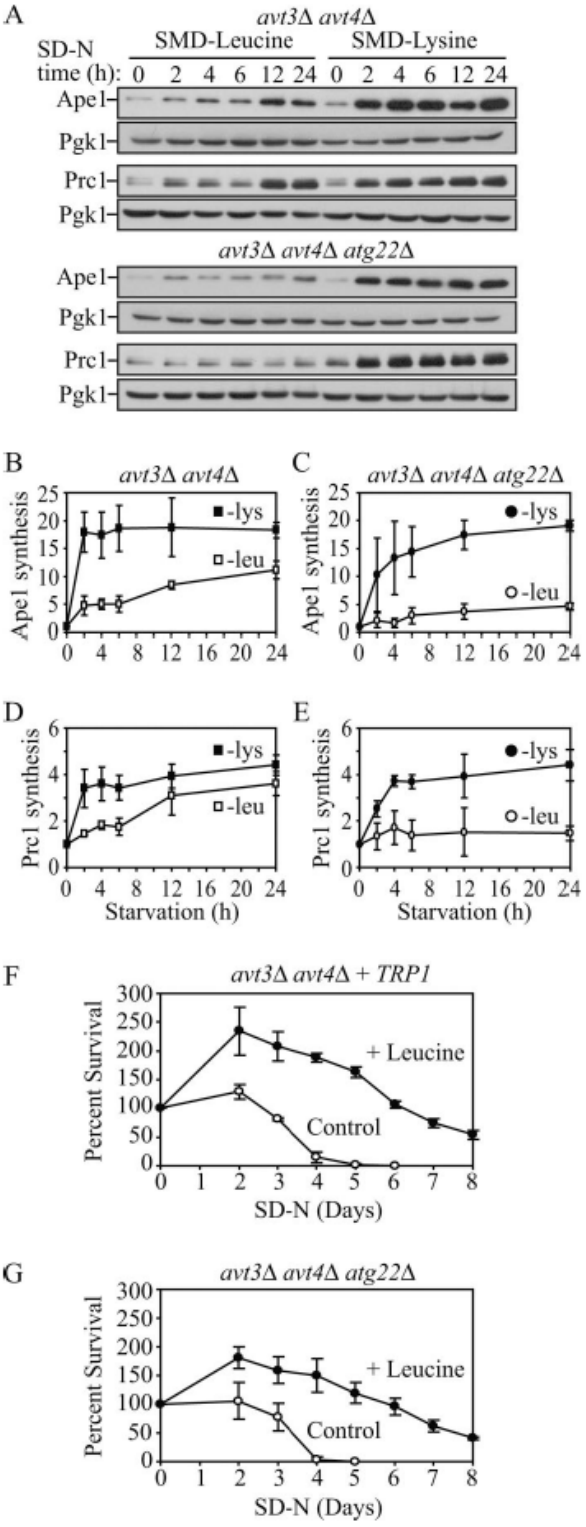
A
avt3Δ avt4Δ
SD-N
SMD-Leucine
SMD-Lysine
time (h): 0 2 4 6 12 24 0 2 4 6 12 24
Ape1
Pgk1
Prc1
Pgk1
avt3Δ avt4Δ atg22Δ
Ape1
Pgk1
Prc1
Pgk1
B
avt3Δ avt4Δ
Ape1 synthesis
-lys
-leu
C
avt3Δ avt4Δ atg22Δ
Ape1 synthesis
-lys
-leu
D
Prc1 synthesis
-lys
-leu
Starvation (h)
E
Prc1 synthesis
-lys
-leu
Starvation (h)
F
avt3Δ avt4Δ + TRP1
Percent Survival
+ Leucine
Control
SD-N (Days)
G
avt3Δ avt4Δ atg22Δ
Percent Survival
+ Leucine
Control
SD-N (Days)

Figure 2.7. **Protein synthesis and survival dependent on autophagic amino acids was reduced in *avt3Δ avt4Δ* mutant cells, and the defect was exacerbated by the *atg22Δ* mutation**. (A) *avt3Δ avt4Δ* (ZFY20) and *avt3Δ avt4Δ atg22Δ* (ZFY22) cells were grown and analyzed for up-regulated protein synthesis as described in the legend to Figure 2.6. (B-E) Quantification of immunoblots from SMD-leucine (open symbols) or SMD-lysine (closed symbols) in the *avt3Δ avt4Δ* (square), *avt3Δ avt4Δ atg22Δ* (circle) cells. Band intensities were quantified as described in the legend to Figure 2.6. The loss of leucine effluxers blocked synthesis of Ape1 and Prc1 during leucine depletion. The *avt3Δ avt4Δ* strain harboring pRS414 (*TRP1*) (F) and *avt3Δ avt4Δ atg22Δ* (G) cells were grown in SMD to mid-log phase and incubated in SD-N or SD-N containing 100 μg/ml leucine. At the indicated days, viability was determined as described in the legend to Figure 2.4. The error bars indicate the SD of three independent experiments. The reduced viability of the *avt3Δ avt4Δ*, and *avt3Δ avt4Δ atg22Δ* mutant cells was partially rescued by addition of leucine.

DISCUSSION

The atg22Δ Mutant is Not Defective in Autophagic Body Breakdown.

One of the main roles of autophagy is to degrade cytoplasm and recycle the resulting macromolecules for reuse in the synthesis of essential components during nutrient stress. Accordingly, autophagic bodies that are delivered into the vacuole lumen must be disintegrated and broken down (Klionsky, 2005). The topic of vesicle breakdown is an important one, as the vacuole is the terminal destination for many cellular delivery pathways; however, little is known about the process of lipid recycling within this organelle. For example, Atg15 is the only putative lipase so far associated with this organelle. In addition, it is not even known how the vacuole membrane is itself protected from degradation. This complication extends to all heterotypic fusion events. That is, the vesicle membrane that fuses with the vacuole must be rapidly removed or protected to prevent its degradation while part of the vacuole limiting membrane and the subsequent loss of vacuolar integrity, which could be deleterious to the cell. Finally, with regard to autophagy, a difference in the susceptibility to lysis of Cvt versus autophagic bodies as suggested by Suriapranata et al. (2000) might provide insight into the origin of the sequestering vesicle membrane, a topic of considerable debate.

As we have demonstrated in this article, in contrast to the previously reported data, Atg22 is not directly involved in intravacuolar vesicle lysis. The steps of autophagy up to and including autophagic body breakdown are essentially normal in the *atg22Δ* mutant, although there is a kinetic delay in breakdown (Figures 2.1 and 2.2). Our data disagree with the conclusion from the previous work (Suriapranata et al., 2000), that the primary

role of Atg22 is in the breakdown of autophagic, but not Cvt bodies. Thus, no data at present suggest a substantial difference between the membranes used for autophagy and the Cvt pathway, nor do they indicate a fundamental difference between autophagic and Cvt bodies with regard to the mechanism of degradation. This finding is supported by recent studies indicating that the origin of the membrane for the Cvt pathway and autophagy is probably the same (Reggiori et al., 2004b).

Atg22 is a Putative Amino Acid Effluxer on the Vacuolar Membrane.

Biochemical analysis of Atg22 indicates that it is an integral membrane protein (Figure 2.3). Localization of Atg22-GFP suggests that this protein is localized on the vacuole-limiting membrane. These data fit well with the predictions based on its amino acid sequence that Atg22 functions as a permease. Analysis of amino acid concentrations suggested that Atg22 is an effluxer for tyrosine, but it also revealed that vacuolar accumulation of leucine in the *atg22Δ* mutant (Figure 2.5). We were unsuccessful in carrying out analyses of amino acid efflux by using vacuoles containing radiolabeled amino acids; thus, we do not have direct evidence for the function of Atg22 as a leucine effluxer. However, the Avt3/4 proteins have been characterized as permeases for leucine and other amino acids in addition to tyrosine. The defect in protein synthesis seen in the absence of leucine in the *atg22Δ* strain along with the viability assays suggested that leucine is also a substrate for Atg22 (Figures 2.4, 2.6, and 2.7).

Release of Amino Acid from the Vacuole Is Essential for Viability as the Last Stage of Autophagy.

The finding that Ape1 synthesis in the *atg22Δ* cells was severely but not completely

blocked in SMD-leucine (Figure 2.6) indicated there might be redundant leucine effluxers that could partially compensate for the defect. At present, only Avt3/Avt4 and Avt6 have been identified as vacuolar amino acid effluxers in *S. cerevisiae*, and leucine has been shown to be a possible substrate of Avt3 and Avt4 (Sato et al., 1984). Analysis of both Ape1 and Prc1 protein synthesis and cell viability in *avt3Δ avt4Δ* and *atg22Δ avt3Δ avt4Δ* strains (Figure 2.7) suggested that all three proteins are redundant leucine effluxers and part of the same family of permeases. In support of this finding, vacuolar amino acid analysis indicated an increase in leucine, isoleucine and tyrosine levels in the double and triple mutants (Figure 2.5). We note that there is precedence for redundancy in vacuolar permeases; the Vba1, Vba2, and Vba3 proteins all seem to function in influx of basic amino acids (Shimazu et al., 2005). To examine the nature of this redundancy, we transformed the *avt3Δ avt4Δ* strain with a plasmid overexpressing the *ATG22* gene under the control of the *CUP1* promoter. Overexpression of Atg22, however, did not rescue the decrease in viability of the *avt3Δ avt4Δ* strain or rescue the defect in protein synthesis in medium lacking leucine (our unpublished data), suggesting that the functions of these permeases are not completely overlapping. Finally, these results verify the previously untested assumption that vacuolar amino acid efflux is essential for cell viability under starvation conditions.

Breakdown of Autophagic Bodies is Kinetically Delayed in the *atg22Δ* Mutant.

Although the steps of autophagy up to and including breakdown are essentially normal in the *atg22Δ* mutant, there is a partial accumulation of autophagic bodies. The present study, however, makes it clear that the *atg22Δ* mutant displays only a kinetic block in breakdown (Figure 2.2). One response of cells to long-term amino acid or nitrogen

starvation is the up-regulation of certain genes, including those for some autophagy-related proteins (such as Atg8) and vacuolar proteinases (such as Pep4, Prb1, and Prc1) (Gasch et al., 2000). Thus, the role of Atg22 as a leucine effluxer provides an explanation for an indirect effect on autophagic body breakdown. The *atg22Δ* mutant will be limited for leucine in strains that are *leu2* auxotrophs when incubated in starvation conditions. As a result, proteins that are normally up-regulated during starvation will not be synthesized. The proteinases Pep4, Prb1, and Prc1 are critical for breakdown of autophagic bodies, and they are normally substantially induced during starvation. The strain used by Suriapranata et al. (2000) as well as those used in the present study are *leu2* mutants. Thus, we propose that the inability to synthesize adequate levels of Pep4, Prb1, and Prc1, which are normally up-regulated approximately eight-, nine-, and sevenfold under nitrogen starvation, respectively (Gasch et al., 2000) (Figures 2.6 and 2.7), could account for the observed kinetic delay in autophagic body degradation.

Recycling Model for Autophagy.

When cells lack essential nutrients, autophagy is induced, which generates an internal nutrient pool to supply the missing components essential for survival (Kuma et al., 2004; Levine and Klionsky, 2004; Lum et al., 2005). However, there are no mechanistic data that specifically connect the breakdown process with subsequent cytosolic protein synthesis. In this study, using genetics and biochemical assays, we have provided this link by demonstrating that 1) Atg22 most likely functions as a leucine effluxer; and 2) vacuolar permeases mediate the connection between autophagy and its associated protein degradation, and maintenance of amino acid levels in the cytosol and hence protein synthesis levels. Thus, our study has allowed us to propose a “recycling” model that

includes the efflux of macromolecules from the vacuole as the final step of autophagy (Figure 2.8).

The vacuole/lysosome is a highly complex organelle that is characterized as having an acidic lumen, and harboring a range of hydrolytic enzymes. These hydrolases are involved in the degradation of various substrates, and in concert with vacuolar permeases, they allow the homeostatic control of cytosolic nutrients used for anabolic and catabolic processes. Importantly, the vacuole it is not a "dead-end" compartment, and this study is the first report with the efflux process being defined as the final step of autophagy.

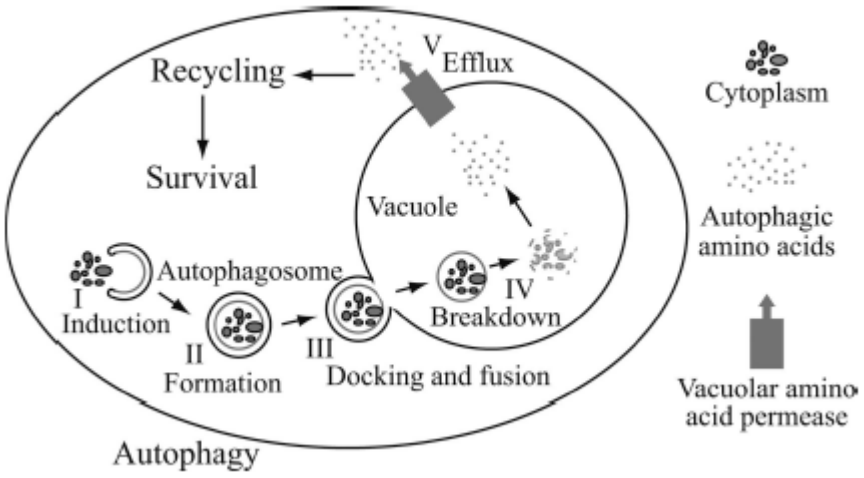

Figure 2.8. **Model for autophagy including the final step of amino acid efflux**. Autophagy is depicted as occurring in five discrete stages as shown. Additional steps including cargo recognition, vesicle nucleation and retrieval of Atg proteins have been omitted for simplicity. See the text for a discussion of the role of efflux.

REFERENCES

Abeliovich, H., C. Zhang, W.A. Dunn, Jr., K.M. Shokat, and D.J. Klionsky. 2003. Chemical genetic analysis of Apg1 reveals a non-kinase role in the induction of autophagy. *Mol Biol Cell*. 14:477-90.

Cheong, H., T. Yorimitsu, F. Reggiori, J.E. Legakis, C.-W. Wang, and D.J. Klionsky. 2005. Atg17 regulates the magnitude of the autophagic response. *Mol Biol Cell*. 16:3438-53.

Epple, U.D., I. Suriapranata, E.L. Eskelinen, and M. Thumm. 2001. Aut5/Cvt17p, a putative lipase essential for disintegration of autophagic bodies inside the vacuole. *J Bacteriol*. 183:5942-55.

Gasch, A.P., P.T. Spellman, C.M. Kao, O. Carmel-Harel, M.B. Eisen, G. Storz, D. Botstein, and P.O. Brown. 2000. Genomic expression programs in the response of yeast cells to environmental changes. *Mol Biol Cell*. 11:4241-57.

Huang, W.-P., S.V. Scott, J. Kim, and D.J. Klionsky. 2000. The itinerary of a vesicle component, Aut7p/Cvt5p, terminates in the yeast vacuole via the autophagy/Cvt pathways. *J Biol Chem*. 275:5845-51.

Kaiser, C.A., and R. Schekman. 1990. Distinct sets of SEC genes govern transport vesicle formation and fusion early in the secretory pathway. *Cell*. 61:723-33.

Kim, J., V.M. Dalton, K.P. Eggerton, S.V. Scott, and D.J. Klionsky. 1999. Apg7p/Cvt2p is required for the cytoplasm-to-vacuole targeting, macroautophagy, and peroxisome degradation pathways. *Mol Biol Cell*. 10:1337-51.

Kim, J., and D.J. Klionsky. 2000. Autophagy, cytoplasm-to-vacuole targeting pathway, and pexophagy in yeast and mammalian cells. *Annu Rev Biochem*. 69:303-42.

Klionsky, D.J. 2005. The molecular machinery of autophagy: unanswered questions. *J Cell Sci*. 118:7-18.

Klionsky, D.J., J.M. Cregg, W.A. Dunn, Jr., S.D. Emr, Y. Sakai, I.V. Sandoval, A. Sibirny, S. Subramani, M. Thumm, M. Veenhuis, and Y. Ohsumi. 2003. A unified nomenclature for yeast autophagy-related genes. *Dev Cell*. 5:539-45.

Kuma, A., M. Hatano, M. Matsui, A. Yamamoto, H. Nakaya, T. Yoshimori, Y. Ohsumi, T. Tokuhisa, and N. Mizushima. 2004. The role of autophagy during the early neonatal starvation period. *Nature*. 432:1032-6.

Levine, B., and D.J. Klionsky. 2004. Development by self-digestion: molecular mechanisms and biological functions of autophagy. *Dev Cell*. 6:463-77.

Lum, J.J., D.E. Bauer, M. Kong, M.H. Harris, C. Li, T. Lindsten, and C.B. Thompson. 2005. Growth factor regulation of autophagy and cell survival in the absence of apoptosis. *Cell*. 120:237-48.

Nelissen, B., R. De Wachter, and A. Goffeau. 1997. Classification of all putative permeases and other membrane plurispanners of the major facilitator superfamily encoded by the complete genome of *Saccharomyces cerevisiae*. *FEMS Microbiol Rev*. 21:113-34.

Noda, T., A. Matsuura, Y. Wada, and Y. Ohsumi. 1995. Novel system for monitoring autophagy in the yeast *Saccharomyces cerevisiae*. *Biochem Biophys Res Commun*. 210:126-32.

Ohki, R., and M. Murata. 1997. bmr3, a third multidrug transporter gene of *Bacillus subtilis*. *J Bacteriol*. 179:1423-7.

Ohsumi, Y., K. Kitamoto, and Y. Anraku. 1988. Changes induced in the permeability barrier of the yeast plasma membrane by cupric ion. *J Bacteriol*. 170:2676-82.

Onodera, J., and Y. Ohsumi. 2005. Autophagy is required for maintenance of amino acid levels and protein synthesis under nitrogen starvation. *J Biol Chem*. 280:31582-6.

Reggiori, F., C.-W. Wang, U. Nair, T. Shintani, H. Abeliovich, and D.J. Klionsky. 2004. Early stages of the secretory pathway, but not endosomes, are required for Cvt vesicle and autophagosome assembly in *Saccharomyces cerevisiae*. *Mol Biol Cell*. 15:2189-204.

Robinson, J.S., D.J. Klionsky, L.M. Banta, and S.D. Emr. 1988. Protein sorting in *Saccharomyces cerevisiae*: isolation of mutants defective in the delivery and processing of multiple vacuolar hydrolases. *Mol Cell Biol*. 8:4936-48.

Russnak, R., D. Konczal, and S.L. McIntire. 2001. A family of yeast proteins mediating bidirectional vacuolar amino acid transport. *J Biol Chem*. 276:23849-57.

Sato, T., Y. Ohsumi, and Y. Anraku. 1984. An arginine/histidine exchange transport system in vacuolar-membrane vesicles of *Saccharomyces cerevisiae*. *J Biol Chem*. 259:11509-11.

Shimazu, M., T. Sekito, K. Akiyama, Y. Ohsumi, and Y. Kakinuma. 2005. A family of basic amino acid transporters of the vacuolar membrane from *Saccharomyces cerevisiae*. *J Biol Chem*. 280:4851-7.

Shintani, T., W.P. Huang, P.E. Stromhaug, and D.J. Klionsky. 2002. Mechanism of cargo selection in the cytoplasm to vacuole targeting pathway. *Dev Cell*. 3:825-37.

Suriapranata, I., U.D. Epple, D. Bernreuther, M. Bredschneider, K. Sovarasteanu, and M. Thumm. 2000. The breakdown of autophagic vesicles inside the vacuole depends on Aut4p. *J Cell Sci*. 113 (Pt 22):4025-33.

Teter, S.A., K.P. Eggerton, S.V. Scott, J. Kim, A.M. Fischer, and D.J. Klionsky. 2001. Degradation of lipid vesicles in the yeast vacuole requires function of Cvt17, a putative lipase. *J Biol Chem*. 276:2083-7.

Thumm, M., R. Egner, B. Koch, M. Schlumpberger, M. Straub, M. Veenhuis, and D.H. Wolf. 1994. Isolation of autophagocytosis mutants of *Saccharomyces cerevisiae*. *FEBS Lett*. 349:275-80.

CHAPTER 4

Dual Positive and Negative Regulatory Roles of the Cyclin-Dependent Kinase Pho85 Orchestrate Induction of Autophagy in *Saccharomyces cerevisiae*

ABSTRACT

As a major intracellular degradation pathway, autophagy is tightly regulated to prevent cellular dysfunction in all eukaryotic cells. The rapamycin-sensitive Tor kinase complex 1 is a major regulator of autophagy. Several other nutrient-sensory kinases also play critical roles to precisely modulate autophagy; however, the network of regulatory mechanisms remains largely elusive. We used genetic analyses to elucidate the mechanism by which the stress-responsive, cyclin-dependent kinase, Pho85 and its corresponding cyclins antagonistically modulate autophagy in *Saccharomyces cerevisiae*. When complexed with cyclins Pho80 and Pcl5, Pho85 negatively regulates autophagy through downregulating the protein kinase Rim15, and the transcription factors Pho4 and Gcn4. The cyclins Clg1, Pcl1 and Pho80, in concert with Pho85, positively regulate autophagy through promoting the degradation of Sic1, a negative regulator of autophagy that targets Rim15. Our results suggest a model in which Pho85 has opposing roles in autophagy regulation.

INTRODUCTION

Eukaryotic cells confronted by various stresses in their intracellar and extracellular environment can initiate an adaptive response, autophagy, for survival (Levine and Klionsky, 2004). As a major intracellular degradation pathway, autophagy helps cells to get rid of long-lived proteins and damaged and/or unused organelles. Autophagy involves a dynamic rearrangement of subcellular membranes to sequester portions of cytoplasm into a double-membrane vesicle, termed an autophagosome, which is delivered to a degradative organelle, the vacule/lysosome, resulting in the breakdown of the contents, and finally, the resulting macromolecules are released back into the cytosol for recycling (Huang and Klionsky, 2007; Yang et al., 2006). Autophagy is an evolutionarily conserved pathway that occurs in all eukaryotic cells (Reggiori and Klionsky, 2002). In yeast, autophagy helps cells survive nutrients limitation; in mammalian cells, autophagy is implicated in many physiological events, such as development and differentiation, antiaging, cell growth control, cancer, and innate and adaptive immunity (Levine and Deretic, 2007; Levine and Klionsky, 2004).

As an intracellular degradative pathway, autophagy is tightly regulated in order to prevent insufficient or excess levels, both of which are harmful for cells. The mechanism of autophagy regulation has been studied extensively. A schematic overview of the key components involved in autophagy regulation is depicted in Figure 4.1A. The target of rapamycin (Tor) signaling pathway plays a major role in regulating autophagy induction (Carrera, 2004). Tor proteins (Tor1 and Tor2) are conserved serine/threonine protein kinases, that are linked to nutritional controls, especially the availability of nitrogen, and they regulate many processes, including protein synthesis and autophagy. Tor proteins

form two functional distinct protein complexes, Tor complex 1 and 2 (TORC1 and TORC2) (Loewith et al., 2002). Only TORC1 has primary functions in autophagy, and is particularly sensitive to the drug rapamycin. In nutrient-rich conditions, TORC1 is active and inhibits autophagy; upon nutrient starvation, TORC1 is inhibited and autophagy is induced. Treatment with rapamycin can largely mimic nutrient starvation, inhibiting TORC1 and allowing the induction of autophagy (Noda and Ohsumi, 1998). However, in mammalian cells, rapamycin is a relatively poor inducer of autophagy (Takeuchi et al., 2005). More recent data reveal that Torin, an ATP-competitive mTOR inhibitor, disrupts mTORC1-dependent phenotypes more completely than rapamycin (Thoreen et al., 2009).

In addition to TORC1, other nutrient-regulated protein kinase signaling pathways are also implicated in autophagy regulation. For example, the Ras/cAMP-dependent protein kinase A (PKA) signaling pathway negatively regulates autophagy; constitutive activation of PKA prevents the induction of autophagy by rapamycin or nutrient starvation, whereas inactivation of PKA induces autophagy in rich conditions without rapamycin (Budovskaya et al., 2004; Schmelzle et al., 2004). Sch9 is a homologue of mammalian protein kinase B (PKB)/Akt or p70S6 kinase (Urban et al., 2007). Simultaneous inactivation of PKA and Sch9 triggers a stronger induction of autophagy that is seen with inactivation of just PKA, and the induction is independent of effects on TORC1; further inactivation of TORC1 causes an additive effect on autophagy (Yorimitsu et al., 2007). These observations suggest a model in which TORC1, PKA and Sch9 cooperatively regulate autophagy, at least in part, in parallel. The Gcn2 kinase signaling pathway is also involved in the regulation of autophagy. In response to amino acid starvation, Gcn2 derepresses *GCN4* mRNA translation. Gcn4 is a master transcriptional activator and initiates transcriptional induction

of nearly all amino acid biosynthetic genes (Hinnebusch, 2005). Moreover, rapamycin-induced TORC1 inactivition activates Gcn2 through dephosphorylation, leading to translational derepression of GCN4 mRNA (Cherkasova and Hinnebusch, 2003; Kubota et al., 2003). Upon loss of Gcn2 or Gcn4, autophagy is impaired (Talloczy et al., 2002).

Pho85, a yeast cyclin-dependent kinase (CDK), is structurally and functionally related to the mammalian kinase, CDK5. It has multiple functions and associates with ten different cyclin regulatory subunits, each of which potentially direct Pho85 to different target substrates. Thus, Pho85 in conjugation with different cyclins can discharge numerous biological functions, including phosphate metabolism, cell cycle control, cell polarity establishment, and the regulation of autophagy (Huang et al., 2007). Pho85 negatively regulates starvation-induced autophagy, antagonistically with a positive regulator of autophagy, Snf1, the closest yeast homologue of the mammalian AMP-activated protein kinase (AMPK) (Wang et al., 2001b). It is unknown, however, which potential cyclin(s) associates with Pho85 to negatively regulate autophagy (Wang et al., 2001b).

Ten Pho85 cyclin (Pcl) partners were identified primarily through sequence homology and two-hybrid screens (Measday et al., 1997). Based on sequence alignment within a region called the “cyclin box”, they are grouped into two subfamilies: the Pcl1,2 subfamily (Pcl1, Pcl2, Pcl5, Pcl9 and Clg1) and the Pho80 family (Pho80, Pcl6, Pcl7, Pcl8, Pcl10). The Pho80-Pho85 complex signals a response to the stress of phosphate starvation. When inorganic phosphate is abundant, the Pho80-Pho85 kinase is active, phosphorylating and inactivating the transcription factor Pho4, maintaining Pho4 cytosolic localization, where it is unable to activate transcription of the phosphate acquisition genes. When inorganic

phosphate becomes limiting, the kinase activity of Pho80-Pho85 is inhibited, thereby allowing the activation of Pho4 and leading to the expression of genes that promote the survival response to phosphate starvation (Carroll and O'Shea, 2002). The Pho80-Pho85 complex also negatively regulates cell entery into a quiescent state (G_0) in response to nutrient availability, through direct phosphorylation and retention of Rim15 in the cytosol (Wanke et al., 2005). Rim15 is a protein kinase, which functions as a key controller of many aspects of the G_0 program through its ability to integrate signaling from TORC1, PKA, Sch9 and Pho80-Pho85 pathways (Swinnen et al., 2006). Moreover, Rim15 is also required for the induction of autophagy that occurs upon inhibition of PKA and Sch9 (Yorimitsu et al., 2007). Another well-studied ancillary partner of Pho85 is the cyclin Pcl5. Pcl5 targets Pho85 specifically to Gcn4, eventually causing the degradation of this transcription factor (Shemer et al., 2002).

Cln1, Cln2 and Cln3 are G_1-specific cyclins that associate with Cdc28, the major yeast CDK required for cell cycle progression (Bloom and Cross, 2007). Pho85 plays a role in the cell cycle when complexed with the related G_1-specific cyclins, Pcl1, Pcl2 and Pcl9, which are expressed specifically in the G_1 phase of the cell cycle (Tennyson et al., 1998). Pcl1,2-Pho85 complexes become essential in cells lacking Cln1 and Cln2 (Espinoza et al., 1994; Measday et al., 1994). Most of the characterized Pho85 substrates that have a role in cell cycle progression are also substrates of Cdc28, such as Rga2 and Sic1. The GTPase-activating protein (GAP) Rga2 is one of the substrates of G_1-specific forms of Pho85 and has a role in polarized growth (Sopko et al., 2007). Sic1 is a stoichiometric, cyclin-dependent kinase (CDK) inhibitor that specifically inhibits S phase Clb cyclin-containing Cdc28 kinase complexes, hence blocking the onset of S phase

(Mendenhall et al., 1995). This inhibition is removed after phosphorylation of Sic1 followed by degradation (Deshaies and Ferrell, 2001). The major kinases involved in controlling Sic1 stability are the Cln-Cdc28 Cdks (Verma et al., 1997). However, Pho85 is also involved in this process because it phosphorylates Sic1 *in vitro* and prompts Sic1 degradation *in vivo* (Nishizawa et al., 1998). A more recent study shows that Pho85 is required for cells arrested in G_1 after DNA damage to return to cell cycle progression, through targeting Sic1 for degradation (Wysocki et al., 2006). However, at this point, it is still unclear which is the actual cyclin(s) of Pho85 required *in vivo* for the phosphorylation and destabilization of Sic1 (Carroll and O'Shea, 2002).

A role of the CDK inhibitor in the regulation of autophagy is suggested by several studies in mammalian cells. p27, a mammalian CDK2-cyclin E inhibitor, has similar functions with the yeast CDK inhibitor Sic1, such as a role in orchestrating the G_1/S transition, although they do not share significant sequence similarity (Bloom and Cross, 2007). In cancer cells, overexpression of p27, or expression of a stabilized, active p27, induces autophagy (Komata et al., 2003; Liang et al., 2007). A recently identified small molecule (CpdA) stabilizes p27, in association with the induction of autophagy (Chen et al., 2008). Nonetheless, overexpression of p27 or stabilization of p27 accompanies cell cycle arrest at G_1. This raises a question as to whether p27 itself, or cell cycle arrest caused by p27 overexpression, contributes to the induction of autophagy. In fact, cell cycle arrest and autophagy share many similarities, but the precise correlation between G_1 arrest and autophagy is still a matter of debate (Huang and Klionsky, 2007). More recent findings in mammalian cell culture show that autophagy occurs but is not required for entrance into G_0 arrest (Valentin and Yang, 2008). It is possible that autophagy and cell cycle arrest may

occur in parallel, or cell cycle arrest may induce autophagy. Using budding yeast as a model system may help to elucidate the mechanisms by which CDK inhibitors regulate autophagy.

Here, we demonstrate the mechanism by which the Pho85 signaling pathway is involved in the control of autophagy. Our work implicates Pho85 as both a negative and a positive regulator of autophagy. We found that the yeast CDK inhibitor, Sic1, functions as a negative regulator of autophagy, which is opposite from the mammalian ortholog, p27. Results from physiological, genetic and biochemical studies reveal a model for the regulation of autophagy by Pho85 (Figure 4.1).

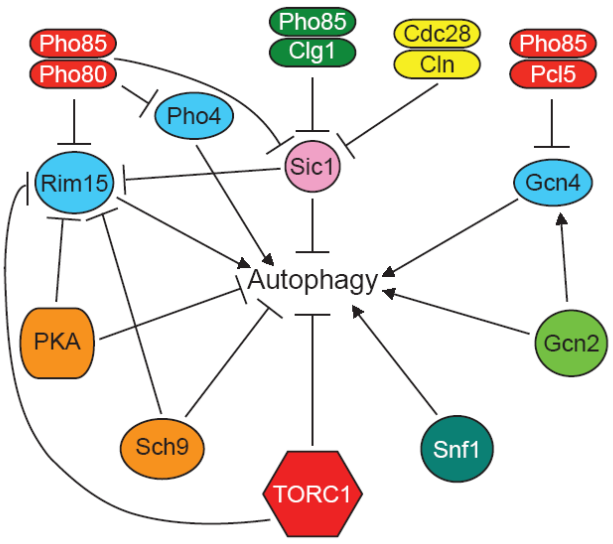

Figure 4.1. Schematic overview of the key components in autophagy regulation. Arrows represent positive regulation; bars represent negative regulation. Cyclins Pho80, Clg1 and Pcl1 (not shown) form complexes with Pho85 to inhibit Sic1.

RESULTS

Pho80 and Pcl5 are the cyclins of Pho85 that participate in the negative regulation of autophagy

Although Pho85 serves as a negative regulator of autophagy (Wang et al., 2001b), it is unclear which Pho85 partner cyclin(s) may be involved, and the mechanism through which Pho85 exerts its effect. Pho80 directs Pho85 to inhibit Rim15 function, and Rim15 is needed for autophagy that is induced by PKA and Sch9 inactivation (Wanke et al., 2005; Yorimitsu et al., 2007). Pcl5 directs Pho85 to initiate the degradation of Gcn4, a protein required for both starvation- and rapamycin-induced autophagy (Shemer et al., 2002; Talloczy et al., 2002). Thus, Pho80 and Pcl5 are potential Pho85 cyclins involved in negative autophagy regulation. In order to measure the level of autophagy induction in the presence of *PHO85* or cyclin knockouts, we used the Pho8Δ60 assay (Noda et al., 1995), which measures autophagy-dependent activation of an altered alkaline phosphatase marker.

Wild-type cells grown in rich medium displayed a basal level of Pho8Δ60-dependent alkaline phosphatase activity, and rapamycin treatment increased the level of activity substantially (Figure 4.2A). In contrast, *atg1*Δ cells showed no increase after rapamycin treatment. In agreement with previous studies (Wang et al., 2001b), deletion of *PHO85* caused a markedly elevated activity of Pho8Δ60 after rapamycin treatment, being ~40-50% higher than that of wild-type cells. As expected, upon rapamycin treatment, *pho80*Δ cells and *pcl5*Δ cells displayed a significant increase of Pho8Δ60 activity, with values similar to that of *pho85*Δcells (Figure 4.2A). Thus, Pho80 and Pcl5 are cyclins of Pho85 that negatively regulate autophagy. Double deletion of both *PHO80* and *PCL5* resulted in

~80% higher activity of Pho8Δ60 than that of wild-type cells, after rapamycin treatment, suggesting that Pho80-Pho85 and Pcl5-Pho85 kinase complexes have an additive effect on autophagy and presumably function in parallel pathways (Figure 4.1).

As part of our effort to elucidate how Pho80-Pho85 and Pcl5-Pho85 negatively regulate autophagy, we wanted to determine which downstream targets might be involved. We first examined the role of downstream targets of Pho80-Pho85, Rim15 and Pho4. The corresponding higher increase of Pho8Δ60 activity beyond the wild type level in *pho80*Δ cells depended to a large extent on the presence of Rim15 and Pho4 (Fig. 1C, 1D). However, deletion of *RIM15* or *PHO4* did not affect the increase of Pho8Δ60 activity in *pcl5*Δ cells, in agreement with the fact that Rim15 and Pho4 are *bona fide* targets of Pho80-Pho85, but not Pcl5-Pho85 (Figure 4.1, 4.2B, 4.2C). Next, we examined the effect on autophagy of loss of Gcn4, a downstream target of Pcl5-Pho85. Knockout of *GCN4* significantly reduced the level of Pho8Δ60 activity in *pcl5*Δ cells (Figure 4.2D). Together, these data suggested that the Pho80-Pho85 and Pcl5-Pho85 kinase complexes contribute appreciably to the negative regulation of autophagy, through their inhibitory roles on Rim15 and Pho4, and on Gcn4, respectively. Further analyses showed that compared to single *rim15*Δ, *pho4*Δ, or *gcn4*Δ mutants or the double *pho4*Δ *gcn4*Δ mutant, the triple *rim15*Δ *pho4*Δ *gcn4*Δ mutant displayed the lowest activity of Pho8Δ60, being ~50% relative to that of wild-type cells, after rapamycin treatment (Figure 4.2E), suggesting that Rim15, Pho4 and Gcn4 have partially additive effects on autophagy, and presumably regulate autophagy in parallel.

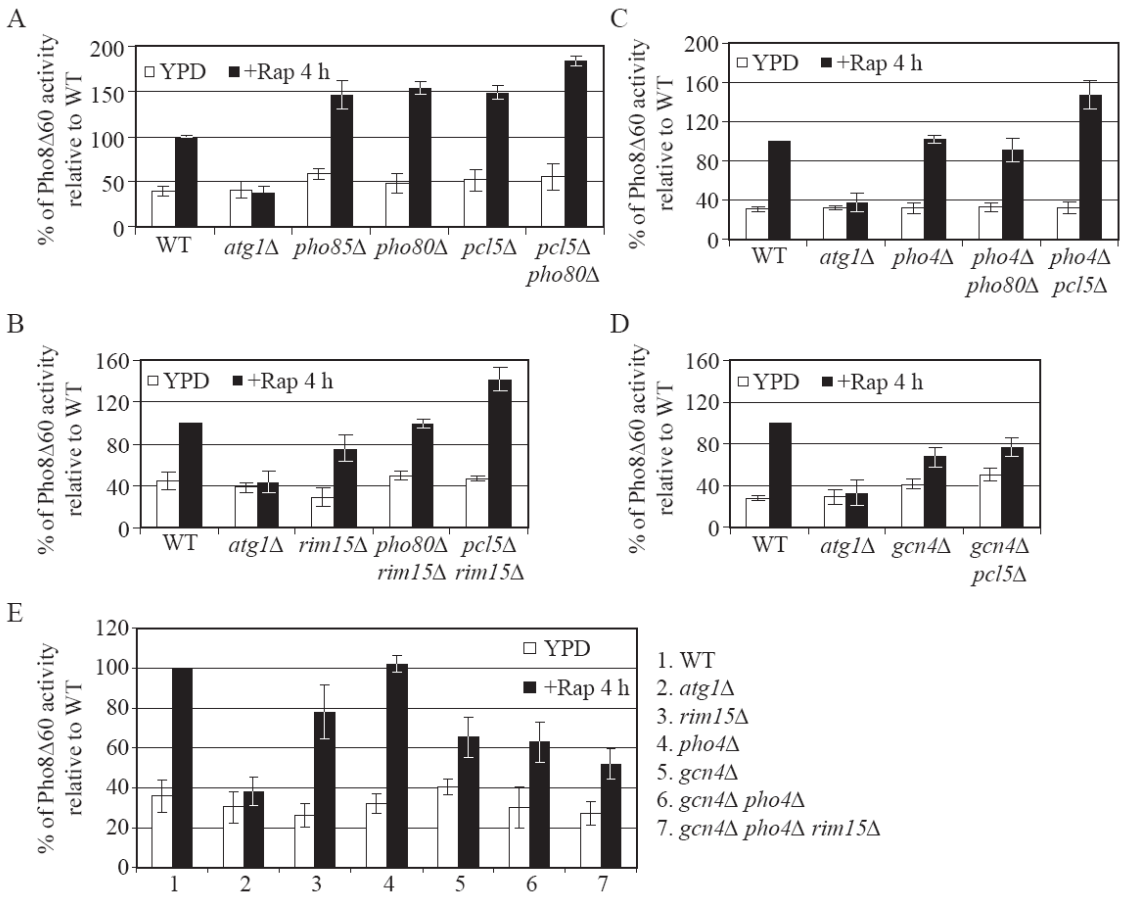

Figure 4.2. Pho80 and Pcl5 are the cyclins of Pho85 that participate in the negative regulation of autophagy. Cells expressing Pho8Δ60 were grown in YPD to midlog phase and then treated with rapamycin for 4 h. The Pho8Δ60 activity was measured as described in Supplemental Experimental Procedures, and was normalized to the activity of wild-type cells with rapamycin treatment, which was set to 100%. Error bars indicate the standard deviation (SD) of three independent experiments. Strains used were wild type (TN124), and *atg1*Δ (HAY572), and in (A) *pho85*Δ (ZFY089), *pho80*Δ (ZFY105), *pcl5*Δ (ZFY099) and *pho80*Δ *pcl5*Δ (ZFY128); in (B) *rim15*Δ (ZFY100), *pho80*Δ *rim15*Δ (ZFY102) and *pcl5*Δ *rim15*Δ (ZFY103); in (C) *pho4*Δ (ZFY135), *pho4*Δ *pho80*Δ (ZFY137) and *pcl5*Δ *pho4*Δ (ZFY143); in (D) *gcn4*Δ (ZFY111), *gcn4*Δ *pcl5*Δ (ZFY112); in (E) *rim15*Δ (ZFY100), *pho4*Δ (ZFY135), *gcn4*Δ (ZFY111), *gcn4*Δ *pho4*Δ (ZFY142) and *gcn4*Δ *pho4*Δ *rim15*Δ (ZFY175).

Sic1 functions as a negative regulator of autophagy

In cancer cells, overexpression of a mammalian CDK inhibitor, p27, induces autophagy (Liang et al., 2007). A recently identified small molecule (CpdA) stabilizes p27, in association with the induction of autophagy (Chen et al., 2008). The yeast CDK inhibitor Sic1 is negatively regulated by Pho85 through phosphorylation (Nishizawa et al., 1998). To gain more insight into the mechanism by which this CDK inhibitor regulates autophagy, we decided to investigate the role of Sic1 in autophagy.

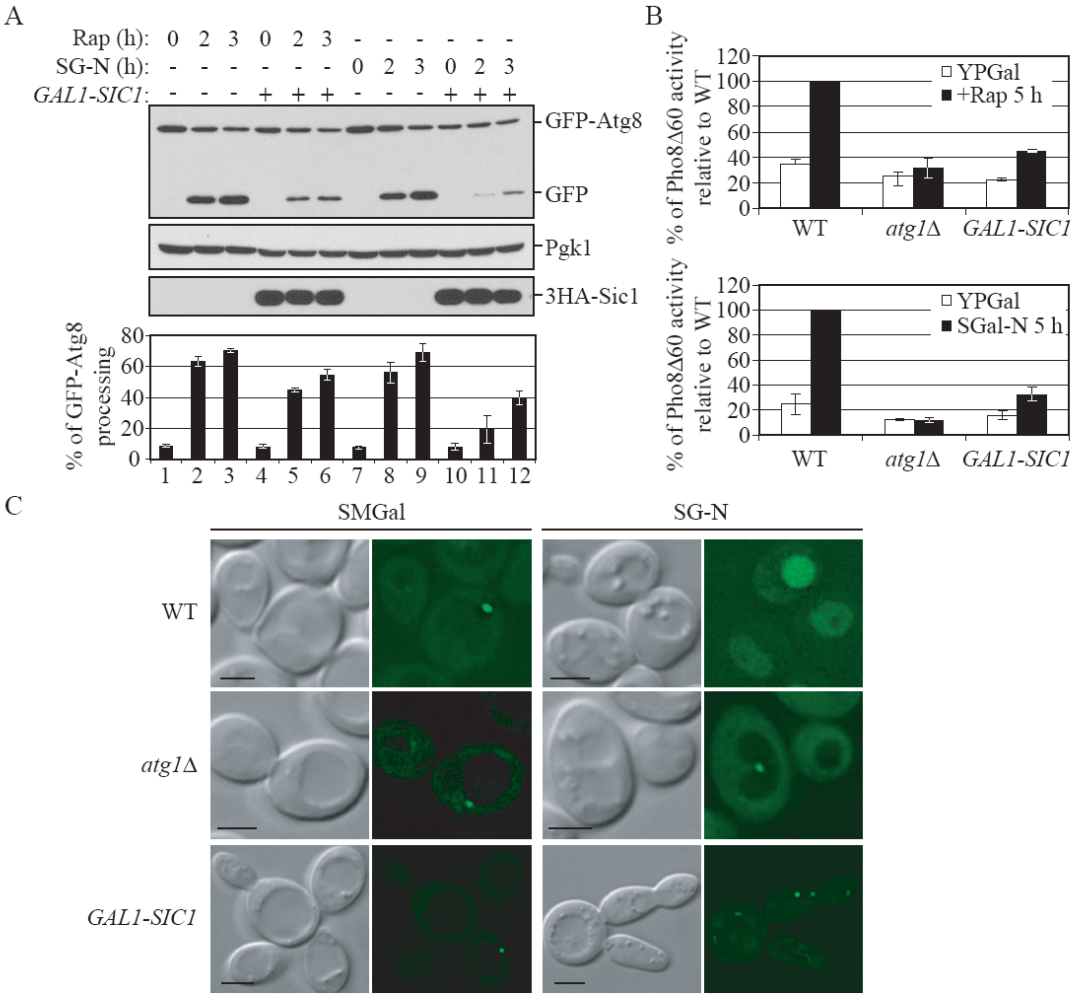

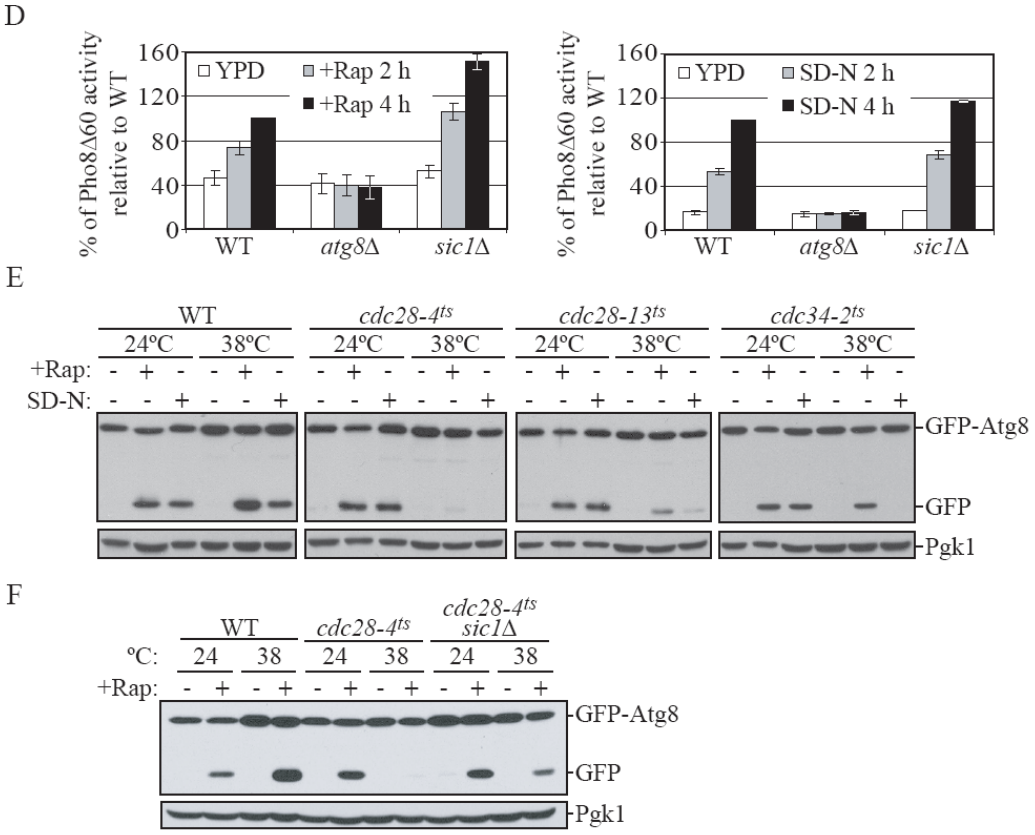

Figure 4.3. Sic1 functions as a negative regulator of autophagy. (A) and (B) Overexpression of Sic1 inhibits rapamycin- and nitrogen starvation-induced autophagy. (A) Wild-type (W3030-1B) cells expressing GFP-Atg8 (pCU-GFP-AUT7(414)) and expressing either 3HA-Sic1 (pZY011), or an empty vector (pTY006), were grown in SMD and shifted to SMGal for 12 h, and then subjected to either rapamycin treatment or starvation treatment (SG-N). At the indicated times, proteins were TCA-precipitated and subjected to immunoblotting with anti-YFP, anti-HA and anti-Pgk1 (loading control) antisera. Percentage of GFP-Atg8 processing was calculated as described in Supplemental Experimental Procedures. Error bars indicate the SD of three independent experiments. (B) Wild-type (ZFY202), *atg1*Δ (TYY181) and *GAL1-SIC1* (ZFY203) cells expressing Pho8Δ60 were grown in YPD and shifted to YPGal for 12 h, and were then treated with rapamycin or shifted to nitrogen starvation (SG-N) medium for 5 h. The Pho8Δ60 activity was normalized to the activity of wild-type cells treated with rapamycin or nitrogen starved, which was set to 100%. Error bars indicate the SD of three independent experiments. (C) Overexpression of Sic1 inhibits delivery of GFP-Atg8 to the vacuole. Wild type (W303-1B), *atg1*Δ (TYY164), and *GAL1-SIC1* (ZFY184) cells expressing GFP-Atg8 (pCU-GFP-AUT7(416)), were analyzed by fluorescence microscopy as

described in Supplemental Experimental Procedures. Bar, 5 μm. (D) Nonspecific autophagy is elevated upon deletion of *SIC1*. Wild-type (TN124), *atg8*Δ (YZX200) and *sic1*Δ (ZFY098) cells expressing Pho8Δ60 were grown to midlog phase and treated with rapamycin, or shifted to nitrogen starvation conditions (SD-N). At the indicated times, the Pho8Δ60 activity was measured, and it was normalized to the activity of wild-type cells with nitrogen starvation or rapamycin treatment for 4 h, which was set to 100%. Error bars indicate the SD of three independent experiments. (E) GFP-Atg8 processing is blocked by inactivation of Cdc28 and Cdc34. Wild type (BY4742) and temperature-sensitive mutants *cdc28-4*^{ts} (D4), *cdc28-13*^{ts} (D13) and *cdc34-2*^{ts} (MTY670) expressing GFP-Atg8 (pCU-GFP-AUT7(416)), were grown in 24°C or 38°C for 3 h, and shifted to nitrogen starvation medium or treated with rapamycin for 2 h. (F) The autophagic defect in the *cdc28-4*^{ts} mutant is partially suppressed by deletion of *SIC1*. Wild-type cells (BY4742) and temperature-sensitive mutants *cdc28-4*^{ts} (D4), and *cdc28-4*^{ts} *sic1*Δ (ZFY258) expressing GFP-Atg8 (pCU-GFP-AUT7(416)), were grown at 24°C or 38°C for 3 h, and treated with rapamycin for 2 h. (E) and (F) TCA-precipitated proteins were subjected to immunoblotting with anti-YFP and anti-Pgk1 (loading control) antisera.

We first asked whether overexpression of Sic1 would induce autophagy in yeast, using a GFP-Atg8 processing assay; Atg8 is associated with autophagosomes and, when delivered into the vacuole, GFP-Atg8 is hydrolyzed to yield free GFP, which thus reflects the level of autophagy (Shintani and Klionsky, 2004b). The wild-type strain was transformed with a plasmid expressing GFP-Atg8 and a plasmid expressing Sic1 driven by the *GAL1* promoter, or an empty vector. After 12 h overexpression of Sic1 in galactose-containing medium, we found that no free GFP was detected in cells, suggesting that autophagy was not induced under this condition (Figure 4.3A, lanes 4 and 10). After rapamycin treatment or starvation for nitrogen, cells harboring the empty vector displayed free GFP, whereas the level of free GFP was substantially reduced in the cells overexpressing Sic1 (Figure 4.3A). Furthermore, overexpression of Sic1 resulted in a markedly reduced activity of Pho8Δ60 after rapamycin treatment or following nitrogen

starvation (Figure 4.3B). A similar result was observed when we examined the effect of Sic1 overexpression on the delivery of GFP-Atg8 to the vacuole by fluorescence microscopy. Wild-type cells grown in SMGal displayed a prominent GFP-Atg8 punctum with a perivacuolar localization that corresponded to the phagophore assembly site (PAS; the organizing site for the autophagosome), as well as diffuse cytosolic staining (Figure 4.3C). When shifted to SG-N, GFP-Atg8 could also be detected within the vacuole lumen. The *atg1*Δ mutant prevented the movement of GFP-Atg8 into the lumen. The overexpression of Sic1 also blocked movement of GFP-Atg8 into the vacuole lumen, indicating a defect in autophagy. Thus, these results suggested that the CDK inhibitor Sic1 has an inhibitory role in the control of autophagy in yeast, which is opposite to the role of p27 in mammalian cells. Moreover, deletion of *SIC1* caused a significantly elevated activity of Pho8Δ60 after rapamycin treatment and a modest increase following starvation, compared to wild-type cells (Figure 4.3D). Taken together, our data indicated that Sic1 functions as a negative regulator of autophagy in parallel with TORC1.

Sic1 is controlled by ubiquitin-dependent protein degradation. Cln-Cdc28 can phosphorylate Sic1, which allows Sic1 to be specifically recognized by the F-box protein Cdc4. Cdc4, Cdc53 and Skp1 constitute a ubiquitin ligase complex (SCF^{Cdc4}) that cooperates with the ubiquitin-conjugating enzyme Cdc34 to promote the ubiquitination of Phospho-Sic1, leading to its degradation, and S phase entry (Feldman et al., 1997; Schwob et al., 1994). Sic1 accumulates in temperature-sensitive mutants such as *cdc28* and *cdc34*, leading to cell cycle arrest at the G_1 phase; whereas deletion of *SIC1* allows *cdc34* mutant to enter into S phase (Schneider et al., 1998; Schwob et al., 1994). To further examine the negative regulation of autophagy by Sic1, we decided to monitor this process in *cdc28* and

cdc34 mutants that stabilize Sic1. Cells expressing GFP-Atg8 were grown at permissive temperature and then shifted to non-permissive temperature, followed by rapamycin treatment or nitrogen starvation. Wild-type cells displayed processing of GFP-Atg8 when autophagy was induced by either condition (Figure 4.3E). In contrast, *cdc28-4*^{ts}and *cdc28-13*^{ts} mutants displayed a significant defect in GFP-Atg8 processing at the non-permissive temperature (Figure 4.3E). *cdc34-2*^{ts} mutant also displayed an autophagic defect at the non-permissive temperature when autophagy was induced by nitrogen starvation, but not rapamycin treatment (Figure 4.3E). We next addressed whether accumulation of Sic1 in these *cdc* mutants is responsible for the autophagic defect. We found that deletion of *SIC1* in the *cdc28-4*^{ts} mutant partially suppressed the defect in GFP-Atg8 processing at non-permissive temperature after rapamycin treatment (Figure 4.3F). Thus, these data suggested that autophagy is inhibited in these *cdc* mutants that are defective in Sic1 degradation and accumulate Sic1.

Pho85 positively regulates autophagy

Pho85 negatively regulates Sic1 (Nishizawa et al., 1998), and our data suggested that Sic1 is a negative regulator of autophagy. Thus, it was tempting to speculate that Pho85 might promote autophagy through downregulation of Sic1, even though Pho85 is also a negative regulator of autophagy. Consistent with this idea, the level of autophagy induced by rapamycin treatment was higher in the double *pho80*Δ *pcl5*Δ mutant than in the single *pho85*Δ mutant (Figure 4.1). This result indicated that loss of *PHO85* might have an inhibitory effect on autophagy when the Pho80 and Pcl5 cyclins that exert a negative effect are deleted (Figure 4.1). To test this hypothesis, we used the Pho8Δ60 assay to monitor the induction of autophagy in *pho80*Δ *pcl5*Δ cells in the presence and absence of *PHO85*.

When treated with rapamycin, or after nitrogen starvation, *pho80*Δ *pcl5*Δ *pho85*Δ cells displayed ~1.5-fold lower activity of Pho8Δ60 than that of *pho80*Δ *pcl5*Δ cells (Figure 4.4A). This result suggested that Pho85 has a positive role in the induction of autophagy, at least in the *pho80*Δ *pcl5*Δ background. To further substantiate the premise that Pho85 promotes autophagy, we chose a different genetic background, the *gcn4*Δ *pho4*Δ *rim15*Δ strain, lacking all three downstream targets of Pho80-Pho85 and Pcl5-Pho85 to negatively regulate autophagy (Figure 4.1). Again, we found that deletion of *PHO85* decreased the level of autophagy, in this case in the *gcn4*Δ *pho4*Δ *rim15*Δ cells, particularly during nitrogen starvation (Figure 4.4B and 4.4C).

Next, we decided to use a chemical genetics approach to eliminate potential confounding effects of the chronic *pho85*Δ mutation. We took advantage of a strain carrying a mutation in the ATP binding pocket of Pho85 ($Pho85^{F82G}$). This mutant retains wild-type function but is rapidly inactivated when treated with the cell-permeable ATP-analogue inhibitor 1-Na-PP1 (Carroll et al., 2001). Cells expressing $Pho85^{F82G}$ were treated with or without 1-Na-PP1, followed by additional treatment with rapamycin to induce autophagy. Consistent with our previous finding that Pho85 is partly a negative regulator of autophagy, *PHO85-F82G* cells displayed an increase of Pho80Δ60 activity when treated with both 1-Na-PP1 and rapamycin, compared to rapamycin alone (Figure 4.4D). In contrast, *PHO85-F82G pho80*Δ *pcl5*Δ cells showed a decrease of Pho8Δ60 activity in the presence of 1-Na-PP1, in agreement with our result that loss of Pho85 inhibited autophagy in the *pho80*Δ *pcl5*Δ background. Notably, 1-Na-PP1 treatment had essentially no effect on rapamycin-induced autophagy in wild-type cells. Taken together, we propose a model in which Pho85 has dual roles in autophagy regulation; that is, it is

both a negative and a positive regulator of autophagy (Figure 4.1).

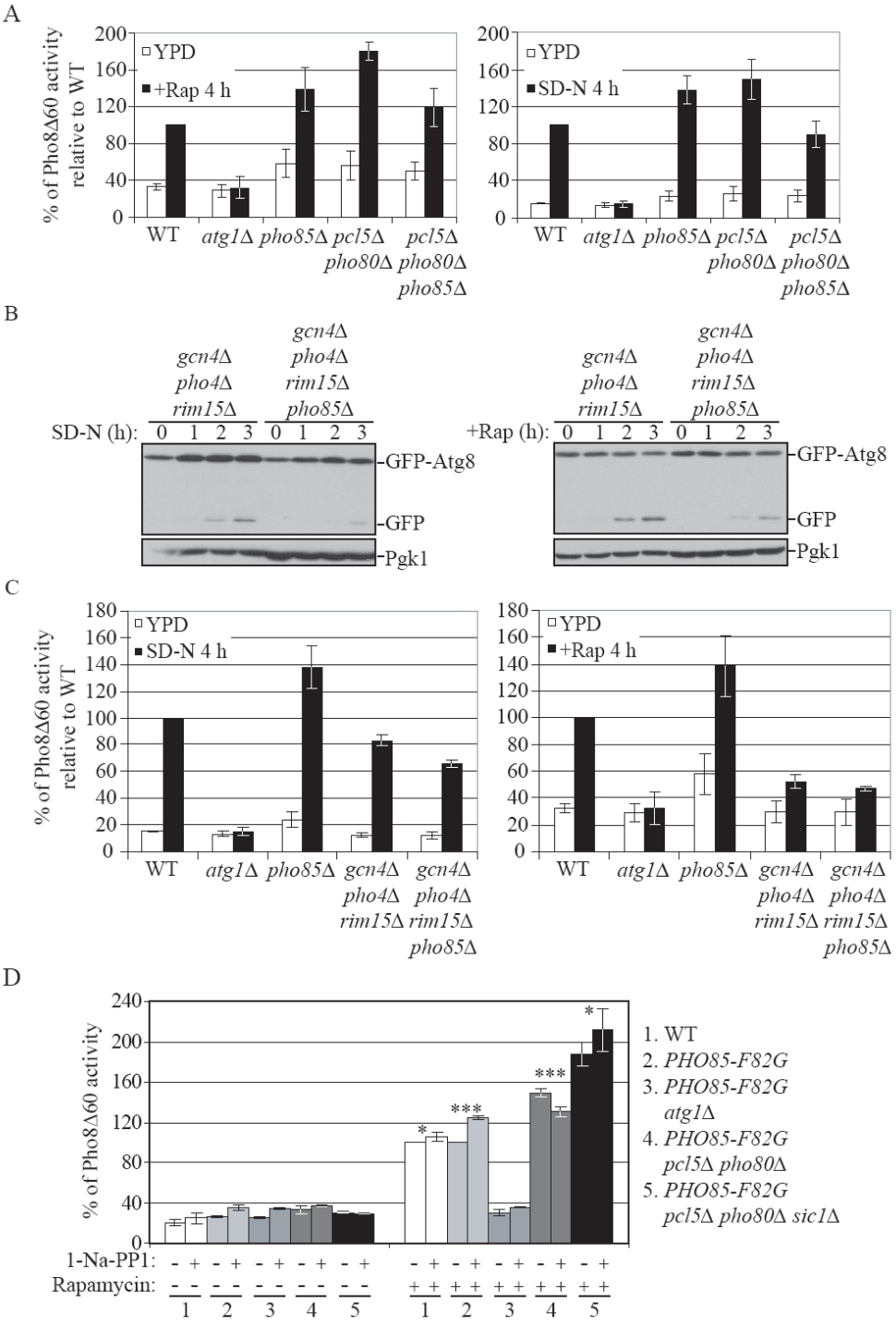

Figure 4.4. Pho85 positively regulates autophagy. (A) Deletion of *PHO85* suppresses autophagy in *pho80*Δ *pcl5*Δ cells. Wild-type (TN124), *atg1*Δ (HAY572), *pho80*Δ *pcl5*Δ (ZFY128) and *pho80*Δ *pcl5*Δ *pho85*Δ (ZFY172) cells were analyzed by the Pho8Δ60 assay, as described in Figure 2D. (B) and (C) Deletion of *PHO85* suppresses autophagy in *gcn4*Δ *pho4*Δ *rim15*Δ cells. (B) *gcn4*Δ *pho4*Δ *rim15*Δ (ZFY152) and *gcn4*Δ *pho4*Δ *pho85*Δ *rim15*Δ (ZFY174) cells expressing GFP-Atg8 (pCU-GFP-AUT7(416)), were grown to midlog phase and shifted to nitrogen starvation medium or treated with rapamycin. At the indicated times, proteins were precipitated with TCA and resolved by SDS-PAGE followed by immunoblotting with anti-YFP and anti-Pgk1 (loading control) antisera. (C) Wild-type (TN124), *atg1*Δ (HAY572), *pho85*Δ (ZFY089), *gcn4*Δ *pho4*Δ *rim15*Δ (ZFY175) and *gcn4*Δ *pho4*Δ *pho85*Δ *rim15*Δ (ZFY177) cells expressing Pho8Δ60 were analyzed by the Pho8Δ60 assay, as described in Figure 2D. (D)Addition of the inhibitor 1-Na-PP1 to block $Pho85^{F82G}$ kinase activity partially suppressed autophagy in the background of *pcl5*Δ *pho80*Δ, and further deletion of *SIC1* relieved the autophagic defect that is seen upon loss of Pho85 activity. Wild-type (ZFY155), *pho85-F82G* (ZFY145), *pho85-F82G atg1*Δ (ZFY213), *pho85-F82G pcl5*Δ *pho80*Δ (ZFY215) and *pho85-F82G pcl5*Δ *pho80*Δ *sic1*Δ (ZFY214) cells expressing Pho8Δ60, were grown in YPD to midlog phase, and treated (+) or untreated (–) for 1 h with 1-Na-PP1, followed by additionally treatment with rapamycin for 5 h to induce autophagy as indicated. Samples were collected and analyzed by the Pho8Δ60 assay. The Pho8Δ60 activity in wild-type cells was normalized to the activity of wild-type cells treated with rapamycin alone, which was set to 100%. The Pho8Δ60 activity in the other four strains was normalized to the activity of *pho85-F82G* cells treated with rapamycin alone, which was set to 100%. Error bars indicate the SD of three independent experiments. * indicates a statistically non-significant difference ($p > 0.05$), *** indicates a statistically significant effect of 1-Na-PP1 versus untreated cells ($p < 0.01$)

Pho85 inhibits Sic1 to positively regulate autophagy

Having established a role of Pho85 as a positive regulator of autophagy, we decided to determine whether Sic1, which is a known Pho85 substrate, was the downstream target of Pho85 for autophagy induction. 1-Na-PP1 treatment caused a decrease in the level of autophagy that was induced by rapamycin in *PHO85-F82G pho80*Δ *pcl5*Δ cells (Figure 4.4D). We further extended our analysis by examining the effect of deletion of *SIC1*.

Without 1-Na-PP1 treatment, there was a marked increase in the level of autophagy induced by rapamycin treatment in *PHO85-F82G pho80*Δ *pcl5*Δ *sic1*Δ cells (Figure 4.4D), with approximately 1.25-fold higher activity of Pho8Δ60 than in *PHO85-F82G pho80*Δ *pcl5*Δ cells. This result suggested that Pho80-Pho85, Pcl5-Pho85, and Sic1, at least in part, negatively regulate autophagy in parallel pathways. When treated with 1-Na-PP1 followed by rapamycin, the *PHO85-F82G pho80*Δ *pcl5*Δ *sic1*Δcells did not display any decrease in the activity of Pho8Δ60, compared to rapamycin treatment alone (Figure 4.4D). This result suggested that the deletion of *SIC1* in the *PHO85-F82G pho80*Δ *pcl5*Δ cells suppressed the inhibition of autophagy that was caused by inactivation of Pho85 after addition of 1-Na-PP-1.

To further confirm our chemical genetics data, we utilized a complementary approach. Instead of using mutants, we decided to overexpress Pho85 and/or Sic1. To this end, we first examined the effect caused by overexpression of Pho85 alone. *GAL1::HIS3* chromosomal tagging was used to replace the endogenous *PHO85* promoter. After 12 h overexpression of Pho85 in galactose-containing medium, GFP-Atg8 was processed in nutrient-rich conditions even without rapamycin treatment (Figure 4.5A), although the level of autophagy induction was low. Additional deletion of *PHO80* and *PCL5*, increased the level of free GFP by ~30-40%, which further confirmed the view that Pho80-Pho85 and Pcl5-Pho85 negatively regulate autophagy. Deletion of *ATG1* completely abolished the induction of autophagy upon overexpression of Pho85, indicating that the induction was Atg1-dependent. A similar result was observed when we examined the effect of Pho85 overexpression on the delivery of GFP-Atg8 to the vacuole by fluorescence microscopy (Figure 4.5B). We then extended our analysis to examine the ability of Pho85 to induce

autophagy by using the quantitative Pho8Δ60 assay. Overexpression of Pho85 caused a significant induction of autophagy in *pho80*Δ *pcl5*Δ *GAL1-PHO85* cells, with approximately 2-fold higher activity of Pho8Δ60 than that of *pho80*Δ *pcl5*Δ cells (Figure 4.5C, open bars). After additional treatment with rapamycin, the activity of Pho8Δ60 dramatically increased, being ~40-50% higher than that of *pho80*Δ *pcl5*Δ cells (Figure 4.5C, closed bars). Taken together, these results further supported the model that Pho85 has dual roles in autophagy regulation.

Next, we examined the effect of overexpressing Sic1 or both Pho85 and Sic1. We again used the *pho80*Δ *pcl5*Δmutant to simplify the analysis by removing these two Pho85-mediated negative regulation pathways (Figure 4.1). To this end, the *pho80*Δ *pcl5*Δ cells and *pho80*Δ *pcl5*Δ *GAL1-PHO85* cells were co-transformed with a plasmid expressing GFP-Atg8, and a plasmid allowing galactose-inducible expression of *SIC1*, or an empty vector. As expected, after 12 h in galactose-containing medium, in *pho80*Δ *pcl5*Δ *GAL1-PHO85* cells containing an empty vector, autophagy was induced without any additional treatment (Figure 4.5D, lane 2); whereas treatment with rapamycin or nitrogen starvation resulted in a significantly elevated level of free GFP (Figure 4.5D, compare lane 5 to 6, and 9 to 10). Sic1 overexpression inhibited autophagy induction (Figure 4.5D, compare lane 5 to 7, and 9 to 11). In contrast, when both Sic1 and Pho85 were overexpressed, the inhibition of autophagy caused by Sic1 overexpression was abolished (Figure 4.5D, compare lane 3 to 4, 7 to 8, and 11 to 12). Taken together, we infer that Pho85 targeted the CDK inhibitor Sic1 for degradation to relieve the inhibitory effect of Sic1 overexpression on autophagy, hence promoting autophagy induction.

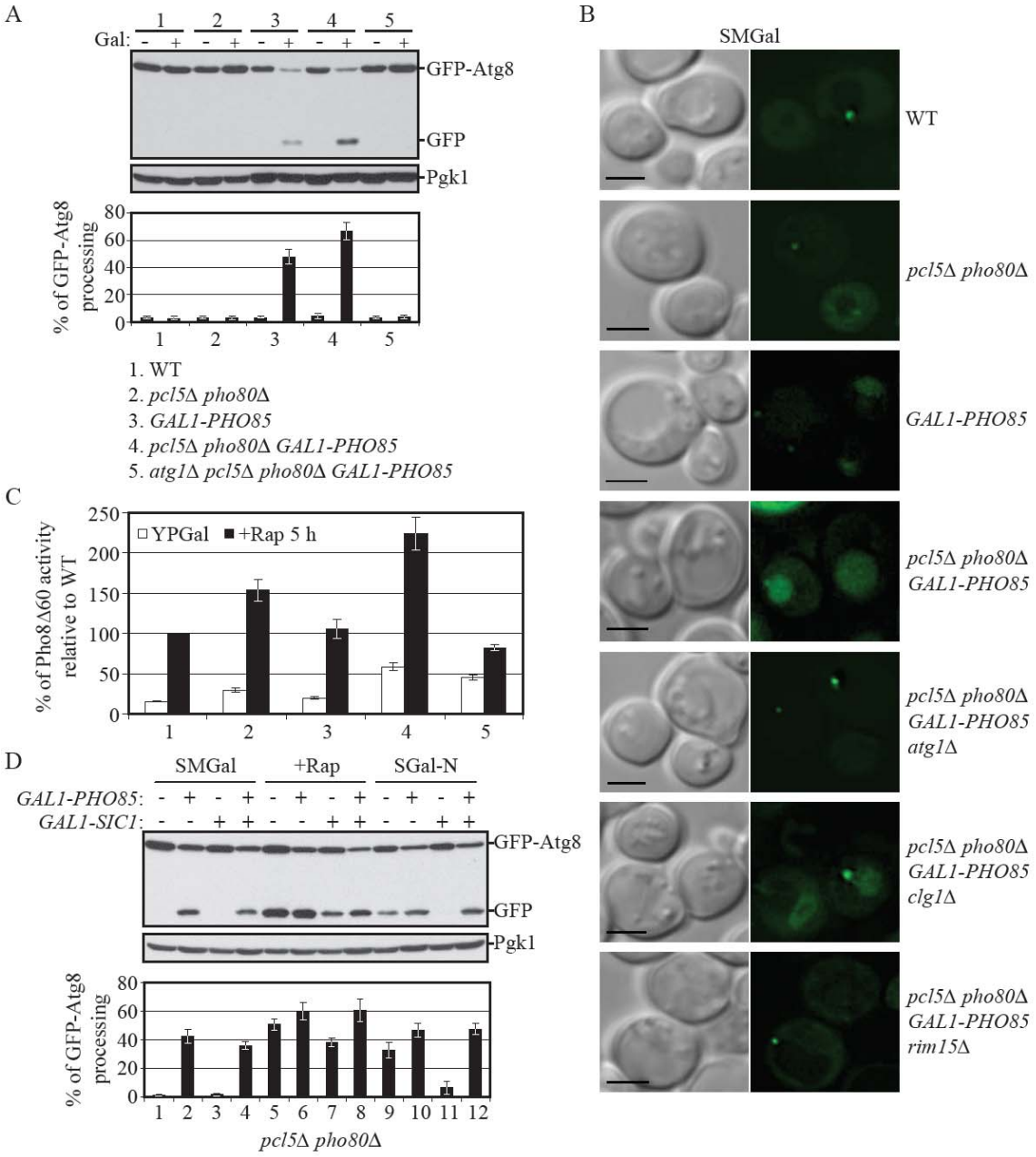

Figure 4.5. Overexpression of Pho85 induces autophagy and relieves the inhibitory effect of Sic1 overexpression on autophagy. (A), (B) and (C) Overexpression of Pho85 induces autophagy. (A) and (B) Wild-type (W3030-1B), *pcl5*Δ *pho80*Δ (ZFY207), *GAL1-PHO85* (ZFY209), *pcl5*Δ *pho80*Δ *GAL1-PHO85* (ZFY208), *atg1*Δ *pcl5*Δ *pho80*Δ *GAL1-PHO85* (ZFY217), *clg1*Δ *pcl5*Δ *pho80*Δ *GAL1-PHO85* (ZFY246) and *pcl5*Δ *pho80*Δ *rim15*Δ*GAL1-PHO85* (ZFY216) cells

expressing GFP-Atg8 (pCU-GFP-AUT7(416)), were grown in SMD and shifted to SMGal for 12 h. In (A), cells that were grown in SMD (–) or SMGal (+) were collected and subjected to immunoblotting, as described in Figure 2A. In (B), cells that were grown in SMGal were analyzed by fluorescence microscopy as described in Supplemental Experimental Procedures. Bar, 2.5 μm. (C) Wild type (ZFY202), *pcl5*Δ *pho80*Δ (ZFY206), *GAL1-PHO85* (ZFY224), *pcl5*Δ *pho80*Δ *GAL1-PHO85* (ZFY225) and *atg1*Δ *pcl5*Δ *pho80*Δ *GAL1-PHO85* (ZFY227) cells were grown in YPD and shifted to YPGal for 12 h, then treated with rapamycin for 5 h and analyzed by the Pho8Δ60 assay. Values were normalized to the activity of wild-type cells with rapamycin treatment, which was set to 100%. Error bars indicate the SD of three independent experiments. (D) In *pcl5*Δ *pho80*Δ cells, overexpression of Pho85 suppresses the autophagic defect resulting from Sic1 overexpression. *pcl5*Δ *pho80*Δ (ZFY207) and *pcl5*Δ *pho80*Δ *GAL1-PHO85* (ZFY208) cells were analyzed by the GFP-Atg8 processing assay, as described in Figure 2A.

Clg1 targets Pho85 to antagonize Sic1 inhibition of autophagy

Having established the positive regulatory role of Pho85 in autophagy, we sought to determine which particular Pho85 cyclin(s) may be involved. A *pcl6*Δ *pcl7*Δ double mutant displays normal induction of autophagy (Wang et al., 2001c). By using the Pho8Δ60 assay, we found essentially normal induction of autophagy in *pcl8*Δ, *pcl10*Δ or *pcl8*Δ *pcl10*Δ double mutant cells (Figure 4.6A). Similarly, *pcl1*Δ, *pcl2*Δ, *pcl9*Δ or triple *pcl1*Δ *pcl2*Δ *pcl9*Δ cells did not display any discernable difference in Pho8Δ60 activity relative to wild-type cells (Figure 4.6B, 4.7A). We then turned to the cyclin Clg1, which belongs to the Pcl1,2 subfamily; the role of Clg1 has not yet been clearly characterized. When treated with rapamycin, cells deleted for *CLG1* displayed a significant reduction in Pho8Δ60 activity, being ~30% lower than that of wild-type cells (Figure 4.7A). This result suggested that Clg1 is a potential cyclin of Pho85 to positively regulate autophagy. When autophagy was induced by nitrogen starvation, however, *clg1*Δ cells displayed no appreciable

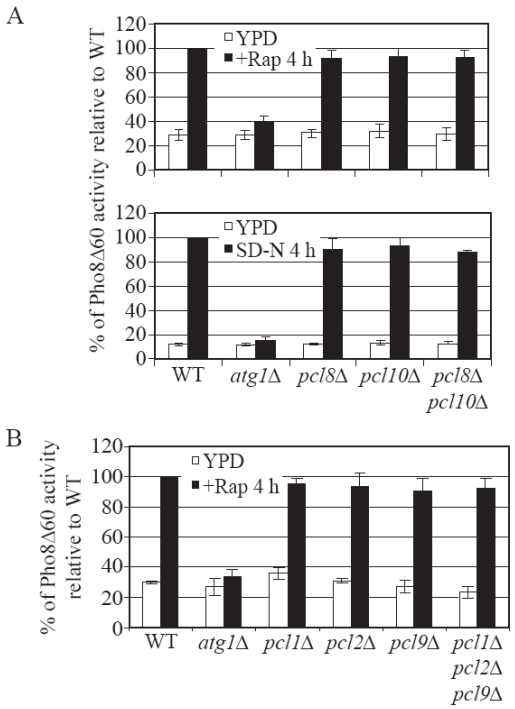

Figure 4.6. Deletion of *PCL8, PCL10, PCL1, PCL2* or *PCL9* reveals a minor effect on autophagy. In (A), Wild-type (TN124), *atg1*Δ (HAY572), *pcl8*Δ (ZFY178), *pcl10*Δ (ZFY179) and *pcl8*Δ *pcl10*Δ (ZFY180) cells; and in (B), Wild-type (TN124), *atg1*Δ (HAY572), *pcl1*Δ (ZFY121), *pcl2*Δ (ZFY130), *pcl9*Δ (ZFY139) and *pcl1*Δ *pcl2*Δ *pcl9*Δ (ZFY129) cells, were analyzed by the Pho8Δ60 assay, as described in Figure 2D.

difference in Pho8Δ60 activity compared to the wild type although further deletion of *PCL1*, *PCL2* and *PCL9* significantly reduced the level of autophagy (Fig. 5A). When autophagy was induced by overexpression of Pho85, deletion of *CLG1* significantly reduced the level of free GFP by ~70-80% (Figure 4.7C). Similarly, there was a reduction in the delivery of GFP-Atg8 to the vacuole (Figure 4.5B). These results suggested that Clg1 is a major cyclin that targets Pho85 to positively regulate autophagy, whereas Pcl1, Pcl2 and Pcl9 might function redundantly with Clg1 in autophagy regulation. To test the

possibility that the autophagic defect seen in *clg1*Δ and *clg1*Δ *pcl1*Δ *pcl2*Δ *pcl9*Δ cells was due to the accumulation of Sic1, we decided to examine the stability of protein A (PA)-tagged Sic1 in the presence of *PHO85* or cyclin knockouts. Deletion of *PHO85* largely stabilized PA-Sic1 (Figure 4.7B), in agreement with previous studies (Nishizawa et al., 1998). Although single deletion of *CLG1*, *PCL1*, *PCL2* or *PCL9* did not appreciably stabilize PA-Sic1, triple knockout *pcl1*Δ *pcl2*Δ *pcl9*Δ cells and quadruple knockout *clg1*Δ *pcl1*Δ *pcl2*Δ *pcl9*Δ cells displayed an approximately 2-fold and 2.5-fold higher amount of PA-Sic1, respectively, compared to wild-type cells (Figure 4.7B). These results suggested that Clg1, Pcl1, Pcl2 and Pcl9 might be functionally redundant cyclins of Pho85 to promote Sic1 degradation.

To further assess whether Clg1-Pho85 regulates autophagy through targeting Sic1 for degradation, we examined the phenotypes associated with co-overexpression of Sic1 and Clg1. *pho80*Δ *pcl5*Δ cells bearing a plasmid expressing Sic1 driven by the *GAL1* promoter displayed a slow growth phenotype on a galactose-containing plate, compared to vector alone; whereas Clg1 overexpression partially suppressed the slow growth phenotype resulting from overexpression of Sic1 (Figure 4.7D). We then asked whether overexpression of Clg1 suppressed the inhibition of autophagy caused by Sic1 overexpression. After 12 h in galactose-containing medium followed by treatment with rapamycin or nitrogen starvation, a *pho80*Δ *pcl5*Δ *GAL1-CLG1* strain overexpressing both Clg1 and Sic1, displayed a substantially greater level of free GFP than the *pho80*Δ *pcl5*Δ strain overexpressing Sic1 alone (Figure 4.7E, compare lane 7 to 8, and 11 to 12). A similar result was observed when we examined the effect of combined overexpression of Clg1 and Sic1on the delivery of GFP-Atg8 to the vacuole by fluorescence microscopy (Figure 4.8).

Thus, Clg1-Pho85 potentially targets Sic1 for degradation to relieve inhibition of autophagy caused by Sic1 overexpression.

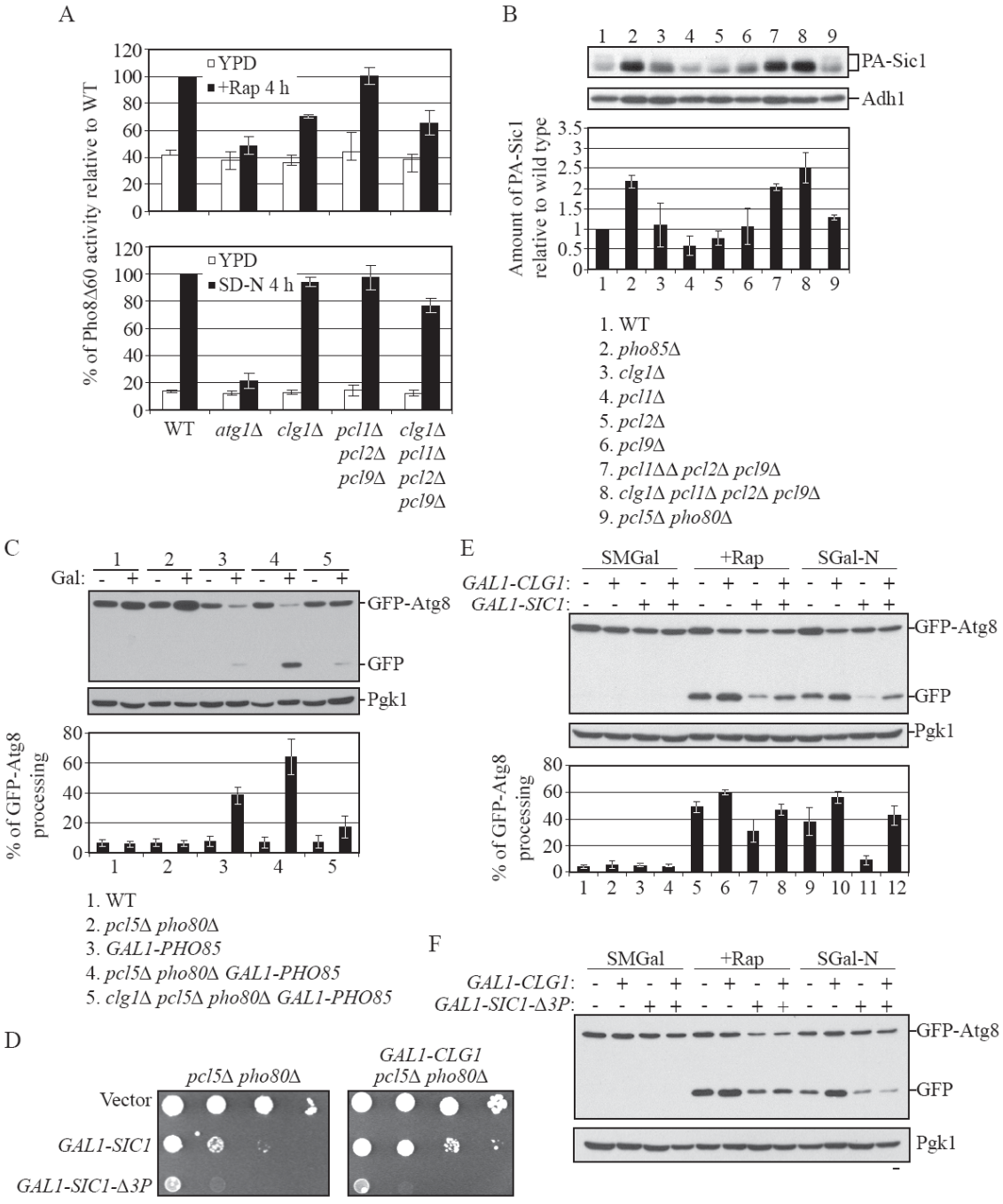

Figure 4.7. Clg1 targets Pho85 to antagonize Sic1 inhibition of autophagy. (A) Deletion of *CLG1* inhibits autophagy induced by rapamycin treatment. Wild-type (TN124), *atg1*Δ (HAY572), *clg1*Δ (ZFY182), *pcl1*Δ *pcl2*Δ *pcl9*Δ (ZFY129) and *clg1*Δ *pcl1*Δ *pcl2*Δ *pcl9*Δ (ZFY183) cells were analyzed by the Pho8Δ60 assay, as described in Figure 2D. (B) Sic1 stability is regulated by Pho85 and its cyclins Clg1, Pcl1, Pcl2 and Pcl9. Wild-type (W303-1B), *pho85*Δ (ZFY088), *clg1*Δ (ZFY228), *pcl1*Δ (ZFY229), *pcl2*Δ(ZFY230), *pcl9*Δ(ZFY231), *pcl1*Δ *pcl2*Δ *pcl9*Δ(ZFY234), *clg1*Δ *pcl1*Δ *pcl2*Δ *pcl9*Δ (ZFY235) and *pcl5*Δ *pho80*Δ (ZFY207) cells, expressing a *CUP1* promoter driven, N-terminal 3×protein A (PA) tagged Sic1 (pZY041), were grown to early log phase (OD_{600} = 0.5-0.6). Immunoblotted proteins were detected with a purified antibody (to detect protein A), and anti-Adh1 antiserum (as a loading control). Band intensities of PA-Sic1 and Adh1 were quantified as described in Supplemental Experimental Procedures. The relative amount of PA-Sic1 in wild-type cells was set to 1 as reference, and error bars indicate the SD of three independent experiments. (C) Deletion of *CLG1* inhibits autophagy induced by overexpression of Pho85 in *pcl5*Δ *pho80*Δ cells. Wild-type (W3030-1B), *pcl5*Δ *pho80*Δ (ZFY207), *GAL1-PHO85* (ZFY209), *pcl5*Δ *pho80*Δ *GAL1-PHO85* (ZFY208) and *clg1*Δ *pcl5*Δ *pho80*Δ *GAL1-PHO85* (ZFY246) cells were analyzed by the GFP-Atg8 processing assay, as described in Figure 4A. (D) In *pcl5*Δ *pho80*Δ cells, overexpression of Clg1 partially suppresses the slow growth phenotype resulting from overexpression of Sic1 wild-type but not the degradation-resistant mutant, Sic1-Δ3P. *pcl5*Δ *pho80*Δ (ZFY207) and *pcl5*Δ *pho80*Δ *GAL1-CLG1* (ZFY220) cells bearing either 3HA-Sic1 (pZY011), 3HA- Sic1-Δ3P (pZY016), or an empty vector (pTY006), were spotted in serial 10-fold dilutions on plates containing galactose and incubated at 30°C for 72 h. (E) and (F) In *pcl5*Δ *pho80*Δ cells, overexpression of Clg1 partially suppresses the autophagic defect resulting from overexpression of wild-type Sic1 but not the degradation-resistant mutant, Sic1-Δ3P. *pcl5*Δ *pho80*Δ (ZFY207) and *pcl5*Δ *pho80*Δ *GAL1-CLG1* (ZFY220) cells expressing either 3HA-Sic1 (pZY011), 3HA- Sic1-Δ3P (pZY016), or an empty vector (pTY006), were analyzed by the GFP-Atg8 processing assay, as described in Figure 2A.

An *in viv*o phosophorylation study suggests that Pho85 phosphorylates one of the consensus sites (Thr5) of Sic1, and at least one of another two sites (Val33 and Ser76), for efficient degradation of Sic1 (Nishizawa et al., 1998). To further clarify the mechanism of Clg1-Pho85 in the destabilization of Sic1, we generated a mutant version of Sic1, Sic1-Δ3P (T5A, T33V, and S76A). This mutant has a severe ubiquitination defect and is largely

stabilized; overexpression of Sic1-Δ3P driven by the *GAL1* promoter strongly inhibits cell

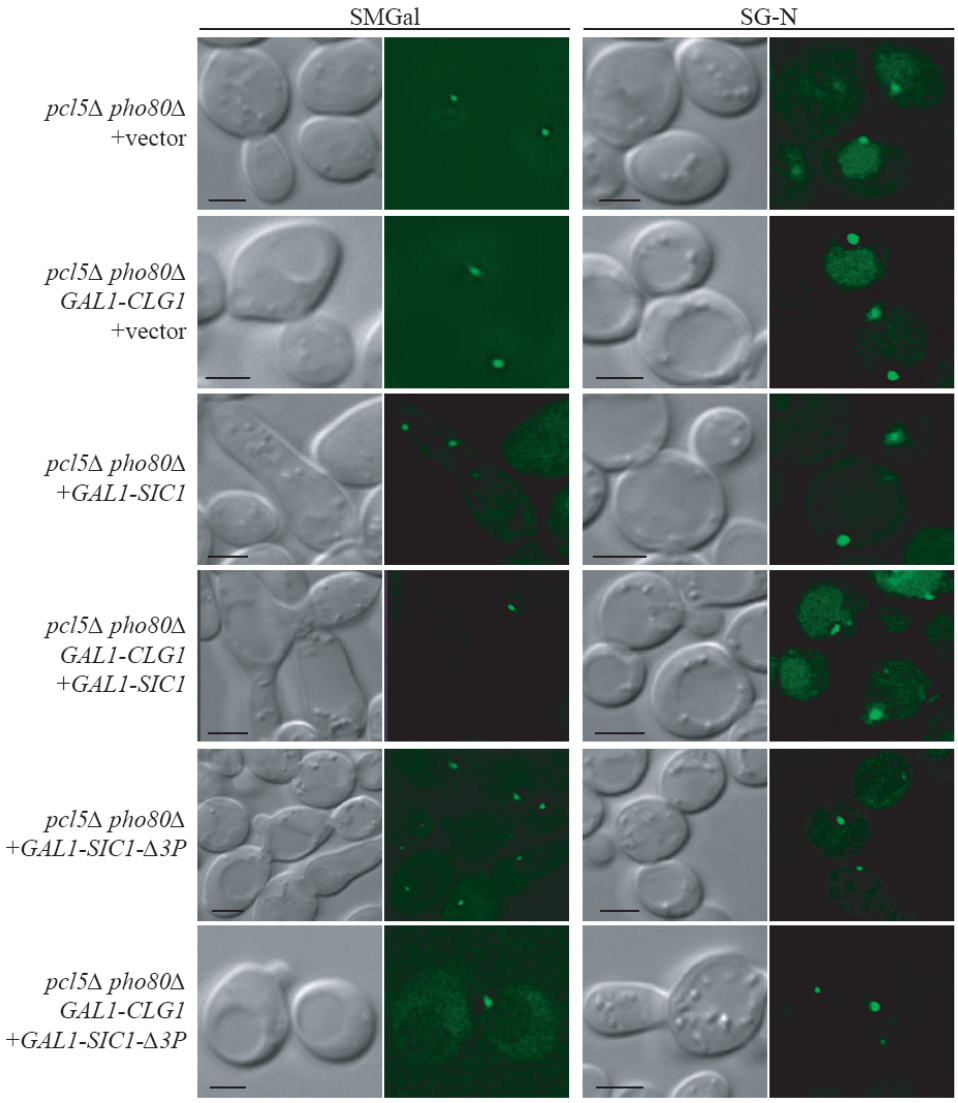

Figure 4.8. Overexpression of Clg1 suppresses Sic1 inhibition of autophagy. *pcl5*Δ *pho80*Δ (ZFY207) and *pcl5*Δ *pho80*Δ *GAL1-CLG1* (ZFY220) cells expressing GFP-Atg8 (pCU-GFP-AUT7(414)) and either 3HA-Sic1 (pZY011), 3HA- Sic1-Δ3P (pZY016), or an empty vector (pTY006), were analyzed by fluorescence microscopy, as described in Supplemental Experimental Procedures. Bar, 2.5 μm.

growth (Verma et al., 1997). As expected, overexpression of Sic1-Δ3P strongly inhibited cell proliferation in both wild-type cells and *GAL1-CLG1* cells (Figure 4.7D). Moreover, overexpression of Clg1 failed to suppress the autophagic defect when Sic1-Δ3P was overexpressed (Figure 4.7F and 4.8), suggesting that Sic1 is degraded in a Clg1-dependent manner, and that this degradation requires phosphorylation of Sic1. Taken together, these results let us propose a model in which the Clg1-Pho85 kinase complex (as well as Pcl1/2/9-Pho85) targets Sic1 for degradation, exerting a positive regulatory effect on autophagy induction (Figure 4.1).

Phosphorylation of Sic1 by Pho85 associated with Clg1, Pcl1 and Pho80

When complexed with Pcl1, Pho85 phosphorylates Sic1 *in vitro* (Nishizawa et al., 1998), although there is no evidence to show that Pcl1 is the actual cyclin required *in vivo* for the phosphorylation and hence destabilization of Sic1. Based on our model that the Clg1-Pho85 kinase complex exerts a positive regulatory effect on autophagy through destabilizing Sic1, we decided to examine whether this complex is able to directly phosphorylate Sic1 in an *in vitro* phosphorylation assay. Pho85 associates with its cyclin partners and hence should co-immunoprecipitate with them (Measday et al., 1997). Immunoprecipitated HA-tagged Clg1 obtained from *PHO85* cells but not from *pho85*Δ cells phosphorylated Sic1, indicating specific phosphorylation by the Clg1-Pho85 complex (Figure 4.9A). As our genetic data suggested that Clg1 is not the sole cyclin that targets Pho85 to positively regulate autophagy, we decided to extend our *in vitro* phosphorylation analysis to cyclins Pcl1, Pcl2, Pcl9, Pho80 and Pcl5. Consistent with the result from Nishizawa et al. (1998), immunoprecipitated HA-tagged Pcl1, but not Pcl2, obtained from *PHO85* cells but not from *pho85*Δ cells, phosphorylated Sic1 *in vitro* (Figure 4.9A and

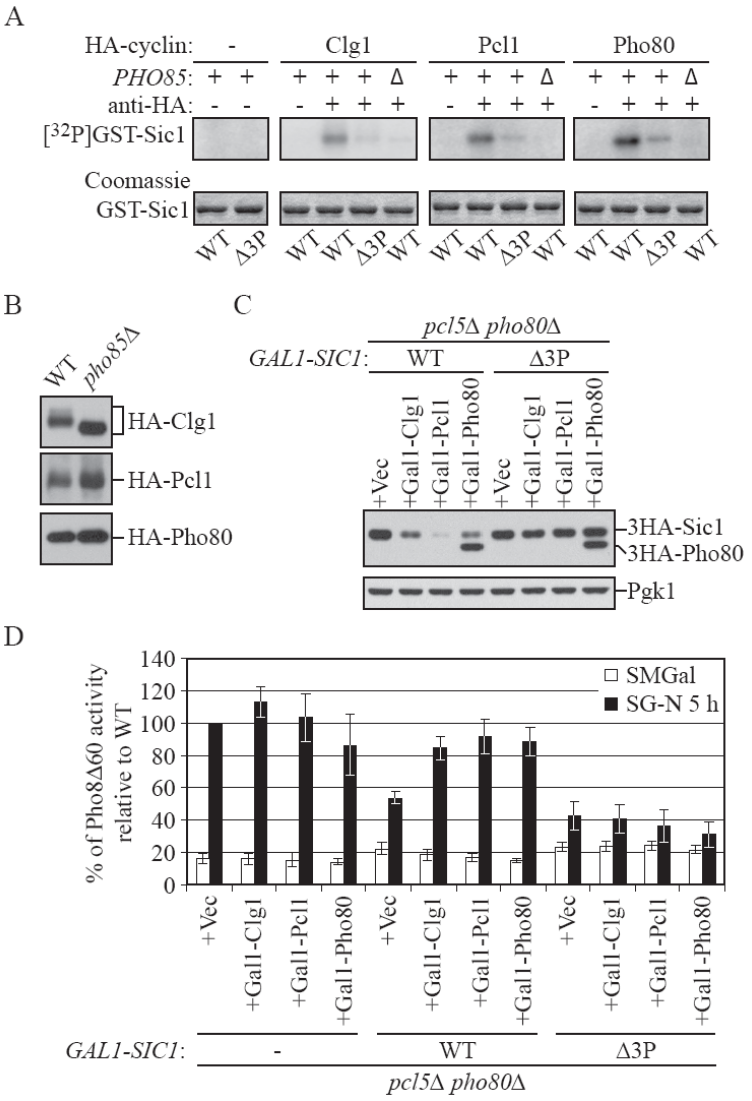

Figure 4.9. Clg1, Pcl1 and Pho80 are cyclin partners of Pho85 for Sic1 phosphorylation. (A) *In vitro* phosphorylation of T5, T33 and S76 in Sic1 by Clg1, Pcl1 and Pho80-associated Pho85 complexes. GST-Sic1 (pZY037) and GST-Sic1-Δ3P (pZY040), expressed and purified from *E.coli*, were used as substrates in *in vitro* kinase assay using immunoprecipitated HA-tagged Clg1 (pZY017), Pcl1 (pZY018), and Pho80 (pZY022) from wild-type (W303-1B) or *pho85*Δ (ZFY088) cells. As a negative control, the antibody was not added (-) to the reaction. Phosphorylated proteins were detected by autoradiography (top) and the protein input was shown by Coomassie Blue staining (bottom). (B) The immunoprecipitates used in (A) were analyzed for the presence of HA-cyclin by immunoblotting using anti-HA antibody. (C) and (D) Overexpression of Clg1, Pcl1

or Pho80 reduced the abundance of overexpressed Sic1 wild type, but not the Sic1-Δ3P mutant, and suppressed the inhibitory effect of overexpression of wild-type Sic1, but not Sic1-Δ3P, on autophagy. *pcl5*Δ *pho80*Δ (ZFY255), *pcl5*Δ *pho80*Δ *GAL1-3HA-SIC1* (ZFY256) and *pcl5*Δ *pho80*Δ *GAL1-3HA-SIC1-Δ3P* (ZFY257) cells expressing either 3HA-Clg1 (pZY017), 3HA-Pcl1 (pZY018), 3HA-Pho80 (pZY022) or an empty vector (pTY006), were grown in SMD and shifted to SMGal for 12 h. In (C), samples were collected and analyzed by immunoblotting using anti-HA and anti-Pgk1 (loading control) antisera; in (D) cells were shifted to SG-N and analyzed by the Pho8Δ60 assay. Values were normalized to the activity of ZFY255 cells bearing pTY006, and subjected to nitrogen starvation, which was set to 100%. Error bars indicate the SD of three independent experiments.

4.10A). Phosphorylated Sic1 was also obtained with Pho80 (Figure 4.9A); however, we could not detect phosphorylation of Sic1 by immunoprecipitated HA-tagged Pcl9 or Pcl5 *in vitro* (Figure 4.10A). Further analysis demonstrated that the Clg1-Pho85, Pcl1-Pho85 or Pho80-Pho85-mediated phosphorylation of Sic1 was significantly reduced by the introduction of the T5A, T33V, and S76A mutations (Sic1-Δ3P) (Figure 4.9A), suggesting that T5, T33 and/or S76 are the Pho85 targets *in vitro* (notably, the residual phosphorylation level in Sic1-Δ3P suggests the presence of an additional site(s) in Sic1 that may be targets *in vitro* by Pho85). Taken together, our data suggested that the Pho85 cyclins Clg1, Pcl1 and Pho80 contribute to the kinase activity of Pho85 towards the T5, T33 and/or S76 sites on Sic1.

To assess the relevance of Sic1 phosphorylation by Clg1-, Pcl1- and Pho80-associated Pho85 complexes *in vivo*, we assayed the effects of overexpression of these cyclins on the stability of Sic1 or Sic1-Δ3P, and hence the effect on autophagy. *pcl5*Δ *pho80*Δ cells bearing chromosomally integrated *GAL1* promotor-driven HA-tagged Sic1 or Sic1-Δ3P, were transformed with a plasmid expressing *GAL1* promotor-driven HA-tagged Clg1, Pcl1, Pcl2, Pcl9, Pho80 or Pcl5, or an empty vector. Although all of the various cyclin-CDK

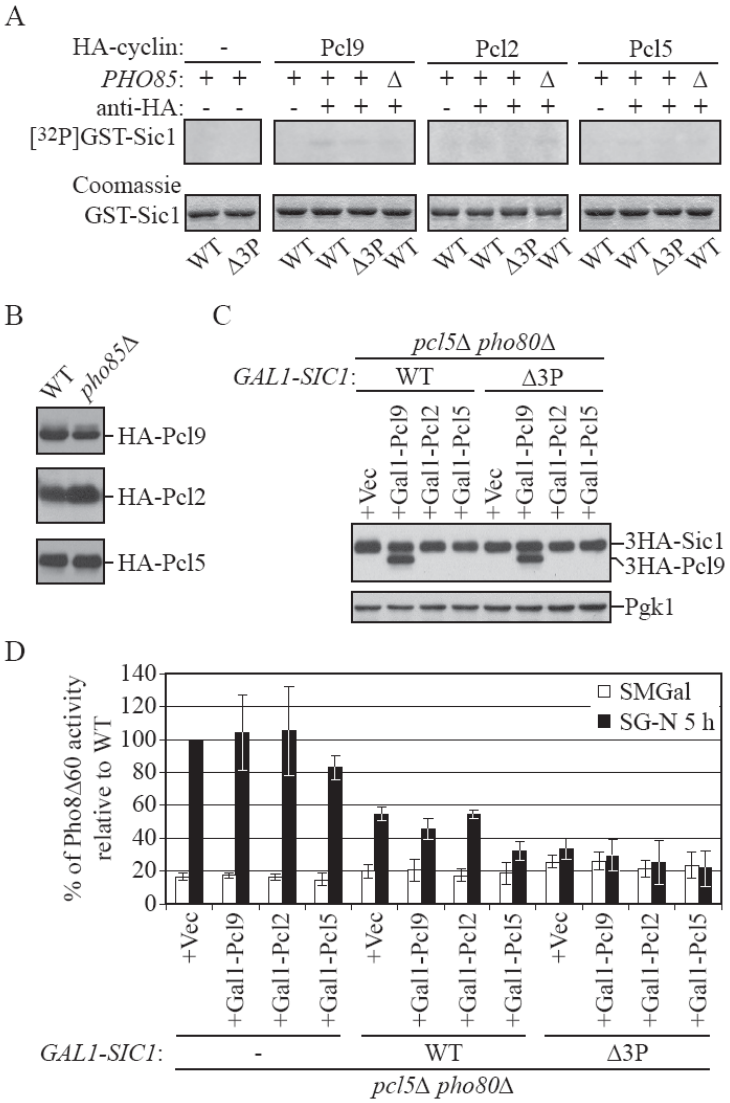

Figure 4.10. Pcl9, Pcl2 and Pcl5 are not cyclin partners of Pho85 for Sic1 phosphorylation. (A) Immunoprecipitated Pcl9-, Pcl2- and Pcl5-associated Pho85 complexes do not phosphorylate Sic1 *in vitro*. GST-Sic1 (pZY037) and GST-Sic1-Δ3P (pZY040), expressed and purified from *E.coli*, were used as substrates in *in vitro* kinase assay using immunoprecipitated HA-tagged Pcl9 (pZY021), Pcl2 (pZY019), or Pcl5 (pZY020) from wild-type (W303-1B) or *pho85*Δ (ZFY088) cells. As a negative control, the antibody was not added (-) to the reaction. Phosphorylated proteins were detected by autoradiography (top) and the protein input was shown by Coomassie Blue staining (bottom). (B) The immunoprecipitates used in (A) were analyzed for the presence of HA-cyclin by immunoblotting using anti-HA antibody. (C) Overexpression of Pcl9, Pcl2 or Pcl5

does not affect the abundance of overexpressed Sic1 wild type or the Sic1-Δ3P mutant. *pcl5*Δ *pho80*Δ *GAL1-3HA-SIC1* (ZFY256) and *pcl5*Δ *pho80*Δ *GAL1-3HA-SIC1-Δ3P* (ZFY257) expressing either 3HA-Pcl9 (pZY021), 3HA-Pcl2 (pZY019), 3HA-Pcl5 (pZY020) or an empty vector (pTY006), were grown in SMD and shifted to SMGal for 12 h, and were analyzed by immunoblotting using anti-HA and anti-Pgk1 (loading control) antisera. (D) Overexpression of Pcl9, Pcl2 or Pcl5 does not suppress the inhibitory effect of overexpression of Sic1 wild type, or the Sic1-Δ3P mutant, on autophagy. *pcl5*Δ *pho80*Δ (ZFY255), ZFY256 and ZFY257 bearing either pZY021, pZY019, pZY020 or pTY006, were grown in SMD and shifted to SMGal for 12 h, then shifted to SG-N for 5 h, and analyzed by the Pho8Δ60 assay. Values were normalized to the activity of ZFY255 cells bearing pTY006, and subjected to nitrogen starvation, which was set to 100%. Error bars indicate the SD of three independent experiments.

complexes displayed similar stability (Figure 4.9B and 4.10B), after 12 h in galactose-containing medium, cells that overexpressed Sic1 alone accumulated Sic1, whereas cells that additionally overexpressed Clg1, Pcl1 or Pho80, but not Pcl9, Pcl2 or Pcl5, displayed a markedly reduced level of Sic1 (Figure 4.9C and 4.10C). Furthermore, the defect of nitrogen starvation-induced autophagy caused by overexpression of Sic1 was almost completely abolished by overexpression of Clg1, Pcl1 or Pho80, but not Pcl9, Pcl2 or Pcl5 (Figure 4.9D and 4.10D). In contrast, in the cells that overexpressed Sic1-Δ3P, the level of Sic1-Δ3P did not decrease appreciably when combined with overexpression of Clg1, Pcl1 or Pho80 (Figure 4.9C). Correspondingly, these cells were unable to relieve the autophagic defect caused by accumulation of Sic1-Δ3P (Figure 4.9D). Taken together, the above results suggested that Pho85 forms complexes with cyclins Clg1, Pcl1 and Pho80 to directly phosphorylate T5, T33 and/or S76 of Sic1, and hence promote autophagy by targeting Sic1 for degradation.

Rim15 is a downstream target of Sic1

To better understand how Sic1 negatively regulates autophagy, we decided to identify which downstream effectors of Sic1 might be involved in autophagy regulation. The data presented above suggested that Pho80-Pho85, Pcl5-Pho85, and Sic1, at least in part, negatively regulate autophagy in parallel pathways. If this is true, one would expect to see that loss of the three downstream targets of Pho80-Pho85 and Pcl5-Pho85 (Figure 4.1) would not suppress the upregulation of autophagy that was seen in the *sic1*Δ mutant. When treated with rapamycin, deletion of *PHO4* had little, if any, effect on Pho8Δ60 activity in *sic1*Δ cells (Figure 4.11A). In contrast, deletion of *RIM15* or *GCN4* resulted in a dramatic decrease in the Pho8Δ60 activity of *sic1*Δ cells (Figure 4.11A). This result suggested that Rim15 and/or Gcn4, but not Pho4, might be downstream targets of Sic1.

We reasoned that if Sic1 inhibits autophagy through downregulating Rim15 and/or Gcn4, then overexpression of Sic1 in mutants lacking Rim15 or Gcn4 would not exaggerate the defect in autophagy. To this end, the *GAL1* promoter was integrated at the *SIC1* locus to allow conditional overexpression of *SIC1* in wild-type, *rim15*Δ, *pho4*Δ and *gcn4*Δ cells. With rapamycin or nitrogen starvation, the level of free GFP processed from GFP-Atg8 was significantly reduced upon overexpression of Sic1 in wild-type, *pho4*Δ and *gcn4*Δ cells (Figure 4.11B). In contrast, in *rim15*Δ cells, there was no discernable difference in GFP-Atg8 processing between the presence and absence of Sic1 overexpression (Figure 4.11B). Furthermore, overexpression of Sic1 resulted in a markedly reduced activity of Pho8Δ60 that was induced by nitrogen starvation, in wild-type, *pho4*Δ and *gcn4*Δ cells, but not *rim15*Δ cells (Figure 4.11C). Notably, deletion of *RIM15*, *PHO4* or *GCN4* does not affect the stability of Sic1 (Figure 4.11D). Thus, these

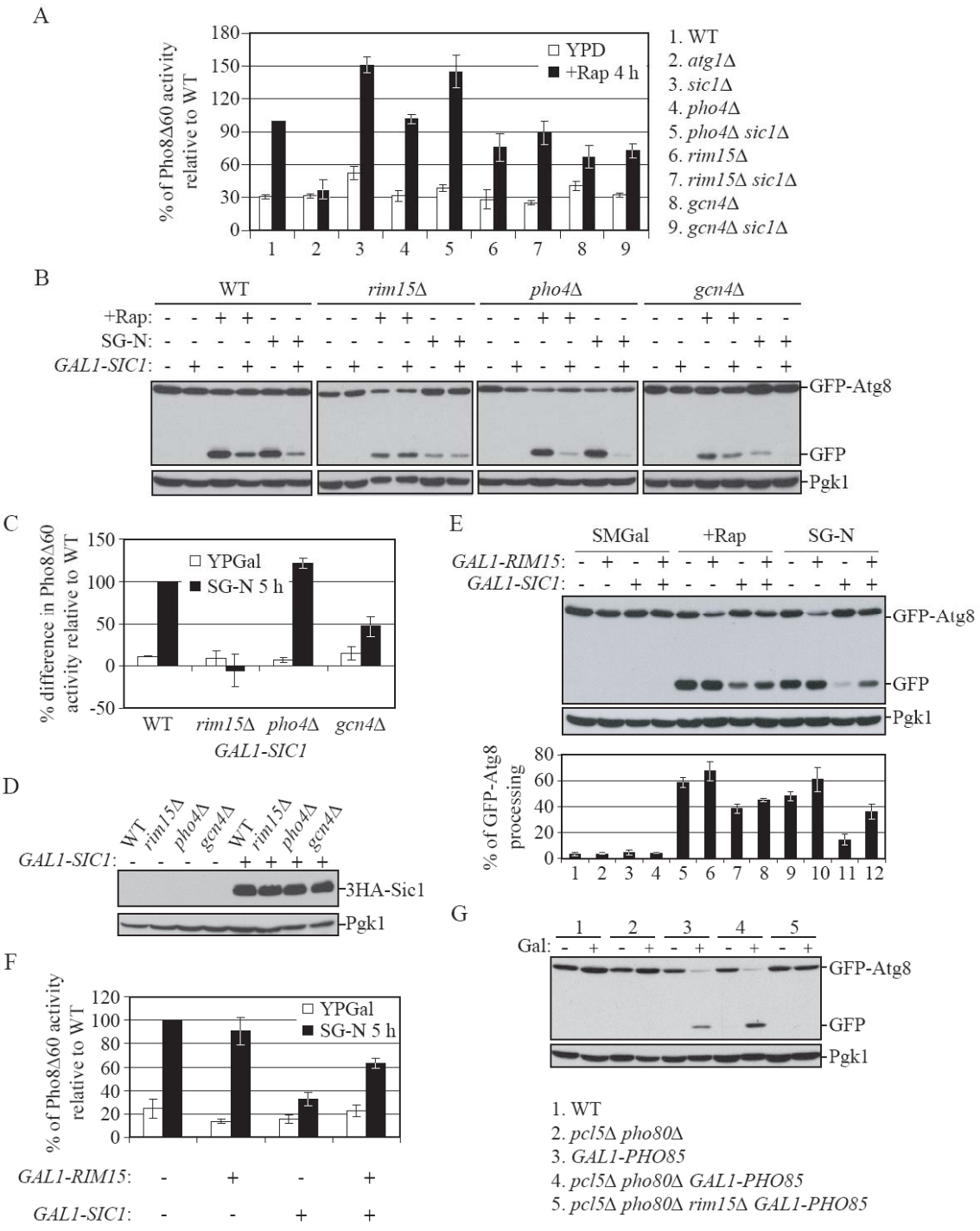
A
% of Pho8Δ60 activity relative to WT
YPD
+Rap 4 h
1. WT
2. atg1Δ
3. sic1Δ
4. pho4Δ
5. pho4Δ sic1Δ
6. rim15Δ
7. rim15Δ sic1Δ
8. gcn4Δ
9. gcn4Δ sic1Δ
B
WT
rim15Δ
pho4Δ
gcn4Δ
+Rap:
SG-N:
GAL1-SIC1:
GFP-Atg8
GFP
Pgk1
C
% difference in Pho8Δ60 activity relative to WT
YPGal
SG-N 5 h
WT
rim15Δ
pho4Δ
gcn4Δ
GAL1-SIC1
D
GAL1-SIC1:
3HA-Sic1
Pgk1
E
SMGal
+Rap
SG-N
GAL1-RIM15:
GAL1-SIC1:
GFP-Atg8
GFP
Pgk1
% of GFP-Atg8 processing
F
% of Pho8Δ60 activity relative to WT
YPGal
SG-N 5 h
GAL1-RIM15:
GAL1-SIC1:
G
Gal:
GFP-Atg8
GFP
Pgk1
1. WT
2. pcl5Δ pho80Δ
3. GAL1-PHO85
4. pcl5Δ pho80Δ GAL1-PHO85
5. pcl5Δ pho80Δ rim15Δ GAL1-PHO85

Figure 4.11. Rim15 is a downstream target of Sic1. (A) Deletion of *RIM15* or *GCN4*, but not *PHO4*, suppresses the upregulation of autophagy in *sic1*Δ cells. Wild-type (TN124), *atg1*Δ (HAY572), *sic1*Δ (ZFY098), *pho4*Δ (ZFY135), *pho4*Δ *sic1*Δ (ZFY141), *rim15*Δ (ZFY100), *rim15*Δ *sic1*Δ (ZFY116), *gcn4*Δ (ZFY111) and *gcn4*Δ *sic1*Δ (ZFY115) cells were analyzed by the Pho8Δ60 assay, as described in Figure 2D. (B) and (C) Overexpression of Sic1 inhibits autophagy in wild-type, *pho4*Δ and *gcn4*Δ cells, but not *rim15*Δ cells. (B) Wild type (W303-1B), *rim15*Δ (ZFY132), *pho4*Δ (ZFY170), *gcn4*Δ (ZFY131), *GAL1-SIC1* (ZFY184), *rim15*Δ*GAL1-SIC1* (ZFY187), *pho4*Δ *GAL1-SIC1* (ZFY188) and *gcn4*Δ *GAL1-SIC1* (ZFY185) cells were analyzed by the GFP-Atg8 processing assay, as described in Figure 2A. (C) Wild-type (ZFY202), *rim15*Δ (ZFY204), *pho4*Δ (ZFY252), *gcn4*Δ (ZFY251), *GAL1-SIC1* (ZFY203), *rim15*Δ *GAL1-SIC1* (ZFY249), *pho4*Δ *GAL1-SIC1* (ZFY250) and *gcn4*Δ *GAL1-SIC1* (ZFY248) cells were analyzed by the Pho8Δ60 assay, as described in Figure 2B. The difference of the Pho8Δ60 activity between the absence and presence of Sic overexpression was normalized to the difference in wild-type cells treated with nitrogen starvation, which was set to 100%. Error bars indicate the SD of three independent experiments. (D) Deletion of *RIM15*, *PHO4* or *GCN4* does not affect the stability of Sic1. Wild type (W303-1B), *rim15*Δ (ZFY132), *pho4*Δ (ZFY170), *gcn4*Δ (ZFY131), *GAL1-3HA-SIC1* (ZFY184), *rim15*Δ *GAL1-3HA-SIC1* (ZFY187), *pho4*Δ *GAL1-3HA-SIC1* (ZFY188) and *gcn4*Δ *GAL1-3HA-SIC1* (ZFY185) cells, were grown to early log phase (OD_{600} = 0.5-0.6). Immunoblotted proteins were detected with anti-HA and anti-Pgk1 (loading control) antisera. (E) and (F) Overexpression of Rim15 partially suppresses the inhibitory effect of Sic1 overexpression on autophagy. (D) Wild-type (W303-1B), *GAL1-RIM15* (ZFY192), *GAL1-SIC1* (ZFY184) and *GAL1-SIC1 GAL1-RIM15* (ZFY193) cells were analyzed by the GFP-Atg8 processing assay, as described in Figure 2A. (E) Wild-type (ZFY202), *GAL1-RIM15* (ZFY253), *GAL1-SIC1* (ZFY203) and *GAL1-SIC1 GAL1-RIM15* (ZFY254) cells were analyzed by the Pho8Δ60 assay, as described in Figure 2B. (G) Deletion of *RIM15* blocks the induction of autophagy upon overexpression of Pho85 in *pcl5*Δ *pho80*Δ cells. Wild-type (W3030-1B), *pcl5*Δ *pho80*Δ (ZFY207), *GAL1-PHO85* (ZFY209), *pcl5*Δ *pho80*Δ *GAL1-PHO85* (ZFY208) and *pcl5*Δ *pho80*Δ *rim15*Δ *GAL1-PHO85* (ZFY216) cells were analyzed by the GFP-Atg8 processing assay, as described in Figure 4A.

results indicated that Rim15, but not Gcn4, might be a downstream target of Sic1.

To further examine this possibility, we generated a strain in which the *GAL1* promoter was integrated in front of both *RIM15* and *SIC1*. When cells were shifted to nitrogen

starvation, the percentage of GFP-Atg8 processing was dramatically increased in cells co-overexpressing Rim15 and Sic1, being ~2.5-fold higher than that of cells overexpressing Sic1 alone (Figure 4.11E, compare lane 11 to 12). Furthermore, the level of Pho8Δ60 activity was significantly elevated (~2-fold increase) in cells co-overexpressing Rim15 and Sic1, compared to that of cells overexpressing Sic1 alone (Figure 4.11F). Thus, these data let us propose a model in which Rim15 acts as a downstream target of Sic1, and overexpression of Rim15 acts to antagonize the inhibition of autophagy caused by Sic1 overexpression.

Based on the above data, Pho85 negatively regulated Sic1, and Sic1 negatively regulated Rim15, which indicated that Rim15 may be essential for autophagy induced by Pho85 overexpression. However, since Rim15 is also under the negative regulation of Pho80-Pho85, a negative regulator of autophagy, loss of Rim15 would presumably suppress both negative and positive regulation of Pho85 (Figure 4.1). To this end, we decided to examine the effect associated with deletion of *RIM15* in the background of *pho80*Δ *pcl5*Δ *GAL1-PHO85*. We found that loss of Rim15 completely abolished the appearance of vacuolar GFP-Atg8 (Figure 4.5B) and free GFP induced by Pho85 overexpression (Figure 4.11G). Thus, these data further strengthened our model that Rim15 is a downstream target of Sic1.

DISCUSSION

The nutritional environment is a critical determinant of cellular behavior. As an intracellular degradative process, autophagy is tightly regulated by intracellular and extracellular nutrient levels. Several key intracellular regulators, many of which are protein kinases, play roles in the regulation of autophagy, including Tor, PKA, Sch9 and Pho85. In this study, we elucidated the mechanism of Pho85 in autophagy regulation, and demonstrated: (1) Pho80 and Pcl5 target Pho85 to negatively regulate autophagy via downregulating Rim15, Pho4 and Gcn4; (2) Sic1 is a negative regulator of autophagy; (3) Clg1, Pcl1 and Pho80 target Pho85 to positively regulate autophagy via destabilizing Sic1; (4) Rim15 acts as a downstream target of Sic1.

Pho85 seems to be involved in at least two types of sensing, including roles in environmental signaling and cell cycle regulation (Huang et al., 2007). The main role of Pho85 in environmental signaling is to turn off activities that are needed only under specific stress conditions. For example, when inorganic phosphate becomes scarce, Pho80-Pho85 is inhibited, thereby allowing activation of Pho4 which promotes the expression of genes involved in phosphate metabolism, and activation of Rim15 which is a key controller of many aspects of the G_0 program. In response to amino acid starvation, the level of the Pcl5 protein is substantially reduced, resulting in hypophosphorylation and stabilization of Gcn4, which activates amino acid biosynthesis genes. We found that both of these two nutrient sensors, Pho80-Pho85 and Pcl5-Pho85, negatively regulate autophagy. Thus, Pho85 links the regulation of autophagy to phosphate and amino acid starvation.

In addition to serving as a repressor of environmental stress responses, Pho85 has important roles in regulating cell-cycle progression (Carroll and O'Shea, 2002). We

investigated one of the targets of Pho85 with well-defined functions in G_1/S progression, the CDK inhibitor Sic1. Sic1 is an inhibitor of S phase Clb cyclin-containing Cdc28 kinase complexes. It is expressed in late M phase and remains stable until the late G_1 phase. Sic1 must be phosphorylated to be targeted for destruction at the end of the G_1 phase, which is a necessary step for initiation of S phase entry and DNA replication (Deshaies and Ferrell, 2001). The major kinases involved in phosphorylating Sic1 are the Cln-Cdc28 kinases, whereas Pho85 serves an accessory role, based on the observations that Pho85 can phosphorylate Sic1 *in vitro* and is required for full phosphorylation of Sic1 *in vivo* (Nishizawa et al., 1998; Verma et al., 1997). Moreover, when DNA damage occurs in G_1, Cln-Cdc28 is downregulated, leading to cell cycle delay. Pho85 is required for the return to cell cycle progression through promoting Sic1 degradation and Cdc28 activation (Wysocki et al., 2006). While most previous work has linked only the roles of Sic1 to cell cycle regulation, our observations indicate that it also functions as a negative regulator of autophagy. Moreover, we found that Pho85 is a positive regulator of autophagy through targeting Sic1 for degradation, and apparently several of the cyclins, including Clg1, form complexes with Pho85 to fulfill this role. Thus, these data demonstrated that Pho85 has two separate and opposite roles in autophagy regulation.

One question is to ask which cyclin partner(s) function together with Pho85 to promote autophagy. We reasoned that since Pho85 promotes the induction of autophagy, then the corresponding cyclin(s) must also be involved in autophagy regulation. We found that deletion of *CLG1* alone, but not other cyclins, significantly reduced the level of autophagy that was induced by rapamycin (Figure 4.6 and 4.7A). On the other hand, when starved for nitrogen, the *clg1*Δ *pcl1*Δ *pcl2*Δ*pcl9*Δ quadruple mutant displayed a

significantly lower Pho8Δ60 activity than the single *clg1*Δ mutant, suggesting that Pcl1, Pcl2 and Pcl9 might have some redundant role with Clg1 in autophagy regulation. Moreover, deletion of *CLG1* significantly inhibited, but did not completely abolish the induction of autophagy by Pho85 overexpression (Figure 4.7C), suggesting that Clg1 is not the sole cyclin that targets Pho85 to positively regulate autophagy. Since Pho85 promotes the induction of autophagy through destabilizing Sic1, then the corresponding cyclin(s) must be also involved in regulation of Sic1 stability. Since Sic1 must be phosphorylated to be targeted for degradation, we then asked which cyclin(s) is responsible for Pho85-associated kinase activity toward Sic1. We found that Clg1 was the primary autophagy-regulating cyclin partner of Pho85 to phosphorylate Sic1 *in vitro* (Figure 4.9A). In addition, we confirmed the previous result from Nishizawa et al. (1998) that the Pcl1-Pho85 (but not Pcl2-Pho85) complex phosphorylates Sic1 *in vitro*. Intriguingly, the stress responsive Pho80-Pho85 complex strongly phosphorylated Sic1 *in vitro*. We further investigated the mutant version of Sic1, Sic1-Δ3P, which contains T5A, T33V and S76A mutations. Sic1-Δ3P was phosphorylated to a significantly lower extent than wild type Sic1 (Figure 4.9A), suggesting at least T5, T33 and/or S76 were phosphorylated *in vitro*. To gain more insight into the physiological relevance of these phosphorylation events *in vivo*, we further examined the effect of overexpression of these cyclins on the regulation of Sic1 stability and the induction of autophagy. Indeed, overexpression of Clg1, Pcl1 or Pho80 significantly reduced the level of wild type Sic1, but not Sic1-Δ3P, and overcame the inhibition of autophagy caused by overexpression of wild type Sic1, but not Sic1-Δ3P (Figure 4.9C and 4.9D). Taken together, these data support our model that Pho85 complexes with cyclins Clg1, Pcl1 and Pho80 to directly phosphorylate T5, T33 and/or

S76 of Sic1, and hence promote autophagy by targeting Sic1 for degradation. The observations that Pho80-Pho85 negatively regulated autophagy through inactivating Rim15 and Pho4, and also positively regulated autophagy through downregulating Sic1, led us to propose that it has dual roles in autophagy regulation (Figure 4.1); however, further studies are clearly needed to clarify the relationship between Clg1, Pcl1 and Pho80 in Sic1 and autophagy regulation. The observation that single *clg1*Δ cells, but not other single *pcl* mutants, showed an autophagic defect (Figure 4.6 and 4.7A), indicated that Clg1 might play a primary role. Pho80-Pho85 is localized exclusively to the nucleus (Kaffman et al., 1998); Clg1 is localized primarily to the nucleus (our unpublished data), whereas Pcl1 localizes partially to the nucleus as well as sites of polarized cell growth (Moffat and Andrews, 2004). Moreover, transcript levels for *CLG1* and *PHO80* are constant throughout the cell cycle, whereas *PCL1* is specifically expressed during the late G_1 phase (Measday et al., 1997). Thus, it is likely that subcellular localization of Pcl-Pho85 complexes and/or the timing of expression of these cyclin genes contributes to the selection of when and where to phosphorylate Sic1 and promote its degradation.

In mammalian cells, the CDK inhibitor p27 functions as a positive regulator of autophagy (Liang et al., 2007). In the present study, however, we found that the yeast CDK inhibitor Sic1 is a negative regulator of autophagy, based on the observations that overexpression of Sic1 or Sic1-Δ3P, a degradation-resistant mutant, significantly inhibited autophagy, and that loss of Sic1 dramatically upregulated autophagy. Moreover, autophagy was inhibited in the *cdc28-4*^{ts} and *cdc34-2*^{ts} mutants, in which Sic1 accumulates (Schwob et al., 1994), whereas deletion of *SIC1* in the *cdc28-4*^{ts} mutant partially suppressed the defect in autophagy induction. These observations fit well with the view that

hyper-accumulation of Sic1 inhibits autophagy. Cells that overexpress the Clb-Cdc28 inhibitor Sic1 accumulate in G_1 phase, and the *cdc34-2*^{ts}, *cdc28-4*^{ts} and *cdc28-13*^{ts} mutants also display a G_1 cell cycle arrest after incubation at nonpermissive temperature (Nugroho and Mendenhall, 1994; Schwob et al., 1994; Verma et al., 1997). Thus, we cannot rule out the possibility that the defect in autophagy caused by hyper-accumulation of Sic1 might be due to cell cycle arrest at the G_1 phase. On the other hand, induction of autophagy under conditions of nutrient limitation often accompanies cell cycle arrest at the G_1 phase. Therefore, it is also possible that cell cycle arrest may not be directly linked to autophagy regulation, and autophagy may occur in parallel with cell cycle arrest. Further analysis is needed to identify the precise correlation between cell cycle arrest and autophagy.

One obvious question is how Sic1 negatively regulates autophagy. Our data suggest that Rim15 acts as a downstream target of Sic1. First, deletion of *RIM15* completely suppressed the upregulation of autophagy in *sic1*Δ cells (Figure 4.11A). Second, inhibition of autophagy caused by Sic1 overexpression did not occur in *rim15*Δ cells (Figure 4.11B and 4.11C). Third, Rim15 overexpression partially suppressed the inhibition of autophagy caused by Sic1 overexpression (Figure 4.11E and 4.11F). Since Sic1 is a stoichiometric inhibitor of Clb-Cdc28 kinases, we asked whether inhibition of Rim15 kinase activity occurs through a physical interaction between Rim15 and Sic1. However, only a weak interaction was detected in co-immunoprecipitation experiments (data not shown). Thus, further study will be needed to elucidate the mechanism by which Sic1 inhibits Rim15. Notably, our data suggest that Rim15 integrates signals from both the negative and positive regulatory pathways of Pho85 to properly control autophagy.

In conclusion, we have elucidated the regulatory mechanism by which Pho85 and its

corresponding cyclins modulate autophagy in yeast. We propose that Pho85, not only integrates nutrient signals via the Pho80-Pho85 and Pcl5-Pho85 cyclin-CDK complexes to negatively regulate autophagy, but that it also integrates information from the cell cycle inhibitor Sic1 via the Clg1-, Pcl1-, and Pho80-Pho85 cyclin-CDK complexes to promote autophagy. Although Pho85 does not play a major role in regulating autophagy compared to the TORC1 complex, the multifunctional CDK Pho85 is critical to ensure appropriate autophagy activity during various extracellular and intracellular stress conditions.

EXPERIMENTAL PROCEDURES

Strains, Plasmids and Media

Yeast strains and plasmids used in this study are listed in Table 4.1 and 4.2.

Strains were grown at 30°C in standard rich medium with 2% glucose (YPD), or 2% galactose plus 2% raffinose (YPGal) as carbon source, or synthetic medium with 2% glucose (SMD), or 2% galactose plus 2% raffinose (SMGal) as carbon source. Rapamycin (dissolved in 90% ethanol/10% Tween-20) was added to the media at a final concentration of 2 μg/ml. For starvation conditions, cells were shifted to SD-N or SG-N medium. 1-Na-PP1 was added to the media at a final concentration of 20 mM for the analysis of the ATP analogue-sensitive mutant PHO85^{F82G}.

Table 4.1. Yeast strains used in this study

Strain	Genotype	Source or Reference
BY4742	*MATa leu2- 0 his3- 1 lys2- 0 ura3- 0*	ResGen/Invitrogen
D4	*MATα ade1 cdc28-4 his3 leu2 trp1*	(Mendenhall et al., 1988)
D13	*MATα ade1 cdc28-13 his3 leu2 trp1*	(Mendenhall et al., 1988)
EY0823	W303-1A *pho85Δ::LEU2 trp1::pho85-F82G::TRP1 pho3Δ ADE2*	(Carroll et al., 2001)
HAY572	TN124 *atg1Δ::URA3*	(Abeliovich et al., 2003)
MTY670	W303-1A *MATa cdc34-2*	(Willems et al., 1996)
TN124	*MATα leu2–3,112 ura3–52 trp1 pho8Δ::PHO8Δ60 pho13Δ::LEU2*	(Noda et al., 1995)
TYY164	W303-1B *atg1Δ::KanMX6*	This study

TYY181	W303-1B *pho13Δ::KanMX6 pho8Δ60::HIS3 atg1Δ::URA3*	(Yorimitsu et al., 2007)
W303-1A	*MATa ade2-1 can1-100 his3-11,15 leu2-3,112 trp1-1 ura3-1*	(Wallis et al., 1989)
W303-1B	*MATα ade2-1 can1-100 his3-11,15 leu2-3,112 trp1-1 ura3-1*	(Wallis et al., 1989)
YZX200	TN124 *atg8Δ::KanMX6*	(Xie et al., 2008)
ZFY088	W303-1B *pho85Δ::HIS3*	This study
ZFY089	TN124 *pho85Δ::URA3*	This study
ZFY098	TN124 *sic1Δ::URA3*	This study
ZFY099	TN124 *pcl5Δ::URA3*	This study
ZFY100	TN124 *rim15Δ::URA3*	This study
ZFY102	TN124 *pho80Δ::URA3 rim15Δ::TRP1*	This study
ZFY103	TN124 *pcl5Δ::URA3 rim15Δ::TRP1*	This study
ZFY105	TN124 *pho80Δ::URA3*	This study
ZFY111	TN124 *gcn4Δ::TRP1*	This study
ZFY112	TN124 *gcn4Δ::TRP1 pcl5Δ::URA3*	This study
ZFY115	TN124 *gcn4Δ::TRP1 sic1Δ::URA3*	This study
ZFY116	TN124 *rim15Δ::URA3 sic1Δ::TRP1*	This study
ZFY121	TN124 *pcl1Δ::URA3*	This study
ZFY128	TN124 *pho80Δ::KanMX6 pcl5Δ::URA3*	This study
ZFY129	TN124 *pcl1Δ::URA3 pcl2Δ::TRP1 pcl9Δ::KanMX6*	This study
ZFY130	TN124 *pcl2Δ::KanMX6*	This study

ZFY131	W303-1B *gcn4Δ::KanMX6*	This study
ZFY132	W303-1B *rim15Δ::KanMX6*	This study
ZFY135	TN124 *pho4Δ::KanMX6*	This study
ZFY137	TN124 *pho80Δ::URA3 pho4Δ::KanMX6*	This study
ZFY139	TN124 *pcl9Δ::KanMX6*	This study
ZFY141	TN124 *sic1Δ::URA3 pho4Δ::KanMX6*	This study
ZFY142	TN124 *gcn4Δ::TRP1 pho4Δ::KanMX6*	This study
ZFY143	TN124 *pcl5Δ::URA3 pho4Δ::KanMX6*	This study
ZFY145	EY0823 *pho13Δ::HIS3 pho8Δ60::URA3*	This study
ZFY152	W303-1B *gcn4Δ::KanMX6 rim15Δ::HIS3 pho4Δ::LEU2*	This study
ZFY155	W303-1A *pho13Δ::HIS3 pho8Δ60::URA3*	This study
ZFY170	W303-1B *pho4Δ::LEU2*	This study
ZFY172	TN124 *pho80Δ::KanMX6 pcl5Δ::URA3 pho85Δ::TRP1*	This study
ZFY174	W303-1B *gcn4Δ::KanMX6 rim15Δ::HIS3 pho4Δ::LEU2 pho85Δ::TRP1*	This study
ZFY175	TN124 *gcn4Δ::TRP1 pho4Δ::KanMX6 rim15Δ::URA3*	This study
ZFY177	TN124 *gcn4Δ::TRP1 pho4Δ::KanMX6 rim15Δ::URA3 pho85Δ::BLE*	This study
ZFY178	TN124 *pcl8Δ::URA3*	This study
ZFY179	TN124 *pcl10Δ::URA3*	This study
ZFY180	TN124 *pcl8Δ:: KanMX6 pcl10Δ::URA3*	This study
ZFY182	TN124 *clg1Δ::BLE*	This study

ZFY183	TN124 *pcl1Δ::URA3 pcl2Δ::TRP1 pcl9Δ::KanMX6 clg1Δ::BLE*	This study
ZFY184	W303-1B *HIS3::GAL1p-3HA-SIC1*	This study
ZFY185	W303-1B *gcn4Δ::KanMX6 HIS3::GAL1p-3HA-SIC1*	This study
ZFY187	W303-1B *rim15Δ::KanMX6 HIS3::GAL1p-3HA-SIC1*	This study
ZFY188	W303-1B *pho4Δ::LEU2 HIS3::GAL1p-3HA-SIC1*	This study
ZFY192	W303-1B *TRP1::GAL1p-3HA-RIM15*	This study
ZFY193	W303-1B *HIS3::GAL1p-3HA-SIC1 TRP1::GAL1p-3HA-RIM15*	This study
ZFY202	W303-1B *pho13Δ pho8Δ60::HIS3*	This study
ZFY203	W303-1B *pho13Δ pho8Δ60::HIS3 TRP1::GAL1p-3HA-SIC1*	This study
ZFY204	W303-1B *pho13Δ pho8Δ60::HIS3 rim15Δ::BLE*	This study
ZFY206	W303-1B *pho13Δ pho8Δ60::HIS3 pho80Δ::LEU2 pcl5Δ::BLE*	This study
ZFY207	W303-1B *pho80Δ pcl5Δ*	This study
ZFY208	W303-1B *pho80Δ pcl5Δ HIS3::GAL1p-3HA-PHO85*	This study
ZFY209	W303-1B *HIS3::GAL1p-3HA-PHO85*	This study
ZFY213	EY0823 *pho13Δ::HIS3 pho8Δ60::URA3 atg1Δ::KanMX6*	This study
ZFY214	EY0823 *pho13Δ pho8Δ60::URA3 pho80Δ::HIS3 pcl5Δ::BLE sic1Δ::KanMX6*	This study

ZFY215	EY0823 *pho13Δ pho8Δ60::URA3 pho80Δ::HIS3 pcl5Δ::BLE*	This study
ZFY216	W303-1B *pho80Δ pcl5Δ HIS3::GAL1p-3HA-PHO85 rim15Δ::LEU2*	This study
ZFY217	W303-1B *pho80Δ pcl5Δ HIS3::GAL1p-3HA-PHO85 atg1Δ::LEU2*	This study
ZFY220	W303-1B *pho80Δ pcl5Δ HIS3::GAL1p-3HA-CLG1*	This study
ZFY224	W303-1B *pho13Δ pho8Δ60::HIS3 TRP1::GAL1p-3HA-PHO85*	This study
ZFY225	W303-1B *pho13Δ pho8Δ60::HIS3 pho80Δ::LEU2 pcl5Δ::BLE TRP1::GAL1p-3HA-PHO85*	This study
ZFY227	W303-1B *pho13Δ pho8Δ60::HIS3 pho80Δ::LEU2 pcl5Δ::BLE TRP1::GAL1p-3HA-PHO85 atg1Δ::URA3*	This study
ZFY228	W303-1B *clg1Δ::BLE*	This study
ZFY229	W303-1B *pcl1Δ::LEU2*	This study
ZFY230	W303-1B *pcl2Δ::KanMX6*	This study
ZFY231	W303-1B *pcl9Δ::LEU2*	This study
ZFY234	W303-1B *pcl1Δ::LEU2 pcl2Δ::KanMX6 pcl9Δ::HIS3*	This study
ZFY235	W303-1B *clg1Δ pcl1Δ pcl2Δ::KanMX6 pcl9Δ*	This study
ZFY246	W303-1B *pho80Δ pcl5Δ clg1Δ::LEU2 HIS3::GAL1p-3HA-PHO85*	This study
ZFY248	W303-1B *pho13Δ::LEU2 pho8Δ60::URA3 gcn4Δ::KanMX6 HIS3::GAL1p-3HA-SIC1*	This study

ZFY249	W303-1B *pho13Δ::LEU2 pho8Δ60::URA3 rim15Δ::KanMX6 HIS3::GAL1p-3HA-SIC1*	This study
ZFY250	W303-1B *pho13Δ::KanMX6 pho8Δ60::URA3 pho4Δ::LEU2 HIS3::GAL1p-3HA-SIC1*	This study
ZFY251	W303-1B *pho13Δ pho8Δ60::HIS3 gcn4Δ::LEU2*	This study
ZFY252	W303-1B *pho13Δ pho8Δ60::HIS3 pho4Δ::KanMX6*	This study
ZFY253	W303-1B *pho13Δ::LEU2 pho8Δ60::URA3 TRP1::GAL1p-3HA-RIM15*	This study
ZFY254	W303-1B *pho13Δ::KanMX6 pho8Δ60::URA3 HIS3::GAL1p-3HA-SIC1 TRP1::GAL1p-3HA-RIM15*	This study
ZFY255	W303-1B *pho13Δ pho8Δ60::HIS3 pho80Δ pcl5Δ*	This study
ZFY256	W303-1B *pho13Δ pho8Δ60::HIS3 pho80Δ pcl5Δ LEU2::GAL1p-3HA-SIC1*	This study
ZFY257	W303-1B *pho13Δ pho8Δ60::HIS3 pho80Δ pcl5Δ LEU2::GAL1p-3HA-SIC1-Δ3P*	This study
ZFY258	BY4742 *cdc28-4 sic1Δ::HIS3*	This study

Table 4.2. Yeast plasmids used in this study.

Plasmid	Vector; Insert	Source	Used in figure(s)
pCU-GFP-AUT7 (416)	pCU-GFP(416); Atg8	(Kim et al., 2001a)	2C, 2E, 4A, 4B, 5B, 7B, 7D, 7F, S2, S3A
pCU-GFP-AUT7 (414)	pCU-GFP(414); Atg8	(Kim et al., 2002)	2A, 4D, 5C, 5D, S7

pTY006	Yes2; *3HA*	(Yorimitsu et al., 2009)	2A, 4D, 5C, 5D, 6A, 6C, 6D, S5, S6, S7A, S7C, S7D
pZY011	Yes2; *3HA-SIC1*	This study	2A, 4D, 5C, S6, S7
pZY016	Yes2; *3HA-SIC1* (T5A T33V S76A)	This study	5D, S6, S7
pZY017	Yes2; *3HA-CLG1*	This study	6A, 6B, 6C, 6D
pZY018	Yes2; *3HA-PCL1*	This study	6A, 6B, 6C, 6D
pZY019	Yes2; *3HA-PCL2*	This study	S8A, S8B, S8C, S8D
pZY020	Yes2; *3HA-PCL5*	This study	S8A, S8B, S8C, S8D
pZY021	Yes2; *3HA-PCL9*	This study	S8A, S8B, S8C, S8D
pZY022	Yes2; *3HA-PHO80*	This study	6A, 6B, 6C, 6D
pZY032	pRS405; *GAL1-3HA-SIC1*	This study	6C, 6D, S8C, S8D
pZY033	pRS405; *GAL1-3HA-SIC1* (T5A T33V S76A)	This study	6C, 6D, S8C, S8D
pZY037	pGEX4T-1; *SIC1*	This study	6A, S8A
pZY040	pGEX4T-1; *SIC1* (T5A T33V S76A)	This study	6A, S8A
pZY041	pCU-PA(416); *SIC1*	This study	S5

Immunoblotting and Quantitative Analysis

Protein samples for western blotting were extracted by TCA precipitation and resolved by SDS-PAGE, followed by immunoblotting with appropriate antiserum or

antibodies, as described previously (Cheong et al., 2005). The band intensity was quantified with ImageJ software (National Institutes of Health). To calculate the percentage of GFP-Atg8 processing, we quantified the band intensity of both free GFP and GFP-Atg8, and calculated the percentage of free GFP relative to the sum of GFP-Atg8 and free GFP. To calculate the relative amount of PA-Sic1, we quantified the band intensity of PA-Sic1 and Adh1, and calculated the amount of PA-Sic1 relative to the amount of Adh1.

Fluorescence Microscopy

Cells were cultured in SMD selective medium to mid-log phase, and then shifted to SMGal selective medium for 12 h. For experiments under growing conditions, cells were pelleted and resuspended in fresh SMGal. For starvation experiments, cells were shifted to SG-N for 3 h, pelleted and resuspended in SG-N. Cells were visualized with a microscope (DeltaVision Spectris; Applied Precision, Issaquah, WA) fitted with differential interference contrast (DIC) optics and Olympus camera IX-HLSH100. The images were deconvolved using softWoRx software (Applied Precision).

Assays for Autophagy

To monitor bulk autophagy, the Pho8Δ60 assay and the GFP-Atg8 processing assay were performed as previously described (Noda et al., 1995; Shintani and Klionsky, 2004b).

In vitro Kinase Assay

GST-Sic1 wild type or GST-Sic1-Δ3P mutant were expressed in *E.coli* and purified using glutathione-Sepharose beads (GE Healthcare). To assay *in vitro* phosphorylation of Sic1 by Pho85 and its cyclin complex, HA-Clg1 (pZY017), HA-Pcl1 (pZY018), HA-Pcl2

(pZY019), HA-Pcl5 (pZY020), HA-Pcl9 (pZY021) and HA-Pho80 (pZY022), fusion proteins were expressed in SMGal medium for 4 h. The cells were disrupted by vortexing with acid-washed glass beads, in lysis buffer (50 mM Tris-HCl, pH7.5, 150 mM NaCl, 1 mM EDTA, 0.2% NP-40, 10% glycerol, 1 mM PMSF, 1X protease inhibitor cocktail, 1X phosphatase inhibitor cocktail [Roche]). HA-tagged fusion proteins were purified from clarified extracts with protein A sepharose beads using monoclonal mouse anti-HA antibody. Kinase reactions were performed with the protein A sepharose beads in kinase buffer (10 mM HEPES, 10 mM $MgCl_2$, 50 mM NaCl, 2 mM EDTA, 1 mM DTT, 0.02% Triton X-100) in a final volume of 30 µl containing 1 µg of indicated GST-Sic1 substrates, 100 µM ATP, 2 µCi of [γ-^{32}P]ATP and incubated for 30 min at 30 °C. Reactions were stopped by adding 10 µl of 4X SDS-PAGE sample buffer and denaturing for 5 min at 90 °C, and then subjected to SDS-PAGE and autoradiography.

REFERENCES

Abeliovich, H., Zhang, C., Dunn, W.A., Jr., Shokat, K.M., and Klionsky, D.J. (2003). Chemical genetic analysis of Apg1 reveals a non-kinase role in the induction of autophagy. Mol Biol Cell *14*, 477-490.

Bloom, J., and Cross, F.R. (2007). Multiple levels of cyclin specificity in cell-cycle control. Nat Rev Mol Cell Biol *8*, 149-160.

Budovskaya, Y.V., Stephan, J.S., Reggiori, F., Klionsky, D.J., and Herman, P.K. (2004). The Ras/cAMP-dependent protein kinase signaling pathway regulates an early step of the autophagy process in *Saccharomyces cerevisiae*. J Biol Chem *279*, 20663-20671.

Carrera, A.C. (2004). TOR signaling in mammals. J Cell Sci *117*, 4615-4616.

Carroll, A.S., Bishop, A.C., DeRisi, J.L., Shokat, K.M., and O'Shea, E.K. (2001). Chemical inhibition of the Pho85 cyclin-dependent kinase reveals a role in the environmental stress response. Proc Natl Acad Sci U S A *98*, 12578-12583.

Carroll, A.S., and O'Shea, E.K. (2002). Pho85 and signaling environmental conditions. Trends Biochem Sci *27*, 87-93.

Chen, Q., Xie, W., Kuhn, D.J., Voorhees, P.M., Lopez-Girona, A., Mendy, D., Corral, L.G., Krenitsky, V.P., Xu, W., Moutouh-de Parseval, L.*, et al.* (2008). Targeting the p27 E3 ligase SCF(Skp2) results in p27- and Skp2-mediated cell-cycle arrest and activation of autophagy. Blood *111*, 4690-4699.

Cheong, H., Yorimitsu, T., Reggiori, F., Legakis, J.E., Wang, C.W., and Klionsky, D.J. (2005). Atg17 regulates the magnitude of the autophagic response. Mol Biol Cell *16*, 3438-3453.

Cherkasova, V.A., and Hinnebusch, A.G. (2003). Translational control by TOR and TAP42 through dephosphorylation of eIF2α kinase GCN2. Genes Dev *17*, 859-872.

Deshaies, R.J., and Ferrell, J.E., Jr. (2001). Multisite phosphorylation and the countdown to S phase. Cell *107*, 819-822.

Espinoza, F.H., Ogas, J., Herskowitz, I., and Morgan, D.O. (1994). Cell cycle control by a complex of the cyclin HCS26 (PCL1) and the kinase PHO85. Science *266*, 1388-1391.

Feldman, R.M., Correll, C.C., Kaplan, K.B., and Deshaies, R.J. (1997). A complex of Cdc4p, Skp1p, and Cdc53p/cullin catalyzes ubiquitination of the phosphorylated CDK inhibitor Sic1p. Cell *91*, 221-230.

Hinnebusch, A.G. (2005). Translational regulation of GCN4 and the general amino

acid control of yeast. Annu Rev Microbiol *59*, 407-450.

Huang, D., Friesen, H., and Andrews, B. (2007). Pho85, a multifunctional cyclin-dependent protein kinase in budding yeast. Mol Microbiol *66*, 303-314.

Huang, J., and Klionsky, D.J. (2007). Autophagy and human disease. Cell Cycle *6*, 1837-1849.

Kaffman, A., Rank, N.M., O'Neill, E.M., Huang, L.S., and O'Shea, E.K. (1998). The receptor Msn5 exports the phosphorylated transcription factor Pho4 out of the nucleus. Nature *396*, 482-486.

Kim, J., Huang, W.P., and Klionsky, D.J. (2001). Membrane recruitment of Aut7p in the autophagy and cytoplasm to vacuole targeting pathways requires Aut1p, Aut2p, and the autophagy conjugation complex. J Cell Biol *152*, 51-64.

Kim, J., Huang, W.P., Stromhaug, P.E., and Klionsky, D.J. (2002). Convergence of multiple autophagy and cytoplasm to vacuole targeting components to a perivacuolar membrane compartment prior to de novo vesicle formation. J Biol Chem *277*, 763-773.

Komata, T., Kanzawa, T., Takeuchi, H., Germano, I.M., Schreiber, M., Kondo, Y., and Kondo, S. (2003). Antitumour effect of cyclin-dependent kinase inhibitors (p16(INK4A), p18(INK4C), p19(INK4D), p21(WAF1/CIP1) and p27(KIP1)) on malignant glioma cells. Br J Cancer *88*, 1277-1280.

Kubota, H., Obata, T., Ota, K., Sasaki, T., and Ito, T. (2003). Rapamycin-induced translational derepression of GCN4 mRNA involves a novel mechanism for activation of the eIF2α kinase GCN2. J Biol Chem *278*, 20457-20460.

Levine, B., and Deretic, V. (2007). Unveiling the roles of autophagy in innate and adaptive immunity. Nat Rev Immunol *7*, 767-777.

Levine, B., and Klionsky, D.J. (2004). Development by self-digestion: molecular mechanisms and biological functions of autophagy. Dev Cell *6*, 463-477.

Liang, J., Shao, S.H., Xu, Z.X., Hennessy, B., Ding, Z., Larrea, M., Kondo, S., Dumont, D.J., Gutterman, J.U., Walker, C.L.*, et al.* (2007). The energy sensing LKB1-AMPK pathway regulates p27(kip1) phosphorylation mediating the decision to enter autophagy or apoptosis. Nat Cell Biol *9*, 218-224.

Loewith, R., Jacinto, E., Wullschleger, S., Lorberg, A., Crespo, J.L., Bonenfant, D., Oppliger, W., Jenoe, P., and Hall, M.N. (2002). Two TOR complexes, only one of which is rapamycin sensitive, have distinct roles in cell growth control. Mol Cell *10*, 457-468.

Measday, V., Moore, L., Ogas, J., Tyers, M., and Andrews, B. (1994). The PCL2 (ORFD)-PHO85 cyclin-dependent kinase complex: a cell cycle regulator in yeast. Science *266*, 1391-1395.

Measday, V., Moore, L., Retnakaran, R., Lee, J., Donoviel, M., Neiman, A.M., and Andrews, B. (1997). A family of cyclin-like proteins that interact with the Pho85 cyclin-dependent kinase. Mol Cell Biol *17*, 1212-1223.

Mendenhall, M.D., al-Jumaily, W., and Nugroho, T.T. (1995). The Cdc28 inhibitor $p40^{SIC1}$. Prog Cell Cycle Res *1*, 173-185.

Mendenhall, M.D., Richardson, H.E., and Reed, S.I. (1988). Dominant negative protein kinase mutations that confer a G_1 arrest phenotype. Proc Natl Acad Sci U S A *85*, 4426-4430.

Moffat, J., and Andrews, B. (2004). Late-G_1 cyclin-CDK activity is essential for control of cell morphogenesis in budding yeast. Nat Cell Biol *6*, 59-66.

Nishizawa, M., Kawasumi, M., Fujino, M., and Toh-e, A. (1998). Phosphorylation of sic1, a cyclin-dependent kinase (Cdk) inhibitor, by Cdk including Pho85 kinase is required for its prompt degradation. Mol Biol Cell *9*, 2393-2405.

Noda, T., Matsuura, A., Wada, Y., and Ohsumi, Y. (1995). Novel system for monitoring autophagy in the yeast *Saccharomyces cerevisiae*. Biochem Biophys Res Commun *210*, 126-132.

Noda, T., and Ohsumi, Y. (1998). Tor, a phosphatidylinositol kinase homologue, controls autophagy in yeast. J Biol Chem *273*, 3963-3966.

Nugroho, T.T., and Mendenhall, M.D. (1994). An inhibitor of yeast cyclin-dependent protein kinase plays an important role in ensuring the genomic integrity of daughter cells. Mol Cell Biol *14*, 3320-3328.

Reggiori, F., and Klionsky, D.J. (2002). Autophagy in the eukaryotic cell. Eukaryot Cell *1*, 11-21.

Schmelzle, T., Beck, T., Martin, D.E., and Hall, M.N. (2004). Activation of the RAS/cyclic AMP pathway suppresses a TOR deficiency in yeast. Mol Cell Biol *24*, 338-351.

Schneider, B.L., Patton, E.E., Lanker, S., Mendenhall, M.D., Wittenberg, C., Futcher, B., and Tyers, M. (1998). Yeast G_1 cyclins are unstable in G_1 phase. Nature *395*, 86-89.

Schwob, E., Bohm, T., Mendenhall, M.D., and Nasmyth, K. (1994). The B-type cyclin kinase inhibitor $p40^{SIC1}$ controls the G_1 to S transition in S. cerevisiae. Cell *79*, 233-244.

Shemer, R., Meimoun, A., Holtzman, T., and Kornitzer, D. (2002). Regulation of the transcription factor Gcn4 by Pho85 cyclin PCL5. Mol Cell Biol *22*, 5395-5404.

Shintani, T., and Klionsky, D.J. (2004). Cargo proteins facilitate the formation of transport vesicles in the cytoplasm to vacuole targeting pathway. J Biol Chem *279*,

29889-29894.

Sopko, R., Huang, D., Smith, J.C., Figeys, D., and Andrews, B.J. (2007). Activation of the Cdc42p GTPase by cyclin-dependent protein kinases in budding yeast. EMBO J *26*, 4487-4500.

Swinnen, E., Wanke, V., Roosen, J., Smets, B., Dubouloz, F., Pedruzzi, I., Cameroni, E., De Virgilio, C., and Winderickx, J. (2006). Rim15 and the crossroads of nutrient signalling pathways in *Saccharomyces cerevisiae*. Cell Div *1*, 3.

Takeuchi, H., Kondo, Y., Fujiwara, K., Kanzawa, T., Aoki, H., Mills, G.B., and Kondo, S. (2005). Synergistic augmentation of rapamycin-induced autophagy in malignant glioma cells by phosphatidylinositol 3-kinase/protein kinase B inhibitors. Cancer Res *65*, 3336-3346.

Talloczy, Z., Jiang, W., Virgin, H.W.t., Leib, D.A., Scheuner, D., Kaufman, R.J., Eskelinen, E.L., and Levine, B. (2002). Regulation of starvation- and virus-induced autophagy by the eIF2α kinase signaling pathway. Proc Natl Acad Sci U S A *99*, 190-195.

Tennyson, C.N., Lee, J., and Andrews, B.J. (1998). A role for the Pcl9-Pho85 cyclin-cdk complex at the M/G_1 boundary in *Saccharomyces cerevisiae*. Mol Microbiol *28*, 69-79.

Thoreen, C.C., Kang, S.A., Chang, J.W., Liu, Q., Zhang, J., Gao, Y., Reichling, L.J., Sim, T., Sabatini, D.M., and Gray, N.S. (2009). An ATP-competitive Mammalian Target of Rapamycin Inhibitor Reveals Rapamycin-resistant Functions of mTORC1. J Biol Chem *284*, 8023-8032.

Urban, J., Soulard, A., Huber, A., Lippman, S., Mukhopadhyay, D., Deloche, O., Wanke, V., Anrather, D., Ammerer, G., Riezman, H*., et al.* (2007). Sch9 is a major target of TORC1 in *Saccharomyces cerevisiae*. Mol Cell *26*, 663-674.

Valentin, M., and Yang, E. (2008). Autophagy is activated, but is not required for the G_0 function of BCL-2 or BCL-X_L. Cell Cycle *7*, 2762-2768.

Verma, R., Annan, R.S., Huddleston, M.J., Carr, S.A., Reynard, G., and Deshaies, R.J. (1997). Phosphorylation of Sic1p by G_1 Cdk required for its degradation and entry into S phase. Science *278*, 455-460.

Wallis, J.W., Chrebet, G., Brodsky, G., Rolfe, M., and Rothstein, R. (1989). A hyper-recombination mutation in *S. cerevisiae* identifies a novel eukaryotic topoisomerase. Cell *58*, 409-419.

Wang, Z., Wilson, W.A., Fujino, M.A., and Roach, P.J. (2001a). Antagonistic controls of autophagy and glycogen accumulation by Snf1p, the yeast homolog of AMP-activated protein kinase, and the cyclin-dependent kinase Pho85p. Mol Cell Biol *21*, 5742-5752.

Wang, Z., Wilson, W.A., Fujino, M.A., and Roach, P.J. (2001b). The yeast cyclins Pc16p and Pc17p are involved in the control of glycogen storage by the cyclin-dependent protein kinase Pho85p. FEBS Lett *506*, 277-280.

Wanke, V., Pedruzzi, I., Cameroni, E., Dubouloz, F., and De Virgilio, C. (2005). Regulation of G_0 entry by the Pho80-Pho85 cyclin-CDK complex. EMBO J *24*, 4271-4278.

Willems, A.R., Lanker, S., Patton, E.E., Craig, K.L., Nason, T.F., Mathias, N., Kobayashi, R., Wittenberg, C., and Tyers, M. (1996). Cdc53 targets phosphorylated G_1 cyclins for degradation by the ubiquitin proteolytic pathway. Cell *86*, 453-463.

Wysocki, R., Javaheri, A., Kristjansdottir, K., Sha, F., and Kron, S.J. (2006). CDK Pho85 targets CDK inhibitor Sic1 to relieve yeast G_1 checkpoint arrest after DNA damage. Nat Struct Mol Biol *13*, 908-914.

Xie, Z., Nair, U., and Klionsky, D.J. (2008). Atg8 controls phagophore expansion during autophagosome formation. Mol Biol Cell *19*, 3290-3298.

Yang, Z., Huang, J., Geng, J., Nair, U., and Klionsky, D.J. (2006). Atg22 recycles amino acids to link the degradative and recycling functions of autophagy. Mol Biol Cell *17*, 5094-5104.

Yorimitsu, T., He, C., Wang, K., and Klionsky, D.J. (2009). Tap42-associated protein phosphatase type 2A negatively regulates induction of autophagy. Autophagy *5*.

Yorimitsu, T., Zaman, S., Broach, J.R., and Klionsky, D.J. (2007). Protein kinase A and Sch9 cooperatively regulate induction of autophagy in *Saccharomyces cerevisiae*. Mol Biol Cell *18*, 4180-4189.

CHAPTER 5

Conclusions and Contributions to the Field

This thesis can be broken down into two parts. In part I, including chapters 1 and 2, I reviewed our current knowledge of autophagy and its related pathways, in terms of the molecular machinery and signaling regulation in yeast and higher eukaryotic cells, with an emphasis on yeast (chapter 1) and on mammals (chapter 2). In both reviews, I discussed the physiological significance of autophagy, and more importantly, highlighted recent advances and pinpointed some unanswered questions remaining in the field. These reviews might provide some clues for our future work in autophagy. In part II, including chapters 3 and 4, I described the advances made contributing to the understanding of autophagy in the yeast *Saccharomyces cerevisiae*. These advances include: i) identification of the molecular mechanism by which Atg22 recycles amino acids to link the degradative and recycling functions of autophagy. These results led us to propose a "recycling" model that includes the efflux of macromolecules from the lysosome/vacuole as the final step of autophagy; ii) identification of the molecular mechanism by which the stress-responsive, cyclin-dependent kinase (CDK) Pho85 and its corresponding cyclins antagonistically modulate the induction of autophagy; iii) discovery of the role of an inhibitor of Clb-Cdc28 kinases, Sic1, in the negative regulation of autophagy and further identification of Rim15 as a downstream target of Sic1.

Permeases Recycle Amino Acids Resulting from Autophagy

Previously, Onodera and Ohsumi showed that in autophagy-defective *atg7Δ* cells, the

total intracellular amino acid pool was dramatically reduced, and bulk protein synthesis was substantially abrogated under nitrogen starvation conditions, compared to the wild type (Onodera and Ohsumi, 2005). They interpreted these results to indicate that free amino acid pools generated during autophagy become a limiting factor for protein synthesis under starvation conditions. This is compatible with a recent report that plasma and tissue amino acid levels, which are critical for the maintenance of energy homeostasis and viability, were reduced in Atg5 knock-out neonatal mice under fasting conditions (Kuma et al., 2004). Because of these observations, we hypothesized that amino acids generated by autophagy are released from the vacuolar/lysosomal lumen into the cytoplasm to be re-utilized for protein synthesis, and this recycling is essential to allow cells to sustain viability during nutrient deprivation. The unanswered question was what factors mediate the connection between the breakdown process and the subsequent cytosolic protein synthesis? Permeases located in the limiting membrane of the vacuole could play such a role for the mobilization of amino acids resulting from autophagy. Thus, we began our analysis by examining a putative vacuolar integral membrane protein, Atg22, with limited homologies with permeases (Nelissen et al., 1997; Ohki and Murata, 1997; Suriapranata et al., 2000).

In chapter 3, I have described the study of the characterization of *ATG22*, which was previously identified as *AUT4*. First, I carefully examined the role of Atg22 in autophagy and breakdown of the autophagic body. A previous report suggested that the breakdown of autophagic bodies depends on Atg22; in contrast, the cytoplasm to vacuole targeting (Cvt) pathway, a type of specific autophagy involved in biosynthetic delivery to the vacuole (Kim and Klionsky, 2000), is reported to be normal in the *atg22Δ* mutant cells

(Suriapranata et al., 2000). The apparent difference in the susceptibility to lysis of Cvt versus autophagic bodies suggested there might be a fundamental difference between the membrane used for autophagy versus the Cvt pathway, and might provide some insight to the origin of the sequestering vesicle membrane, a topic of considerable debate. In contrast to previously published data, I found that the steps of autophagy up to and including breakdown are essentially normal in the *atg22Δ* mutant. I monitored non-specific autophagy through the Pho8Δ60 assay (Noda et al., 1995) (measuring bulk autophagy of the cytosol), and processing of GFP-tagged Atg8 (Cheong et al., 2005) (monitoring the efficiency of delivery and lysis of the autophagic body). In addition, I followed the maturation of prApe1, a marker for specific autophagy, in the Cvt pathway-defective *vac8Δ* background (Cheong et al., 2005). In all cases, I found essentially normal kinetics for both the Cvt pathway and autophagy in the absence of Atg22. In particular, there was no evidence for a substantial difference in the lysis of Cvt versus autophagic bodies. Thus, my data suggest that the membrane origin for the autophagy and Cvt pathways is probably the same, as supported by Reggiori et al (2004).

Second, the loss of viability seen in the *atg22*Δ mutant, which is auxotrophic for leucine, could be rescued by addition of leucine or complementation of the *leu2* defect by transforming the cells with a plasmid carrying a *LEU2* gene. These results suggested that Atg22 might function as a leucine effluxer on the vacuolar membrane. This conclusion is supported by analysis of vacuolar amino acid levels, which suggest that Atg22 appears to be part of the same family with Avt3 and Avt4, two other vacuolar amino acid permeases (Russnak et al., 2001), which mediate the efflux of leucine and other amino acids; however, since I was unsuccessful in carrying out analyses of amino acid efflux using vacuoles

containing radiolabeled amino acids, I do not have direct evidence for the function of Atg22 as a leucine effluxer.

Third, to identify the connection between autophagy and maintenance of amino acid levels and hence protein synthesis, I carried out a protein synthesis assay by measuring two vacuolar proteinases, Ape1 and Prc1, which are normally upregulated during nitrogen starvation (Onodera and Ohsumi, 2005). Under autophagy-induced conditions in synthetic complete medium lacking only leucine, the *atg22Δ* mutant shows a severely reduced level of Ape1 and Prc1 synthesis; these proteins are hardly detected in the *atg22Δ avt3Δ avt4Δ* mutant. I interpret my data to indicate that the defect in the efflux of autophagy-derived amino acids causes the defect in protein synthesis. The latter is presumably needed for the maintenance of cell viability upon starvation.

Finally, this work has led us to propose a "recycling" model that includes the efflux of macromolecules from the lysosome/vacuole as the final step of autophagy. This model explains the starvation-sensitivity of the *atg22*Δ mutant, which is otherwise normal for autophagy. That is, *atg22*Δ cells are able to carry out the initial steps of autophagy including the formation of autophagosomes, their fusion with the vacuole, and the breakdown of the autophagic bodies. In contrast, leucine and other amino acids accumulate within the vacuole lumen and are not released back into the cytosol. The release of autophagic amino acids is necessary for the maintenance of protein synthesis and viability during starvation conditions. This work provides the first mechanistic data to specifically connect the breakdown process of autophagy with subsequent cytosolic protein synthesis. In addition, this work points out the physiological significance of the recycling step of autophagy.

Cyclin-dependent kinase Pho85 and its Cyclin Complex Antagonistically Modulate the Induction of Autophagy

Previous work has indicated that Pho85 is a negative regulator of autophagy (Wang et al., 2001). However, it remains elusive which potential cyclin(s) associate with Pho85 to play this role. The multifunctional CDK Pho85 has ten different cyclins and each cyclin potentially directs Pho85 to different target substrates to fulfill different roles. Based on these observations, we began our analysis to carefully examine the role of Pho85 and its individual cyclins in autophagy.

In chapter 4, I first demonstrated that cyclins Pho80 and Pcl5 complex with Pho85 to negatively regulate autophagy. Pho80-Pho85 and Pcl5-Pho85 are two nutrient sensors, which sense phosphate and amino acid starvation, respectively. Thus, my work provides evidence to indicate how autophagy is regulated under phosphate and amino acid starvation conditions. I further demonstrated that Pho80-Pho85 and Pcl5-Pho85 kinase complexes contribute appreciably to the negative regulation of autophagy, through their inhibitory roles on Rim15 and Pho4, and on Gcn4, respectively. This is consistent with previous observations that Rim15 and Gcn4 are required for autophagy induction (Talloczy et al., 2002; Yorimitsu et al., 2007).

Second, my work has led to the idenfication of the dual roles of Pho85 in autophagy induction. That is, Pho85 is both a positive and negative regulator of autophagy. The positive regulatory role of Pho85 can be seen in the *pcl5*Δ *pho80*Δ background where the Pho80 and Pcl5 cyclins that exert a negative effect are deleted, and also in the *gcn4*Δ *pho4*Δ *rim15*Δ background where all three downstream targets of Pho80-Pho85 and Pcl5-Pho85 to negatively regulate autophagy are deleted. Overexpression of Pho85 led to the induction of autophagy, whereas further deletion of *PHO80* and *PCL5* elevated the level of

autophagy induction. All of these observations provided the first evidence to support the view that Pho85 has a positive regulatory role in autophagy induction. This important discovery is quite intriguing, and fits well with the fact that Pho85 in conjugation with different cyclins can discharge numerous biological functions (Huang et al., 2007).

Third, another important finding in this work is that the CDK inhibitor Sic1 functions as a negative regulator of autophagy. This is based on the observations that overexpression of Sic1 inhibits autophagy, whereas deletion of *SIC1* dramatically increased the level of autophagy induced by rapamycin treatment. While most previous work has linked the roles of Sic1 only to cell cycle regulation, our study assigns new function to Sic1, a negative regulator of autophagy. However, in mammalian cells, overexpression of the CDK inhibitor p27, or expression of a stable p27 mutant, is sufficient to induce autophagy (Liang et al., 2007). At this moment, we cannot explain the reason for these totally opposite roles of this CDK inhibitor in autophagy regulation between yeast and mammalian cells. Nonetheless, I also found that autophagy was inhibited in the *cdc34-2*^{ts} mutant, in which Sic1 accumulates (Schwob et al., 1994), and in the *cdc28-1*^{ts}, *cdc28-4*^{ts} and *cdc28-13*^{ts} mutants, in which inactivation of Cdc28 causes hypophosphorylation of Sic1, leading to its accumulation (Schneider et al., 1998), whereas deletion of *SIC1* in the *cdc28-4*^{ts} mutant partially suppressed the defect in autophagy induction. These observations fit well with the view that hyper-accumulation of Sic1 inhibits autophagy.

Fourth, the mechanism by which Pho85 positively regulates autophagy is also carefully elucidated. Since Pho85 is known to phosphorylate Sic1 and prompt its degradation (Nishizawa et al., 1998), and Pho85 mediates Sic1 degradation to allow Cdc28 activation and reentry into the cell-cycle after DNA damage-induced G_1 arrest (Wysocki et

al., 2006), I hypothesized that the CDK Pho85 exerts its positive regulatory role in autophagy induction through targeting Sic1, a negative regulator of autophagy, for degradation. I took advantage of an analogue-sensitive mutant *PHO85-F82G* to prevent the synthetical lethal effect upon double deletion of *PHO85* and *SIC1*, and found that deletion of *SIC1* in the *PHO85-F82G pcl5*Δ *pho80*Δ cells suppressed the inhibition of autophagy that was caused by inactivation of Pho85. I also observed that overexpression of Pho85 abolished the inhibitory effect of Sic1 overexpression on autophagy. These results led us to propose a model that Pho85 targets Sic1 to relieve the autophagy defect after Sic1 overexpression.

Fifth, my work further found that Pho85 complexes with cyclins Clg1, Pcl1 and Pho80 to promote Sic1 degradation, exerting a positive regulatory effect on autophagy induction. Since Sic1 must be phosphorylated to be targeted for destruction (Deshaies and Ferrell, 2001), an apparent question is to ask whether Clg1-, Pcl1- and Pho80-Pho85 complexes are able to phosphorylate Sic1. I performed an *in vitro* phosphorylation study and provided direct evidence to show that immunoprecipitated HA-tagged Clg1, Pcl1 and Pho80, but not Pcl2, Pcl5 and Pcl9, obtained from *PHO85* cells but not from *pho85*Δ cells, phosphorylated Sic1 *in vitro*. I further investigated the mutant version of Sic1, Sic1-Δ3P, which contains T5A, T33V and S76A mutations. Sic1-Δ3P was phosphorylated to a significantly lower extent than wild-type Sic1, suggesting at least T5, T33 and/or S76 were phosphorylated *in vitro*. To gain more insight into the physiological relevance of these phosphorylation events *in vivo*, I further examined the effect of overexpression of these cyclins on the regulation of Sic1 stability and the induction of autophagy. Indeed, overexpression of Clg1, Pcl1 or Pho80 significantly reduced the level of wild-type Sic1,

but not Sic1-Δ3P, and overcame the inhibition of autophagy caused by overexpression of wild-type Sic1, but not Sic1-Δ3P. Thus, my work not only addressed the previous unanswered question as to which cyclins of Pho85 regulate Sic1 stability *in vivo*, and showed that Clg1, Pcl1 and Pho80 redundantly fufill this role, but also unraveled an exciting link between cyclins, Sic1 and autophagy; that is, the cyclins Clg1, Pcl1 and Pho80, in concert with Pho85, promote the degradation of Sic1, resulting in the elevation of the magnitude of autophagy. However, to bring our story full circle, further work remains to be done to show that i) Clg1-, Pcl1- and Pho80-Pho85 complexes indeed phosphorylate Sic1 *in vivo* using an *in vivo* phosphorylation assay; ii) immunoprecipitated Pho85 obtained from wild-type cells but not from *clg1*Δ *pcl1*Δ *pho80*Δ cells, phosphorylate Sic1 *in vitro*; iii) triple knockout *clg1*Δ *pcl1*Δ *pho80*Δ cells display an accumulation of Sic1. Further analysis also needs to be carried out to elucidate the mechanism by which Clg1-, Pcl1- and Pho80-Pho85 complexes synergistically regulate Sic1 stability and the magnitude of autophagy. In fact, Pho80-Pho85 is localized exclusively to the nucleus (Kaffman et al., 1998); Clg1 is localized primarily to the nucleus (our unpublished data), whereas Pcl1 localizes partially to the nucleus as well as sites of polarized cell growth (Moffat and Andrews, 2004). Moreover, transcript levels for *CLG1* and *PHO80* are constant throughout the cell cycle, whereas *PCL1* is specifically expressed during the late G_1 phase (Measday et al., 1997). Thus, it is likely that subcellular localization of Pcl-Pho85 complexes and/or the timing of expression of these cyclin genes contributes to the selection of when and where to phosphorylate Sic1 and promote its degradation.

Sixth, another achievement of my work is the identification of Rim15 as the

downstream target of Sic1 in autophagy regulation. Thus, Rim15 is under the negative regulation of both Pho80-Pho85 and Sic1. This intriguing finding inferred that Rim15 integrates signals from both the negative and positive regulatory pathways of Pho85 to properly control autophagy. The main question that remains to be further investigated is how does Sic1 negatively regulate Rim15? At least four nutrient-sensory kinases converge on Rim15 regulation through controlling the nucleocytoplasmic distribution of Rim15 (Swinnen et al., 2006), such that Pho80-Pho85 negatively regulates Rim15 through phosphorylating Rim15 and promoting the association of Rim15 with 14-3-3 proteins in the cytoplasm (Wanke et al., 2005). Thus, it is possible that Sic1 negatively regulates Rim15 through controlling the nucleocytoplasmic distribution of Rim15. We checked the localization of GFP-Rim15 by using the kinase-inactive GFP-Rim15^{K823Y} and GFP-Rim15^{C1176Y} fusion proteins, which accumulate in the nuclei of rapamycin-treated *rim15Δ* cells, as shown previously by Wanke et al. (2005). We found that deletion of *SIC1* did not induce the nuclear import of GFP-Rim15 in nutrient-rich conditions. In addition, when Sic1 wild type or Sic1-Δ3P was overexpressed, we did not observe a clear defect in the movement of Rim15 into the nucleus. However, there was a decrease in the percentage of the cells with clear nuclear staining of GFP-Rim15 when cells were treated with rapamycin. One explanation for this observation is that the nuclear localization of Rim15 may not be directly correlated with its activity. Since Sic1 is a stoichiometric inhibitor, we then asked whether inhibition of Rim15 kinase activity occurs through a physical interaction between Rim15 and Sic1. However, only a weak interaction was detected in co-immunoprecipitation experiments. Thus, Sic1 might inhibit Rim15 indirectly. Since Sic1 is an inhibitor of S phase Clb cyclin-containing Cdc28 kinase complexes (Mendenhall

et al., 1995), it is possible that Clb-Cdc28 phosphorylates and activates Rim15, and, thereby, Sic1 indirectly inhibits Rim15 through inhibiting Clb-Cdc28. Further study will be needed to elucidate the mechanism by which Sic1 negatively regulates Rim15.

Finally, the correlation between cell cycle regulation and autophagy induction is still a matter of debate. Sic1 has roles in controlling both the G_1/S phase transition and the exit from mitosis, hence preventing premature onset of S phase and ensuring genome integrity (Mendenhall et al., 1995). Deletion of *SIC1* causes premature DNA replication from fewer origins, and extension of the duration of S phase. Deletion of *SIC1* also results in the defect in the initiation of mitosis, inefficient separation of sister chromatids during anaphase, leading to partial mitotic arrest, with a high rate of chromosomal damage (Nugroho and Mendenhall, 1994). In addition, I found that deletion of *SIC1* dramatically increased the level of autophagy induced by rapamycin treatment. Thus, it is reasonable to conclude that autophagy is upregulated in order to help cells mitigate genome damage caused by loss of Sic1, and this notion is also consistent with a previous report in mammalian cells that autophagy plays roles in preventing genomic instability (Karantza-Wadsworth et al., 2007; Mathew et al., 2007). Another concern in this field is that since overexpression of Sic1 or inactivation of *CDC34* or *CDC28* leads to G_1 cell cycle arrest (Nugroho and Mendenhall, 1994; Schwob et al., 1994; Verma et al., 1997), we cannot rule out the possibility that the defect in autophagy caused by hyper-accumulation of Sic1 might be due to cell cycle arrest at the G_1 phase. On the other hand, induction of autophagy under conditions of nutrient limitation often accompanies cell cycle arrest at the G_1 phase. Moreover, Rim15 functions as a positive regulator of autophagy, and is also essential for the cells to enter the G_0 phase (cell cycle arrest at the G_0/G_1 phase) in reponse to nutrient starvation (Swinnen et al., 2006).

I reasoned that if cell cycle arrest leads to an autophagic defect, then it would be contradictory to the fact that Rim15 is required for autophagy. Therefore, it is also possible that cell cycle arrest may not be directly linked to autophagy regulation, and autophagy may occur in parallel with cell cycle arrest. Further analysis is clearly needed to clarify the precise correlation between cell cycle arrest and autophagy.

In conclusion, my work largely contributes to our current understanding of autophagy, a precisely controlled process. It elucidated a quite complex regulatory nework by which Pho85 and its corresponding cyclins modulate autophagy in yeast. We believe that potential future work will further extend our knowledge about this important intracellular degradative pathway.

REFERENCES

Cheong, H., Yorimitsu, T., Reggiori, F., Legakis, J.E., Wang, C.-W., and Klionsky, D.J. (2005). Atg17 regulates the magnitude of the autophagic response. Mol Biol Cell *16*, 3438-3453.

Deshaies, R.J., and Ferrell, J.E., Jr. (2001). Multisite phosphorylation and the countdown to S phase. Cell *107*, 819-822.

Huang, D., Friesen, H., and Andrews, B. (2007). Pho85, a multifunctional cyclin-dependent protein kinase in budding yeast. Mol Microbiol *66*, 303-314.

Kaffman, A., Rank, N.M., O'Neill, E.M., Huang, L.S., and O'Shea, E.K. (1998). The receptor Msn5 exports the phosphorylated transcription factor Pho4 out of the nucleus. Nature *396*, 482-486.

Karantza-Wadsworth, V., Patel, S., Kravchuk, O., Chen, G., Mathew, R., Jin, S., and White, E. (2007). Autophagy mitigates metabolic stress and genome damage in mammary tumorigenesis. Genes Dev *21*, 1621-1635.

Kim, J., and Klionsky, D.J. (2000). Autophagy, cytoplasm-to-vacuole targeting pathway, and pexophagy in yeast and mammalian cells. Annu Rev Biochem *69*, 303-342.

Kuma, A., Hatano, M., Matsui, M., Yamamoto, A., Nakaya, H., Yoshimori, T., Ohsumi, Y., Tokuhisa, T., and Mizushima, N. (2004). The role of autophagy during the early neonatal starvation period. Nature *432*, 1032-1036.

Liang, J., Shao, S.H., Xu, Z.X., Hennessy, B., Ding, Z., Larrea, M., Kondo, S., Dumont, D.J., Gutterman, J.U., Walker, C.L.*, et al.* (2007). The energy sensing LKB1-AMPK pathway regulates p27(kip1) phosphorylation mediating the decision to enter autophagy or apoptosis. Nat Cell Biol *9*, 218-224.

Mathew, R., Kongara, S., Beaudoin, B., Karp, C.M., Bray, K., Degenhardt, K., Chen, G., Jin, S., and White, E. (2007). Autophagy suppresses tumor progression by limiting chromosomal instability. Genes Dev *21*, 1367-1381.

Measday, V., Moore, L., Retnakaran, R., Lee, J., Donoviel, M., Neiman, A.M., and Andrews, B. (1997). A family of cyclin-like proteins that interact with the Pho85 cyclin-dependent kinase. Mol Cell Biol *17*, 1212-1223.

Mendenhall, M.D., al-Jumaily, W., and Nugroho, T.T. (1995). The Cdc28 inhibitor p40SIC1. Prog Cell Cycle Res *1*, 173-185.

Moffat, J., and Andrews, B. (2004). Late-G1 cyclin-CDK activity is essential for control of cell morphogenesis in budding yeast. Nat Cell Biol *6*, 59-66.

Nelissen, B., De Wachter, R., and Goffeau, A. (1997). Classification of all putative permeases and other membrane plurispanners of the major facilitator superfamily encoded by the complete genome of *Saccharomyces cerevisiae*. FEMS Microbiol Rev *21*, 113-134.

Nishizawa, M., Kawasumi, M., Fujino, M., and Toh-e, A. (1998). Phosphorylation of sic1, a cyclin-dependent kinase (Cdk) inhibitor, by Cdk including Pho85 kinase is required for its prompt degradation. Mol Biol Cell *9*, 2393-2405.

Noda, T., Matsuura, A., Wada, Y., and Ohsumi, Y. (1995). Novel system for monitoring autophagy in the yeast *Saccharomyces cerevisiae*. Biochem Biophys Res Commun *210*, 126-132.

Nugroho, T.T., and Mendenhall, M.D. (1994). An inhibitor of yeast cyclin-dependent protein kinase plays an important role in ensuring the genomic integrity of daughter cells. Mol Cell Biol *14*, 3320-3328.

Ohki, R., and Murata, M. (1997). bmr3, a third multidrug transporter gene of *Bacillus subtilis*. J Bacteriol *179*, 1423-1427.

Onodera, J., and Ohsumi, Y. (2005). Autophagy is required for maintenance of amino acid levels and protein synthesis under nitrogen starvation. J Biol Chem *280*, 31582-31586.

Russnak, R., Konczal, D., and McIntire, S.L. (2001). A family of yeast proteins mediating bidirectional vacuolar amino acid transport. J Biol Chem *276*, 23849-23857.

Reggiori, F., Wang, C.-W., Nair, U., Shintani, T., Abeliovich, H., and Klionsky, D.J. (2004). Early stages of the secretory pathway, but not endosomes, are required for Cvt vesicle and autophagosome assembly in *Saccharomyces cerevisiae*. Mol Biol Cell *15*, 2189-2204.

Schneider, B.L., Patton, E.E., Lanker, S., Mendenhall, M.D., Wittenberg, C., Futcher, B., and Tyers, M. (1998). Yeast G1 cyclins are unstable in G1 phase. Nature *395*, 86-89.

Schwob, E., Bohm, T., Mendenhall, M.D., and Nasmyth, K. (1994). The B-type cyclin kinase inhibitor p40SIC1 controls the G1 to S transition in *S. cerevisiae*. Cell *79*, 233-244.

Suriapranata, I., Epple, U.D., Bernreuther, D., Bredschneider, M., Sovarasteanu, K., and Thumm, M. (2000). The breakdown of autophagic vesicles inside the vacuole depends on Aut4p. J Cell Sci *113 (Pt 22)*, 4025-4033.

Swinnen, E., Wanke, V., Roosen, J., Smets, B., Dubouloz, F., Pedruzzi, I., Cameroni, E., De Virgilio, C., and Winderickx, J. (2006). Rim15 and the crossroads of nutrient signalling pathways in *Saccharomyces cerevisiae*. Cell Div *1*, 3.

Tallóczy, Z., Jiang, W., Virgin, H.W., IV., Leib, D.A., Scheuner, D., Kaufman, R.J., Eskelinen, E.-L., and Levine, B. (2002). Regulation of starvation- and virus-induced autophagy by the eIF2α kinase signaling pathway. Proc Natl Acad Sci U S A *99*, 190-195.

Verma, R., Annan, R.S., Huddleston, M.J., Carr, S.A., Reynard, G., and Deshaies, R.J. (1997). Phosphorylation of Sic1p by G_1 Cdk required for its degradation and entry into S phase. Science *278*, 455-460.

Wang, Z., Wilson, W.A., Fujino, M.A., and Roach, P.J. (2001). Antagonistic controls of autophagy and glycogen accumulation by Snf1p, the yeast homolog of AMP-activated protein kinase, and the cyclin-dependent kinase Pho85p. Mol Cell Biol *21*, 5742-5752.

Wanke, V., Pedruzzi, I., Cameroni, E., Dubouloz, F., and De Virgilio, C. (2005). Regulation of G_0 entry by the Pho80-Pho85 cyclin-CDK complex. EMBO J *24*, 4271-4278.

Wysocki, R., Javaheri, A., Kristjansdottir, K., Sha, F., and Kron, S.J. (2006). CDK Pho85 targets CDK inhibitor Sic1 to relieve yeast G1 checkpoint arrest after DNA damage. Nat Struct Mol Biol *13*, 908-914.

Yorimitsu, T., Zaman, S., Broach, J.R., and Klionsky, D.J. (2007). Protein kinase A and Sch9 cooperatively regulate induction of autophagy in *Saccharomyces cerevisiae*. Mol Biol Cell *18*, 4180-4189.